STUDIES ON LEACHING BEHAVIOUR OF SODIUM BOROSILICATE GLASSES

by

Deborah Lynn Moir

Submitted in partial fulfillment of the requirements
for the degree of Doctor of Philosophy

at

Dalhousie University
Halifax, Nova Scotia
1989 September

THIS THESIS IS DEDICATED TO

My dog, David Letterman and Cap'n Crunch

TABLE OF CONTENTS

LIST OF ILLUSTRATIONS

Page

Page

Page

LIST OF TABLES

ABSTRACT

A combination of instrumental neutron activation analysis (INAA) and epithermal INAA (EINAA) methods has been developed for the simultaneous determination of multi-element concentrations. The elements measured includes Al, As, Ba, Ca, Ce, Co, Cr, Cs, Eu, Fe, Hf, I, K, La, Mg, Mn, Mo, Na, Nd, Ni, Pr, Rb, Sb, Sc, Si, Sm, Sn, Sr, Ta, Tb, Ti, Tm, U, V, W, Yb, Zn and Zr in glasses, and Al, Ce, Cs, Fe, La, Mn, Mo, Na, Nd, Ni, Pr, Sm, U and W in leachates. The precision and accuracy of the methods have been found to be within ±10% in most cases.

Boron has been determined by an indirect INAA method applicable to samples containing > 1000 μg of B and by a spectrophotometric method suitable for 1 to 4 ppm B. A spectrophotometric method has modified for measuring Si (5-100 ppm) in leachates in the presence of F^- ions.

The suitability of sodium borosilicate glasses as host matrices for high-level waste has been evaluated by static leaching with distilled deionized water (DDW), synthetic granitic ground water (GGW) and synthetic Grande Ronde basaltic groundwater (BGW). The effects of leachant composition and pH, temperature (40° and 90°C), time (3-84 d), and surface area to volume ratio (0.010, 0.10 and 0.85 cm^{-1}) have been investigated.

Results indicated a strong influence of the leachant composition through both its pH and nature as well as concentrations of ions present on the leach rate. In general, total mass loss was the highest in BGW primarily due to its high pH (>9). The presence of certain ions such as carbonates and sulfates in leachants increased its aggressiveness possibly through the formation of soluble complexes. The pH (4.5 - 7.5) of DDW and GGW influenced the precipitation of some elements such as La, Sm and U. Leach rates at 90° were 5-30 times higher than at 40°. Activation energies (32-63 kJ/mol) calculated for I-117 glass at 3 different SA/V ratios compares well with those reported in literature. The normalized elemental mass losses showed that the rate of leaching decreased with increasing SA/V ratio. The concentrations of La, Mn, Sm and U in leachate sampled at 90°C were lower compared to that after cooling to room temperature. Application of long-term dissolution models suggest that the primary mechanism of glass leaching is diffusion for up to 84 d.

ABBREVIATIONS

AAS - Atomic absorption spectroscopy
ACS - American Chemical Society
ADC - Analog-to-digital convertor
AECL - Atomic Energy of Canada Limited
AF - Advantage factor
ASTM - American Society for Testing Materials
BGW - Basaltic groundwater
CEC - Commission of the European Communities
CR - Cadmium ratio
CRM - Certified reference material
CRNL - Chalk River Nuclear Laboratories
DDW - Distilled deionized water
DHBA - Dihydroxybenzoic acid
DUSR - Dalhousie University SLOWPOKE reactor
DWRG - Defense Waste Reference Glass
EINAA - Epithermal instrumental neutron activation analysis
EPMA - Electron probe microanalysis
FEP - Fluorinated ethylene propylene
FWHM - Full width at half-maximum
GGW - Granitic groundwater
HLW - High-level waste
ICP-AES - Inductively coupled plasma atomic emission spectroscopy
IR - Infra-red
IUPAC - International Union of Pure and Applied Chemistry
LEPD - Low energy photon detector
LOD - Limit of detection
MCA - Multichannel analyzer
MCC - Materials Characterization Center
NAA - Neutron activation analysis
NBS - National Bureau of Standards
ND - Nuclear Data
NRCC - National Research Council of Canada
PFA - Perfluoroalkoxy
PNAA - Preconcentration Neutron Activation Analysis
PNL - Pacific Northwest Laboratories
PVA - Polyvinyl alcohol
RNAA - Radiochemical Neutron Activation Analysis
SEM - Scanning electron microscope
SIMS - Secondary ion mass spectroscopy
SRL - Savannah River Laboratories
SRM - Standard reference material
SRP - Savannah River Plant
TINAA - Thermal instrumental neutron activation analysis
TN - Tracor Northern

ACKNOWLEDGMENTS

I would like to express my deepest gratitude to Prof. Amares Chatt for his guidance and advice during the course of this study. All the help received from him academically or otherwise is gratefully acknowledged.

I wish to acknowledge the SLOWPOKE-II reactor staff, Dr. Jiri Holzbecher and Mr. Blaine Zwicker for their assistance in the irradiation of samples, as well as Dr. Holzbecher for helpful discussions and advice.

I would also like to thank the other members of the SLOWPOKE research group for their friendship and support, and in particular Dr. R.R. Rao for his invaluable advice during the course of this work.

I thank Dr. G. Bidoglio (CEC, Ispra Establishment, Italy), Dr. R.H. Brill (Corning, U.S.A.) and Dr. T.T. Vandergraaf (AECL-RC, WNRE, Canada) for providing glass samples.

Finally, I gratefully acknowledge the Sumner Foundation, the Natural Sciences and Engineering Research Council of Canada, and Dalhousie University for the financial support through which this work was made possible.

CHAPTER 1

INTRODUCTION AND OBJECTIVES

The use of nuclear power for the generation of electricity has led to concern over the problem of safe disposal of radioactive waste products arising from the processing of spent fuel elements. The spent fuel is highly radioactive due to the presence of actinides such as Am, Cm, Np and Pu, as well as fission products such as the nuclides of I, Pd, Sr, Tc and Zr. Since the half-lives of most of these nuclides are very long (viz. 28a - 1.6×10^7a), they will be in existence for lengthy periods of time. Presently, spent reactor fuel is stored in pools at the reactor sites, and liquid wastes from reprocessing are stored in underground tanks usually at the treatment site. The lifetime of these tanks is of the order of a few decades, and already leaks have been reported (85MILE1). As a result, a permanent and safe disposal procedure and site needs to be developed.

The sea-dumping of medium-level radioactive wastes and shallow land burial of low-level wastes began in 1951 (82SIMO1). Burial of the high-level waste (HLW) in geological formations (granite, salt domes or basalt) appears to be the most favoured disposal option, although other proposals have included burial in the sub-seabed or under ice and such exotic schemes as rocketing the waste into space or injecting it under the earth's crust.

The technical management of the high-level waste (HLW) may be divided into four sub-systems: (1) storage, (2) radionuclide immobilization,

(3) isolation and (4) post-emplacement (79ROY1). The schemes for immobilization and isolation will involve a sequential set of barriers consisting of the host rock, canister and the waste form, and further details are given in Section 2.B. These barriers deal with control of either the radionuclide source or the transport of the radionuclides.

Research on the solidification of HLW was initiated in the 1950's. Over thirty years of research has yet to yield a waste-form composition that can suitably accommodate all types of nuclear waste. Glass has been regarded as one of the most promising waste forms for HLW for several reasons. For example, it is generally not affected by variation in waste composition; its amorphous lattice structure allows for a high loading capacity of waste oxides; it has good chemical, mechanical and thermal stability; it resists leaching by water; it has a low susceptibility to structural damage by radiation; raw materials for its production are readily available; and the technology for its fabrication on a large scale is well established. Different compositions of glass have been selected by different countries, including aluminosilicate, alkali-borosilicate, phospho-aluminosilicate, and phosphate glasses. The concentration of waste products to be incorporated into the glass varies from one country to another; and values between 2 and 30% by weight have been suggested. The United States with vast areas available for repositories is mostly interested in low load percentages; whereas European countries and Japan, where land available is at a minimum, are studying higher waste loading. In addition to glasses, other waste forms such as ceramic, sphene (glass ceramic), zeolites, titanate ceramic (SYNROC) and cements are under consideration.

In order to evaluate the suitability of long-term storage of the glass in a repository, leach tests are being carried out by many researchers. These tests simulate the situation in which waste forms accidentally come in contact with groundwater, dissolve in it and thereby release radionuclides. The possibility exists that these radionuclides may form anionic complexes with the ligands present in the groundwater and migrate across the geochemical barrier to the environment. Obviously the release of nuclides will be governed by a number of parameters including temperature, waste form and leachant compositions, pH, glass surface area to leachant volume ratio (SA/V), canister and backfill materials and oxic/anoxic conditions. Much of the research done so far concentrated on only one or two of the above factors in a short time frame, and the applicability of these results to the prediction of the behaviour of radionuclides has been questioned.

One of the objectives of the work reported in this thesis was to design long-term static leaching experiments for evaluating the effects of individual parameters such as glass type, leachant composition and pH, SA/V ratio and time on the rates of leaching of elements from simulated vitrified HLW. The results obtained from the preliminary work were then used in designing subsequent main experiments. The objectives of the main experiments were to study the effects of four parameters (temperature, leachant composition, pH and SA/V) ratio simultaneously. A comparison of the rates of leaching as affected by these factors was made.

Temperatures of 40° and 90°C were selected for investigation so as to represent two of the more likely temperatures which might be

encountered by groundwaters should the integrity of the repository and waste package be accidentally breached. The protective canister encasing the glass is expected to last for about 10 000 years. It is anticipated that after about 500 years the temperature of the repository will be in the region of 30-60°C, so that an experimental temperature of 40°C is certainly reasonable. However, if the canister does not last as long as expected, the second temperature of 90°C will represent the worst case scenario, since the temperature of the repository within the first 70 years after burial should be around 100°C.

The leachant composition encompasses both the ionic concentration of the solution as well as its pH. A large number of the leaching studies reported thus far involved the use of distilled or deionized water as the leachant. Since an accident in a real repository would allow the infiltration of groundwaters or brines, the use of deionized water alone as the leachant is not realistic. Leachants were chosen in our work to represent typical waters which the glass might encounter in a geologic repository (viz. synthetic granitic groundwater and synthetic Grande Ronde basaltic groundwater). In addition, distilled deionized water was included among the leachants for comparison purposes. The above 3 leachants represented a wide range of ionic concentrations and solution pH (6.10-9.35). Many of the previous studies focused on groundwaters with low concentrations of anionic species. However, a number of elements of interest in waste disposal become more mobile in the presence of certain anions. One of the purposes of the leaching studies done in this work was to investigate the effects of the presence of high concentrations of carbonate and sulfate ions in the leachant through the

use of the basaltic groundwater on the leaching rates.

The glass surface area to leachant volume (SA/V) ratio may strongly affect the leach rate through solubility and saturation controls. In many previous studies the Materials Characterization Center (MCC) standard SA/V ratio ($0.10cm^{-1}$) or another single SA/V ratio was employed. However, since the repository can be breached to different degrees by water under actual conditions, different SA/V ratios should be investigated. To this end the effects of three different SA/V ratios were examined (0.010, 0.10 and 0.85 cm^{-1}) in the present work. Powdered glass was used in some studies reported in literature to achieve a higher SA/V ratio without reducing the leachant volume so drastically that there is insufficient leachate left for subsequent analysis. Although this approach can significantly increase the glass surface area, it does introduce new problems since the leaching mechanism can be vastly different for powdered glass compared to a monolithic sample. In view of this possibility, experiments in our studies were designed so that monolithic glass samples could be leached at each SA/V ratio investigated.

Most researchers conducting leaching studies at elevated temperatures sampled the leachate after the solution had cooled to room temperature. Although it is a very convenient means of sampling, the question arises whether an error is introduced in doing so. If a species with temperature-dependent solubility is leached it may precipitate onto the glass surface during cooling which will change the solution composition and lead to an under-estimation of the extent of leaching. One of the objectives of this study was to determine whether a difference did exist between an aliquot of leachate sampled at the elevated experimental temperature and

a sample of the same leachate taken after it had cooled to room temperature.

Glass dissolution models are commonly employed for long-term extrapolation of leaching data. A comprehensive model which takes into account all leaching parameters is so far unavailable primarily due to the difficulty in formulating a model which compensates for the changing chemical processes of the reaction with time. In order to determine the glass dissolution processes at work, three pre-existing and simple models have been applied to our data.

In early studies leach rate calculations were based on total mass loss of the glass specimens (85IAEA1). These measurements were made by weighing the specimens before and after leaching, and the difference in weights was used to calculate the leach rate. Although this method is adequate for determining the overall leach rate and durability of a glass, it does not provide any information about the leaching characteristics of individual elements. Since not all elements leach at the same rate, the need for a technique which can measure elemental concentrations in solution becomes obvious. Some components of the glass may be preferentially dissolved by a process termed selective leaching, while others are dissolved congruently, i.e. in proportion to the chemical composition of the glass. As a result the concentrations of specific elements may vary greatly in solution. It is more advantageous to gather information on the leaching behaviour of specific elements which act as chemical analogues for the lanthanides and actinides of concern in HLW.

Most researchers carried out their analyses of selective elements in

the waste forms and leachate solutions using either atomic absorption spectrometry (AAS) or inductively coupled plasma-atomic emission spectrometry (ICP-AES). Although these techniques could be advantageously used for leachants, in the case of solid glass and leachates containing particulate matter digestion of the sample is both necessary and difficult. Concentrated hydrofluoric acid is generally used for dissolution, which could present a problem for most spectrometers. A fairly large sample volume is required for sequential multi-element analysis by the above techniques. Neutron activation analysis (NAA), on the other hand, may be advantageously used to analyze solid glass samples with a minimum of sample handling and preparation which might otherwise introduce contamination. In addition, small volumes of leachate samples may be analyzed with good sensitivity and accuracy by NAA.

One of the objectives of this work was to develop an instrumental neutron activation analysis (INAA) method employing thermal as well as epi-cadmium neutrons for the simultaneous determination of multi-element concentrations in samples of simulated vitrified high-level wastes and their leachates (87MOIR1). The method should allow for the determination of the maximum number of elements with the minimum number of irradiation, decay and counting periods and should be of high precision and accuracy. The precision and accuracy of the NAA methods developed here were evaluated by analyzing certified reference materials (CRM). Limits of detection for all elements present were calculated and reported.

Borosilicate glasses present a problem when INAA is used as the analytical technique. This is due to the high thermal neutron cross-section of boron (759 barns), which thus absorbs thermal neutrons very

readily, subsequently reducing the neutron flux. The activity of a sample of borosilicate glass will be lower than expected, giving incorrect values for elemental composition if the comparator standards do not contain an identical amount of boron. The boron content of the glass must be known accurately in order to be able to correct for this flux reduction. Although ^{11}B undergoes an (n,γ) reaction to form ^{12}B, its half-life is only 20.4 ms. This half-life is far too short to permit an irradiated sample to be counted using the available pneumatic transfer system. Because of this difficulty, alternative methods for the determination of boron in borosilicate glass were required. Two such methods were adapted for use in this work. The magnitude of the flux reduction is proportional to the concentration of boron present in a sample and can be determined by measuring the activity of an easily activated element (69SELE1, 81SALE1). This is the basis of a method for determining boron in glass indirectly by NAA. The second method is a variation of the well-known spectrophotometric method for the analysis of boron using methylene blue to form a complex, followed by extraction into 1,2-dichloroethane (69SCHL1). The reliability and sensitivity of the indirect INAA method for measuring the boron content of samples has been compared with the spectrophotometric method, and both have been subsequently applied in the routine determination of boron in glass and leachates.

The determination of silicon by INAA is normally accomplished through the use of the $^{29}Si(n,p)^{29}Al$ reaction. Since the neutron cross section of ^{29}Al is so low (560 mbarns), it is really only applicable to samples which contain percentage quantities of silicon. This presented a problem for

the determination of Si in leachates as the concentrations were expected to be <100 ppm. Hence, as in the case of boron, an alternative method was needed. Silicon can also be determined spectrophotometrically. However, unlike many other elements, the number of methods available is limited to two: either by yellow silicomolybdate or through reduction to molybdenum blue. Several different procedures exist for the determination of Si by molybdenum blue; however, the methods suffer from several interferences including that of fluoride which is a component of the leachants in this work. Two previously developed methods using molybdenum blue (59GRAF1, 70DUCE1) were combined and modified slightly to eliminate the fluoride interference and permit the determination of Si in the leachates. The precision and accuracy of the method were checked using a CRM.

In summary, the objectives of this thesis were to design long-term static leaching experiments for evaluating the effects of four parameters simultaneously. These parameters included temperature, leachant composition using three leachants of different ionic strengths and pH, and SA/V ratio. An investigation of the difference in elemental concentrations of leachate sampled at room temperature and that sampled at elevated temperature was carried out. Simple leaching models were applied to the data obtained in this work in order to understand the glass dissolution mechanism. An INAA method was developed for the determination of multi-element concentrations in glass used in leaching experiments and in the resulting leachates and precipitates. Since boron is not easily determined by INAA, two alternative procedures involving indirect INAA and spectrophotometry were adapted for use on glass and leachate.

Similarly, Si in leachates could not be determined by INAA, so a method employing molybdenum blue was developed.

CHAPTER 2

LITERATURE SURVEY

2.A. INTRODUCTION

The safety analysis of a potential repository for high-level wastes (HLW) requires information on the rates of release of radionuclides from the waste form to the surrounding area. The chapter provides a brief summary of the literature available on the major waste forms of interest as well as the factors which influence their leaching performance.

2.B. THE DISPOSAL SYSTEM

The disposal system for HLW is divided into three subsystems: (1) near-field region, (2) geosphere or far-field and (3) biosphere. Near-field is defined as "the excavated repository with its contents and parts of host rock which are or could be altered by construction of the repository or waste emplacement" (85IAEA2). The bulk of undisturbed host rock containing the waste repository makes up the geosphere, while the biosphere is generally referred to as any part of the earth's environment where biological processes could have an influence on radionuclides released from the repository.

This system of barriers can be further sub-divided. The near-field is comprised of the following three components: (1) the waste package, (2) the repository including its barriers and (3) the host medium. In addition, the geosphere and biosphere representing natural barriers may

be again divided into: (1) geologic containment, (2) geochemical layers and (3) the environment (Fig. 2.1).

Very little work has been done on the interactions of all components of the waste package which simulate the repository near-field. This is because a number of different geologic formations are under consideration as locations for waste repositories around the world. A description of the various components of the near-field which are under consideration are presented, beginning with the waste form and progressing towards the repository rock.

2.B.1. Waste Form

The waste form is important because it could affect near-field conditions through Eh, pH and groundwater silica saturation. The primary functions of the waste form are to ensure chemical and physical stability and thereby lower the release of radionuclides. It should have good thermal conductivity, resist mechanical shock, and be compatible with other near-field components.

2.B.2. Liner Material

Leachability of waste forms such as glass, which undergoes surface cracking during cooling due to differences in the expansion coefficients of the glass and container, can be significantly decreased through the use of a liner. A typical low-thermal conductivity material such as woven alumina felt may be used.

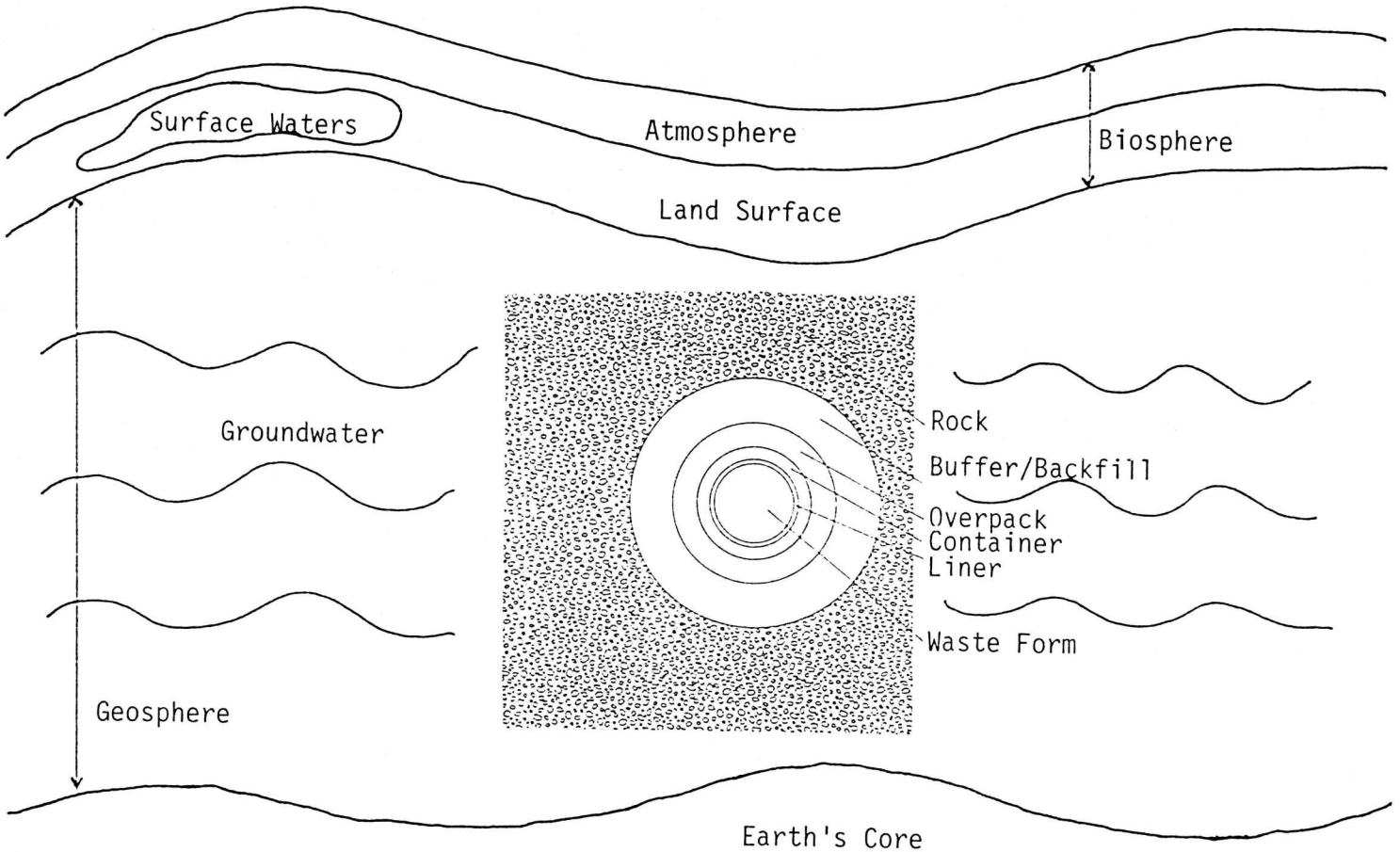

Figure 2.1. The multi-barrier geological isolation system for high-level radioactive waste.

2.B.3. Canister

The primary function of the waste canister is to withstand mechanical and chemical impact which may occur during transport, emplacement and filling of the repository. Materials suggested for containers are primarily stainless steels, although Cu, Al_2O_3, ZrO_2, $MgAl_2O_4$, Ti, Ti alloys, Pb and Ni-Cr alloys have been considered. The material chosen for the canister should have little effect on the leaching of the waste form. In the case of steels there may be a significant effect as a result of iron hydroxide or silicate formation which will increase the rate of leaching and sorption of radionuclides.

2.B.4. Overpack

An overpack is used to help avoid mechanical damage to the canister during its transportation and emplacement, to prevent contamination by transfer of surface materials and to help provide containment for final storage of the waste. Different overpack materials have been considered, but the reference overpack is an iron-alloy which is separated from the container wall by a narrow air space.

2.B.5. Backfill/Buffer

Backfill is used to control access of water to the waste form, to condition the groundwater chemical composition, to retard migration of radionuclides and to help distribute stresses on the waste package caused by geological pressures. Backfill material used will probably contain bentonite clay. A mixture of 1/4 bentonite clay and 3/4 crushed rock is

defined as the reference backfill material. These clays are used as ion-exchangers for radionuclides, and to reduce access of water to the waste form because they swell when wetted.

2.B.6. Repository

The repository is the underground facility in which waste can be placed for long-term storage. This category also includes any engineered barriers which separate the host rock and waste package, as well as structural supports, materials used to seal shafts or boreholes and tunnel backfill material. The minimum waste package design should be able to isolate the waste form from water without the use of further constructed barriers. Materials which are under consideration for repository backfills are clay, sand, vermiculite, magnesia and crushed host rock.

2.B.7. Geologic Environment

The geologic environment consists of the host rock and surrounding geologic media. This medium helps to control movements of groundwaters which could potentially corrode the waste canister and leach the waste form. The most desirable properties of host rock are high strength, thermal conductivity and sorptive capacity, low thermal expansion and a minimum amount of flowing water or brine. The five main rock types under consideration are salt (dome or bedded), granite, argillaceous, tuff and basalt. A comparison of repository conditions for three of the candidate formations is given in Table 2.1 (83MEND1).

Table 2.1. Comparison of repository conditions for three host rock formations (83MEND1)

ROCK	BASALT	TUFF	SALT
THERMAL CONDUCTIVITY (W/m^{o}C)	2.2	1.8	3.6
THERMAL EXP. COEFFICIENT ($^{o}C^{-1}$)	$7x10^{-6}$	$4x10^{-6}$	$45x10^{-6}$
APPARENT POROSITY (%)	1	18	2
MAX. ALLOWABLE TEMP.(^{o}C)	300	300	250
FLOW (m/yr PORE VELOCITY)	<1	<3000	<0.01
FLUID			
pH	9.5	7.3	6.3
Eh (V)	-0.5	0.0	-0.1
DISSOLVED SILICA (ppm)	40	60	<0.01
MAJOR ANIONS (ppm)			
HCO_3^-/CO_3^{2-}	80	120	900
Cl^-	200	7	250000
SO_4^{2-}	100	20	50
F^-	30	2	<0.01
MAJOR CATIONS (ppm)			
Na^+	300	50	60000
K^+	10	5	5000
Ca^{2+}	2	15	80000
Mg^{2+}	0.05	2	1000

2.B.7.A. Rock Salt

The main advantage of using rock salt is the absence of flowing water or brine. It also has a high thermal conductivity, is easily mined underground and is capable of healing openings due to plastic flow. On the other hand, if water comes in contact with rock salt, its high solubility and the presence of variable amounts of other minerals which constitute corrosive brines, act as distinct disadvantages. In addition there is the occasional presence of gas and brine pockets which have a low sorptive capacity for radionuclides. The plasticity of salt leads to the waste canister being subjected to full stresses.

2.B.7.B. Granite

Crystalline rock such as granite is quite massive and rigid and is not expected to alter significantly within the time frame considered in assessment of a waste repository. This type of rock is slightly porous, has a low hydraulic conductivity, and when fractured it is very permeable and undesirable for waste disposal. Properties which do help to favour crystalline rocks as potential repositories are high thermal conductivity, low thermal expansion and the presence of ferrous iron minerals which help influence groundwater redox potentials. Plutons in the Canadian Shield are being examined as part of the research in the Canadian Nuclear Fuel Waste Management Program. This has prompted the use of granitic groundwater in this work.

2.B.7.C. Argillaceous Rock

This rock type refers to sedimentary materials and applies to a wide range of formations including clays, marls, shales and slates. They have a low thermal conductivity, low permeability and a high retention capacity. Their compressive strength is quite low and mining operations can be expected to be more difficult than in hard rock.

2.B.7.D. Tuff

Tuff is a rock formed by accumulation of glassy fragments erupted from volcanoes. Its interaction with water may result in formation of quartz and feldspar or even zeolites. Devitrified welded tuffs have a high density, compressive strength, thermal conductivity, low-to-moderate porosity and are to a certain degree fractured.

2.B.7.E. Basalt

Basalt is formed by cooling molten volcanic material which contracts upon cooling. It is relatively hard and has a high compressive strength. Columbia River basalts are being considered as the host repository rock at the Hanford disposal site in Richland, Washington U.S.A., and thus basaltic groundwaters have been investigated in this work.

2.C. WASTE FORMS

Materials which have been used for the immobilization of low- and medium-level wastes are unsuitable for HLW because of their low resistance to radiation and poor thermal stability. Many different waste forms for HLW have been suggested and tested. Alkali borosilicate glas-

ses are considered to be the most likely candidates. The following section presents a brief description of a few of the waste forms under consideration for HLW immobilization.

2.C.1. Glasses

2.C.1.A. Inorganic Glasses

Many inorganic elements and compounds melt to form liquids with viscosities similar to that of water. A rapid crystallization of the liquid will take place upon cooling at its freezing point. Small droplets of the liquid can be supercooled below the freezing point, but this cooling will eventually lead to crystallization. Several materials exist which melt to form very viscous liquids. If one of these liquids is kept for some time at a temperature only a little below its freezing point, it will slowly crystallize due to the fact that its crystalline phase is more thermodynamically stable than its liquid phase. If instead of maintaining a constant temperature, the liquid is cooled from a point only slightly above the freezing point, then depending upon the rate of cooling, crystallization may or may not occur. At high rates of cooling it is possible to reduce the temperature to a desired extent without crystallization taking place. The liquid's viscosity will increase as the temperature is decreased until it becomes so high that the material appears to be a solid. This solid is referred to as glass. The American Society for Testing Materials (ASTM) defines glass as " an inorganic product of fusion which has been cooled to a rigid condition without crystallizing" (67RAWS1).

It is possible to explain the relationship between liquid, crystal-

line and glassy phases of a material by means of a volume-temperature diagram. Liquid is cooled from an initial state 'a' with the volume of a given mass decreasing steadily along the line 'ab'. Assuming the rate of cooling is sufficiently slow and that nuclei are present, crystallization will occur at temperature T_f (Fig. 2.2). This is accompanied by a decrease in volume 'bc'. If the solid is cooled further the volume decreases along the line 'cd'. However, if the rate of cooling is rapid then crystallization will not take place at T_f, and instead the volume of this supersaturated liquid will decrease along the line 'be' which is a smooth continuation of 'ab'. At a temperature designated as T_g, the glass-transition temperature, the curve of the liquid undergoes a change in direction and continues almost parallel to the contraction curve (cd) of the crystalline phase. The material is a glass below T_g, while it is a supercooled liquid between T_g and T_f. If the temperature of the glass is held constant at a point T, only a little below T_g, the volume decreases slowly until it reaches a point on the dotted line, which happens to be a continuation of the contraction curve. The properties of a glass depend on the rate at which it has been cooled. The exact value of T_g will also depend on the rate of cooling; with T_g being lower the smaller the rate.

The discontinuity at T_g is due to failure of the material to adjust itself at finite rates of cooling to changing temperature conditions. It is expected that a similarity would exist in structures of the liquid and glassy forms of a material. This has been confirmed by X-ray diffraction patterns. Structures of the two forms are characterized by a lack of long-range order; i.e., a lack of a systematic repetition over

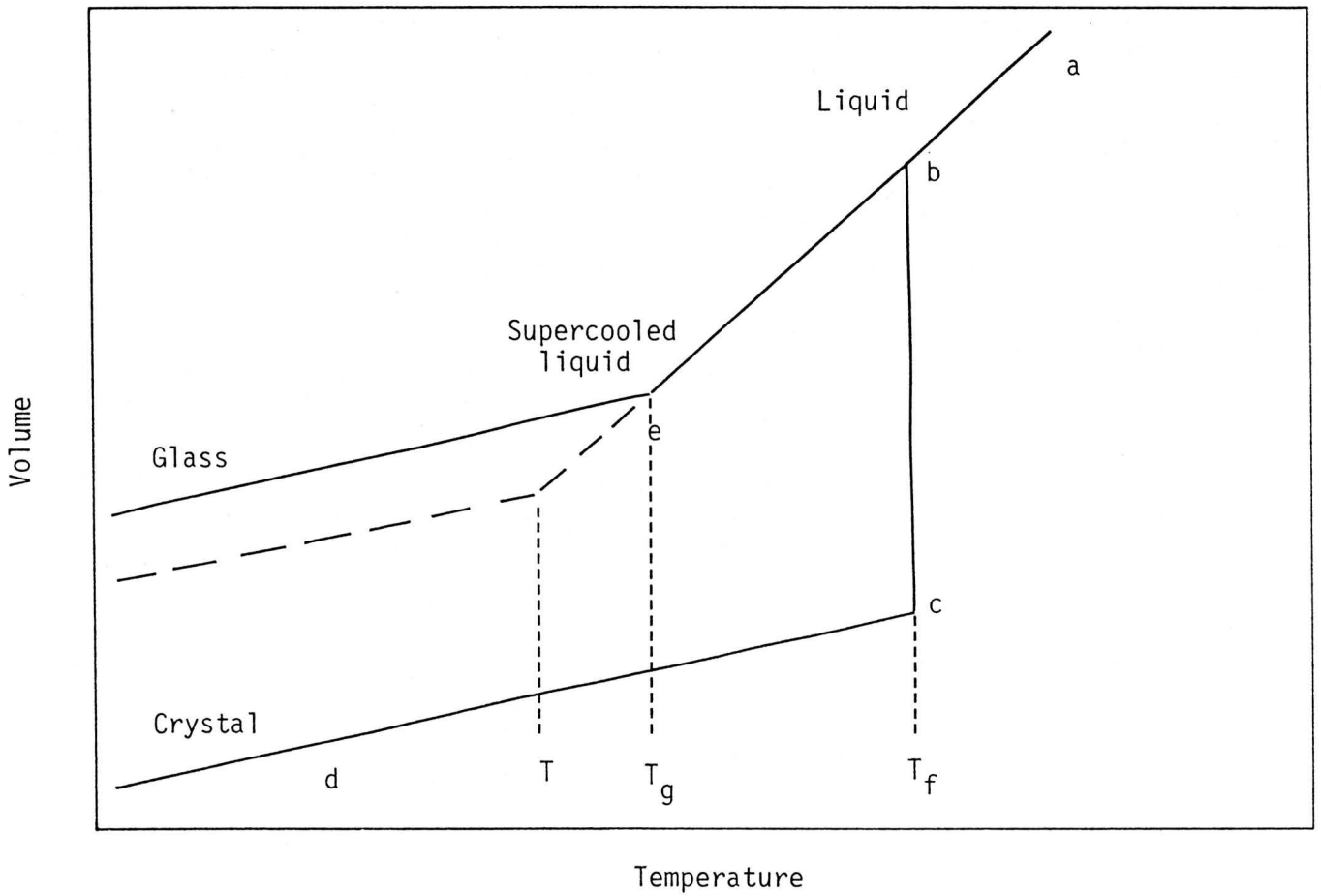

Figure 2.2. The relationship between volume and temperature for glassy, liquid and solid states (83GRAU1). T_f: melting temperature, T_g: glass transformation temperature.

long distances of atoms in unit cells as seen for crystalline compounds. The only elements which form glasses by themselves are those found in Groups V and VI. Both sulfur and selenium will form glasses readily. The following oxides will also form glasses: SiO_2, GeO_2, B_2O_3, P_2O_5, As_2O_3, and Sb_2O_3 if cooled very rapidly. Oxides of SiO_2, GeO_2, B_2O_3, P_2O_5 and As_2O_3 may be melted with a second oxide or mixture and cooled to form a glass. There are limits to the percentages of other oxides which can be added. There is also a second group of oxides, called conditional glass-forming oxides, which will not form glasses by themselves but will do so when melted with a quantity of a second oxide or mixture which includes TeO_2, SeO_2, MoO_3, WO_3, Bi_2O_3, Al_2O_3, Ga_2O_3 and V_2O_5.

2.C.1.A.1. Borosilicate Glass

The most widely applied waste form for HLW immobilization is borosilicate glass. A large variety of chemical compositions have been proposed and are being evaluated. Typical ranges for some of the major oxide components are 20-30 wt% waste oxides, 30-40 wt% SiO_2, 5-10 wt% B_2O_3 and 10-15 wt% alkali oxides and other additives. The compositions and waste loadings of typical borosilicate glasses being considered by several countries are shown in Table 2.2. Processing temperatures for borosilicate glasses are in the range 1100-1200°C in most cases. Borosilicate glasses tend to be far less corrosive than phosphate glasses and can withstand higher temperatures before devitrification. Many countries considering the use of borosilicate glass have proposed lower waste loading although loadings as high as 35 wt% are still being suggested in the United States. Some of the advantages of borosilicate

Table 2.2. Compositions and waste loadings of typical glasses proposed for waste immobilization

COMPONENT (wt%)	76-68[a] U.S.A.	ABS-39[b] Sweden	Glass[c] 209 U.K.	Glass[d] SON 58.30. 20.U2 France	Glass GP98/12[e] Federal Republic of Germany
Al_2O_3	-	3.1	5.11	0.10	2.2
B_2O_3	9.5	19.1	11.12	19.0	10.5
BaO	0.6	-	0.38	-	-
CaO	2.0	-	-	-	3.5
CeO_2	-	-	0.99	-	-
Cr_2O_3	-	-	0.56	0.20	-
Cs_2O	1.1	-	0.77	-	-
Fe_2O_3	9.6	5.7	2.73	0.60	-
La_2O_3	-	-	0.44	-	-
Li_2O	-	-	3.99	-	-
Nd_2O_3	-	-	1.82	-	-
MgO	-	-	6.34	-	1.8
MnO_2	-	-	-	-	-
MoO_3	2.3	-	1.77	-	-
Na_2O	12.5	11.1	8.30	9.40	14.9
NiO	0.2	-	0.36	0.10	-
P_2O_5	-	-	0.24	-	-

* component included with fission products
a, b, d, e 83GRAU1
c 80CHAP1

Table 2.2. Continued

COMPONENT (wt%)	76-68[a] U.S.A.	ABS-39[b] Sweden	Glass[c] 209 U.K.	Glass[d] SON 58.30. 20.U2 France	Glass GP98/12[e] Federal Republic of Germany
PdO	0.5	-	0.44	-	-
Pr_2O_3	-	-	0.43	-	-
Rb_2O	-	-	0.105	-	-
RuO_2	1.1	-	0.68	-	-
SiO_2	39.8	48.5	50.88	43.60	48.2
SrO	-	-	0.32	-	-
TiO_2	3.0	-	-	-	3.9
U_3O_8	1.3	-	0.059	3.60	*
Y_2O_3	-	-	0.17	-	-
ZnO	5.0	-	0.44	-	-
ZrO_2	1.8	-	1.43	-	*
SO_4	-	-	0.095	-	-
Fission Products	-	9.0	-	22.7	15.0
Actinides	4.4	1.66	-	-	-

* component included with fission products
a, b, d, e 83GRAU1
c 80CHAP1

Weight percentages of glasses may not add up to 100%. Values given were the only ones available.

glass are low leachability, excellent radiation stability, low volatility, relative insensitivity to decomposition and good mechanical strength while in canisters. The primary concerns over the use of borosilicate glass as a waste matrix are its tendencies for devitrification, cracking and leaching at high temperature, high pressure water and brine (80CRAN1). Sodium borosilicate glasses have been extensively used in the work reported in this thesis.

2.C.1.A.2. Sodium Calcium Aluminosilicate Glass

Sodium calcium aluminosilicate glasses were first developed for waste immobilization at the Atomic Energy of Canada Limited Chalk River Nuclear Laboratories (CRNL) during 1958-1962. Although these glasses are regarded as the most durable for HLW immobilization purposes, they are not considered as serious matrices because of their high processing temperatures ($\sim$1400°C). Low leach rates as well as leachant pH values which did not exceed 9 were observed when calcium aluminosilicate glasses were leached (82HARV1). A sodium calcium aluminosilicate glass (AECL 981) was used in the preliminary leaching studies in this work.

2.C.1.A.3. High Silica Glass

Natural glasses with high silica contents (obsidians and tektites) are known to have survived for extended periods of time in both lunar and terrestrial environments and to have better leaching characteristics than borosilicate glass. These glasses, however, are formed at very high temperatures ($\sim$1600°C) which will result in Ru and Cs being driven off completely (80CRAN1).

2.C.1.A.4. Phosphate Glass

Phosphate glasses are produced by mixing waste with either phosphorus pentoxide or phosphoric acid and then melting at 1100°C. Phosphate glasses can incorporate about the same waste loading as borosilicate glass, but due to their relatively low formation temperatures (∿900°C) and hence lower volatilization losses for Cs and Ru, phosphate glasses received a lot of early attention as a HLW immobilization matrix. In addition, phosphate glass has a high solubility for waste oxides, especially MoO_3, and sulfates. Development efforts on these glasses have decreased, however, primarily due to two main deficiencies: (1) corrosive nature towards metallic and ceramic containers and (2) tendency to undergo devitrification at relatively low temperatures (∿400-500°C) which results in a significant loss of chemical durability (80CRAN1).

2.C.1.A.5. Lead-iron Phosphate Glass

Lead phosphate glasses have not been considered of much use because of their low durability in solution. However, lead-iron phosphate glasses have been proposed as a new primary disposal matrix for HLW. These glasses are chemically stable due to the effect of iron on the structure. The addition of 9 wt% iron oxide to lead metaphosphate glass ($Pb(PO_3)_2$) has been shown to increase durability by 10000 times. Tendencies for phosphate glass to crystallize is also surpressed by the presence of iron (85SALE1, 85SCHI1). This durability is due to iron's ability to strengthen bonding of the ends of the chains to the glass structure.

2.C.2. Glass Ceramics

Glass ceramics were prepared in an attempt to improve the thermodynamic stability of glass by inducing crystallization of desired phases. These waste forms are produced by sintering or hot-pressing a mixture of waste and glass frit at low temperatures. Ceramic is formed by adding nucleating agents to the glass melt, and then cooling in a controlled manner so that small crystals are produced which are held together by the glass phase (80CRAN1). The glass ceramics have good thermal shock resistance, low leach rates and a high temperature stability, but a very complex processing technology and a relatively small size.

2.C.3. Ceramics

2.C.3.A. Supercalcines

Supercalcine powder is a crystalline assemblage of mutually compatible, refractory and leach resistant solid solution phases which incorporate HLW ions. It is produced by adding constituents to HLW followed by calcination and sintering at temperatures approaching 1100°C. Supercalcine has the advantage over borosilicate glass because it can accept a much higher waste loading (up to 60 wt%), and has good leach resistance and high thermal stability. The question of concern is whether an equilibrium assemblage of species can be assured, as well as whether stability of the various crystals under heat, radiation, transmutation and leaching stress can be maintained (80CRAN1).

2.C.3.B. SYNROC or Synthetic Rock

SYNROC is a three-phase crystalline titanate ceramic. The three

principal phases are barium hollandite ($BaAl_2Ti_6O_{16}$), zirconalite ($CaZrTi_2O_7$) and perovskite ($CaTiO_3$) in the proportions 40, 35 and 25 wt%, respectively. SYNROC also contains a rutile phase (TiO_2) as well as small amounts of metal alloys. Natural mineral radioactivity is contained in the crystal lattices of the three phases, and it is expected that HLW elements may be contained as well. Analogues of these mineral phases occur naturally, and they have survived severe environmental conditions for millions of years. An overall level of 10-20 wt% HLW is the range that this ceramic can be expected to accept.

There are several different types of SYNROC. Their compositions vary slightly depending upon the type of waste they are designed to accept. The basic composition is referred to as SYNROC B (given above). SYNROC C has been developed to immobilize HLW from light-water reactors (82RING1); it has a composition of 35, 30, 20 and 15 wt% of hollandite, zirconalite, perovskite and rutile, respectively. SYNROC D has been developed to immobilize wastes produced by the U.S. defense program which contains large amounts of Na, Al and transition metals (82RING1). A new formulation of SYNROC is SYNROC E which uses the idea of synthetic rutile microencapsulation. A fifth type of SYNROC ceramic is SYNROC F, which represents the conversion of spent nuclear fuel into a leach resistant waste form (83KESS1); it consists of a pyrochlore-type phase, $CaUTi_2O_7$, plus hollandite and rutile.

2.C.4. Clay Ceramics

Clay ceramics have been formed by adding aluminum silicate clays such as kaolin or bentonite to waste which then forms an insoluble

cancrinite-type material. Upon firing a nephaline-type product is formed. This waste form is quite inferior to glass with regards to leach resistance (80CRAN1).

2.C.5. Concretes

Concretes, although successfully used to immobilize low- and medium-level wastes for HLW, provide an inferior product at a higher cost than borosilicate glass (80CRAN1). Concrete has not been seriously considered for HLW because of its high water permeability and resulting high leach rate.

2.C.6. Calcine

Calcine is obtained by dehydration and denitration of waste solutions at temperatures between 400 and 900°C (80LEVI1). The result is an amorphous mixture of oxides of fission products, actinides and corrosion products in the form of a powder. Ordinary calcine is not stable because of its large surface area and the properties of some of its oxides. Calcine is generally an intermediate product used in the formation of other wastes and for interim storage only.

2.C.7. Multibarrier Waste Forms

The multibarrier concept attempts to separate the radionuclide-bearing inner core from the environment by using coatings and metal matrices. These coatings may be carbon, alumina or SiC. This waste form then exhibits an enhanced inertness due to improved leach resistance and mechanical strength. The main question regarding the

feasability of using this waste form concerns the high complexity in terms of cost and production of an acceptable material (79RUSI1).

2.C.7.A. Metal Matrices

Most waste forms can be dispersed in a metal matrix which allows for better heat transfer and an additional leaching barrier. Low-melting alloys such as Pb-Sb/Sn or Al-Si can be cast around the particle of waste. The problems with this matrix exist in securing a void-free matrix, controlling the radionuclide volatility, possibly lower waste loading and higher corrosion (80CRAN1).

2.C.7.B. Supercalcine-coated Matrices

Supercalcine powder is produced by spray-calcining liquid waste to which Al_2O_3, CaO, SiO_2 and SrO have been added. After heat treatment, the amorphous supercalcine crystallizes into solid solution phases. Coatings for supercalcine provide an additional protective barrier. The most widely used coatings are a 40 μm pyrolytic carbon (PyC) layer for decreased leachability and a 60 μm Al_2O_3 layer to increase resistance against oxidation (79RUSI1).

2.D. LEACHING PARAMETERS

Among the most important variables which affect the leaching process are time, glass composition, leachant composition, backfill and canister materials, pH, surface area to volume ratio, temperature, groundwater flow rate, radiation effects, oxic/anoxic atmospheres and the effects of alteration of the leached surface. The following section describes

some of the experiments which have been conducted on the effects of major leaching parameters.

2.D.1. Glass Composition

Nogues reviewed the durability of seven different glasses in distilled water at 90°C for 28 d duration (82NOGU1). Twenty-eight days were sufficient for all seven glasses to show surface deterioration. He found that a critical concentration of $SiO_2 + Al_2O_3 + Fe_2O_3 > 55\%$ or $SiO_2 + Al_3O_3 > 53\%$ had to be present in glass in order for it to be leach resistant. The Al_2O_3 content seemed to be an important parameter in controlling the rate of leaching. Addition of Al_2O_3 between 2 and 5% resulted in a large increase in durability. As the Al_2O_3 content increased, resistance to leaching was decreased in acidic and increased in neutral and basic solutions (82CLAR1). Fe_2O_3 is less effective in this role. With the addition of Al_2O_3 and Fe_2O_3, the SiO_2 content is sufficiently reduced so as to prevent a continuous SiO_2 framework. Al_2O_3 and Fe_2O_3 are both unstable at low pH, and once they are leached, SiO_2 is unable to hold the glass framework together. In basic solution SiO_2 readily dissolves. Species such as Al_2O_3 can stabilize the glass surface up to pH 10.7, at which point its dissolution occurs by AlO_2^- (82CLAR1).

Glass composition is a major factor in influencing alkali leaching through alteration of the diffusion coefficients of alkali elements in glass. McGrail tested the effect of various oxides on this coefficient (84MCGR1). He started with a basic glass composition of $14Na_2O{\cdot}10B_2O_3{\cdot}76SiO_2$ and substituted CaO, ZnO, Fe_2O_3, ZrO_2, TiO_2 or MoO_3 for SiO_2, and leached the glasses in deionized water at 90°C. Substitution

of these oxides for SiO_2 reduced the sodium diffusion coefficient, D_{Na}. The largest overall reduction in the diffusion coefficient occurred when CaO was used as the substitution. The extent of Na leaching did not always correspond to changes in D_{Na}. For instance, substituting oxides lowered D_{Na}, but Na release was often higher (84MCGR1). Wicks observed that waste durability improved up to a waste oxide loading of 35%, beyond which there was very little change (86WICK1).

Instead of basing long-term behavior of waste forms on extrapolation of short-term studies, it has been suggested that a study be carried out on natural glass samples in the geologic record. Allen suggested the use of orange basaltic sideromelane rock which contains considerable amounts of B_2O_3, little or no Al_2O_3 and smaller amounts of CaO, Na_2O and SiO_2 (82ALLE1). Several samples of 10-100 000 years old showed no sign of alteration. A surface rind was observed which was composed of iron-rich clays, and this rind appeared similar to gel layers found on borosilicate glasses. This rind contained about 10-20 wt% water and was almost completely depleted of Na and Ca. Iron, on the other hand, seemed to be concentrated in the rind. Allen had observed that natural glasses produced 13 million years ago by volcanic eruption and isolated from contact with water appeared fresh and transparent (82ALLE1). He estimated that devitrification of this glass at 0°C would require about 10 million years. It was pointed out by Heimann, however, that these ancient glasses were never subjected to the aggressive environments which waste glasses can be expected to face. If natural glasses are leached under the humid conditions expected in a repository, they would rapidly deteriorate (86HEIM1). The compositions and waste loadings of several

typical glasses under consideration have already been shown in Table 2.2.

2.D.2. Leachant Solutions

The leachant solution used in an experiment is extremely important. The leach rates observed and the compositions of corroded glass surfaces depend on the nature of the leachant. Various leachant solutions have been tested, which may be divided into three subgroups: (1) deionized or distilled water, (2) granitic, silicate and basalt groundwaters and (3) brines.

2.D.2.A. Deionized Water

Much of the research conducted so far involved the use of distilled or deionized water as a leachant solution. Realistically this is not a suitable test solution since in an accidental scenario the glass would come in contact with groundwaters or brines. Higher leach rates have been reported for waste forms leached in deionized water. Sale observed that glass leached in distilled or deionized water formed insoluble compounds such as $Fe(OH)_3$, $Mn(OH)_2$, $MnCO_3$, $SrCO_3$, $CaCO_3$, $Ti(OH)_4$, UO_3 or $UO_2(OH)_2$. The leach rates decreased with time, usually due to the approach of solubility limits for elements released (84SALE1). Distilled deionized water (DDW) has been used in the work reported in this thesis for comparison purposes.

2.D.2.B. Brines

It has been reported that brine solutions decrease the rate of

leaching. Based on release of Cs which had the highest leach rate, Cs release decreased with increasing salinity (80BRAI1). While Na and K slowed the rate, Mg caused it to increase (84GRAM1). Saturation was achieved faster in brines because an increase in the solution salinity results in less ion exhange between alkali species in the glass and hydrogen ions in solution. Magnesium chloride on the other hand increased releases through the formation of magnesium silicates, thereby decreasing the silicon saturation of the leachate solution. A second study showed that the release of elements was slower in brine at the early stages of leaching, while in later stages the decrease in high salinity solutions was not as great as for other solutions (83STRA1). In contrast, release of Cs did not decrease in brine. This was attributed to the formation of a glass precipitation layer made up of magnesium silicate which did not have an affinity for Cs. Brine solutions were not used in the present work.

2.D.2.C. Groundwaters

The compositions of several synthetic groundwaters which have been used in leaching experiments are shown in Table 2.3. Basalt and granite groundwaters have been used in this study.

Silicate water was reported to be less aggressive than deionized water (84BIBL1). Release of elements in silicate were about one half that observed in deionized water (84STRA1). Strachan (83STRA1) found the leachability trends for the sodium borosilicate SRL-131 glass in various leachants at two different temperatures as follows: (1) at 40°C: deionized water > silicate water > brine = synthetic groundwater; and

Table 2.3. Composition of synthetic groundwater leachant solutions

COMPONENT	SCSSS[a]	GRANITIC[b] ROCK	SYNTHETIC[c] AQ 293	WNRE[d] SYNTH.
Al	< 0.5	-	-	-
B	< 0.3	-	-	-
Ca	14600 ± 300	10-40	37.5	15000
Ce	< 0.5	-	-	-
Cl	34300 ± 1700	4-15	93	34260
Cs	0.2 ± 0.1	-	-	-
F	-	0.5-5	0.7	-
Fe	0.74 ± 0.09	0.02-5	-	-
HCO_3^-	-	90-275	100	10
HS^-	-	0-0.5	-	-
K^+	72 ± 4	1-5	5	50
Li^+	-	-	-	-
Mg^{2+}	187 ± 5	1-10	7.5	200
Mn	-	0.01-0.5	-	-
Mo	< 0.5	-	-	
Na	6200 ± 100	10-100	42	5050
NO_3^-	46 ± 10	-	-	50
Si	14 ± 2	3-14 (SiO_2)	-	15
SO_4^{2-}	727 ± 21	0.5-15	7.5	790
Sr^+	17.3 ± 0.5	-	-	20
Ti	< 0.2	-	-	-
Y	< 0.1	-	-	-
Zn	0.18 ± 0.04	-	-	-

(all concentrations in ppm unless otherwise noted)

Only the main components of the groundwaters are given

SCSSS = Standard Canadian Shield Saline Solution
WNRE = Whiteshell Nuclear Research Establishment

a 84HEIM1
b 84ALLA1
c 79ALLA1
d 82HAYW1

(2) at 90°C: deionized water = synthetic groundwater > silicate water > brine. The low leaching in salt brine points to the effect of ionic strength on leach mechanisms. Rates of silanol condensation increased with increasing ionic strength (83STRA1). Based on the release of boron, leaching of sodium borosilicate SRL-131 glass was highest in deionized water followed by silicate water, brine and synthetic groundwater at 40°C. Only a thin amorphous gel layer was observed on glass at this temperature (85STRA1). At 90°C, glass leached fastest in deionized water followed by silicate, synthetic groundwater and then brine; and a much thicker alteration layer was observed.

Hermansson leached French Cogema type JSS-A glass in doubly distilled water and silicate water at 90°C under Ar atmosphere in the presence of crushed Stripa granite (84HERM1). Most elements, except Al and Fe showed increased rates of release with time in both waters. Molybdenum and boron were leached more extensively in silicate water.

In both deionized and silicate waters a negative rate of release for Cs occurred (83STRA1). This was attributed to Cs being sorbed by a zinc silicate layer which formed on the corroded glass. Dissolved constituents asymptotically reached a steady-state in silicate waters (84STRA2).

Savage leached UK-209 glass in granodiorite and deionized water at 100°C and 50 MPa. Silica solubility was higher than for an amorphous-silica system at 100°C, 101.3 kPa due to partial ionization of solvated silica monomers (H_4SiO_4) producing $H_3SiO_4^-$ at pH < 8. There was no tendency for species leached from glass and granodiorite to be higher than from glass alone (82SAVA1).

Van Iseghem observed that at different temperatures weight losses were highest in clay water (82VANI1). This might have been due to the absence of saturation effects as cations and anions present in the clay water do not influence corrosion stability. Glass matrix cations such as Ca^{2+}, Mg^{2+} or Sr^{2+} might have been adsorbed on clay particles present in solution. Wet clay was found to corrode waste faster than either distilled water or clay-water mixtures which might have been caused by cation exchange reactions between waste and clay.

2.D.3. Effect of pH

The pH of a solution can have an important effect on the leach rate. At low pH, alkali ions in the glass undergo an ion exchange with hydrogen ions in the solution as confirmed by tests conducted on conventional high-silica glass (84RIGB1). As a result, a layer of hydrated silica is formed which serves as a protective surface for glass (84RIGB1). In alkaline solutions the silica network is attacked, and glass leaching is accelerated (78BOUL1). Waste storage glass differs in that the depleted surface layer is not always protective. In this case the rate-limiting step is removal of alkali ions from the glass rather than diffusion of cations through the surface film, and thus the rate of leaching increases in acidic solution. The effect of pH changes on the leach rate of sodium borosilicate glasses has been studied in the present work.

In a static leach test on powdered PNL 76-68 glass, Grambow found Fe was the first element to precipitate at a pH near 6, followed by rare-earth elements (82GRAM1). As the pH increased, Zn precipitated

along with alkaline earth elements. At all values of pH, matrix dissolution was the controlling mechanism, as long as solubility limits were not exceeded. When solution concentrations of various elements were raised to the levels where new solid forms occurred these new forms regulated solution concentration.

In a similar study also by Grambow (82GRAM1), the solubilities of Ca, Fe, Si, Zn and rare earth elements were tested in an MCC-5S Soxhlet test. The Ca concentration was found to be governed by calcite formation ($CaCO_3$). Complexes of chloride, nitrate, molybdate, phosphate, carbonate, sulfate and anionic boron species, as well as hydrolysis species, were considered but found to be of little importance at pH values < 9, while at $pH > 9$, only $CaCO_3$ contributed to soluble Ca. Iron was found to leach at a rate similar to that of Si at $pH < 2$, because the solubility limit of amorphous $Fe(OH)_3$ was not exceeded. Above pH 2 the rate of loss of Fe was less than Si, and $Fe(OH)_3$ precipitated on the glass surface forming an insoluble layer. Zinc was leached less than Si at $pH > 7$, as it was controlled by a phase similar to $Zn(OH)_2$. At $pH < 7$, however, Zn was leached congruently with Si.

Within the neutral pH range Wicks found that the silica solubility did not change for TDS-131 glass leached in deionized water at 90°C, while at higher pH it was significant. Waste corrosion was minimal at pH 6-8.5 (82WICK1).

2.D.4. Effect of Temperature

Temperature studies consistently showed that as temperature increased so did the rate of leaching. Dissolution was observed to

increase by one to two orders of magnitude between 100-350°C (80CHAP1). In addition, it was found that the effects of temperature were less than those expected after extrapolation of data from 100° to 200°C (81ALTE1). Strachan found that release of elements such as Na, Li, Cs, B, Si, Al, Ca and Sr in distilled water at 40°C was lower than at 90°C (84STRA1). Both 40° and 90°C temperatures have been used in our work.

The saturation fraction of silicic acid plays an important role in determining glass reactivity (85STRA1). Solubility of SiO_2 was reduced in solutions of high ionic strength. Temperature was observed to have two effects: (1) kinetic - which slowed the rate of reaction by 1-2 orders of magnitude when the temperature was lowered from 90-40°C; and (2) a complicating effect was produced which made predicting the change in chemistry of the solid/solution system more difficult. Chemistry of the leachate and solubility of the solids change with temperature.

An uptake of large amounts of water by high-silica glass at 220°C had been reported to occur. This uptake was found to depend solely on temperature. A large increase in water occurred at the early stages followed by a linear decrease with time (85YAMA1).

Silica dissolution increased less than a factor of 10 at room temperature compared to 90°C in an experiment conducted by Wicks in which TDS-131 glass was leached in deionized water at neutral pH (82WICK1). The leach rate was increased at higher pH. As temperature increased, diffusion-controlled dissolution became less important, and above 300°C network dissolution was the dominant mode.

The MCC Static Leach Test, the most commonly used leaching procedure, calls for samples to be cooled to room temperature before

aliquots are extracted for analysis. A species which has a temperature dependent solubility may precipitate onto the glass surface during cooling thus changing the solution composition (86MEAN1).

Means (86MEAN1) investigated this problem by leaching powdered MCC 76-68 glass in synthetic Grande Ronde basaltic groundwater at either 90 or 190°C. In one set of experiments samples and leachant were kept in contact at all times, while in the second set they were separated during heating and cooling. In both cases a skeletal or honeycomb appearance formed on the altered layer which was characteristic of leached glass. This layer was formed by the removal of soluble elements from the glass surface. There did not appear to be any difference in the two cases at 90°C suggesting precipitation was not occurring with cooling. At 190°C glass leached in isolation showed deeper and wider honeycomb structures, and there was evidence of surface precipitation. Glasses in contact with leachant at 190°C were richer in Zn and Fe as well as Ca and P. These elements concentrated in the altered layer, and along with Fe precipitated on the surface during cooling. This can have serious ramifications as calcium phosphates, which are highly insoluble at high pH, may adsorb or co-precipitate U. In the present work both hot and cooled leachates and the precipitates have been analyzed.

2.D.5. Effect of Surface Area to Volume Ratio

SA/V ratio can greatly influence leach rates of waste forms. Silica makes up the skeleton of glass, and its rate of leaching establishes the rate at which glass degrades. Leaching of silica is limited in a closed system by the saturation concentration of dissolved silica. Under static

leaching conditions the concentration of dissolved silica increases with time. As its concentration approaches the saturation value, the leach rate decreases. In the case where the rate of leaching is governed by diffusion-controlled mass transfer, the following equation applies:

$$R_i = \frac{VdC}{dt} = kSA(C_s - C) \qquad (2.1)$$

where V is leachant volume, SA is surface area of the waste form and C_s is saturation concentration. Integration of this equation gives:

$$C = C_s(1 - e^{-(kSAt/V)}) \qquad (2.2)$$

which predicts that SAt/V determines the rate of approach to saturation (82AVAG1).

In an extensive study it was observed that with increasing SA/V ratio the elemental release decreased (83PEDE1). A higher SA/V ratio resulted in a smaller reaction layer thickness and an increased abundance of surface precipitates containing Zn, Si and Fe. Neither congruent dissolution nor thinning of the reaction layer was observed. Reaction layer thickness increased with time for all SA/V ratios. As SA/V increased, dissolution rates for some elements decreased, most notably for Si and Ca. At a SA/V = 1 m^{-1} most glass components leached at comparable rates. An actual repository leaching experiment in which glass was in contact with Stripa groundwater produced lower leach rates than did laboratory situations due to higher SA/V ratios for samples in

the lab (84CLAR1).

SA/V ratio affects the kinetics of glass dissolution in the following ways (82PETI1):

(1) pH increases because of the diffusion of alkali ions in solution, which may alter the corrosion mechanism from diffusion-controlled ($t^{1/2}$) to the one controlled by dissolution of the network (t). If this occurs, the result will be an enhancement of the rate of dissolution. It has been suggested that dissolution would be prevented by release of boron which acts as a buffer.

(2) A saturation effect occurs due to the accumulation of dissolved species, which slows down the rate of dissolution. The release rate is then controlled by the saturation solubility of the waste form.

Petit (82PETI1) conducted experiments in which some samples were given renewed leachant solutions, and others were not. If the solution was not renewed, the mass of the waste form block decreased rapidly at first and built-up a surface layer. This layer disappeared and mass decreased slowly with time. There did not appear to be a saturation effect, and dissolution seemed to be congruent. The first part of the leaching process was dominated by interdiffusion. This layer formed faster than it dissolved, which enriched the leachate solution in dissolved species, and they slowed further interdiffusion. The layer was then attacked and dissolved. Dissolution proceeded congruently at an increased rate along with precipitation of reaction products (82PETI1).

Petit also leached monolithic glass in renewed leachant pre-saturated by powdered glass (82PETI1). The solid samples dissolved very rapidly and only a thin hydrated layer formed on the surface. When

the leachant solution was filtered to remove the glass powder before leaching began, the blocks degraded much slower; illustrating how important undissolved glass powder and colloids are in leaching.

Van Iseghem observed that SA/V ratios influenced all borosilicate glasses he leached at 90°C. High SA/V ratio conditions expected should not be harmful by themselves (85VANI1). Three different SA/V ratios (0.010, 0.10 and 0.85 cm^{-1}) have been investigated in this work.

2.D.6. Backfill Materials

The nature of elements present in canister and backfill materials, bedded salt, clays and sea sediments can have a tremendous effect on the corrosivity of leachants.

Lead in the leaching environment in the form of a canister material has been shown to have a significant effect on corrosion of glass. Barkatt leached powdered TDS-131 glass in deionized water at 70°C in the presence of pure lead spheres. He found that the initial leach rate was depressed but after 15 d the rates, excluding those of Si and Fe, became unaffected (84BARK1). The leach rate for Si decreased considerably in the presence of lead while iron's was enhanced by a factor of five.

Wicks investigated the effects of various potential canister and overpack metals on SRP glass at 90°C in deionized water and simulated basaltic groundwater. No significant effects were observed in the presence of 304-L stainless steel, Ticode 12, E-Brite, Iconel 600 or 409 and 430 ferric steels. The glass, however, was affected by low carbon steel or lead. The results obtained were the same in both leachants; that is the effects of lead were beneficial while those of the steel were

detrimental (86WICK2).

TDS-131 glass containing 3.7 wt% Al_2O_3 along with MCC glass 76-68 (0.02 wt% Al_2O_3) were leached in both the absence and presence of alumina, aluminum or a combination of both. All three additives caused an initial decrease in the leach rate for Si (by a factor of 80) and for B and the alkali and alkaline earth metals by a factor of 6.

Several studies have been conducted in which glass was leached in the presence of clays (81LANZ1, 82LANZ1, 83LANZ1, 84CLAR1). Clays are capable of retaining cationic species while anions can migrate through. At a temperature of 50°C, the releases found for glass leached in clay pastes were higher than for a dynamic study with slowly renewed water. The results were similar at 80°C suggesting that elements released from glass were being absorbed by the clay, so that the glass continued to leach as if it was in contact with the original fresh solution. In other words, the presence of this absorbing clay medium tended to stop saturation conditions (83LANZ1).

Bentonite, proposed as the reference backfill, has been shown to strongly influence corrosion of glass. Hermansson (85HERM1) found that in the presence of bentonite or bentonite saturated water, B and Mo were present only in small amounts. He found that glasses most severely attacked were those in bentonite saturated water or in the presence of corrosion products (85HERM1).

Wicks leached glass in three phases: (1) in the presence of salt, basalt, shale, granite and tuff, but without host rock, (2) in the presence of five different groundwaters with and without host rock and (3) in the presence of canister, overpack metal and backfill (82WICK2).

Leachability was found to decrease in the presence of rock and salt. Elements such as Fe, Mn and Mg had low leach rates which correspond to retention within leached surface layers. In the presence of groundwater and host rock, leachability decreased further. Rock-equilibrated groundwater was the most aggressive. Backfill material was found to influence release rates the most.

2.D.7. Pressure

Very little work has been conducted on the effects of pressure by itself on the rate of waste form leaching. In addition, whatever has been done is quite contradictory. Scholze (82SCH01) observed an increase in pressure from 16 to 130 bars slightly increased the waste form weight loss (<20%). Between 15 and 300 bars pressure the rate of leaching was found to be unaffected according to Altenheim (81ALTE1). To the contrary, Chapman (80CHAP1) found that the rate of glass dissolution decreased with increasing pressure.

Wicks leached TDS-131 glass in deionized water at 90°C at four different pressures and two SA/V ratios: 14.7 psi, SA/V = 10:1 cm^{-1}; 1000 psi, SA/V = 10:1 cm^{-1}; 14.7 psi, SA/V = 1:10 cm^{-1}; 1500 psi, SA/V = 1:10 cm^{-1}. No significant effects of pressure were observed up to 1500 psi. Glass leached at high pressures did, however, contain a more adherent surface layer (82WICK1).

2.D.8. Effects of Radiation

Solidified waste forms containing HLW are subjected to radiation from the decay of fission products, activation products and actinides

from within the waste itself. The radiation will mainly be due to gamma, beta and alpha particles, while neutrons and fission fragments will contribute to a much lesser extent. The number of displaced atoms per nuclear reaction was found to be approximately 10^{-2} for beta and gamma decay, approximately 10^{3} for alpha decay and approximately 10^{5} for spontaneous fission. It is generally believed that the most significant source of radiation in HLW will be the alpha decays of actinides (79MALO1), however, beta decay from fission products such as ^{90}Sr and ^{137}Cs will predominate for the first one thousand years. Changes in volume, leach rate, stored energy, microstructure and mechanical properties of the waste form may result from this radiation (80ANTO1). Unfortunately, due to the difficulties in working with radioactive samples most leach experiments have been conducted on non-radioactive waste forms.

Most of the data available shows that leach rates are virtually unaffected by radiation damage at or beyond saturation doses for actinide doped glasses (83WEBB1). An experiment by Pederson et al. (83PEDE2) showed that the leach rate increased by less than a factor of 3 at a dose of 10^{25} alpha decays/m^3.

A study was carried out on the effects of radiation damage on Teflon PFA leaching vessels (83STRA2). It was believed that the [F^-] would increase with increasing dose, thus creating a bias in the test in terms of the complexing power of F^- and by generating acid. At dose rates of 1 x 10^5 rad/h it was necessary to exclude air from the leaching vessel in order to stop formation of HNO_3 from the oxidation of N_2 present. In gamma fields ranging from 4.7 x 10^4 to 1.8 x 10^6 rad no detectable bias in the leaching of glass in PFA Teflon in the presence of air or Ar was

observed, provided total exposure didn't exceed 1 x 10^5 rad. As the exposure increased beyond this limit, larger quantities of HF were produced in an Ar atmosphere, and HF/HNO_3 in air. It was suggested that for exposures to exceed 1 x 10^5 rad leaching vessels should be made of Pt, Pd or Au.

Transient species formed by radiolysis can affect glass leaching. The effect depends upon the repository conditions to which the waste form would be exposed. Gamma radiolysis of air-equilibrated water enhanced corrosion of borosilicate glass by a factor of seven (83PEDE2). The leachant solution became acidic due to formation of nitric acid produced by radiolysis of air in the presence of water. Formic acid and oxalic acid were found in solutions with CO_2. Similar tests conducted on deaerated deionized water showed significantly lower leach rates.

2.D.9. Effects of Eh

A small number of researchers investigated the effects of oxidizing and reducing atmospheres on the rate of glass leaching. It is believed that after the repository environment has been initially disturbed initial redox conditions will be slowly re-established. The redox environment can partially dictate the extent of radionuclide migration. Groundwater in tuff and salt (84JANT1) is expected to be slightly anoxic (0.0 to -0.1V), while that of basalt will be strongly anoxic (-0.45 $\pm$ 0.05V).

An interaction between the waste form and package becomes important if one of the components is redox active. Examples are crushed basalt used as a backfill and iron as the canister material. Basalt is believed

to control Eh-pH levels because it contains the redox-active component ferrous silicate (84JANT1). Eh-pH diagrams predicted the formation of ferrous silicate in anoxic conditions, the same as for the oxygenated case, however, instead the solution was depleted in iron, and silica was mobile.

As Eh becomes more reducing cationic species react with solid phases much more easily. Lower leach rates are to be expected for certain species in reducing environments where less soluble reduced forms are produced. Bidoglio observed lower leach rates for ^{99}Tc, ^{237}Np and ^{239}Pu under reducing conditions (86BIDO1).

2.D.10. Glass Corrosion

Glass corrosion may occur in either one or a combination of three ways: (1) reaction with corrosive materials to form new compounds on the surface, (2) preferential dissolution leaving a leached surface or (3) continuous dissolution exposing fresh glass.

Water attack on glass occurs due to the presence of reasonably soluble components in glass such as alkali elements. However, the presence of lime and certain oxides increases water resistance. Dissolution of glass and release of alkali ions into solution results in an increased pH which helps in the attack of other components.

The first stage in the chemical attack of glass and water involves an exchange between H^+ and Na^+ ions (80KENN1). As a result the attack is influenced by the alkali content of glass. Corrosion of glass is governed by the unending silica network, and terminal structure which associates alkali ions with the network. This terminal end which

associates Na^+ is the point of consideration in the dissolution process:

$$\text{-Si-O-(Na)} + H_2O \longrightarrow \text{-Si-OH} + Na^+ + OH^- \qquad (2.3)$$

An oxygen-sodium bond near the glass/water interface is broken by migration of a Na^+ ion and then an oxygen atom dissociates a water molecule to satisfy its force field through the use of an H^+ ion. In the process a free hydroxyl ion forms which plays a role in the second step.

$$[\text{-Si-O-Si-}] + OH^- \longrightarrow \text{-SiOH} + \text{-SiO}^- \qquad (2.4)$$

In this step the Si-O-Si bond is broken. One end then becomes a silanol by transfer of a proton (or hydroxyl ion attachment); the other end forms a structure which can dissociate another water molecule:

$$[\text{-Si-O}^-] + H_2O \longrightarrow \text{-SiOH} + OH^- \qquad (2.5)$$

Glass constituents may be classified according to the way they are leached (82HALL1). Major network elements are leached at a constant rate from the surface of waste forms. Some elements are removed by ion-exchange with protons in the leachant solution according to a $t^{1/2}$ time dependence which suggests removal by diffusion mechanisms from beneath the surface. The result is a hydrated surface layer depleted in these elements (84MCGR1, 82HALL1, 85HAAK1). An electrical charge develops on the glass surface due to adsorption and desorption of ions.

This surface charge attracts counter-ions and repels co-ions. Along with a mixing tendency due to thermal motion, this surface charge results in the formation of a double layer consisting of a charged glass surface with counter-ions over co-ions in a diffused manner. Electrokinetics depends on the potential at the plane of shear between the surface and solution. This potential is called the zeta potential (85LEE1). Leaching of glass results in a higher concentration of ions in solution, so that a lower zeta potential is expected due to compression of the diffuse part of the double layer. Adsorption of multivalent ions can also affect the zeta potential.

Colloids may exist naturally as clay, quartz, feldspar, micas and oxyhydroxides of Al, Si and Fe, humic acid or bacteria. Mobility of a radionuclide in contact with minerals depends upon the chemical state of the element. Formation of colloids is possible for actinides in their lower oxidation states. These may be true radiocolloids (aggregates of the radionuclide) or psuedocolloids (material in the groundwater onto which the radionuclide has sorbed) (82OLOF1). Stability of colloids is related to the zeta potential. Surface charges on colloids can prevent their coagulation and precipitation from solution. Colloids may be attached to a surface by electrostatic attraction, Van der Waals forces or by chemical bonding (86VILK1). If the colloidal particle can get close enough to the surface for Van der Waals forces or chemical bonding to occur, it can stick to another particle or a surface of like charge. In dilute solutions the thickness of the double layer is usually greater than the range of these forces. Colloids may also be repelled by a hydration layer barrier (steric hindrance). Colloids can reduce solution

saturation by removing elements.

In the presence of $AlCl_3$, the zeta potential of SRL-131 glass was observed by Lee (85LEE1) to reverse signs, indicating Al^{3+} had penetrated the double layer and reacted with the surface. When leached in $CaCl_2$, $MgCl_2$ or $ZnCl_2$, the zeta potential became positive and then went to zero.

Colloids were not found by Lee in $CaCl_2$, $MgCl_2$ or $ZnCl_2$ solutions because of their low surface potentials, and because colloids formed would be attracted to the surface by Van der Waals forces. In deionized water or $AlCl_3$ high surface potentials caused colloids to remain in solution.

2.D.11. The Reaction Layer

Surface layer compositions of waste forms depend heavily on the nature of the leaching solution. As the glass dissolves metal cations are released, combine with OH^- or CO_3^{2-} in solution to form insoluble compounds which then re-precipitate on the glass surface. Usually Na, B, Li and Cs are depleted, while elements such as U, Mn, Fe, Sr, Gd, Nd, Ca and Ti are enriched relative to the bulk glass (80KENN1, 82STAP1, 83SALE1, 82SALE1, 84KRIS1, 85APTE1, 85BANB1).

Flintoff (85FLIN1) leached unannealed samples of DWRG glass in deionized water, Grande Ronde simulated groundwater and MCC reference brine at 90°C. He found two basic types of surface layers formed: a porous layer extending uniformly over the surface and an outer layer of crystalline precipitates. The porous layer was greatest in deionized water and smallest in brine (85FLIN1).

Silica was found to be relatively insoluble and usually formed part

of the reaction layer in the form of a gel enriched with other insoluble elements, whose release was controlled by Si (85APTE1). A study by Pickering (82PICK1) involved leaching GP98/12 glass doped with UO_2 and PuO_2 as well as C31-3EC doped with ^{237}Np and ^{241}Am in distilled water and brine at room temperature and elevated pressure. A surface layer was observed which consisted of two distinct layers. For GP98/12 glass the outer layer was enriched in Ca, while for C31-3EC both layers were depleted in this element. Layers for both waste forms were enriched in Ce, Nd, Ti, Zn, Zr, U, Np and Pu while depleted in Na, Cs, Si, Ba and Ca. Because C31-3EC had a higher Al_2O_3 content, it formed an Al-rich layer. Such glasses tended to form Al hydroxides at the glass/water interface which buffers solution pH. GP98/12 did not have a high enough Al content to buffer the pH until it rose to 9-10 and $Ca(OH)_2$ precipitated.

Surface layers formed by leaching SRP waste had excess amounts of non-radioactive elements such as Ni, Fe and Mg present and deficiencies in glass frit components such as Si and Na. The layers found on this glass when leached in basalt, tuff, shale and granite groundwaters were similar to those leached in deionized water. A Mg-oxychloride layer was formed in brine (86WICK1).

Disagreement exists as to whether reaction layers formed are protective and thereby decrease the leach rate. Three models exist:

(1) The reaction layer represents a rate-limiting diffusional barrier to water and H_3O^+ ions moving into the glass and for leached material leaving the glass for solution. Release of material into solution and growth of the reaction layer are proportional to the square

root of time. Leach rate is inversely proportional to reaction layer thickness (84CHIC1).

(2) The reaction layer does not present a barrier to leaching. Any decrease in leaching with time is due to the approach of glass components to saturation limits. Leach rate is independent of reaction layer thickness, and release of Si is controlled by the rate of solution transport away from the glass (84CHIC1).

(3) A passive reaction layer forms on the glass surface which in turn lowers glass reactivity. The rate of leaching is not related to the reaction layer thickness (84CHIC1).

Chick (84CHIC1) leached glass in deionized water at 90°C using the MCC-1 leach test. Samples were pre-leached, leached in a saturated solution, or leached with the leachant changed regularly. In fresh water the leach rate for samples with reaction layers was almost as high as for samples with no layer. When the leachant solution was replaced, the reaction layer was observed to grow. Layer growth was proportional to elemental release (84CHIC1).

In some cases two or three reaction layers were observed (84STRA2, 83ISHI1). The layer closest to the uncorroded glass was rich in rare earth elements, insoluble oxides, hydroxides and hydrated iron, while the middle layer was concentrated in iron. The outer layer contained Zn and Si, if leached in deionized water, or Mg and Si if leached in brine (84STRA2).

CHAPTER 3

DEVELOPMENT OF ANALYTICAL METHODS

3.A. INTRODUCTION

In recent years different types of waste form have been considered and evaluated for the immobilization of high-level radioactive wastes. Alkali borosilicate glasses, in particular, sodium borosilicates, are considered to be the most likely candidates. Leach tests conducted on these glasses measure the quantity of elements released and they are expressed relative to the amount of the element originally present in the glass. Thus, there is a need for a complete elemental analysis of the simulated waste oxide-loaded glass and its leachates. This analysis should include the major, minor and trace element content.

Experiments can be done using glasses doped with actinides and fission products of concern. However, the lengths of the experiments are not close to the time required for these radionuclides to decay to a sufficiently low level so that they can be considered harmless for handling purposes. On the other hand, chemical analogues of the radionuclides of interest can be incorporated into the glass and used to predict their behaviour. The lanthanides are of particular interest, and they may be used to simulate the behaviour of the actinides. It is then of particular importance that the concentrations of the lanthanides in glasses as well as leachates be accurately determined.

There are several different 'standard leach tests' proposed by various organizations and a number of slightly modified versions are

available. No single test has been universally agreed upon as superior to the others. The lack of a single standardized leach test makes comparisons of results between different laboratories difficult, and this difficulty will only increase as more and more work becomes focused on tests which include components of the waste package beyond the waste form alone.

Early leach studies were usually limited to weight loss measurements or to the chemical analysis of only a few elements. However, lately multi-element analysis is becoming more routine, as is the use of the scanning electron microscope (SEM), electron probe microanalysis (EPMA), secondary ion mass spectroscopy (SIMS) and other surface analysis techniques.

At the present time a final decision concerning the selection of a site for HLW repositories has yet to be made. Therefore, it is impossible to exactly determine the environment that will be encountered by the waste form assembly. This uncertainty has led the scientific community to study a wide range of repository conditions. The experimental parameters investigated in several studies are generally temperature, pressure, pH, effects of radiation, choice of backfill and canister material, surface area to volume ratio, types of glass used, time, groundwater flow rate and composition and the effects of oxidizing or reducing atmospheres. In most studies these parameters are investigated independently of one another although they are interrelated. A more realistic study should attempt to combine several of the variables.

The objectives of the work described in this chapter include the

development of an instrumental neutron activation analysis (INAA) method of high precision and accuracy for the characterization of the major, minor and trace elements in glasses. Epithermal and thermal INAA methods have been developed for the determination of up to 41 elements. Different types of interference have been studied. The precision, accuracy and detection limits of the method have been evaluated. The levels of boron in glass have been measured using an indirect INAA method as well as by spectrophotometry; the two procedures have been compared, and the problems encountered discussed. The principles of NAA, experimental procedures and results are discussed in this chapter.

Additionally, static leaching experiments have been designed in which parameters such as time, temperature, leachant composition and pH, and surface area to volume ratio have been studied simultaneously and comparisons are made. Chemical analyses of the resulting leachate solutions have been carried out using an INAA method developed specifically for this work, as well as by spectrophotometric methods modified for the determination of boron and silicon.

3.B. PRINCIPLES OF NEUTRON ACTIVATION ANALYSIS

3.B.1. Activation Analysis

Activation analysis is an elemental determination technique in which the nuclei of stable isotopes are subjected to bombardment by sufficiently energetic particles to produce nuclides which emit radiation during their decay. Different types of particles can be used in activation analysis including neutrons, photons, protons, deuterons, alpha particles, etc. The types and energies of radiation emitted, and

half-lives are characteristic of each nuclide making the identification of the parent element possible. Although first proposed in 1936 by von Hevesy and Levi (72DES01), it was not until the mid-1940's that activation analysis became recognized as a highly sensitive technique. This interest in activation analysis was further sparked by the development of nuclear reactors with neutron fluxes of the order of 10^{12} to 10^{14} n cm^{-2} s^{-1} and computerized gamma-ray spectrometers. The majority of the elements in the periodic table can now be determined in the parts per million (ppm) or parts per billion (ppb) range.

3.B.2 Neutron Activation Analysis

Of all the activation techniques available, neutron activation analysis (NAA) is most commonly employed. Some of the lighter elements such as B, C, O, N, etc. and a few of the heavier elements such as Pb, Bi, Tl, etc. cannot be analyzed by NAA due to the low natural abundances of their stable isotopes of interest, low probability of reaction (cross section) and/or the production of nuclides with properties which are not convenient for measurement.

Several different forms of NAA exist and are performed depending upon the background matrix and the nuclides of interest. Preconcentration neutron activation analysis (PNAA) is the case in which the element of interest is concentrated from the interfering matrix prior to irradiation. If the irradiation is followed by a chemical separation of the element of interest then the procedure is called radiochemical neutron activation analysis (RNAA). Both PNAA and RNAA usually involve a number of steps such as digestions and wet chemical separations if they are to

be applied to natural samples and thus can be quite time consuming. Furthermore short-lived nuclides cannot be utilized in RNAA. Radiochemical neutron activation analysis requires the addition of carriers to correct for the loss of the elements of interest, while PNAA is unable to make use of the reagent blank-free determinations.

A third type of NAA is the instrumental neutron activation analysis (INAA) - a non-destructive technique in which the sample is used either as is or is simply dried and then packaged for irradiation. The primary advantages of INAA over other analytical techniques are thus its non-destructive nature, freedom from reagent blanks, the capability of carrying out simultaneous multi-element measurements, excellent selectivity, sensitivity, and high precision and accuracy. In the present work, INAA has been extensively used.

3.B.2.A. Thermal Instrumental Neutron Activation Analysis (TINAA)

Neutrons of three broad energy groups are produced in a nuclear reactor. These are classified as follows: (1) thermal neutrons with energies of approximately 0.025 eV at 20°C, (2) fast neutrons which have energies >1 MeV and (3) epithermal neutrons with energies between 0.1 and 1 MeV. Thermal neutrons comprise approximately 50-90% of the flux of a nuclear reactor. These neutrons exhibit an energy distribution which is approximately that of gas molecules in thermal equilibrium at room temperature and is best described by a Boltzmann-type distribution. Thermal neutrons are responsible for the (n,γ) reactions which are most often employed for analytical measurement purposes. Fast neutrons can induce reactions such as (n,p), $(n,2n)$, (n,α), (n,np), (n,n'),

(n,2p), etc. The last class of neutrons, the epithermal neutrons, show a skewed energy distribution which is similar to that of the thermal neutrons. Due to the fact that these neutrons are only partially moderated they are still capable of producing (n,p) and (n,α) reactions. These reactions can cause interferences in TINAA and will have to be studied in the context of the sample matrix used.

3.B.2.B. Epithermal Instrumental Neutron Activation Analysis (EINAA)

There are certain elements which possess a higher epithermal or resonance neutron cross section than thermal cross section. These differences in the cross sections of elements may be advantageously used to enhance the activity of interest while reducing that of the matrix, thus resulting in more accurate quantitative determinations. Some interferences from nuclides produced on activation by thermal neutrons may also be reduced by irradiating with epithermal neutrons. The EINAA technique has been used in this work to analyze samples of glass and leachate.

The total flux in a reactor consists of thermal, fast and epithermal neutrons. When using TINAA it is not necessary to filter the fast and epithermal neutron components as these are quite small compared to the thermal component. To employ EINAA however, the thermal neutron flux must be significantly reduced, if not completely eliminated, without the epithermal neutron flux being affected. The fast neutron flux will remain constant, and although small when compared to the epithermal fraction, it can still cause higher order reactions.

Some materials have a high thermal neutron absorption cross section

and a lower epithermal neutron cross section and can be effectively used to absorb most of the thermal neutrons present in the flux while allowing higher energy neutrons to pass through. Cadmium and boron are two materials which can be used to filter thermal neutrons. The use of cadmium or boron shields in reactors will give a flux of neutrons consisting primarily of epithermal and fast neutrons. The neutron cut-off energy is the lowest energy at which neutrons would be absorbed by a material, and is 0.4 MeV for cadmium compared with 0.6 MeV for boron. A pneumatic site lined with 1 mm-thick Cd has been installed at the Dalhousie University SLOWPOKE-2 Reactor (DUSR), and it has been used in the present work to develop an EINAA method.

The cadmium ratio, CR, is the measured ratio of two activities produced with and without the presence of a cadmium shield for a given position and may be used to determine whether EINAA would be advantageous compared to TINAA. The cadmium ratio is defined as:

$$CR = \frac{\sigma_{th}\ \Phi_{th}}{I_o\ \Phi_{epi}} + 1 \qquad (3.1)$$

where σ_{th} is the thermal neutron cross section, Φ_{th} is the thermal neutron flux, I_o is the resonance integral or epithermal neutron cross section and Φ_{epi} is the epithermal neutron flux. Generally the CR is measured with reference to gold as the $I_o/\ \sigma_{th}$ ratio for gold is known very accurately. The CR of all other nuclides can then be derived from the $I_o/\ \sigma_{th}$ ratios.

The advantage factor, AF, is perhaps a more useful term. This

refers to the ratio of the sum of the cadmium ratios of the background nuclides, $(CR)_b$, to the cadmium ratio of the nuclide of interest, $(CR)_i$:

$$AF = \frac{(CR)_b}{(CR)_i} \qquad (3.2)$$

This term relates to the enhancement of the activity of interest against the sum of the background activities. Studying the advantage factors of elements of interest can help in determining the applicability of EINAA to a sample. Obviously, if the advantage factor is greater than 1 it would not be advantageous to irradiate the sample in an epithermal flux, as this would simply increase the background activity with respect to that of the sample.

3.B.3. Concentration Determination Methods

3.B.3.A. The Absolute Method

The concentration of a nuclide present in a sample and thereby the concentration of parent element from which it was produced, is related to the activity of the nuclide measured as the area under a photopeak. This radioactivity produced can be determined by Equation 3.3:

$$A = \frac{Nw\Phi\sigma\theta\varepsilon\ (1-\exp(-\lambda t_i))\ (\exp(-\lambda t_d))\ (1-\exp(-\lambda t_c))}{M} \qquad (3.3)$$

where:

A = activity (disintegrations s^{-1}) of the nuclide of interest at time

T where $T = t_i + t_c + t_d$

N = Avagadro's number (6.023×10^{23} atoms $mole^{-1}$)

w = weight of the element of interest (g)

Φ = flux of the bombarding particles (n $cm^{-2}s^{-1}$ in the case of neutrons)

σ = activation cross section of the target nuclide (cm^2)

θ = abundance of the isotope of interest

ε = efficiency of the detector

M = atomic weight of the element of interest (g $mole^{-1}$)

λ = decay constant of the nuclide produced and is equal to the natural log of 2 (ln2) divided by the half-life of the product nuclide (inverse time)

t_i = length of irradiation (time)

t_d = decay period which is the length of time between the end of the irradiation and the beginning of the counting time (time)

t_c = length of counting (time)

The ease of accomplishing NAA is controlled by several factors. The cross section, natural abundance of the target isotope, and the half-life of the nuclide produced are all constant. The sample matrix and the activities of interfering nuclides can, however, play a part in the value of detection limit of the element. This value can be improved by the judicious choice of irradiation, decay and counting periods. Thus a reliable determination of the concentration of an element may be determined using Equation 3.3. However, it requires a prior knowledge of accurate values for Φ, σ, ε, θ and λ. Often these parameters are not known with a high degree of certainty and thus errors

can occur. The absolute method for measuring elemental levels has not been used in the present work for this reason.

3.B.3.B. The Elemental Comparator Standard Method

The comparator method is much simpler and more accurate than the absolute method of analysis. In this case the activity of the sample is compared to that of the elemental standard of known concentration. It makes the assumption that all the other parameters in Equation 3.3 are the same. Provided the values of t_i, t_c and t_d are exactly the same for the sample and standards the comparator equation can be used directly, otherwise corrections must be made.

$$W_x = \frac{W_s \, A_x}{A_s} \tag{3.4}$$

where W denotes the weight, A the activity and the subscripts s and x stand for standard and sample respectively. The above equation is of course only applicable if all other parameters are exactly the same. The comparator standard method has been used in the present work for calculating elemental concentrations.

3.B.3.C. The Certified Reference Material Comparison Method

The final method for determining concentrations is through the use of a certified reference material (CRM) with a matrix similar to that of the sample. Many of the concentrations of elements present in CRMs are known with a high degree of accuracy so that Equation 3.4 may be used,

substituting the values of the elemental comparator standards for those of the CRM. The disadvantage in using this method lies in the precision of the certified values of the elements. The precisions for CRMs are generally determined as the average of three different analytical techniques and laboratories, which increases the uncertainty of the reported value to between ±10 and 25% as opposed to less than 10% for single techniques such as NAA. A second disadvantage in using CRMs is that normally not all elemental levels are certified and the element of interest may fall in this group. In addition reference materials are expensive and not that common. Certified reference materials may be put to better use if they are employed to evaluate the accuracy of an analytical method rather than the determination of elemental concentrations. In this work the comparator method has been employed for concentration determinations, and at least one or more CRMs have been analyzed to evaluate the accuracy of measurements.

3.B.4. Systematic Errors

Neutron activation analysis, like other analytical techniques, suffers from systematic errors which may occur if suitable precautions are not taken or appropriate corrections not made. The major errors include sample geometry, dead time and pulse pile-up losses, variations in the reactor flux and competing reactions. In addition, there are a number of errors which could occur during the sample preparation step. Some of the errors relevant to the present work are discussed below.

3.B.4.A. Sample Geometry

One major source of error in NAA is the effect of differences in size, shape, matrix and positioning of the irradiation vial on the detector during counting. Samples and standards should be of similar size, activity, amount and matrix in order to give comparable background and peak counts.

An inhomogeneous distribution of elements in the standards, a difference in the heights of samples and standards or the placement on and distance of the samples and standards from the detector can all contribute to poor results. The identical positioning of samples and standards on the detector, is extremely important due to the size of the detector window. The active detector window is small and the solid angle depends on the semiconductor crystal shape and size. If the positions of the standards vary from that of the samples then the activities being detected are also different; consequently, the results will be in error. The distances of the samples and standards from the detector window is also important as this will reduce the solid angle.

For the experiments conducted in this work precautions were taken to minimize errors due to variation in geometry of samples and standards. This was accomplished through the use of special irradiation vial holders which ensured a reproducible geometry each time.

3.B.4.B Dead Time Losses

When a gamma-ray from a sample impinges on a detector, the signal produced is transformed into an electrical signal, which is amplified and then sent to the analog-to-digital converter (ADC) and stored in the

appropriate channel of a multi-channel analyzer (MCA). At some point in time during these processes, the ADC may be busy processing data so that it is not available to receive more signals from the detector. This period of time during which the ADC is busy is called the dead time, and any data which arrives within that time is lost. The type of ADC used can be extremely important as some are capable of converting data faster than others, and are thus better suited for counting more active samples. There are several ways in which to correct for dead time losses and a thorough study has been previously done in this laboratory (80DESI1). Dead time losses in this work were corrected for by maintaining sample and standard matrices and activities comparable, thus keeping losses approximately the same.

3.B.4.C. Flux Variations

Neutron activation analysis requires a stable, reproducible and homogeneous neutron flux for reliable results. This is particularly important if comparator standards are used in the analysis, as the method assumes that all parameters, other than the weight and activity, in Equation 3.1 are identical for the standards and samples. If this assumption cannot be made then correction factors must be applied.

One method which can be used to correct for fluctuations in the flux is to map variations in each irradiation site with distance and time and then calculate a correction factor. This method is only of use if the flux is stable over time. Such mapping has been carried out at the DUSR Facility, and it has been found to be constant with time and between sites for the inner pneumatic irradiation sites. Vertical and horizontal

flux variations were found to be less than $\pm 1\%$ cm^{-1} for the inner sites (78RYAN1) and $\pm 5\%$ cm^{-1} for the outer sites. The vertical flux variations in the Cd-site were found to be higher in the centre ($\pm 4.3\%$ cm^{-1}) than on the outer edges of the site ($\pm 2.4\%$ cm^{-1}).

A second procedure is to irradiate both the sample and standard at the same time, thus exposing them to the same neutron flux. While this may be suitable for long-lived nuclides, problems may occur in the determination of short-lived nuclides, as the standard and sample would both need to be counted at the same detector within a short time.

A third method is to correct for flux variations by making use of neutron flux monitors. Flux monitors are usually elemental wires of extremely high purity ($\geq$ 99.99%) and which produce nuclides with a half-life similar to the nuclide of interest. They can be used to determine a correction factor which may be applied to the samples and standards. Since the DUSR neutron flux was found to be highly stable, homogeneous and reproducible, there was no need to use the above two methods.

3.B.4.D. Interferences Due to Competing Reactions and Overlapping Gamma-rays

Reactions of the (n,γ) type are most common in INAA. This reaction occurs when a neutron impinges on the target nucleus followed by the emission of gamma-rays. As has already been discussed the reactor flux contains thermal, epithermal and fast neutrons. Although their fraction is small, the presence of the epithermal and fast neutrons cannot be ignored, and the possibility exists for higher order reactions to occur

and cause interference.

A reaction involving epithermal or fast neutrons may be detrimental if the nuclide produced is the same as that produced by the (n, γ) reaction of the isotope of interest. Because there is no way of differentiating between the sources of the nuclides, it is impossible to calculate after irradiations the amount of the isotope of interest which is present in the sample. A correction can be made if the interfering isotope produced other nuclides with different and interference-free photopeaks. The amount of interfering isotope present could then be determined and its contribution to the nuclide of interest calculated and subtracted from the common peak. This approach was applied in this work in the determination of Mg in the presence of Al and Si, since Si contributes to ^{28}Al activity via the $^{28}Si(n,p)^{28}Al$ reaction and Al contributes to ^{27}Mg activity through the reaction $^{27}Al(n,p)^{27}Mg$. If the element of interest is preconcentrated, or if the interfering isotope is removed prior to irradiation, this problem can be eliminated beforehand.

In some cases fast reactions may have beneficial results, especially in the case where a nuclide does not undergo (n,γ) reaction or does not produce a nuclide which is convenient from the measurement point of view. An example of a beneficial higher order reaction which was made use of in this work is the determination of Ni by $^{58}Ni(n,p)^{58}Co$ reaction.

Interferences may also occur due to overlapping of photopeaks. When two different nuclides have closely lying photopeaks and no other peaks are available for measurement then the differences in half-lives becomes important. If the half-lives are sufficiently different, it is

possible to count the activities of the photopeaks when both are present and then again when only the longer-lived one remains. The activity of the longer-lived nuclide can be subtracted from the overall activity to obtain the activity due to the shorter-lived one. An example of an interference due to overlapping photopeaks is that of ^{82}Br, ^{76}As and ^{122}Sb with photopeaks at 554, 559 and 564 keV respectively. Both ^{82}Br and ^{122}Sb have other photopeaks and nuclides (^{80}Br and ^{124}Sb) which may be used for their determinations; however, in the case of ^{76}As this is the only nuclide and energy which may be used. Unfortunately, the half-lives of these three nuclides are also similar (35.3, 26.3 and 64.8 h), so that correction factors for Br and Sb must be applied before the activity due to ^{76}As can be calculated.

3.B.4.E. Detectors

There are a number of gamma-ray detectors available. These include scintillation counters, gas proportional counters, geiger counters, track detectors and semiconductor detectors. Generally light emission and track detectors are not used in INAA. Semiconductor detectors have superior resolution and selectivity compared to the remaining types; however, the efficiency is poor. Scintillation counters have a greater efficiency than the semiconductor detectors, but the resolution and hence selectivity are poorer. Gas proportional counters are of little use in NAA due to their lack of selectivity and resolution.

In this work semiconductor detectors were employed exclusively. There are three types of such detectors available: lithium-drifted

silicon Si(Li), lithium drifted germanium Ge(Li), and hyperpure or intrinsic germanium. The shape and size of the detector crystal determines the energy range of the gamma-rays which can be efficiently detected. Many different crystal shapes are available. These range from the thin planar crystal which is best suited for low energy gamma-rays, a medium-to-large sized coaxial (cylinder) detector which covers a wide energy range, or a bullet-shaped crystal which has the greatest efficiency between 300-800 keV and is used for intermediate energy range. The thallium doped sodium iodide (NaI(Tl)) detector has excellent efficiency but poor resolution, and is commonly used in RNAA and PNAA and in tracer studies.

3.C. EXPERIMENTAL

3.C.1. Solid Glasses

3.C.1.A. Description of Glasses

3.C.1.A.1. Preliminary Experiments

The glasses investigated in the preliminary experiments were of diverse types and oxide loadings and were obtained from several different sources. These included: Corning Glass JL (The Corning Museum of Glass, Corning, N.Y., U.S.A.) - a sodium calcium aluminosilicate glass taken from a 4th century A.D. glass factory in Galilee; Atomic Energy of Canada Limited (AECL, Pinawa, MB) Glass 200 - a sodium borosilicate glass; AECL Glass 981 - a sodium calcium aluminosilicate glass; and the Commission of the European Communities (CEC) Glass - a simulated waste oxide-loaded sodium borosilicate glass. All glass samples were in the form of fine powders (100-400 mesh) except the CEC glass which consisted

of granules of about 1.5 mm diameters.

3.C.1.A.2. Main Experiments

Samples of I-117 glass, provided in cylindrical form by the CEC Joint Research Centre, Ispra Establishment, Italy, were used in the main leaching experiments. It is a simulated waste oxide-loaded sodium borosilicate glass very similar to the CEC glass used in the preliminary leaching studies. The cylinders were cut into wafers using an Isomet 11-1180 low speed saw (Buehler Limited) with a high concentration diamond wafering blade. Since three different surface area to volume ratios (0.010 cm^{-1}, 0.10 cm^{-1} and 0.85 cm^{-1}) were investigated in this work, the dimensions of these wafers varied. All wafers were washed in 2-propanol in an ultrasonic bath and dried in acetone to remove loosely attached particles and cooling solution.

3.C.1.B. Analysis of Glass Samples

Randomly selected specimens of I-117 glass wafers were crushed into a fine powder using a Bel-Art micro-mill grinder with a hard-faced blade. Two separate batches of I-117 glass were received from the CEC for experiments. Batch 1 glass was used in experiments at SA/V = 0.010 cm^{-1} and 0.10 cm^{-1}, while batch 2 glass was employed only at SA/V = 0.85 cm^{-1}. Both batches of glass were analyzed. The methods used for the preparation of the glass samples for analysis were identical for the preliminary as well as the main experiments. Approximately 100 mg of glass were weighed into a 1 mL polyethylene irradiation vial. This weight was found to be optimum, as a smaller value resulted in sample

inhomogeneity, and a larger weight gave too great an activity. The capsules were sealed by heating the lip between the cap and container to melt the plastic.

3.C.1.C. Elemental Comparator Standards

The preparation of elemental comparator standards involved pipetting a known volume of standard solution (Spex Hi-Pure Plasma Emission Spectroscopy Standard, or BDH or Alpha atomic absorption standard solution) of the element of interest into a 1 mL sample vial. The amount of standard solution added to the vials depended upon the cross section of the element of interest and normally the number of μg added was such as to give a comparable number of counts as the samples. The appropriate volume of the stock standard solution was pipetted to give that weight. In many cases a dilution of the stock solution was needed because a volume of at least 50 μL was necessary to ensure the homogeneity of the standard prepared. The comparator standards were prepared on background matrices similar to those of the actual samples; in this case it was silica gel (BDH) due to the high silica content of the glasses.

Often multi-element standards were run, and in these instances the elements were grouped together according to their half-lives and non-interfering gamma-rays. Standards were prepared in sets of 6 for the elements with medium-lived nuclides and a minimum of 3 for those with long-lived nuclides.

The borosilicate glasses required that special sets of standards be prepared with an added quantity of boron (Spex Hi-Pure ICP standard solution or J.T. Baker solid H_3BO_3) equal to that present in the glass.

The reasons for adding the boron to the standards and the methods used to determine the concentration of boron in the glass is explained in a later section.

3.C.1.D. Irradiation and Counting Equipment and Schemes

Each sample vial was placed in the appropriate sized outer irradiation vials as dictated by the site to be used. The DUSR has a total of 8 pneumatic sites available; 5 inner sites and 2 outer sites are used for thermal neutron irradiations and 1 cadmium-site which is used for epithermal neutron irradiations. The inner sites require the use of medium-sized irradiation vials (7 mL), while the outer sites and the cadmium site require large vials (27 mL).

All irradiation vials were made of high-purity polyethylene. The DUSR flux has been found to be very stable. Both vertical and horizontal flux variation of the inner sites is less than $\pm$ 1% cm^{-1}, while for the outer sites the variation is approximately $\pm$ 5% cm^{-1} (78RYAN1). The positioning of sample vials is more important for the cadmium site because of its design and the larger flux variation (85HOLZ1). There is a hole in the bottom centre of the Cd-shield for air, through which a leakage of thermal neutrons occurs; moreover, a substantial vertical flux gradient exists which is higher at the bottom. For irradiations in the cadmium site, first the bottom-half of the large irradiation vial (27mL) was filled by blank small irradiation vials (2/5 dram), and then the sample vials were placed on top of them.

Inner site irradiations involved placing the sample in the bottom of a medium-sized vial (7 mL) and a blank vial on top. The blank served

to stop the sample from moving inside the outer vial during transfer to and from the reactor core, and thus helped to avoid its accidental opening. Fig. 3.1 illustrates the types of vials used depending on the site.

Nuclear data for the nuclides observable by EINAA and INAA are given in Tables 3.1 and 3.2, respectively. Nuclides observed by EINAA were detected using two irradiation-decay-counting schemes of t_i = 2-5 min, t_d = 7-10 min and t_c = 10 min, and t_i = 1 h, t_d = 2 d and t_c = 6 h. The scheme for the longer-lived nuclides was t_i = 7 h, t_d = 5-28 d and t_c = 12h. All samples were counted on a Canberra 60 cm^3 Ge(Li) detector (1.88 keV FWHM at 1 332 keV photopeak of ^{60}Co and peak to Compton ratio of 35:1), an APTEC 25 cm^3 bullet-shaped coaxial hyperpure germanium detector (2.08 keV FWHM at 1 332 keV peak of ^{60}Co and peak to Compton ratio of 17:1), an APTEC planar 500 mm^2 hyperpure germanium low energy photon detector, LEPD (560 eV FWHM at 122 keV photopeak of ^{57}Co), and EG&G Ortec GEM Series hyperpure germanium coaxial detector (1.68 keV FWHM at 1 332 keV peak of ^{60}Co and peak to Compton ratio of 63:1).

The Canberra Ge(Li) detector was coupled to a TN-11 MCA and Digital Electronics Corporation (DEC) PDP 11/05 microprocessor through an Ortec 472 spectroscopy amplifier and a 50 MHz Tracor Northern (TN) 1301 ADC, or to a Canberra Jupiter Series 80 MCA with a DEC PDP 11V03L minicomputer through another Ortec 472 amplifier attached to a 100 MHz Canberra 8621 ADC. The APTEC bullet amplifier was attached to a 4096 channel Nuclear Data (ND) ND66 MCA through a Link 8010 pulse processor and a Link 8020/4 ADC. The LEPD detector was also connected to the Canberra 8621 ADC and the Jupiter Series 80 MCA as in the case of the Ge(Li). The GEM Series

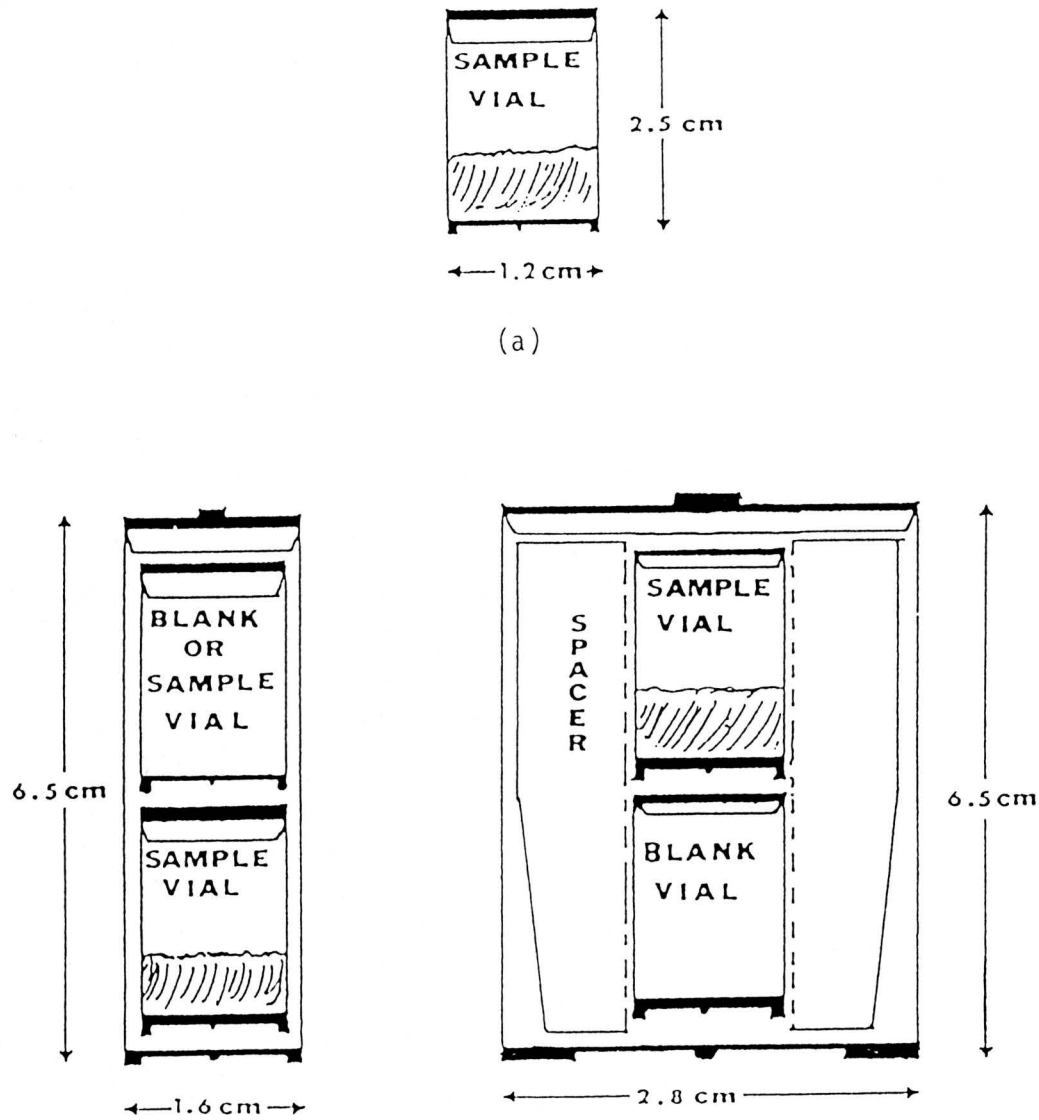

Figure 3.1. The types of irradiation vials used in experiments (88FONG1):

(a) polyethylene sample vial,

(b) inner site irradiation vial containing two sample vials and

(c) outer site irradiation vial containing a sample and a blank vial held in a spacer.

Table 3.1. Nuclear data nuclides observable in glass through a short irradiation using EINAA

ELEMENT	REACTION	NUCLIDE PRODUCED	HALF-LIFE	PHOTOPEAK ENERGY (keV)
$^{27}_{13}Al$	(n,γ)	$^{28}_{13}Al$	2.31 min	1779
$^{138}_{56}Ba$	(n,γ)	$^{139}_{56}Ba$	1.42 h	166
$^{79}_{35}Br$	(n,γ)	$^{80}_{35}Br$	17.5 min	617
$^{48}_{20}Ca$	(n,γ)	$^{49}_{20}Ca$	8.70 min	3083
$^{37}_{17}Cl$	(n,γ)	$^{38}_{17}Cl$	37.3 min	1642
$^{127}_{53}I$	(n,γ)	$^{128}_{53}I$	25.0 min	443
$^{41}_{19}K$	(n,γ)	$^{42}_{19}K$	12.4 h	1525
$^{139}_{57}La$	(n,γ)	$^{140}_{57}La$	40.3 h	1596
$^{26}_{12}Mg$	(n,γ)	$^{27}_{12}Mg$	9.47 min	1014
$^{55}_{25}Mn$	(n,γ)	$^{56}_{25}Mn$	2.58 h	1811
$^{100}_{42}Mo$	(n,γ)	$^{101}_{42}Mo$	14.6 min	191
$^{23}_{11}Na$	(n,γ)	$^{24}_{11}Na$	15.0 h	1369
$^{29}_{14}Si$	(n,p)	$^{29}_{13}Al$	6.56 min	1273
$^{152}_{62}Sm$	(n,γ)	$^{153}_{62}Sm$	46.8 h	69
$^{86}_{38}Sr$	(n,γ)	$^{87m}_{38}Sr$	2.81 d	388
$^{50}_{22}Ti$	(n,γ)	$^{51}_{22}Ti$	5.79 min	320
$^{238}_{92}U$	(n,γ)	$^{239}_{92}U$	23.5 min	74
$^{51}_{23}V$	(n,γ)	$^{52}_{23}V$	3.75 min	1434

Table 3.2. Nuclear data for nuclides observable in glass through a long irradiation using INAA

ELEMENT	REACTION	NUCLIDE PRODUCED	HALF-LIFE	PHOTOPEAK ENERGY (keV)
^{75}As	(n,γ)	^{76}As	26.3 h	559
^{130}Ba	(n,γ)	^{131}Ba	11.8 d	496
^{81}Br	(n,γ)	^{82}Br	1.48 d	777
^{140}Ce	(n,γ)	^{141}Ce	32.4 d	145
^{59}Co	(n,γ)	^{60}Co	5.27 a	1332
^{50}Cr	(n,γ)	^{51}Cr	27.7 d	320
^{133}Cs	(n,γ)	^{134}Cs	2.06 a	795
^{151}Eu	(n,γ)	^{152}Eu	12.7 a	1408
^{58}Fe	(n,γ)	^{59}Fe	45.1 d	1099
^{180}Hf	(n,γ)	^{181}Hf	42.5 d	482
^{41}K	(n,γ)	^{42}K	12.4 h	1525
^{98}Mo	(n,γ)	^{99}Mo	66.2 h	141
^{146}Nd	(n,γ)	^{147}Nd	11.1 d	531
^{58}Ni	(n,p)	^{58}Co	70.8 d	811
^{141}Pr	(n,γ)	^{142}Pr	19.3 h	1574
^{85}Rb	(n,γ)	^{86}Rb	18.6 h	1076
^{45}Sc	(n,γ)	^{46}Sc	83.9 d	889
^{116}Sn	(n,γ)	^{117m}Sn	14.0 d	159
^{159}Tb	(n,γ)	^{160}Tb	72.1 d	298
^{232}Th	(n,γ,β^-)	^{233}Pa	27.4 d	312
^{169}Tm	(n,γ)	^{170}Tm	129 d	84
^{186}W	(n,γ)	^{187}W	23.9 h	686
^{168}Yb	(n,γ)	^{169}Yb	30.7 d	198
^{174}Yb	(n,γ)	^{175}Yb	4.19 d	396
^{64}Zn	(n,γ)	^{65}Zn	244 d	1115
^{94}Zr	(n,γ)	^{95}Zr	64.4 d	757

hyperpure germanium detector was connected to an APTEC PC-MCA through an Ortec 572 spectroscopy amplifier and an APTEC ADC-80.

The energy range of the LEPD was between 50-200 keV, while the bullet system was optimum for a range of 200-900 keV. The Ge(Li) detector was used to study the entire energy spectrum. The detector system used depended upon the samples, and the nuclides to be detected.

3.C.1.E. Boron Determinations

3.C.1.E.1. Indirect Instrumental Neutron Activation Analysis

Boron is a difficult element to determine by INAA because of the very short half-life of ^{12}B (20.4ms). In addition, ^{10}B absorbs thermal neutrons very readily thereby reducing the thermal neutron flux. The magnitude of the reduction of the flux is proportional to the concentration of boron present, and can be determined by the presence of an indicator element. This forms the basis of a method for determining boron in solid glass samples. The indicator element could be an easily activated element such as indium or vanadium. Needless to mention that this element must not be initially present in the sample of interest.

For the application of this technique to the glasses it was initially decided to work with a liquid vanadium sample and a solid boron sample for making standards. This was to keep the conditions similar to those of the glass and to eliminate problems due to inhomogeneity; however, it was later found that a liquid boron standard was more advantageous to use. Boron standards (Spex Hi-Pure Plasma Emission Spectroscopy Standard or Spex Hi-Pure H_3BO_3) containing 1000 μg to 8000 μg of B were added to a 1 mL irradiation vial containing approximately 100mg

silica gel. A 1 mL sample of vanadium solution (10 μg/mL) was added along with 1 μg of Sm and 10000 μg of Na in the case of the CEC glasses. The Na and Sm were added in order to give a high background similar to the glasses. Along with each set of standards 100 mg samples of glass were also spiked with the vanadium solution and analyzed by the same procedure. All samples and standards in a set were irradiated under the same conditions. For AECL Glass 200 a t_i = 10 s, t_d = 1 min and t_c = 5 min were used. Because of the much higher activity of the CEC glass, the conditions were slightly different: t_i = 5 s, t_d = 5min and t_c = 5 min. The 1434 keV photopeak of ^{52}V produced by the $^{51}V(n, \gamma)^{52}V$ reaction was assayed. A minimum of 100 μg of boron per 1 μg of vanadium was necessary to produce a statistically significant number of counts. Other elements besides vanadium were investigated. These included In, Ti and Se; however, none of these produced as satisfactory results as V.

3.C.1.E.2. Spectrophotometric Method

The spectrophotometric method for the determination of boron using methylene blue/1,2-dichloroethane is well known (69SCHL1). This procedure is well suited for glass which has to be dissolved in HF forming BF_4^- and the method relies on the formation of a complex between BF_4^- and methylene blue.

The boron concentration of samples to be analyzed should be between 1 and 4 μg/mL for the method to be applicable. The approximate amount of glass needed to give this concentration was weighed into a 125 mL FEP Teflon bottle. About 30-50 mL of 50% HF were used to dissolve the AECL

Glass 200 and the CEC glasses, while a mixture of 10 mL of concentrated H_2SO_4 and 30 mL of HF were required to completely dissolve NBS 92 glass. The solutions were then transferred quantitatively to a 100 mL or 1 L polyethylene volumetric flask and diluted to the volume.

Glass samples, standards and blanks were prepared in the identical fashion using the following procedure: 2 mL of the sample (either deionized water for the blanks, standard or glass sample) were pipetted into a 125 mL FEP Teflon bottle, followed by 10 mL of 1.25 M H_2SO_4 and 8 mL of 5% HF. This mixture was tightly capped and permitted to stand overnight (16h), whereupon 30 mL of distilled deionized water, 10 mL of 0.001 M methylene blue solution and 25 mL of 1,2-dichloroethane (BDH Omnisolv) were added. The solution was shaken vigorously for 1 min to extract the boron, and then 10 mL of the organic layer was pipetted into a 50 mL polyethylene volumetric flask. The flask was made up to volume with 1,2-dichloroethane, and boron analysis was carried out spectrophotometrically at 660 nm using an LKB Novaspec spectrophotometer. Standards used ranged in value from 0.5 to 10 μg/mL and were prepared from a 1000 ppm stock solution of H_3BO_3 (Spex Hi-Pure).

3.C.1.F. Silicon Determinations

The determination of silicon by spectrophotometry, unlike that of other widely distributed elements, is essentially limited to two methods involving yellow silicomolybdate and the molybdenum blue. These methods are interfered with by the presence of Al, As, Ge, P and Ti, each of which forms a complex with molybdic acid and can be reduced to molybdenum blue. The formation of silicomolybdate and the corresponding molybdenum

blue is significantly affected by acidity and the concentration of molybdenum trioxide. Silicomolybdic acid exists in α - and β - forms of which the β - form is more intensely coloured. The reduction of β -silicomolybdate produces a blue mixture of pentavalent and hexavalent molybdenum referred to as molybdenum blue.

Many variations of the molybdenum blue method exist, and although most are sufficiently sensitive, they often suffer from several shortcomings including a low tolerance for diverse ions, in particular anions. These limitations became apparent in the determination of silicon in the leachates due to the presence of fluoride ions. Fluoride ion was an initial component of the BGW leachant, and a trace of hydrofluoric acid was added to all stored leachate samples before boron and silicon analyses to acidify the solutions and ease the determination of the boron through formation of BF_4^-. Unfortunately fluoride ion causes a severe interference in the formation of silicomolybdate. To circumvent this interference a combination of methods by Graff and Langmyhr (59GRAF1) and Duce and Yamamura (70DUCE1) was used. The procedure is given below.

A volume of less than 5 mL of the sample solution containing 5-100 μg silicon was pipetted into a 100 mL polyethylene beaker. Forty mL of 25% $AlCl_3 \cdot 6H_2O$ solution were added to complex the fluoride ions. The mixture was permitted to stand for 30 min to ensure complete complexation. The solution pH was adjusted to 1.1 using 3M H_2SO_4. In order to stabilize the β -silicomolybdate which initially formed, 10 mL of acetone were added, followed by 5 mL of 10% ammonium molybdate heptahydrate, and the pH adjusted to 1.3 using H_2SO_4. After approximately

10 min, 10 mL of 0.75M-0.75M oxalic acid- tartaric acid mixture were added, and a 2 mL aliquot of a reducing agent (0.2% 1-amino-2-naphthol-4-sulfonic acid, 10.8% sodium bisulfite and 0.8% sodium hydroxide) was added after 45 s. The acetone also served to speed up the rate of formation of molybdenum blue and increased the intensity of the colour. The samples were permitted to stand for 20 min and then diluted to 100 mL before being monitored at 795 nm. Standards and blanks were prepared and analyzed in the same manner.

To check the precision and accuracy of the method a biological material with an Si value in the appropriate range was chosen. The material selected was NBS SRM 1572 Citrus Leaves. It was necessary to digest the samples before the analysis could be carried out. This was accomplished by digesting with concentrated ultrapure HNO_3 (Seastar), followed by concentrated Ultrex HCl to remove any interfering nitrate. The samples were then transferred to 50 mL polyethylene flasks, and 1 mL of concentrated HF (Mallinkrodt Analytical Reagent) was added before the samples were diluted to volume with distilled deionized water. The CRM was then analyzed for Si as described in the previous paragraphs.

3.C.2. Leaching Procedures

3.C.2.A. Preliminary Experiments

Two different sized FEP Teflon bottles (Nalgene) were used, viz. 125 and 500 mL. All bottles were rinsed with 4M ULTREX nitric acid followed by distilled deionized water. Samples of glass were weighed directly into these bottles, and a specified volume of leachant - either distilled deionized water or synthetic groundwater was added. The

composition of the groundwater is shown in Table 3.3 (82VAND1). The bottle size and the volume of leachant added depended upon the SA/V ratio desired. All experiments were done at room temperature and under atmospheric oxic conditions. The parameters investigated for each experiment are shown in Table 3.4. Samples of the leachate solutions were removed at weekly intervals for analysis. The sampling procedure involved pipetting a 1 mL sample into a precleaned 1 mL irradiation vial and evaporating it to dryness under an IR lamp prior to irradiation.

3.C.2.B. Main Experiments

The leachant solutions selected for the main experiments were distilled deionized water (DDW), a synthetic granitic groundwater (GGW) which was based upon actual groundwater compositions (82MATT1, 82VAND1) and synthetic Grande Ronde basaltic groundwater (BGW) (84GRAY1) with initial pH values of 6.10, 7.42 and 9.35, respectively. The BGW composition was chosen to represent a common basaltic groundwater which occurs in North America. Ultrapure salts (BDH Analar Analytical Reagents, and Merck Suprapur) were used to prepare the synthetic groundwaters. The calculated compositions of these groundwaters are given in Table 3.5. All pH measurements were done using an Orion ROSS Ag/AgCl combination pH electrode attached to a Fisher Accumet Model 810 pH meter, and standardized with Fisher reference buffer solutions of pH 4.00, 7.00 and 10.00. The pH of the leachants were constant from day to day, and the pH of the deionized water was slightly acidic (6.10) due to dissolved carbon dioxide. No efforts were made to exclude atmospheric gases such as O_2, CO_2 and N_2, and therefore the solutions were assumed to

Table 3.3. Composition of synthetic granitic groundwater used in preliminary leaching experiments

COMPONENT	CONCENTRATION (mg/L)[a]
Ca^{2+}	17.2
Cl^-	57.4
F^-	0.226
K^+	3.46
Mg^{2+}	8.47
Na^+	8.38
NO_3^-	1.67
pH = 6.30	

a 82VAND1

Table 3.4. Parameters used in preliminary leaching experiments

GLASS TYPE	GLASS WT (g)	LEACHANT	VOLUME (mL)	SA_2 (cm^2)	SA/V (cm^{-1})
AECL 981					
1	1.0455	DW	100	1100	11
2	3.0629	GW	450	3300	7.3
AECL 200					
1	0.9988	DW	100	470	4.7
2	3.1867	GW	450	1500	3.4
CEC					
1	1.5558	DW	225	23	0.10
2	3.5266	GW	450	52	0.12
Corning JL					
1	1.5449	DW	450	2000	4.4

DW = Deionized Water

GW = Groundwater

SA = glass surface area

SA/V = glass surface area to leachant volume

Table 3.5. Compositions of synthetic groundwaters used in main leaching experiments

COMPONENT	SYNTHETIC GRANITIC GROUNDWATER[a] (mg/L)	SYNTHETIC GRANDE RONDE BASALTIC GROUNDWATER[b] (mg/L)
Ca^{2+}	5.04	2.81
Cl^-	18.1	281
F^-	0.249	33.4
HCO^-_3	10.8	102
K^+	3.54	3.41
Mg^{2+}	4.13	-
Na^+	8.51	397
NO^-_3	1.52	-
Si	-	35.5
SO^{2-}_4	8.62	173
pH	7.42	9.35

a 82MATT1, 82VAND1
b 84GRAY1

contain these gases under ambient conditions.

The wafered glass samples were of three different dimensions depending upon the SA/V ratio required ($0.010 cm^{-1}$, $0.10\ cm^{-1}$ or $0.85\ cm^{-1}$). Due to the unavailability of a sufficient amount of glass and the requirement of a large enough volume of leachant for sampling to conduct an experiment at SA/V = $1.0\ cm^{-1}$, it was decided that the third SA/V ratio to be investigated would be $0.85\ cm^{-1}$. In order to obtain this larger surface area, two wafers of glass were used. The exact dimensions of the cut glass specimens were measured using calipers. Various parameters of each experiment are shown in Table 3.6. All glass specimens were washed twice in 2-propanol in an ultrasonic bath for 5 min and dried with acetone at least 12h prior to the start of the actual leaching experiment.

The glass samples were suspended in 30 mL FEP Teflon bottles (Nalgene) using the following procedure. A square of Teflon mesh ($1\ cm^2$) was heat sealed using a soldering iron so that individual threads could not pull loose. A length of monofilament fishing line or Teflon thread was used to hold the glass in place against the mesh and to help keep the mesh/glass assembly at the bottom of the bottle and thus completely submerged in the leachate. The mesh, fishing line and Teflon thread were all analyzed using INAA to check for contaminating elements which might be leached out during the experiments. No elements of concern were detected. The required volume of leachant solution was added to each bottle using a buret. The volume of leachant added was based on the measured surface area of the glass specimen and SA/V ratio desired.

All leaching experiments were run at two temperatures, namely 40° and 90°C in Haake constant temperature baths for up to 84 d. The baths were

Table 3.6. Parameters used in main leaching experiments

EXPT.	GLASS TYPE	DIAMETER (cm)	THICKNESS (cm)	SA (cm^2)	LEACHANT VOLUME (mL)	SA/V (cm^{-1})
1[a]	I-117-B1	0.395	0.065	0.3368	33.68	0.010
2	I-117-B1	0.990	0.070	1.757	17.57	0.10
3[b]	I-117-B2	0.990 0.990	0.410 0.070	2.815 1.757	TOTAL 5.38	0.85

SA = glass surface area

SA/V = glass surface area to leachant volume

a - sliced glass cylinders were cut into quarters - i.e. samples were sector-shaped

b - two disks of glass were used for each sample bottle to increase the total glass surface area

equilibrated for 12 h before use, and the desired temperature did not vary by more than ±2°C at any time. Because of the length of time over which these experiments were conducted and the elevated temperature (90°C), Fisher stabilized bath oil (flash point 180°C) rather than water was used as the heating medium. The bottle assemblies were placed in the baths and allowed to reach their maximum temperatures, at which time they were removed; as much oil as possible wiped off, cooled and then weighed. As the oil could not be completely removed from the bottle exterior, a comparison of the weights of the individual bottles prior to leaching with that after leaching was done. Blanks for each leachant were handled in the exact same manner as the samples.

On a specified sampling day (viz. 3, 7, 14, 21, 28, 35, 56 or 84 d), a bottle was removed from the bath and the glass specimen(s) taken out of leachate solutions. A 4 mL aliquot of hot leachate (40° or 90°C) was pipetted into a pre-weighed 7 mL polyethylene irradiation vial in the case of DDW and GGW or into a 27 mL vial in the case of BGW. Because of the much smaller overall volume of leachate in the experiment conducted at SA/V = 0.85 cm^{-1}, only 1 mL aliquots were pipetted.

The bottle was then resealed and the remaining contents allowed to cool to room temperature, after which an additional 4 mL or 1 mL aliquot was pipetted into a second vial. Both irradiation vials and the remaining leachate in the bottle were weighed. The densities of all three leachants had been determined so that the actual volumes delivered into the vials could be calculated. The leachate remaining in the bottle was filtered through a 0.40 μm Nuclepore membrane before the pH, boron and silicon contents were determined.

To remove any adsorbed species on the Teflon mesh support, fishing line or thread and the inner walls of the bottle, a 1% (by volume) solution of ultrapure Seastar nitric acid was added to the bottles such that its volume was equal to that of the original leachant added. This solution was heated to 90°C for approximately 12 h. After cooling to room temperature, a 4 mL (or 1 mL) aliquot of this acid strip solution was pipetted into a 7 mL irradiation vial regardless of the original leachant used. All pipetted leachates and acid strip solutions were evaporated to dryness under an IR lamp.

The leached glass specimen was washed with distilled deionized water followed by acetone, allowed to dry in air for 48 h; any loose precipitate found was removed and added to that collected on the Nuclepore membrane before weighing, after which the sample was stored in a clean vial. Air drying was found to give the same weight as drying the sample at 110°C for 12h.

The weights of the individual components (hot- and cold-sampled leachates, remaining contents of bottle before filtering and the glass) were added together and the total weight was compared to the original weight. If the difference was excessive the results were to be discarded because of water loss during leaching. This was only found to be a problem in the third experiment ($SA/V = 0.85\ cm^{-1}$) where a very small leachant volume was used. To help reduce this problem the bottles were removed periodically and weighed. If the water loss was higher than 10% by weight a small amount of deionized water was added to bring the leachant volume back to its original value.

3.C.2.C. Comparator Standards

The preparation of elemental comparator standards involved pipetting a known volume of an Alpha or BDH atomic absorption standard solution or a Spex Hi-Pure Plasma Emission Spectroscopy Standard solution of the element of interest into either a 1 mL, 7 mL or 27 mL irradiation vial. Leachate standards were evaporated directly without a background matrix. All leachate standards used in the preliminary experiments were pipetted into 1 mL vials. Three sets of leachate standards were prepared for the main experiments; in 7 mL vials, in 27 mL vials and on Nuclepore membranes placed in 1 mL vials. Filter standards were prepared by pipetting the liquid standard onto a Nuclepore membrane supported between 2 glass rings. A maximum of 1 mL of standard could be pipetted as otherwise the weight of the liquid caused the membrane to collapse inside the rings. The filter was dried before packing in the vial.

3.C.2.D. Irradiation and Counting

Once the leachates were evaporated to dryness they were prepared for irradiation. Leachates used in the preliminary experiments were simply capped and sealed. However, in the case of the main experiments, to avoid the possibility of dried sample on the vial bottom from flaking up and thereby changing the sample geometry, inverted irradiation vial caps were pushed to the bottom of each vial. This prevented dried sample from moving inside the vial. To hold this inverted cap in place in the 27 mL vials it was necessary to cut a 7 mL vial to fit snugly between the inverted cap and the actual vial lid. A similar procedure was employed for the Nuclepore membranes. All membranes were folded into 1 cm

squares and pushed to the bottom of 1 mL irradiation vials followed by an inverted cap. To stop this cap from slipping, the vials were cut 3 mm from the top of the spacer, and the original lid put in place and then heat-sealed.

3.D. RESULTS AND DISCUSSION

3.D.1. Characterization of Glasses

3.D.1.A. TINAA and INAA Methods

The concentrations of minor and trace elements in a glass matrix are difficult to determine by INAA due to the interferences caused by the presence of some of the major elements. Activities due to ^{24}Na, ^{28}Al, and ^{56}Mn interfered in the measurement of short-lived nuclides. Irradiation of samples with epithermal neutrons helps to reduce the interferences caused by these nuclides. The epithermal neutron absorption cross section for ^{23}Na is significantly lower than its thermal neutron cross section (σ_{th} = 530 mb and σ_c = 340 mb), thus the activity due to ^{24}Na nuclide can be minimized.

The EINAA method developed here allows for reliable determinations of 17 elements through short- and medium-lived nuclides. The method involves irradiation of the samples in a permanently installed cadmium-shielded site for 2-5 min, decay for 7-10 min and counting for 10 min. The irradiation and decay times were chosen so that the optimum amount of glass (100 mg) could be irradiated and counted within a reasonable period of time before most of the nuclides of interest had decayed. The optimum decay time was found to be 10 min as it allowed sufficient time for the activity to drop to a level which could easily

be handled, yet the presence of the shorter-lived nuclides such as ^{28}Al ($t_{1/2}$ = 2.31 min) could still be detected without causing spectral interference.

In addition, concentrations of several elements were determined through long-lived nuclides by irradiating the samples in the mixed (mostly thermal neutron) flux of the reactor for 7h, allowing them to decay for 28 d and counting for 12 h. Very intense activities due to ^{140}La, ^{153}Sm and ^{24}Na gave high dead times, and made the determination of K, Pr, and W extremely difficult. These three elements produce nuclides with medium half-lives (^{42}K = 12.4 h, ^{142}Pr = 19.3 h and ^{187}W = 23.9 h) which had completely decayed by 21 d when measurements of other nuclides without interference can be made. Shorter irradiations (1h) in the cadmium-shielded site did not activate the elements sufficiently to allow detection, while an irradiation of this length in a thermal site again resulted in too high an activity to count. To eliminate this problem, the glass was irradiated with thermal neutrons for 10 min, allowed to decay for approximately 2 d and counted for 6 h. It was then possible to determine these remaining elements.

3.D.1.B. Interfering Reactions and Gamma-rays

There were several interfering reactions which required correction factors to be introduced in order to obtain elemental concentrations of good accuracy. Correction for the production of ^{28}Al due to the $^{28}Si(n,p)^{28}Al$ reaction had to be done since all glass samples contained approximately 50% SiO_2. Ultrapure Si comparator standards (SiO_2 Spex Hi-Pure) were irradiated and counted under the identical conditions as the

samples. The number of counts of $^{28}Al/\ \mu g$ Si was calculated from these standards. Once the Si concentration in the samples had been determined via the 1273 keV peak of ^{29}Al produced by the $^{29}Si(n,p)^{29}Al$ reaction, a correction was then applied to the ^{28}Al activity from ^{27}Al and ^{28}Si in order to obtain the ^{28}Al activity due to $^{27}Al(n,\gamma)^{28}Al$ alone. A similar correction was then applied for the secondary reaction $^{27}Al(n,p)^{27}Mg$. The contribution of Al towards ^{24}Na by means of the $^{27}Al(n,\alpha)^{24}Na$ reaction was found to be insignificant.

Interferences caused by overlapping photopeaks are controlled by a combination of factors: the resolution of the detector, the concentrations of the elements of interest and the energy of the photopeaks and their abundances. An example of an interference due to overlapping gamma-rays is that of the 554 keV photopeak of ^{82}Br, 559 keV for ^{76}As and 564 keV for ^{122}Sb. While the concentration of Br can be determined through other interference-free peaks or by its medium-lived nuclide ^{80}Br, and Sb may be assayed by the long-lived nuclide ^{124}Sb, As can only be sensitively determined using the 559 keV peak. This problem can be solved with the use of a high resolution detector provided the relative concentrations of these elements are favourable.

As mentioned, in some cases nuclides and their less abundant photopeaks must be chosen over others to avoid interferences. This was the situation in the determination of Sm. The 69.6 keV, 47.0 keV and 41.5 keV photopeaks of ^{153}Sm were chosen over the 103 keV peak of the same nuclide to avoid contributions from ^{155}Sm (104.2 keV), ^{151}Pm (101 keV and 105 keV) and ^{239}Np (106 keV). In the case of ^{134}Cs, the 796 keV photopeak was selected rather than the 603 keV peak to eliminate the possible

interference by ^{124}Sb at this energy.

Sometimes it is impossible for the detector to resolve overlapping peaks or to assay the concentration through another peak or nuclide. Such a situation exists in the determination of Zn in the presence of Tb and Eu. The photopeaks of ^{65}Zn (1115.5 keV) and ^{160}Tb (1115.3 keV) are too close for most detectors to resolve adequately, and the presence of the photopeak of ^{152}Eu at 1112.2 keV further complicates the matter. In addition ^{65}Zn does not have another suitable photopeak, and, while a second Zn nuclide, ^{69m}Zn ($t_{1/2}$ = 13.9 h), does exist its half-life is too short for it to be used for the determination of Zn in glass because of the high background. The intensity of the 1115.3 keV peak of ^{160}Tb is small, however, the cross section and abundance of this target isotope require a necessary correction to be applied. This correction may be made in two ways. The first method would involve allowing the ^{160}Tb nuclide to decay for at least 10 half-lives before the ^{65}Zn peak could be measured. Since the half-life of ^{160}Tb is 72d, this procedure is undesirable because of time constraints, even though the activity of ^{65}Zn could still be measured ($t_{1/2}$ = 243 d). The second method, and the one employed in this study, is to determine the ^{160}Tb contribution to the 1115.3 keV peak and subtract it from the 1115.5 keV peakof ^{65}Zn. The concentration of Tb in the samples was first calculated by means of interference-free peaks at 298 keV and 879 keV, and the ratio between this and the activity at 1 115.3 keV was calculated and applied to the ^{65}Zn peak. Corrections for the presence of Eu depend upon the relative concentration in the sample and the resolution of the detector used. If the peaks due to ^{152}Eu and ^{65}Zn cannot be resolved, then a similar

correction for the presence of Eu must be applied as for ^{160}Tb using an interference-free photopeak of ^{152}Eu such as 1 408 keV. In this study, the peaks at 1112.2 keV due to ^{152}Eu and 1115.5 keV from ^{65}Zn were suitably resolved by the detectors, and the relative concentration of Eu compared to Zn was small so that correction was not necessary.

A primary interference in the analysis of samples by INAA is that caused by a fissionable element. Even if only a small amount of such an element is present, it can cause significant errors in the determination of some elements. A characteristic feature of nuclear fission is the asymmetric division of the nucleus (72DES01). This division leads to the formation of a number of different fission products. Over 400 fission products have been identified with the normal range being Z = 30 to Z = 68 and A = 75 to A = 160.

The three glasses provided by the CEC and used in this work contained uranium. ^{235}U is a fissionable material and thus it is expected that some contribution to the peaks of other nuclides by fission products might occur. The determinations of Ce, La and Mo could be expected to be severly hampered unless a correction for U was applied. In order to make this correction the concentration of uranium in the sample was first determined by means of the 74 keV photopeak of ^{239}U. Once the concentration of U was known, standards of a similar concentration were irradiated and counted under the same conditions as the samples. The resulting fission products and their activities were then determined. Sensitivities in counts/ μg U were calculated for all the products observed. These sensitivities could then be used to correct all subsequent samples of glass containing uranium for contributions to

relevent peaks from fission products provided the INAA conditions were the same. Table 3.7 lists the fission products and their sensitivities in terms of counts/ μg U which were observed.

Of the three CEC glasses which contained uranium, only I-117 Batch 1 required a fission correction to be made. The other two glasses had uranium concentrations which gave negligible fission product contributions.

The background activity is often larger at the lower energy range of a gamma-ray spectrum due to the Compton effect and characteristics of the sample and detector. Because this is often the region where the majority of photopeaks of interest occur, the background matrix is of extreme importance in preparing standards for short- and medium-lived nuclides. In the case of standards prepared for glasses and MESS-1 sediment, silica gel was used because of the high SiO_2 concentrations found in these samples. The contribution of ^{28}Si to the activity, due to the production of ^{28}Al, results in high background activities. This high background should be duplicated in the standards, otherwise its activity would be lower than for the samples, and the number of counts of activity per μg of standard would be too high leading to lower results. For the preparation of Na, Mg and Al standards, silica gel could not be used as the matrix due to the interferences described previously. Sugar was therefore used as the matrix support. The higher background from SiO_2 was not needed in the case of these elements because their measured photopeaks were of higher energy and occurred in regions of low background activity. The choice of the matrix for the long-lived nuclides was not as crucial, since the long decay times involved usually ensured a low

Table 3.7. Uranium fission products observed after 1 h irradiation-1h decay - 1h counting

FISSION PRODUCT	PHOTOPEAK ENERGY (keV)	SENSITIVITY (counts/ µg U)
^{99}Mo	140	294 ± 18
^{141}Ce	145	14.7 ± 2.0
^{99}Mo	182	53.0 ± 4.3
^{239}Np	210	1840 ± 200
^{239}Np	228	4890 ± 90
^{149}Pm	286	243 ± 19
^{148m}Pm	312	85.1 ± 11.0
^{239}Np	334	656 ± 38
^{131}I	365	13.9 ± 1.0
^{172}Er	383	143 ± 20
^{140}Ba	424	0.176 ± 0.040
^{115m}Cd	482	0.711 ± 0.077
^{140}La	487	74.2 ± 10.9
^{103}Ru	496	2.27 ± 0.17
^{147}Nd	531	2.64 ± 0.23
^{140}Ba	537	3.44 ± 0.28
^{148m}Pm	630	1.02 ± 0.07
^{131}I	637	0.548 ± 0.076
^{127}Sb	685	0.256 ± 0.072
^{99}Mo	739	4.97 ± 0.21
^{95}Zr	757	1.00 ± 0.11
^{95}Nb	766	0.232 ± 0.052
^{140}La	816	24.5 ± 3.6
^{140}La	1596	45.0 ± 4.2

background around the photopeaks of interest. However, SiO_2 was still used as the matrix for the long-lived nuclides.

3.D.1.C. Precision and Accuracy of the Methods

In order to evaluate the precision and accuracy of the methods developed, an appropriate certified reference material (CRM) should be analyzed using the same procedure. In the case of glass it was difficult to obtain a suitable CRM. Most of the glass CRM available were not useful for analysis by INAA because they were monolithic in form rather than powdered. This caused a problem since the CRM sample size was too large to fit in the irradiation vials, and often the intense activities encountered made counting of desired nuclides virtually impossible. Such was the case with NBS Trace Elements in Glass SRM 611, 613, 615 and 617 which contained a variety of trace elements in concentrations of 500, 50, 1 and 0.02 ppm respectively. These glass specimens were all disks of $\sim$1.0 mm thickness and 10.5 mm diameter. The glass disks could not be crushed and a smaller sample size used because of inhomogeneity. Due to the intense activity of some of the nuclides formed, in particular ^{24}Na, ^{28}Al, ^{116m}In, ^{115m}In and ^{114m}In, it was virtually impossible to count the samples even after a short irradiation of 1 min. The presence of In in the samples further complicated the matter as the nuclides of this element have a large number of photopeaks and tended to mask most other photopeaks. Moreover, most of the commercially available CRM lacked the high lanthanide concentrations needed to represent the simulated waste oxide-loaded glasses.

The NBS SRM 92 Glass was finally chosen as it was in powdered form

and contained many of the major elements found in the simulated waste oxide glasses. The NBS glass had a certified value for B_2O_3; however, it was very low (0.700%) and was only suitable for analysis by the spectrophotometric method and not by indirect activation analysis. Since this CRM did not fulfill all the requirements, another type of reference material had to be analyzed. The NRCC Marine Sediment (RM MESS-1) was selected because of its high SiO_2 content (64%) and the number of rare earth elements in it. Both the SRM and RM were analyzed by the INAA methods developed in this study, and the results are presented in Tables 3.8 and 3.9, respectively. The relative standard deviations (R.S.D.) for most of the nuclides are less than $\pm$10% and are considered to be acceptable at the level specified.

The agreement between the values obtained in this work and the certified ones is generally within $\pm$10% where such comparisons can be made. Many of the elements in the CRM and RM used have not been certified and often values have not been previously reported by researchers. The deviations between the values reported here and the certified values for SiO_2 may be attributed to the fact that the 1273 keV photopeak of ^{29}Al produced by the reaction $^{29}Si(n,p)^{29}Al$, is very close to the single escape peak of ^{28}Al at 1268 keV. This interference is resolvable through judicious choice of decay time; however, it does introduce an error in the final Si value. This error may be subsequently reflected in the results obtained for Mg due to the competing reaction $^{27}Al(n,p)^{27}Mg$.

3.D.1.D. Limits of Detection

The detection limit of an element in a sample is expressed as the

Table 3.8. Elemental content of NBS Low Boron Glass (SRM 92)

ELEMENT	CONCENTRATION	LOD	NBS VALUE[a]
Al_2O_3, %	6.74 ± 0.07	0.0200	
As	371 ± 29	0.599	
B_2O_3[b], %	0.73 ± 0.03	0.000161	0.70 ± 0.03
BaO, %	0.157 ± 0.001	0.00162	
CaO, %	8.76 ± 0.33	0.256	(8.3)
Ce	1.57 ± 0.32	0.468	
Co	3.23 ± 0.26	0.178	
Cs	1.21 ± 0.06	0.127	
Fe	414 ± 6	65.7	
Hf	3.16 ± 0.17	0.103	
K_2O, %	0.666 ± 0.030	0.239	(0.6)
La	152 ± 10	15.6	
MgO, %	0.734 ± 0.005	0.650	(0.1)
Na_2O, %	13.9 ± 0.1	0.0373	(13.1)
Rb	31.9 ± 2.2	1.74	
Sc	0.223 ± 0.016	0.0127	
SiO_2, %	72.7 ± 6.3	11.5	(75.0)
Sm	0.426 ± 0.023	0.00975	

(all concentrations in ppm unless otherwise noted)
Numbers in brackets () are information values only.
a 82NBS1
b Determined by spectrophotometry

Table 3.8. Continued

ELEMENT	CONCENTRATION	LOD	NBS VALUE[a]
Th	0.345 ± 0.043	0.0545	
U	0.855 ± 0.026	0.125	
Yb	0.151 ± 0.017	0.0585	
ZnO, %	0.333 ± 0.003	0.000738	(0.2)

(all concentrations in ppm unless otherwise noted)
Numbers in brackets () are information values only.
a 82NBS1
b Determined by spectrophotometry

Table 3.9. Elemental content of NRC Marine Sediment (RM MESS-1).

ELEMENT	THIS WORK	FONG et al.[a]	NRC VALUE[b]	LOD
Al_2O_3, %	11.1 ± 0.4	11.3 ± 0.2	11.03 ± 0.38	0.0294
As	11.5 ± 0.9	11.0 ± 0.3	10.6 ± 1.2	0.11
Ba	266 ± 29	263 ± 3.52		22.2
Br	140 ± 9.6	73.2 ± 5.5		0.371
CaO, %	0.604 ± 0.180	0.60 ± 0.07	0.674 ± 0.064	0.120
Ce	82.2 ± 6.3	80.2 ± 4.8		0.621
Cl, %	0.87 ± 0.05	0.84 ± 0.03	0.82 ± 0.07	0.0256
Co	13.3 ± 1.1	11.6 ± 0.71	10.8 ± 1.9	0.299
Cr	70.4 ± 0.9	70.9 ± 5.32	71 ± 11	0.722
Cs	3.78 ± 0.10	4.35 ± 0.16	(4)	0.298
Eu	1.44 ± 0.027	1.46 ± 0.023		0.0936
Fe, %	3.02 ± 0.08	3.17 ± 0.13	3.05 ± 0.17	0.0184
Hf	19.3 ± 0.5	18.5 ± 1.5		0.154
I	67.1 ± 0.4	41.3 ± 2.4		6.51
K, %	1.86 ± 0.12	2.05 ± 0.59	2.24 ± 0.04	0.0264
La	45.6 ± 1.7	45.9 ± 4.94		0.0680
MgO, %	1.61 ± 0.08	1.38 ± 0.17	1.44 ± 0.09	0.0706
Mn	538 ± 42	514 ± 21	513 ± 25	11.4

(all concentrations in ppm unless otherwise noted)

a 87FONG1
b 80MACD1

Table 3.9. Continued

ELEMENT	THIS WORK	FONG et al.[a]	NRC VALUE[b]	LOD
Na_2O, %	2.50 ± 0.13	2.55 ± 0.08	2.50 ± 0.15	0.0232
Nd	45.2 ± 1.9	45.6 ± 5.7		6.53
Rb	80.9 ± 5.7	93.1 ± 4.2		3.08
Sc	10.1 ± 0.6	11.7 ± 1.1		0.0194
SiO_2, %	64.0 ± 2.0	64.7 ± 1.3	67.5 ± 1.9	9.01
Sm	7.72 ± 0.34	6.42 ± 0.81		0.0174
Ta	1.14 ± 0.13	1.57 ± 0.038		0.111
Tb	2.68 ± 0.34	1.63 ± 0.72		0.0593
Th	14.6 ± 1.0	14.7 ± 1.2		0.0828
TiO_2, %	0.908 ± 0.067	0.900 ± 0.62	0.905 ± 0.028	0.0597
Tm	2.23 ± 0.50	1.40 ± 0.58		0.0735
U	3.64 ± 0.52	3.54 ± 0.54		0.312
V	75.4 ± 4.9	68.9 ± 2.1	74.2 ± 2.7	5.25
Yb	4.07 ± 0.23	3.93 ± 0.31		0.621

(all concentrations in ppm unless otherwise noted)

a 87FONG1
b 80MACD1

level at which an observed signal is considered sufficient to be recognized by a detector. The formula used to calculate a detection limit changes with the definition and assumptions made. This means that a range of values for the detection limits for the same sample can be obtained. The detection limits involving radioactivity measurements are most often described according to the definitions of Currie (68CURR1) as shown below:

$$L_C = 2.33 \sqrt{\mu_B} \tag{3.5}$$

$$L_D = 2.71 + 4.65 \sqrt{\mu_B} \tag{3.6}$$

$$L_Q = 50 \ (1 + (1 + \mu_B / 12.5)^{1/2}) \tag{3.7}$$

where μ_B is the limiting or "true" mean of the blank; L_C is the decision (critical) limit and is the level at which the signal is first detected; L_D is the limit of detection at which an analytical procedure may be relied upon to lead to qualitative detection; and L_Q is the determination limit at which a procedure will be sufficiently precise to give a quantitative estimate.

A new set of definitions has recently been given by IUPAC and which have been modified by Long and Winefordner (83LONG1) and an American Chemical Society (ACS) committee (80MACD1):

$$LOD = S_b + 3\sigma \tag{3.8}$$

$$LOQ = S_b + 10\sigma \tag{3.9}$$

where S_b is the measured average blank; LOD is the limit of detection and LOQ is the limit of quantitation. This last set of equations are still not widely used. For this reason, the detection limits calculated in this study were based on the definitions of Currie. Limits of detection (Equation 3.5) for the elements are presented in the respective tables for each of the glasses and NRC RM MESS-1.

It is apparent that the detection limit calculated depends on the sample weight, the contribution of the Compton continuum (called background) and the irradiation conditions. Precision is higher for signals which are above the limit of detection. It is obvious that the detection limit is dependent on the standard deviation of the background activity, and thus the samples with high backgrounds show poorer detection limits.

3.D.1.E. Indirect INAA and Spectrophotometric Methods for Boron

One of the common methods of separation of boron from borosilicates is the fusion with sodium carbonate and then extraction of the cooled melt with acid. Boron can be distilled as volatile trimethyl borate (b.p. 65°C) in order to isolate it from the remainder of the elements before analysis. This method is quite long and laborious, and the chances of contamination are therefore increased. A simpler, less time-consuming method for the analysis of boron in glass and leachate was needed.

Boron is rather difficult to determine by conventional INAA. The isotope ^{10}B has a low abundance (19.7%) and a high thermal neutron capture cross section (4017 b) but produces a stable isotope ^{7}Li through (n,α) reaction. On the other hand, ^{11}B has a high abundance (80.3%) but low

cross section (0.005 b) and produces a very short-lived nuclide ^{12}B (20.4 ms). With such a short half-life a very fast transfer system is required to ensure that the sample reaches the detector before it has significantly decayed. At the present time the DUSR facility does not have a system capable of such a quick transfer.

As mentioned previously, ^{10}B has a high thermal neutron cross section which considerably reduces the thermal neutron flux available. Since the magnitude of this reduction can be related to the concentration of boron present, its concentration can be determined indirectly by the presence of an indicator element. A simple method of indirect activation analysis for boron in organic compounds and biological materials (69SELE1) and in aqueous solutions (81SALE1) is based upon the use of an easily activated element, such as indium or vanadium. Of course the element chosen must not be present in the material of interest to begin with. The technique involves the irradiation of a solid sample of the indicator element surrounded by the material to be analyzed. A linear/logarithmic function exists between the activity of the indicator element and the amount of boron in the sample:

$$\log A = \log A_o - bm \qquad (3.10)$$

where A is the observed activity, A_o is the activity in the absence of boron, m is the weight of boron in the sample and b is a constant.

The indirect INAA method has been found to be most reliable for samples with high boron concentrations, as at least 100 μg B/ μg V is necessary to observe a statistical difference in the number of counts (Fig. 3.2). A CRM with a suitable high concentration was not available

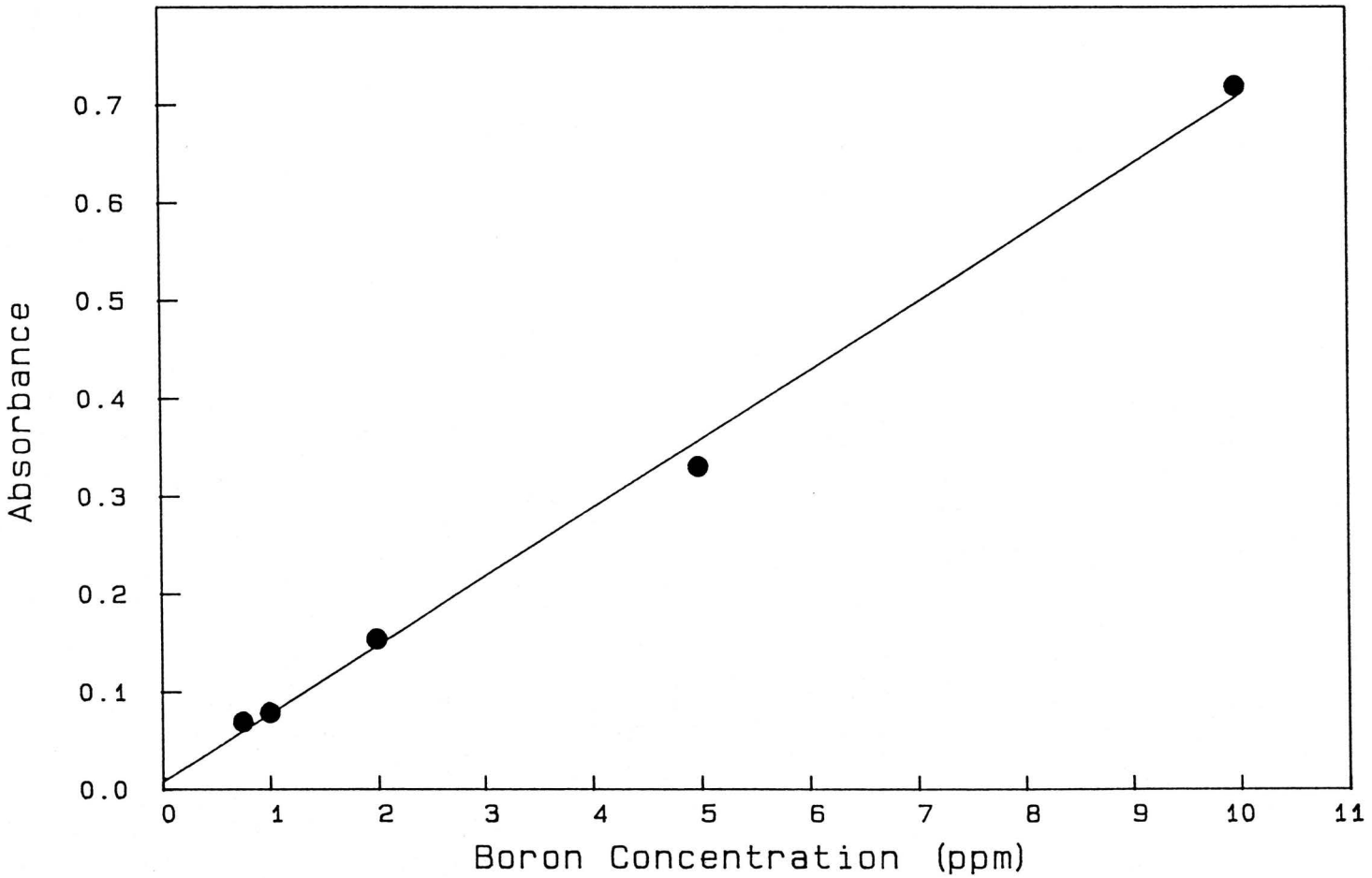

Figure 3.2. Calibration curve used for the determination of boron by a spectrophotometric method using methylene blue and 1,2-dichloroethane.

in powdered form to test this method, but it was applied to AECL 200 glass and the results were compared with another method (Table 3.10) which showed good agreement.

Many photometric methods are used for the determination of boron, and a large number of them are based on a complex formed between boric acid and anthraquinone derivatives in sulfuric acid. One such method involving the use of carminic acid (76MARC1) was investigated here. Carmine is a glycoside derivative of α-hydroxyanthraquinone. It belongs to the group of reagents which are characterized by their ability to form coloured complexes with boron in concentrated H_2SO_4 medium. Boron forms the B^{3+} cation in the concentrated acid and BO^+ in less concentrated H_2SO_4. Carmine is red whereas the boron complex is violet-blue. The reaction is very slow, reaching a maximum absorbance within 45-60 min and remaining stable for a few hours. Oxidizing agents, highly charged cations and nitrate and fluoride anions interfere in the boron determination making this a poor choice of methods for glass dissolved in HF. It is, however, quite sensitive for water samples containing less than 5 ppm of boron (Fig. 3.3). Zirconium nitrate had been suggested as a means of removing the fluoride interference (85TROL1), but it was found that the F^- concentration was so high for our samples dissolved in HF that it was not possible to remove it completely, and the absorbances recorded were all zero.

A similar photometric determination has been described for boron in geological samples after complexation with 2-ethyl-1,3-hexanediol and extraction into chloro-form (85TROL1). This reagent forms a weak chelate with boron which is highly soluble in chloroform; however, boron in the

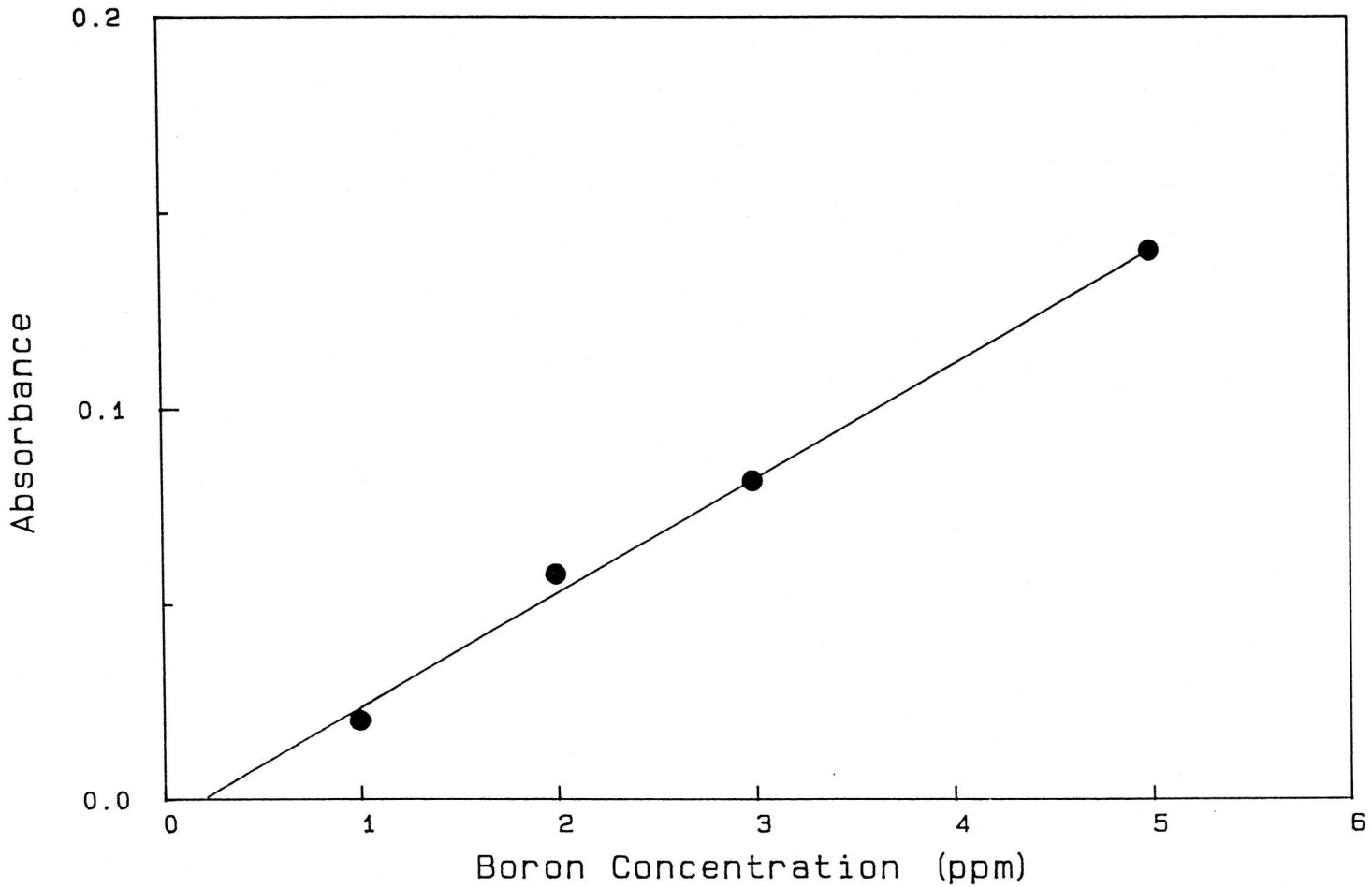

Figure 3.3. Calibration curve used for the determination of boron by a spectrophotometric method using carmine reagent.

form of the BF_4^- anion is not able to form an extractable complex, and therefore it is not applicable to samples of glass dissolved in HF. The photometric procedure may, however, be applied to leachate samples. It became apparent that cooling the samples as suggested impeded the formation of the coloured complex as the absorbances of all standards were zero. In addition, although the procedure clearly states that the cooling should be carried out, the results and discussion show that cooling the samples to 10°C during addition of the carmine reagent and H_2SO_4 causes the complex to form much more slowly.

The spectrophotometric method for the determination of boron using methylene blue/1,2-dichloroethane worked very well for glasses dissolved in HF. Originally 125 mL polyethylene bottles were found to be satisfactory for the reaction. However, after the bottles had been used several times, it was observed that a linear calibration curve was no longer obtained over the previous standard range. The polyethylene bottles were replaced with 125 mL FEP Teflon bottles and this problem eliminated. It appeared that the polyethylene bottles began to be affected by the reagents on prolonged usage, and they adsorbed boron from solution.

It had been reported that boric acid reacts with 2,6-dihydroxybenzoic acid (DHBA) to form an anionic complex which can be associated with cationic dyes and then extracted into chloroform (82OSHI1). Garcia et al. developed a method aimed at avoiding the extraction (85GARC1). They investigated the interaction between the boron complex and dyes and selected crystal violet. The addition of this dye to an aqueous solution of boric acid and DHBA results in a blue ternary complex which is unstable and gradually precipitates upon standing. Polyvinyl alcohol (PVA) was

added to stabilize this complex. The best results were to have been obtained when the PVA was added with an acidified dye as the absorbance due to boron was then constant for about 4h.

The above procedure was applied to leachate samples with boron concentrations in the appropriate range (12-180 ng/mL); unfortunately, it did not appear to work. At no time did a blue complex form regardless of the solution pH, and all absorbances of the standards were zero. In addition, the presence of PVA caused foaming which made the dilution in the volumetric flask very difficult and of questionable accuracy.

The spectrophotometric method based on methylene blue/1,2-dichloroethane was used in the present work for the determination of boron in both solid and liquid samples. This method was found to be most reliable for samples in the range of 1-4 ppm B, and the linearity of the curve could be extended to 10 ppm (Fig. 3.4). The results obtained for AECL Glass 200 (22.3 $\pm$ 1.3 wt% B_2O_3) were very close to those obtained for this glass by the indirect INAA method (22.3 $\pm$ 1.6 wt% B_2O_3) as shown in Table 3.10. The result for SRM NBS 92 glass (0.735 $\pm$ 0.032 wt% B_2O_3) was similarly close to the certified value (0.700 $\pm$ 0.030 wt% B_2O_3 (Table 3.8)).

Specific activities of the elemental comparator standards used for AECL Glass 200 and the glasses provided by the CEC were corrected for reduction in thermal neutron flux due to boron from the addition of H_3BO_3 or a liquid boron standard (Spex Hi-Pure). A comparison between the values obtained in this study and those reported by AECL for four elements in the two glasses (200 and 981) shown in Table 3.11 indicates the reliability of the methods developed.

The calculation of correction factors for the CEC Glass and the two

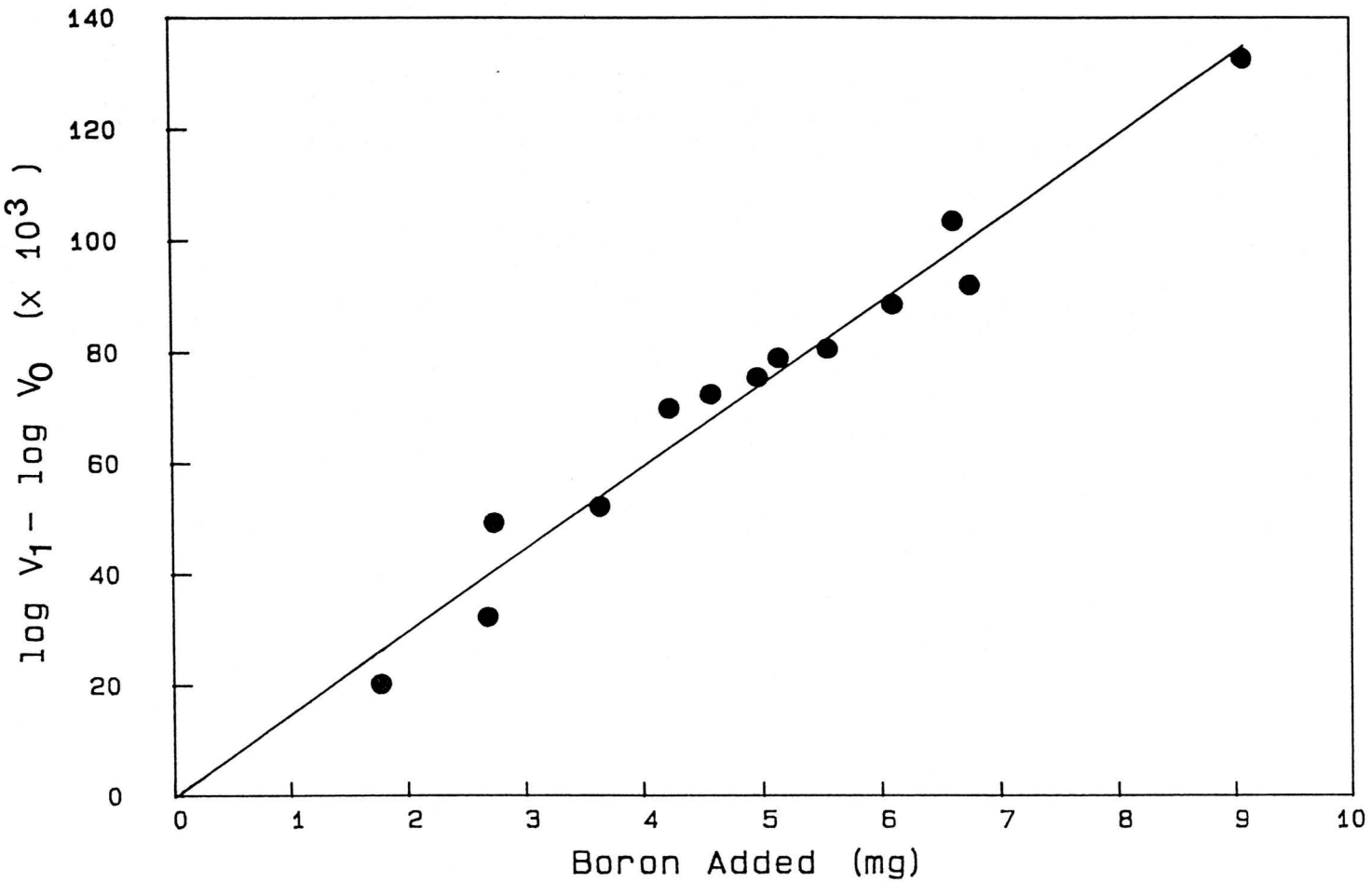

Figure 3.4. Calibration curve used for the determination of boron by an indirect INAA method.

Table 3.10. Comparison of INAA and spectrophotometric methods for boron determinations in AECL Glass 200

	INDIRECT INAA METHOD % B_2O_3 BY WEIGHT	SPECTROPHOTOMETRIC METHOD % B_2O_3 BY WEIGHT
	24.5	24.0
	22.1	21.3
	22.0	21.4
	20.6	22.3
AVERAGE	22.3 $\pm$ 1.6	22.3 $\pm$ 1.3

Table 3.11. Composition of AECL Glasses 200 and 981

(A) AECL Glass 200

COMPONENT	THIS WORK	AECL	LOD
Al_2O_3, %	0.647 ± 0.119	-	0.00871
CaO, %	≤ 0.217	-	-
Na_2O, %	16.3 ± 0.8	16.66	0.0824
SiO_2, %	64.0 ± 2.5	64.62	7.70

(B) AECL Glass 981

COMPONENT	THIS WORK	AECL	LOD
Al_2O_3, %	21.8 ± 1.7	22.39	0.00160
CaO, %	12.2 ± 0.4	12.81	0.407
Na_2O, %	9.43 ± 0.16	9.0	0.0406
SiO_2, %	55.6 ± 1.6	54.90	18.68

batches of I-117 glass was more difficult. The indirect INAA method of analysis was not very practical because this glass was so active after a 5 s irradiation that at least a 5-10 min decay was required before it could be counted. The ^{52}V nuclide ($t_{1/2}$ = 3.75 min) had decayed significantly by that time and the results obtained were inconsistent due to poor counting statistics. More success was obtained using spectrophotometry. Provided all the glass samples were first finely ground in the micro-mill, they could then be dissolved in HF and diluted for analysis. This was, in fact, done on all three CEC glasses and the results are given in the respective tables (3.12, 3.13 and 3.14). An expected (calculated) value of 15.00% B_2O_3 was given by the CEC for the three glasses, and as may be seen the values obtained by this spectrophotometric method are very close to the quoted value.

3.D.1.F. Elemental Content of Glasses

The correction of all elemental comparator standards with the necessary amount of boron was done and used for the determination of elemental concentrations in borosilicate glass. This permitted the subsequent characterization of all glasses. Results of these characterizations are given in Tables 3.11-3.15.

3.D.2. Characterization of Leachates

3.D.2.A. Preliminary Experiments

The glass leachate samples were analyzed by conventional INAA only. Concentrations of potentially interfering elements such as Na were sufficiently low that INAA methods could be used without the worry of high

Table 3.12 Elemental content of CEC Glass

ELEMENT	CONCENTRATION	LOD
Al_2O_3, %	4.32 ± 0.30	0.0317
B_2O_3[a], %	17.9 ± 1.0	0.000161
BaO, %	0.309 ± 0.018	0.00978
CeO_2, %	0.764 ± 0.036	0.000297
Co	1.18 ± 0.36	0.101
Cr	919 ± 68	3.96
Eu	7.72 ± 0.81	0.0527
Fe_2O_3, %	3.73 ± 0.21	0.0453
Hf	204 ± 9	0.416
La_2O_3, %	0.368 ± 0.023	0.00185
MgO, %	7.10 ± 0.49	0.618
MoO_3, %	1.56 ± 0.22	0.00156
Na_2O, %	14.5 ± 1.5	0.144
Nd_2O_3, %	0.772 ± 0.089	0.00223
NiO, %	3.71 ± 0.36	0.00415
Sc	0.0760 ± 0.0095	0.0154
SiO_2, %	52.0 ± 13.3	15.5
Sm	1.24 ± 0.30	0.000393

(all concentrations in ppm unless otherwise noted)
a - Determined by spectrophotometry

Table 3.12. Continued

ELEMENT	CONCENTRATION	LOD
Ta	0.180 ± 0.021	0.106
Th	22.9 ± 1.8	2.10
U_3O_8, %	0.00104 ± 0.00008	0.0000968
Yb	38.8 ± 7.1	2.79
ZnO	0.644 ± 0.006	0.000944
ZrO_2, %	1.04 ± 0.09	0.0196

(all concentrations in ppm unless otherwise noted)

Total weight percentage of glass exceeds 100% due to large uncertainties in values obtained for some oxides

a - Determined by spectrophotometry

Table 3.13. Composition of I-117 Glass (Batch 1)

Oxide	Weight %	LOD
Al_2O_3	4.02 ± 0.03	0.133
BaO	0.503 ± 0.033	0.00673
B_2O_3[a]	15.9 ± 0.5	0.000161
CeO_2	0.774 ± 0.012	0.000333
CoO	0.0117 ± 0.0006	0.0000248
Cr_2O_3	0.199 ± 0.008	0.000547
Cs_2O	0.00828 ± 0.00031	0.0000234
Eu_2O_3	0.0000890 ± 0.0000092	0.00000719
Fe_2O_3	4.36 ± 0.07	0.0392
HfO_2	0.0260 ± 0.0011	0.000119
K_2O	< 0.452	
La_2O_3	0.891 ± 0.102	0.00196
MnO_2	0.986 ± 0.016	0.00989
MoO_3	0.156 ± 0.008	0.00402
Na_2O	19.0 ± 0.4	0.143
Nd_2O_3	0.719 ± 0.006	0.00221

a - Determined by spectrophotometry

Table 3.13. Continued

Oxide	Weight %	LOD
NiO	0.350 ± 0.012	0.00571
Pr_2O_3	0.271 ± 0.017	0.0466
Sc_2O_3	$9.73 \times 10^{-6} \pm 1 \times 10^{-8}$	0.00000329
SiO_2	49.7 ± 17.1	28.3
Sm_2O_3	0.847 ± 0.045	0.000308
SnO	0.0893 ± 0.0037	0.0178
SrO	0.258 ± 0.037	0.166
Tb_2O_3	0.000370 ± 0.000018	0.0000115
U_3O_8	0.0517 ± 0.0006	0.0000965
WO_3	0.00845 ± 0.00075	0.00182
Yb_2O_3	0.00257 ± 0.00045	0.000114
ZnO	0.0345 ± 0.0021	0.00147
ZrO_2	1.30 ± 0.03	0.0144

a - Determined by spectrophotometry

Table 3.14. Composition of I-117 Glass (Batch 2)

Oxide	Weight %	LOD
Al_2O_3	2.85 ± 0.24	0.117
BaO	0.270 ± 0.007	0.00424
B_2O_3[a]	15.5 ± 1.1	0.000161
CeO_2	0.655 ± 0.026	0.000221
CoO	0.0146 ± 0.0031	0.0000394
Cr_2O_3	0.205 ± 0.013	0.000226
Cs_2O	0.000467 ± 0.000021	0.0000193
Eu_2O_3	≤ 0.0000890	
Fe_2O_3	4.15 ± 0.34	0.0367
HfO_2	0.0213 ± 0.0009	0.0000308
K_2O	≤ 0.378	
La_2O_3	0.555 ± 0.045	0.000501
MnO_2	0.980 ± 0.031	0.00898
MoO_3	0.210 ± 0.069	0.00121
Na_2O	18.1 ± 0.6	0.132
Nd_2O_3	0.776 ± 0.046	0.00152

a - Determined by spectrophotometry

Table 3.14. Continued

Oxide	Weight %	LOD
NiO	0.340 ± 0.020	0.00253
Pr_2O_3	0.281 ± 0.053	0.0465
Sc_2O_3	≤ 0.00000274	
SiO_2	48.0 ± 1.4	26.7
Sm_2O_3	0.773 ± 0.035	0.153
SnO	0.0893 ±	0.00295
SrO	0.252 ± 0.006	0.0774
Tb_2O_3	≤ 0.00000931	
U_3O_8	0.00245 ± 0.00015	0.000190
WO_3	≤ 0.00102	
Yb_2O_3	0.00270 ± 0.00008	0.00192
ZnO	0.0451 ± 0.0028	0.00126
ZrO_2	0.923 ± 0.036	0.0110

a - Determined by spectrophotometry

Table 3.15. Elemental content of Corning JL Glass

ELEMENT	CONCENTRATION	LOD
Al_2O_3, %	1.69 ± 0.34	0.0191
Ba	258 ± 11	33.1
Br	15.7 ± 0.6	2.74
CaO, %	8.72 ± 1.42	0.0483
Ce	11.6 ± 0.5	0.648
Cl, %	0.859 ± 0.077	0.0433
Co	6.01 ± 0.30	0.108
Cr	10.9 ± 0.6	0.707
Cs	13.8 ± 0.8	0.109
Eu	0.740 ± 0.013	0.388
Fe_2O_3, %	0.307 ± 0.031	0.0113
Hf	1.06 ± 0.09	0.120
La	8.82 ± 0.27	3.71
MgO, %	0.778 ± 0.064	0.498
MnO, %	0.129 ± 0.018	0.00334
Na_2O, %	15.6 ± 0.7	0.0546
Sc	0.864 ± 0.041	0.0122
SiO_2, %	59.3 ± 5.9	17.3

(all concentrations in ppm unless otherwise noted)

Table 3.15. Continued

ELEMENT	CONCENTRATION	LOD
Sm	1.23 ± 0.15	0.0453
Ta	0.143 ± 0.007	0.0508
Th	0.782 ± 0.056	0.0786
Yb	0.640 ± 0.062	0.445
Zn	49.9 ± 3.4	3.17

(all concentrations in ppm unless otherwise noted)

Total weight percentage of glass is less than 100% as not all components could be determined by INAA

activities of ^{24}Na masking the photopeaks of other nuclides. Two different irradiation-decay-counting schemes were used: 10min-1min-10min and 7h-2d-12h. The shorter irradiation scheme was chosen because it allowed the determination of the short-lived nuclides such as ^{24}Na, ^{28}Al and ^{49}Ca without the problem of high activity. A longer irradiation was necessary to determine the concentrations of lanthanide and other longer-lived nuclides. A 7 h rather than 16 h irradiation time was decided upon due to the large number of samples which were to be analyzed and due to the lack of time and irradiation sites available. Because the elemental concentrations of the leachate solutions were very low a short decay period of only 2 d was necessary for accumulating sufficient counts under the photopeaks of interest.

3.D.2.B. Main Experiments

Due to the high sodium and chloride ion concentations of the basaltic groundwater (BGW), EINAA had to be used for the analysis of the leachates. Since the cadmium site could only accommodate large irradiation vials, the leachates were irradiated in the 27mL vials. All leachate samples were analyzed for their short- and medium-lived nuclides using an irradiation-decay-counting scheme of 10min-1min-10min. The distilled deionized water (DDW) and granitic groundwater (GGW) leachates were irradiated in inner sites and the BGW only in the cadmium site. Longer-lived nuclides were activated by irradiating for 3-7 h, allowing to decay for 3 d and counting for 3-6 h. Since the largest irradiation vials were used for BGW, only outer irradiation sites could then be used for the long thermal irradiations. The irradiation-decay-counting scheme initially used for the

leachate from the SA/V experiment at 0.10 cm^{-1} was 7h-3d-6h. However, due to the enormous number of samples and the time constraints, the two subsequent experiments employed a scheme of 3h-3d-3h. Only the filtered leachate samples were still irradiated for 7 h.

As mentioned previously the precision and accuracy of the method used for the determination of Si in the leachate solutions were checked using NBS SRM 1572 Citrus Leaves. It was difficult to find suitable CRMs with desired Si levels. The Citrus Leaves were not certified for Si; however, an information value was available (0.19% Si). The range of the method used was 5-100 µg Si (Fig. 3.5). The Si content of this material is given in Table 3.16. It is evident that the relative standard deviation is less than ±10%, and the agreement between the information value and that obtained from the analysis is quite good.

3.E. SUMMARY

Two relatively simple INAA methods have been developed for the simultaneous determinations of major, minor and trace elements in glasses. These methods consist of 3 irradiations, 3 decay and 3 counting periods which allow the detection and quantification of approximately 40 elements.

The EINAA method is particularly suited for the determination of elements through medium-lived nuclides since the activities of major nuclides such as ^{28}Al and ^{24}Na are suppressed. Interferences from competing reactions and overlapping gamma-rays were studied to select the most appropriate nuclides and their photopeaks. The precision and accuracy of these methods have been evaluated by analyzing certified reference materials, and the precision has been found to be generally

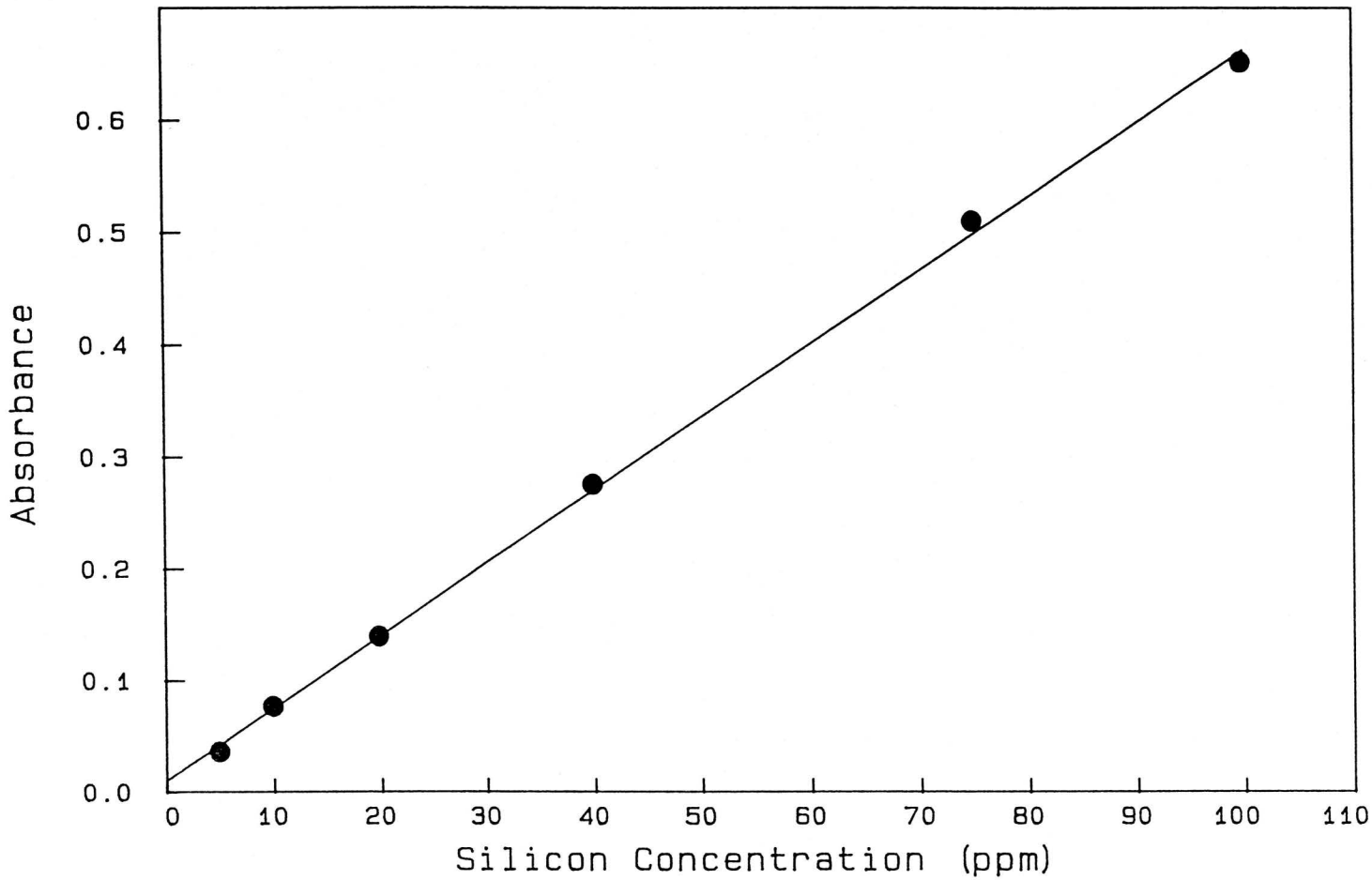

Figure 3.5. Calibration curve used for the determination of silicon by a spectrophotometric method using molybdenum blue.

Table 3.16. Determination of Si in NBS Citrus Leaves (SRM 1572) by molybdenum blue

Sample	This work	LOD	NBS[a]
Citrus Leaves	0.184 ± 0.009%	0.000500%	0.19%

a - information value 85MURA1

within ±10%, and the accuracy was usually within ±5-10%.

The determination of boron in the glass was not possible by conventional INAA; consequently, two alternative methods were employed. Values obtained by these methods for the sample glass were comparable. However, due to the high activities encountered when most glasses were irradiated, the indirect INAA method was found to be less versatile than the spectrophotometric procedure. The latter method has been found to be most useful for boron in the range 0.5-10.0 ppm, while the indirect INAA method was applicable only at higher concentrations (≥1% B).

In addition to the elemental characterization of the glasses, static leaching experiments have been done to study the effects of time, temperature, leachant composition and pH, and surface area to volume ratio on the rate of leaching of elements from simulated waste oxide-loaded glass. The experiments have been designed to collect leachate solutions and precipitates. An INAA method has been developed specifically for the determination of leached elements which involves 3 irradiations, 2 decay and 2 counting periods. The determination of boron in the leachates has been accomplished through the use of the spectrophotometric method using methylene blue and 1,2-dichloroethane, while silicon has been determined by a colorimetric method of molybdenum blue which has been adapted specifically for the leachate solutions. The accuracies of the methods have been evaluated using certified reference materials and found to be good.

CHAPTER 4

LEACHING STUDIES

4.A. INTRODUCTION

One of the main requirements of glass used to immobilize high-level radioactive wastes is that it should possess a high resistance to leaching by groundwater in a repository. Despite all precautions and safeguards, the possibility still exists for the glass to come in contact with groundwater and undergo degradation. Tests must then be conducted to determine the chemical resistance of any glass proposed as an immobilized waste form. This chapter presents the results and discussion of static leaching studies done on three different types of glass under various conditions of temperature, time, SA/V ratio and leachant composition. A simplified leaching model has been applied to some of the data in an attempt to understand the glass dissolution mechanisms.

4.B. CALCULATIONS OF LEACH RATES

The rate of leaching a glass sample can be expressed in various forms. The most common method of expressing leach rate is the normalized form given as:

$$R_i = \frac{M_i}{M_{i,o}} \cdot \frac{W_o}{\Delta t SA} \qquad (4.1)$$

where R_i is the leach rate of element 'i' which is expressed in g $m^{-2}d^{-1}$,

M_i is the mass of the element 'i' dissolved in time Δt, $M_{i,o}$ is the initial mass of the element 'i' in the glass, W_o is the initial weight of the glass or waste form and SA is the surface area of the waste form.

A second form commonly used is the penetration rate, $(PR)_i$, in cmd^{-1}.

$$(PR)_i = \frac{R_i}{\rho} = \frac{M_i \, V}{M_{i,o} \, SA \, \Delta t} \tag{4.2}$$

where ρ is the density of the waste form in g cm^{-3} and V is the volume of the waste form in cm^3.

Other methods used to express rates of leaching are cumulative penetration and cumulative fraction released:

$$(CP)_i = \frac{M_i}{M_{i,o}} \cdot \frac{V}{SA} \tag{4.3}$$

$$(CF)_i = \frac{M_i}{M_{i,o}} \tag{4.4}$$

In these cases $(CP)_i$ is the cumulative penetration based on element 'i', which implies that the waste form surface has been depleted of element 'i' to that depth; $(CF)_i$ is the cumulative fraction of element 'i' released, and M_i is the cumulative amount of element 'i' leached from the waste form.

In this study the release of a component from the glass has been expressed in terms of the normalized mass loss. This term is given by:

$$(NL)_i = \frac{M_i}{M_{i,o}} \cdot \frac{W_o}{SA} \qquad (4.5)$$

where $(NL)_i$ is the normalized mass loss of element 'i'. This unit was chosen to allow easier comparison between the results calculated in this study. In the preliminary experiments normalized leach rates were used. The glasses used in these initial studies were in powder form which could not be accurately weighed after leaching, and thus it was not possible to calculate total normalized mass loss for them.

The total normalized mass loss comprises all the constituents released from the glass; including all dissolved species, colloids and precipitates. Theoretically the mass loss calculations do not include any materials present in the surface layer, provided it adheres to the glass. Obviously, some material may become dislodged during the preparation of the samples for mass loss measurements. This may help to account for some of the scatter in the data points.

All curves in the plots of leach rate and total and normalized elemental mass loss presented in this chapter were drawn by hand. This is a common method of preparing plots in leaching studies. Due to the limited number of points available in each study, and the fact that only one point exists for each day sampled, it was not possible to use a computer program to draw these lines.

4.C. PRELIMINARY EXPERIMENTS

The glass samples in the preliminary experiments were subjected to

short- as well as long-term (up to 2 years although only data up to 168 d has been shown) static leaching. The leach rates for the various glasses have been expressed in terms of g m^{-2} d^{-1} (Equation 4.1). The rates observed for sodium in three glasses, and for samarium, lanthanum and molybdenum for the CEC glass, using two different leachant solutions are presented in Figs. 4.1 - 4.6.

A comparison of leach rates for sodium in three glasses, namely CEC, AECL 200 and AECL 981, shows that the AECL Glass 981 (Fig. 4.1) is the most leach resistant. The leach rate is 100 times slower for this glass leached in both deionized water and synthetic groundwater as compared to the other two glasses. The AECL Glass 981 is a sodium calcium alumino-silicate glass. Such glasses are very durable; however, they have not received much attention for waste immobilization because of their high processing temperature of 1400°C (82HARV1). This high temperature makes them unattractive compared to the lower melting borosilicate glasses from the manufacturing standpoint. One of the reasons for the stability of the sodium calcium aluminosilicate glasses is thought to be due to the formation of a mineralized altered layer on the surface of the glass setting up an equilibrium with the leachant solution.

The surface area to volume (SA/V) ratio may also have contributed to the lower leach rate observed for AECL Glass 981. The experiments conducted on this glass had the highest SA/V ratio in both deionized water and the synthetic groundwater as shown in Table 3.4. The SA/V ratio can significantly alter the rate of leaching. It has been reported that the rate of release of elements from glass decreases with increasing SA/V ratio (83PEDE1).

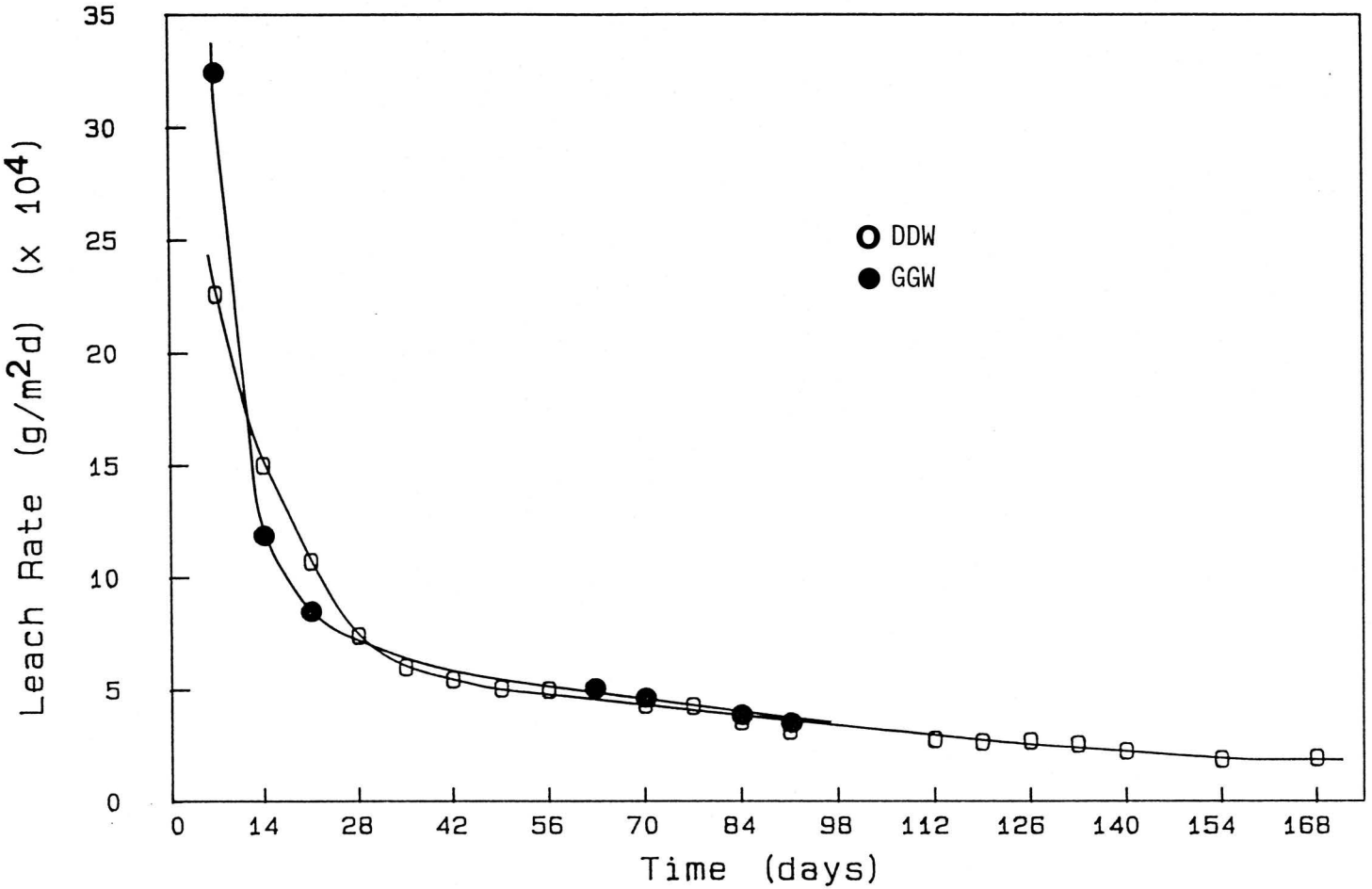

Figure 4.1. Comparison of the leach rate of Na from AECL 981 Glass leached in distilled deionized water and synthetic groundwater.

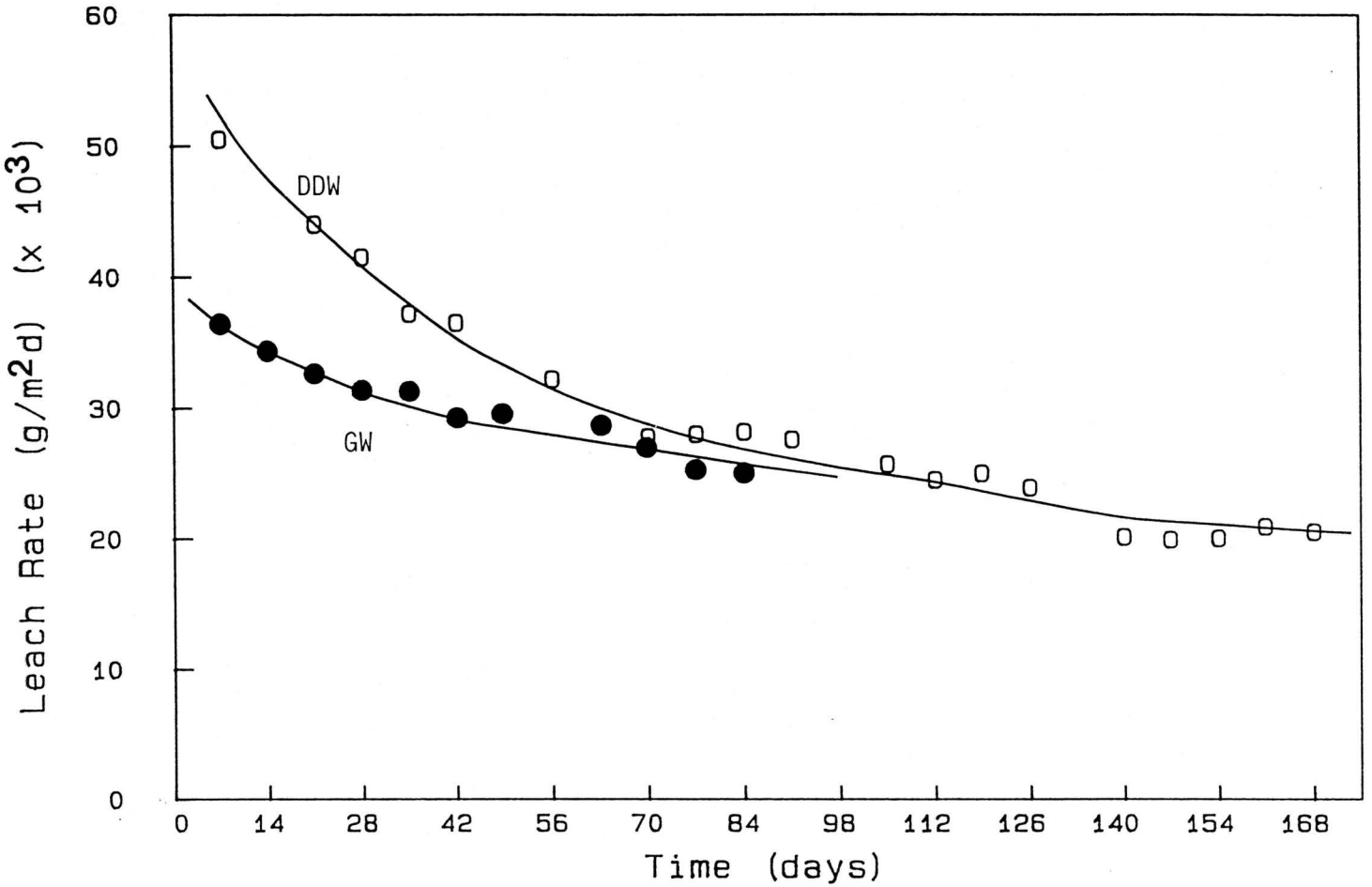

Figure 4.2. Comparison of the leach rates of Na from AECL 200 Glass leached in distilled deionized water and synthetic groundwater.

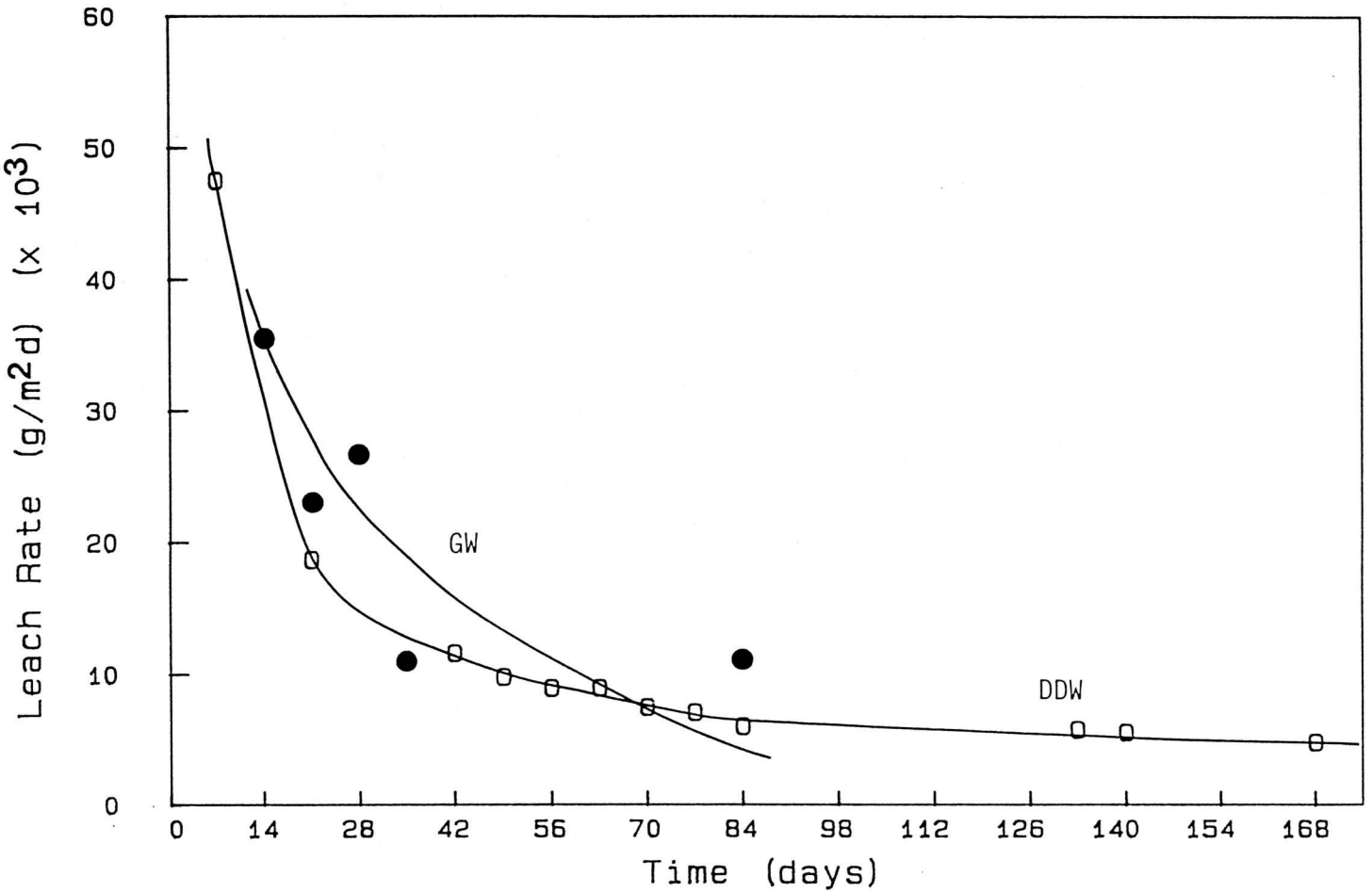

Figure 4.3. Comparison of the leach rate of Na from CEC Glass leached in distilled deionized water and synthetic groundwater.

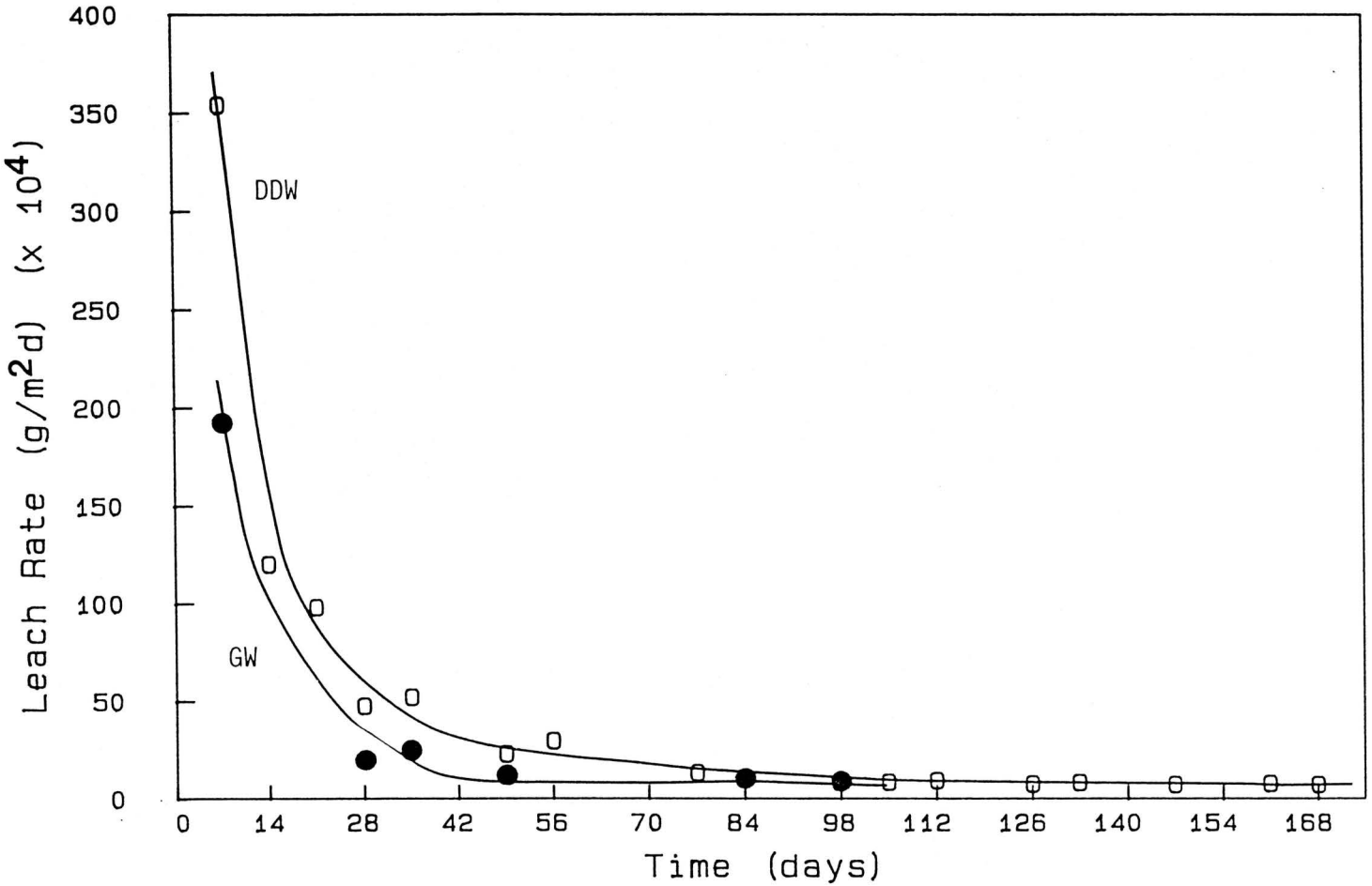

Figure 4.4. Comparison of the leach rate of La from CEC Glass leached in distilled deionized water and synthetic groundwater.

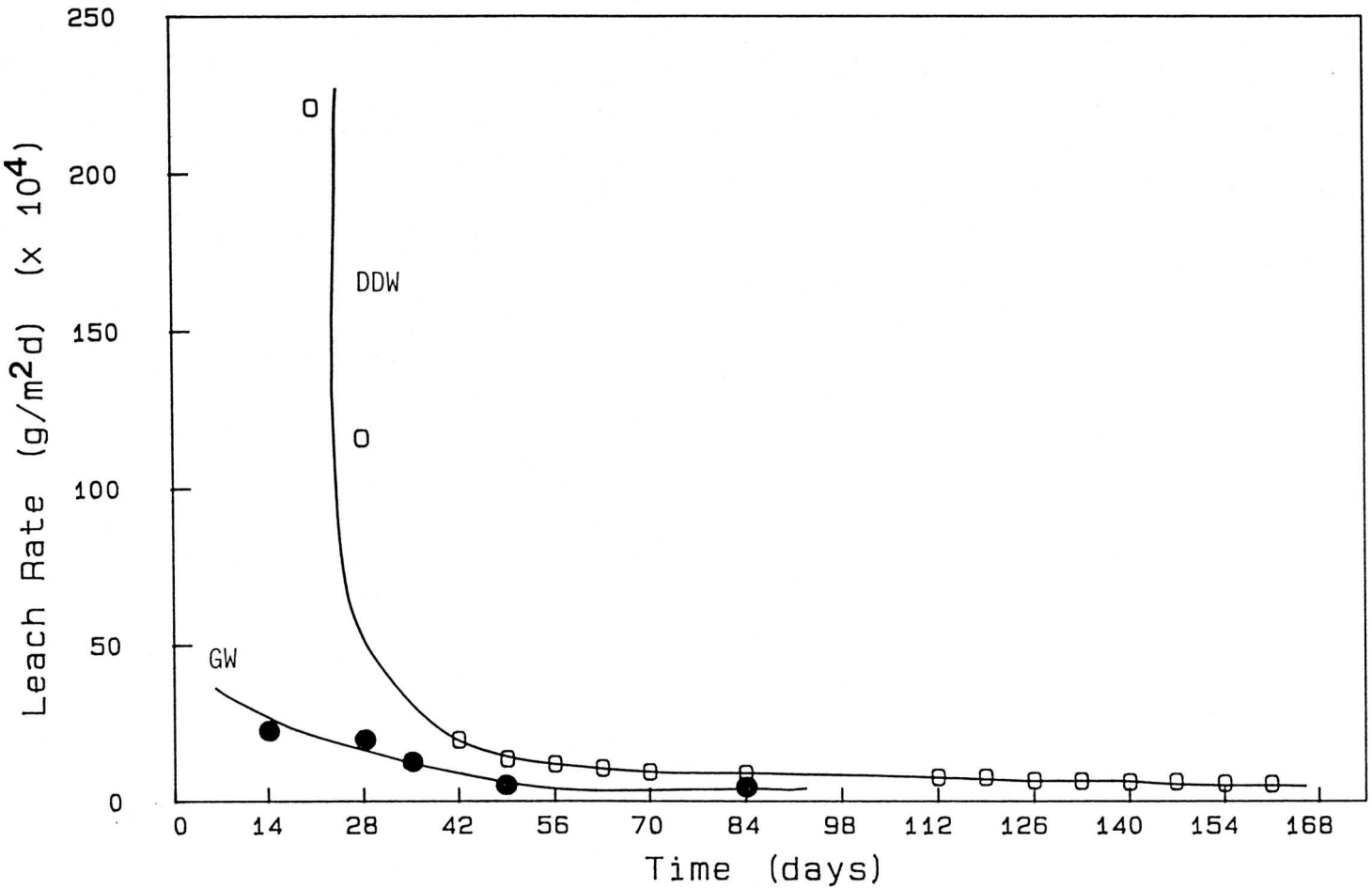

Figure 4.5. Comparison of the leach rate of Sm from CEC Glass leached in distilled deionized water and synthetic groundwater.

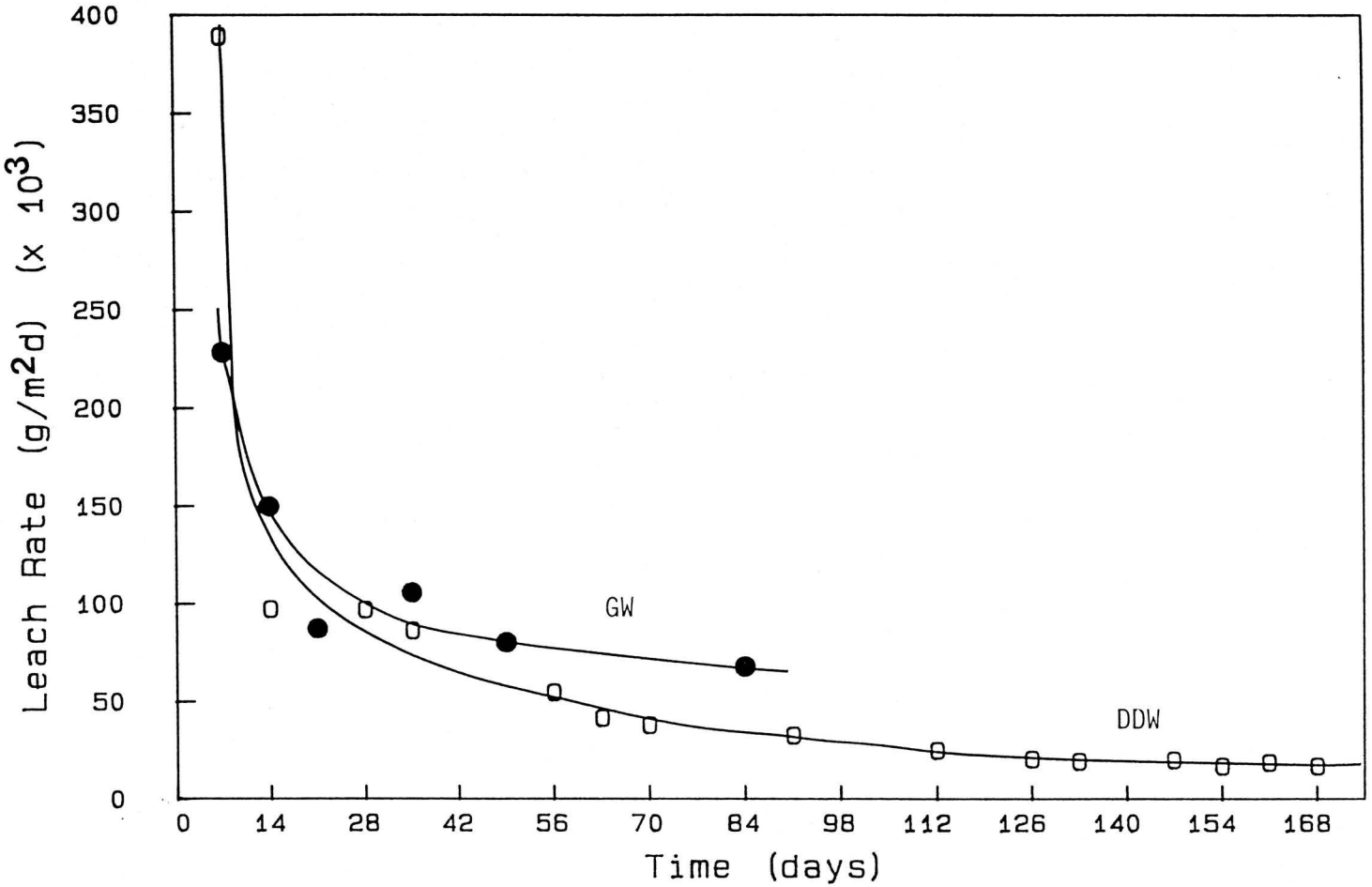

Figure 4.6. Comparison of the leach rate of Mo from CEC Glass leached in distilled deionized water and synthetic groundwater.

For borosilicate glasses, the silica content of the glass is believed to be the controlling factor in the dissolution process (81MALO1,83GRAU1); it slows down when the leachant reaches the saturation concentration of silica. Durability of sodium borosilicate glasses has been reported to increase with increasing silica content. The comparison of the two borosilicate glasses, AECL Glass 200 and CEC Glass (Fig. 4.1 and 4.3), does not really show this trend. The higher silica containing glass (AECL Glass 200) is slightly less durable. It should be pointed out here that the simulated waste oxide loadings of these two glasses are quite different, which may partially account for the difference in the leach rates. The increase in glass durability with increased waste oxide content is explained by the fact that the addition of oxides of multiply charged cations such as Al^{3+} or Zn^{2+} decreases the leach rate for Na^{+} ions and the silica network itself. This is due to buffering by Al^{3+} or Zn^{2+} species. In addition, the dissolution rate may be slowed by the readsorp-tion of leached cations onto the glass surface, and by the formation of an altered layer deposited on the glass surface (83SALE1).

A comparison of the leach rates for all elements (Figs. 4.1 to 4.6) leached from the glasses shows that the rates are lower in groundwater than in deionized water. Obviously, groundwater is a less aggressive leachant than deionized water.

4.D. MAIN EXPERIMENTS

4.D.1. Effects of Leachant Composition and pH

The distilled deionized water (DDW) and granitic groundwater (GGW) leachates sampled at 90°C in the experiments at SA/V = 0.010 cm^{-1} and for

GGW only at SA/V = 0.10 cm^{-1} showed an unexpected pH trend. The pH of these solutions were observed to initially decrease followed by a slow rise (Figs. 4.7 and 4.8). Blank solutions also exhibited lowering of pH to 4.34 and 4.44 (from 6.10 and 7.42) after 84d leaching for DDW and GGW, respectively. The pH of the BGW leachates at 90°C changed very little from their initial value of 9.35 (Fig. 4.9). It had been expected that as the glass leached the pH of the DDW and GGW leachate would rise significantly to values between pH 9 and 10 due to the exchange of H^+ ions in solution with alkali cations, specifically sodium, in the glass. Initially it was thought that a contaminant might have been unintentionally introduced through the monofilament fishing line employed to support the glass or the bottle itself. To test this hypothesis an experiment was run in which various weights of fishing line from 0.01 g to 1 g were leached in DDW, GGW and BGW at 90°C for 7d. Once again the samples of DDW and GGW experienced constant drops in pH to approximately 4.2 from 6.10 and 7.42, respectively. The pH of the BGW samples remained constant around 9.6. This indicated that the amount of fishing line used did not influence the pH, suggesting the line was not the cause of the drop in pH. The results of this experiment are shown in Table 4.1.

Since the fishing line did not appear to be the source of the problem, a test was devised to determine whether oil used as the heating medium in the baths was contaminating the leachates leading to a decrease in pH. A second constant temperature bath was set up in which water was substituted for the oil. Five blank solutions each of DDW, GGW and BGW without mesh or fishing line were leached for 7d at 90°C in the water bath, and a similar set of solutions was immersed in the oil bath. The

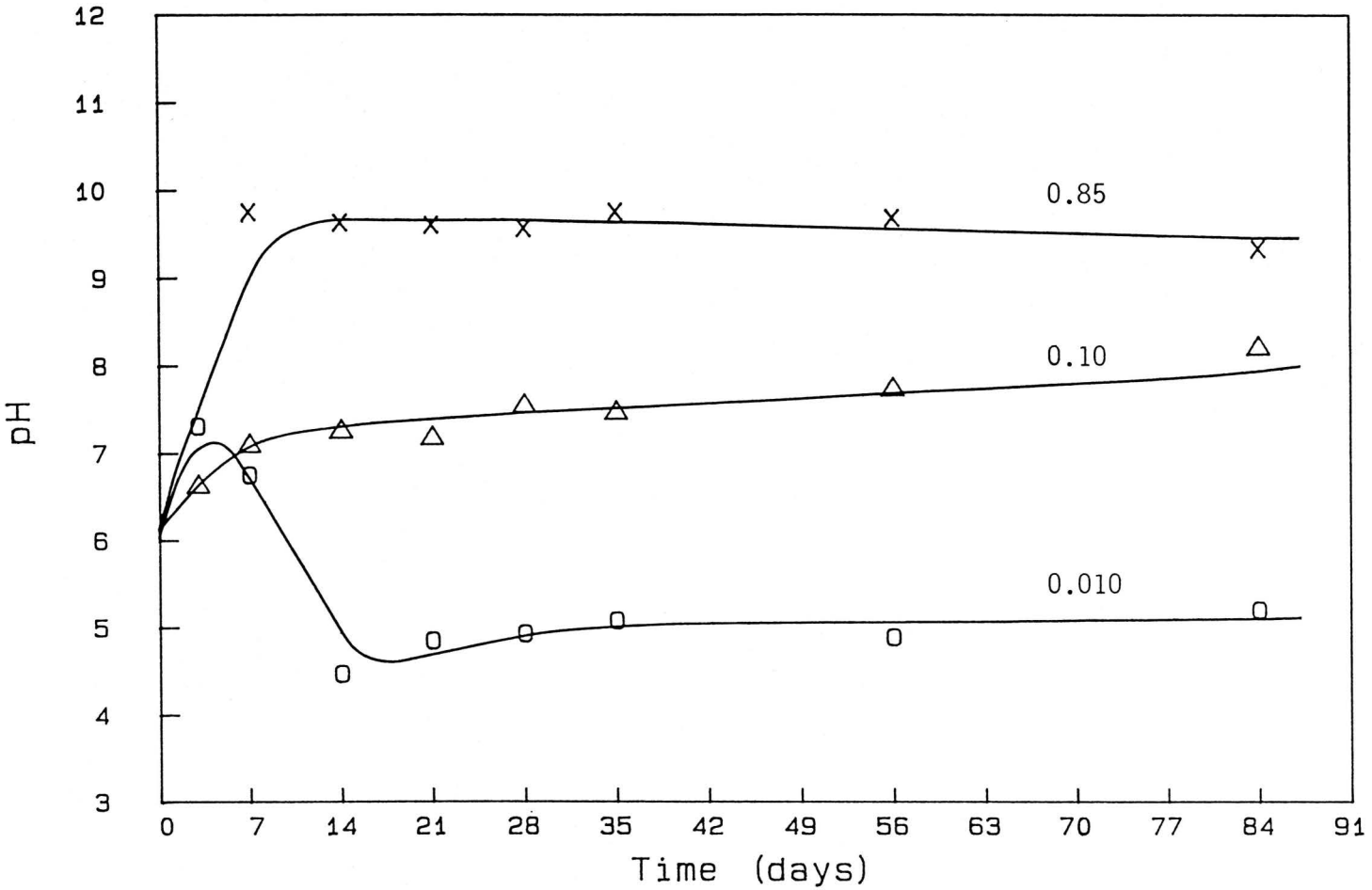

Figure 4.7. Plots of leachate pH for I-117 Glass leached in distilled deionized water at SA/V = 0.010, 0.10 and 0.85 cm^{-1} and 90°C.

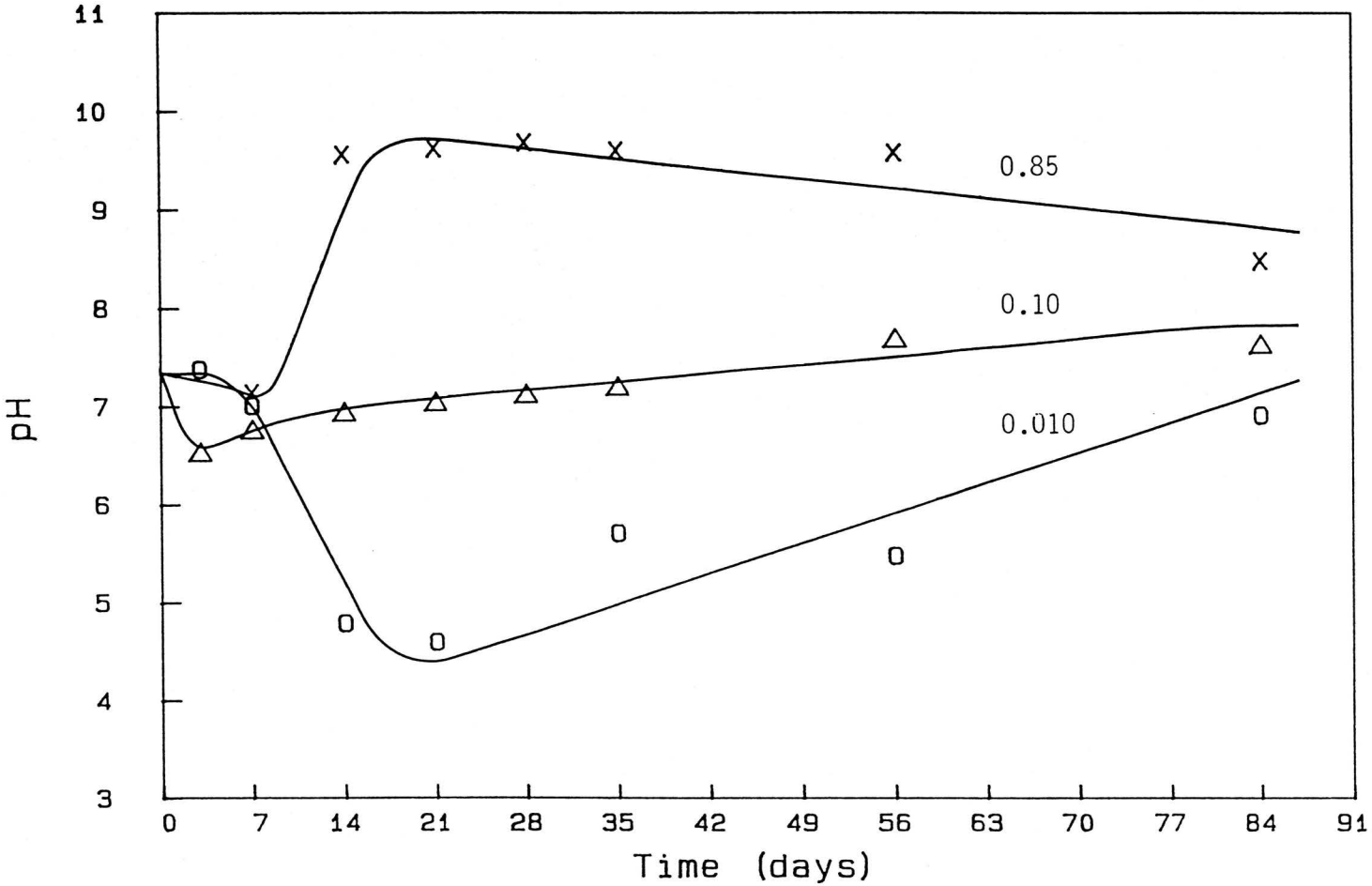

Figure 4.8. Plots of leachate pH for I-117 Glass leached in synthetic granitic groundwater at SA/V = 0.010, 0.10 and 0.85 cm^{-1} and $90^{o}C$.

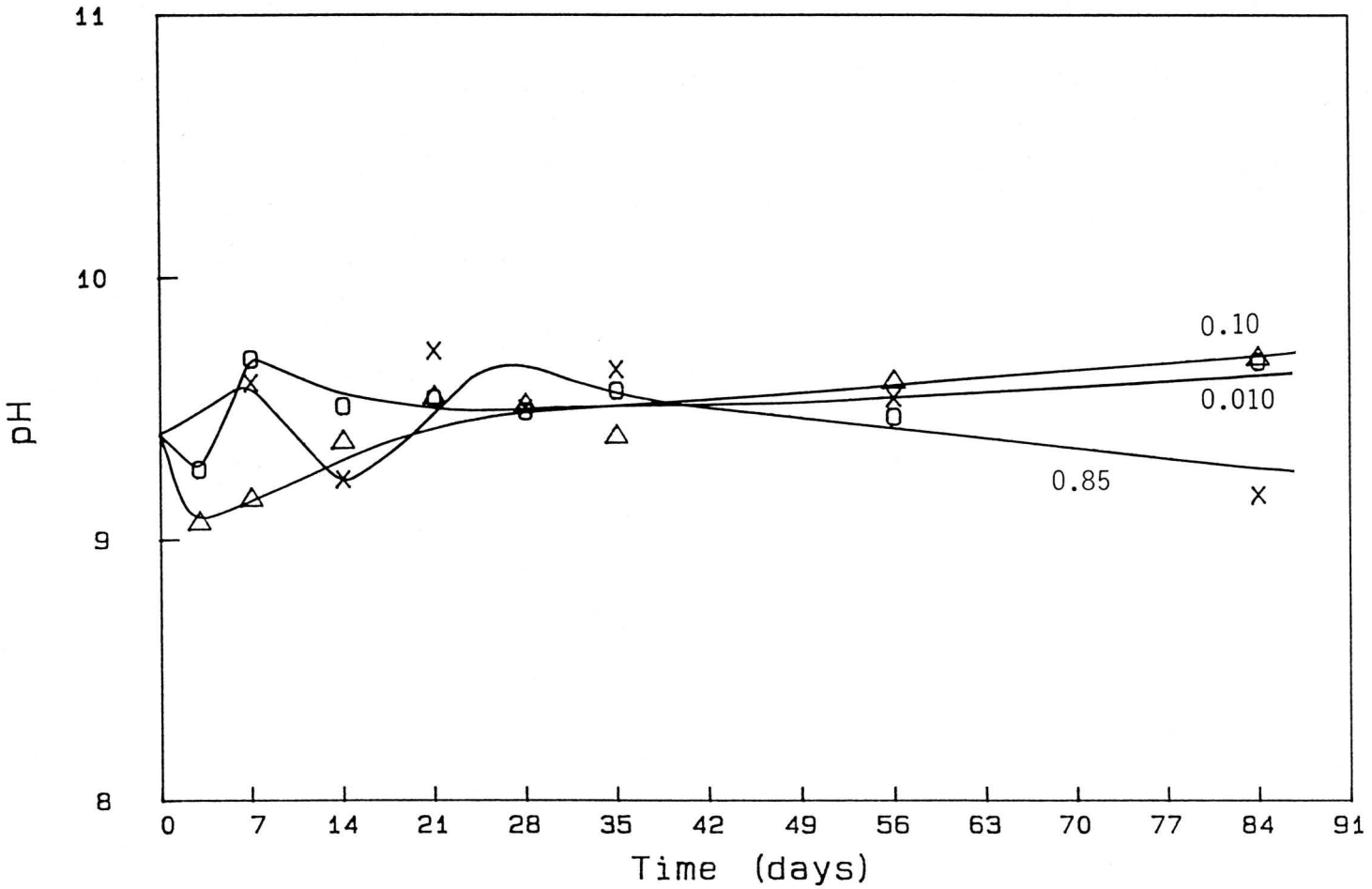

Figure 4.9. Plots of leachate pH for I-117 Glass leached in synthetic Grande Ronde basaltic groundwater at SA/V = 0.010, 0.10 and 0.85 cm^{-1} and $90^{o}C$.

Table 4.1. pH of leachant solutions as a function of weight of Trilene XL Monofilament Fishing Line for 7d at 90°C

LEACHANT	SAMPLE WEIGHT		pH
DDW	0.0107		3.50
DDW	0.0493		4.32
DDW	0.2511		4.22
DDW	0.5021		4.28
DDW	1.0552		4.30
		pH_{avg}	4.12
GGW	0.0101		4.11
GGW	0.0512		4.52
GGW	0.2497		4.28
GGW	0.5039		4.18
GGW	1.0425		4.26
		pH_{avg}	4.27
*BGW	0.0107		9.72
BGW	0.0514		9.76
BGW	0.2512		9.30
		pH_{avg}	9.59

DDW pH_i = 5.98

GGW pH_i = 7.42

BGW pH_i = 9.77

Leachant volumes = 17.57 mL

* Only 3 weights were leached due to the lack of sufficient fishing line

results shown in Table 4.2 were similar suggesting that oil was not influencing the pH. Again the blank solutions of DDW in both baths showed sharp pH decreases. The blank solutions of GGW did not experience a pH decrease in this test. No explanation can be put forward at this stage.

Wicks et al. (82WICK2) had suggested that the use of Teflon bottles might be responsible for a similar pH lowering of leachates in their experiments, through the release of fluoride ions and the subsequent formation of HF causing the decrease in pH. The samples of DDW, GGW and BGW leachate after 7 and 84d of leaching at SA/V = 0.010 cm^{-1} and 90°C were analyzed in the present work for fluorine by INAA through the $^{19}F(n,\gamma)^{20}F$ reaction. Because ^{20}F has a short half-life (11.0s), the leachates were irradiated for 30s, allowed to decay for 15s and counted for 30s using the ND-66 gamma-ray spectrometry system. Since the leachate at this SA/V ratio experienced the largest decrease in pH, it was assumed that if fluoride ion was the cause of the problem then these solutions would have the highest concentrations of the element. The results are given in Table 4.3. As may be seen no fluorine was detected above that which was expected in GGW and BGW leachates. The fluorine concentration in the DDW leachates analyzed at 84 d was higher than expected, but this is most likely due to experimental error. In any event none of the fluorine concentrations determined in the leachates were high enough to suggest that the formation of HF was responsible for the decrease in pH.

Various explanations can be put forward for the pH variations. It could simply be a characteristic of the glass. Sodium, as previously mentioned, is one element which is reported to help control the leachate pH. The exact mechanism for the release of sodium from glass is still not

Table 4.2. Comparison of the pH of blank leachant solutions heated for 7d at 90°C in a constant temperature oil bath and water bath

WATER BATH	OIL BATH
DEIONIZED WATER	DEIONIZED WATER
pH	pH
5.47	5.15
3.85	4.89
4.74	3.81
3.70	3.98
4.71	3.82
pH_{avg} 4.49	pH_{avg} 4.33
GRANITIC GROUNDWATER	GRANITIC GROUNDWATER
pH	pH
8.36	6.99
7.44	7.03
8.81	7.64
7.76	7.09
8.69	7.82
pH_{avg} 8.21	pH_{avg} 7.31

Deionized Water pH_i = 5.81

Granitic Groundwater pH_i = 7.44

Leachant volume = 17.50 mL

Table 4.3. Fluorine content of leachates collected after 7 and 84d of leaching at SA/V = 0.10 cm^{-1} and 90°C as determined by INAA

LEACHANT	DAY	FLUORINE CONTENT	
		LEACHANT	GROUNDWATER
DDW	7	$\leq$ 4.61	-
GGW	7	$\leq$ 3.54	0.249
BGW	7	25.9	33.4
DDW	84	10.5	-
GGW	84	$\leq$ 3.05	0.249
BGW	84	20.6	33.4

(all concentrations in ppm unless otherwise noted)

^{20}F - $t_{1/2}$ = 11s, t_i = 30s, t_d = 15s, t_c = 30s

certain. It has been suggested that sodium exchanges with H^+ or H_3O^+ resulting in an increased OH^- content in the solution, or a non-bridging oxygen in the silica lattice reacts with water diffusing in the glass:

$$\text{-Si-O-Na} + H^+ \longrightarrow \text{-Si-O-H} + Na^+ \qquad (4.6)$$

$$\text{-Si-O}^- + H_2O \longrightarrow \text{-Si-OH} + OH^- \qquad (4.7)$$

The process is then closely followed by diffusion of sodium and hydroxyl ions into solution (85GARL1). Tait and Mandolesi observed a similar low sodium release, as found in our work, in deionized water (SA/V = 0.10 cm^{-1}) at 25, 70 and 99°C using a waste-free as well as a 2% waste-loaded sodium borosilicate glass leached for up to one year; the pH of leachates remained < 7.0 throughout (85IAEA1).

Boron may also influence the pH of the leachate as it is released from the glass. In some of the experiments (DDW and GGW at SA/V = 0.010 and 0.10 cm^{-1}) boron appears to be leaching congruently with sodium (Fig. 4.10). When the normalized elemental mass losses of sodium and boron are equal then they have been removed from the glass in the same proportions as their concentrations in the original unaltered glass. Boron could be leached diffusively and congruently with sodium because boron cannot be attacked by water until an associated alkali ion has been exchanged with H^+ or H_3O^+. Boron can also be removed by water which penetrates the gel layer and not the glass indicating that first the glass must be reduced to gel by removal of Na^+ (82HALL1). It appears that boron is buffering the pH of the DDW and GGW solutions at SA/V = 0.010 and 0.10 cm^{-1} at 90°C, since these are the only cases where sodium and boron leach conguently

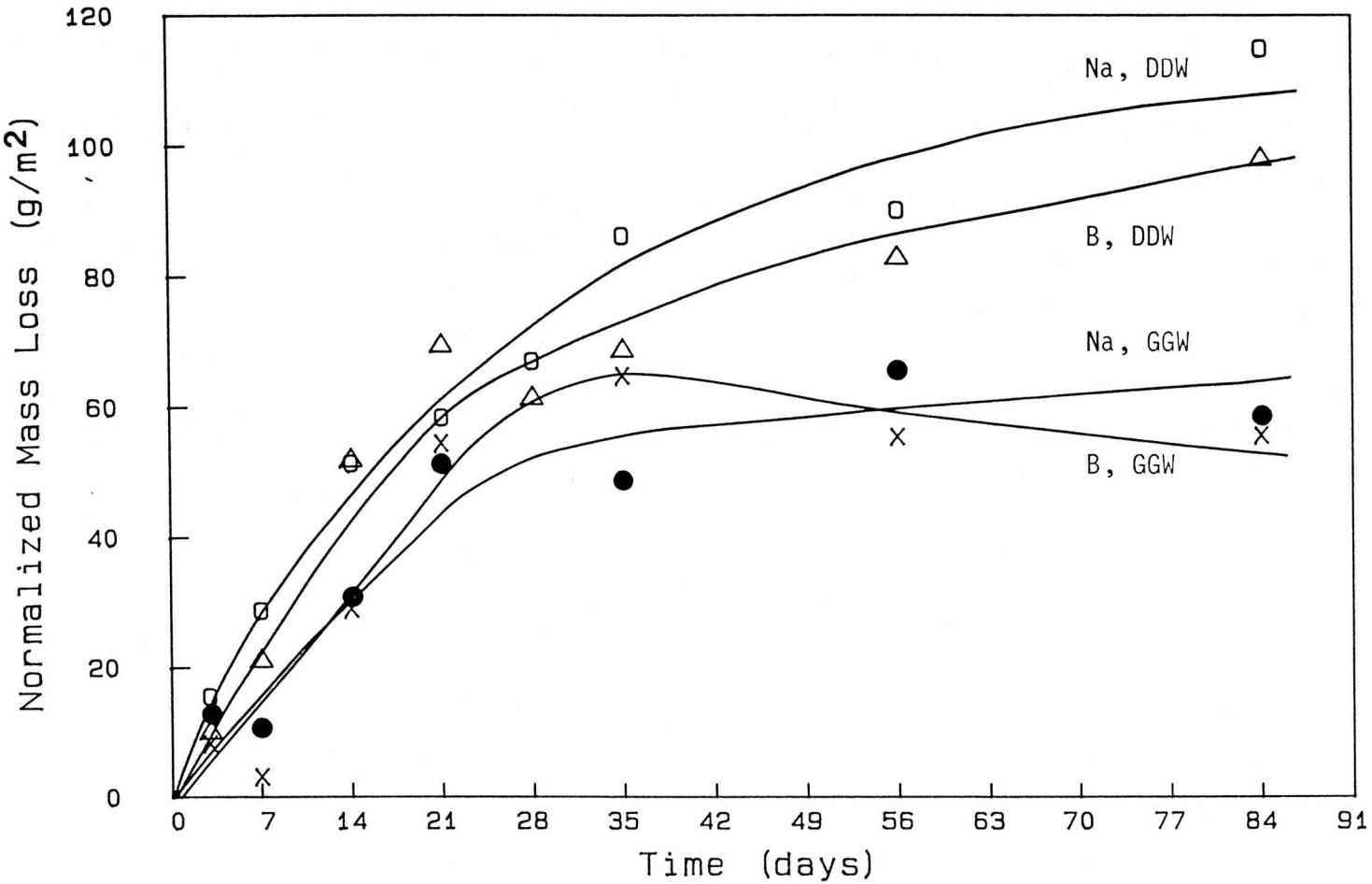

Figure 4.10. Normalized elemental mass loss results for sodium and boron leached from I-117 Glass in distilled deionized water and synthetic granitic groundwater at SA/V = 0.010 cm^{-1} and 90°C.

(Fig. 4.10). The pH of DDW and GGW leachates rises at SA/V = 0.85 cm^{-1} very quickly to 9.5, and the normalized mass loss of Na^+ is 3 times higher than boron (Fig. 4.11). The buffer capacity of the BGW leachant solution was about 15 higher than that of the GGW solution (4.7×10^{-4} M and 2.8×10^{-5} M respectively), which may explain why the pH of BGW leachate was virtually unaffected by either sodium or boron release.

The evidence for a lower than expected sodium release is further supported by the normalized elemental mass loss for this element in BGW leachate. Normally, as the SA/V ratio increases the normalized elemental mass loss decreases (83PEDE1); however, the sodium release in BGW at 90°C and 0.10 cm^{-1} is about 10 times higher than at 0.010 cm^{-1}. A similar observation is made by comparing sodium release of all leachates at 0.85 cm^{-1} with those at 0.10 cm^{-1} (Fig. 4.12). The sodium mass losses at 0.85 cm^{-1} are consistently higher than at 0.10 cm^{-1}, which is the opposite of the expected trend. Sodium is the only element measured which shows this discrepancy. It should be noted here that in the experiments at 0.85 cm^{-1} a different batch of glass was used than at 0.010 or 0.10 cm^{-1}. It is possible that the sodium in the second batch of glass was not homogeneous. If this element was more concentrated in the outer portions of the glass then sodium would leach at a faster rate. Thus the sodium normalized mass losses would not follow the expected trend with SA/V ratio, and the pH of the leachate would increase more rapidly than at either 0.010 or 0.10 cm^{-1}.

At 40°C the normalized mass losses of sodium and boron are expected to be much lower than at 90°C and the pH is not expected to change drastically from its initial value (Figs. 4.13-4.15). This was in fact observed except at SA/V = 0.85 cm^{-1} in BGW leachate (Fig. 4.15). Surpris-

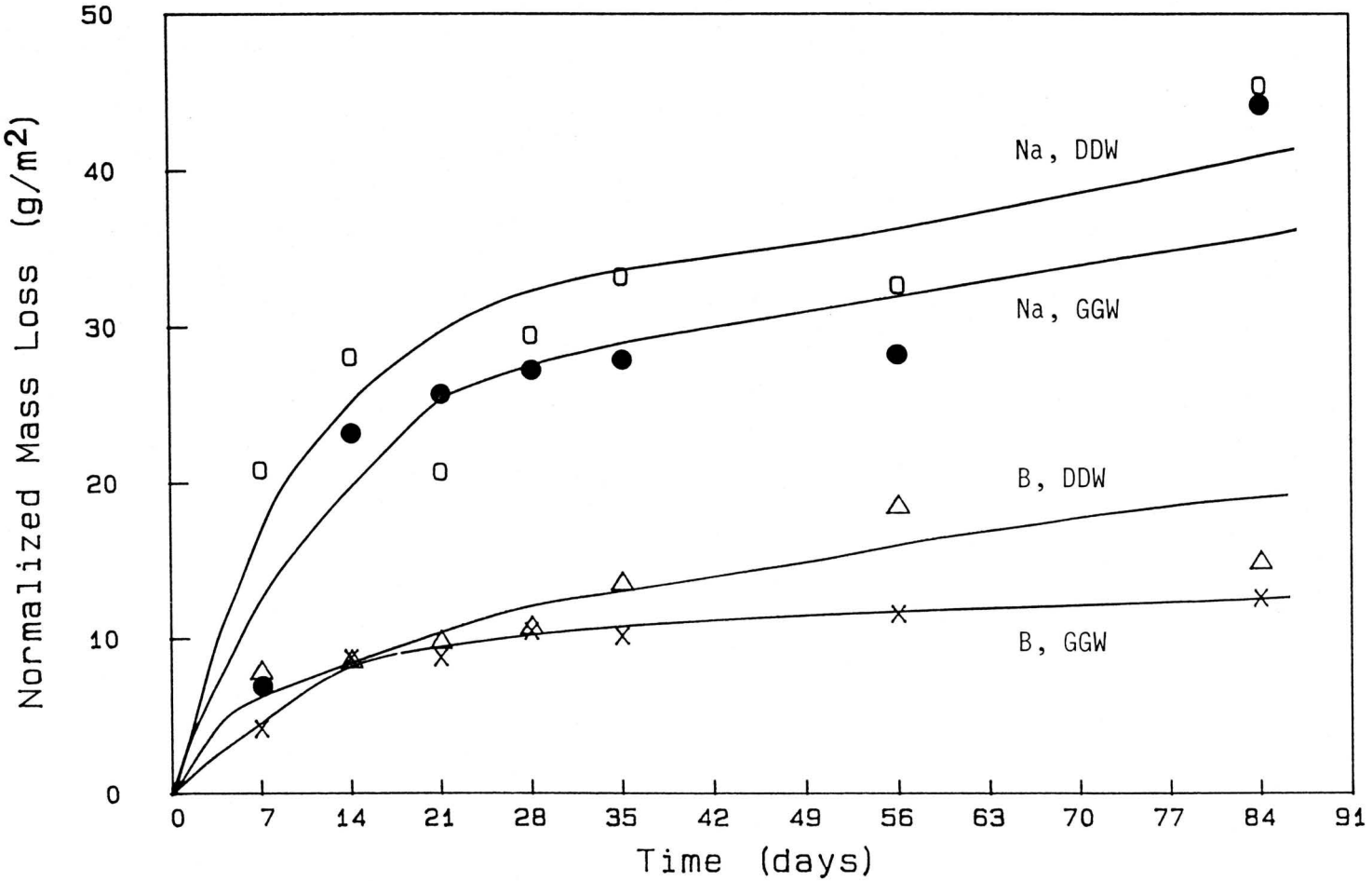

Figure 4.11. Normalized elemental mass loss results for sodium and boron leached from I-117 Glass in distilled deionized water and synthetic granitic groundwater at SA/V = 0.85 cm^{-1} and 90°C.

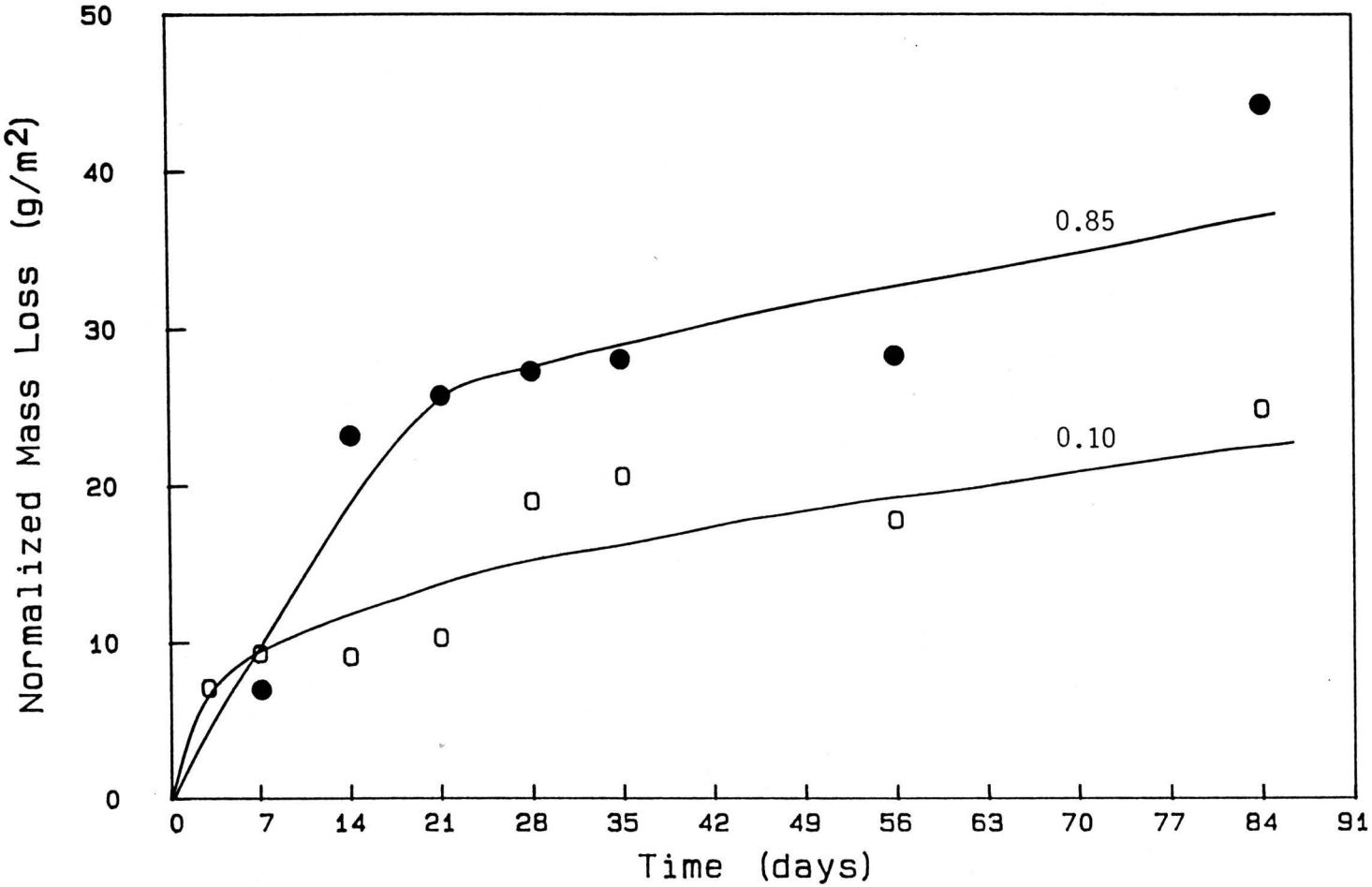

Figure 4.12. Comparison of the normalized elemental mass loss results for sodium leached from I-117 Glass in synthetic granitic groundwater at SA/V = 0.10 and 0.85 cm^{-1} and 90°C.

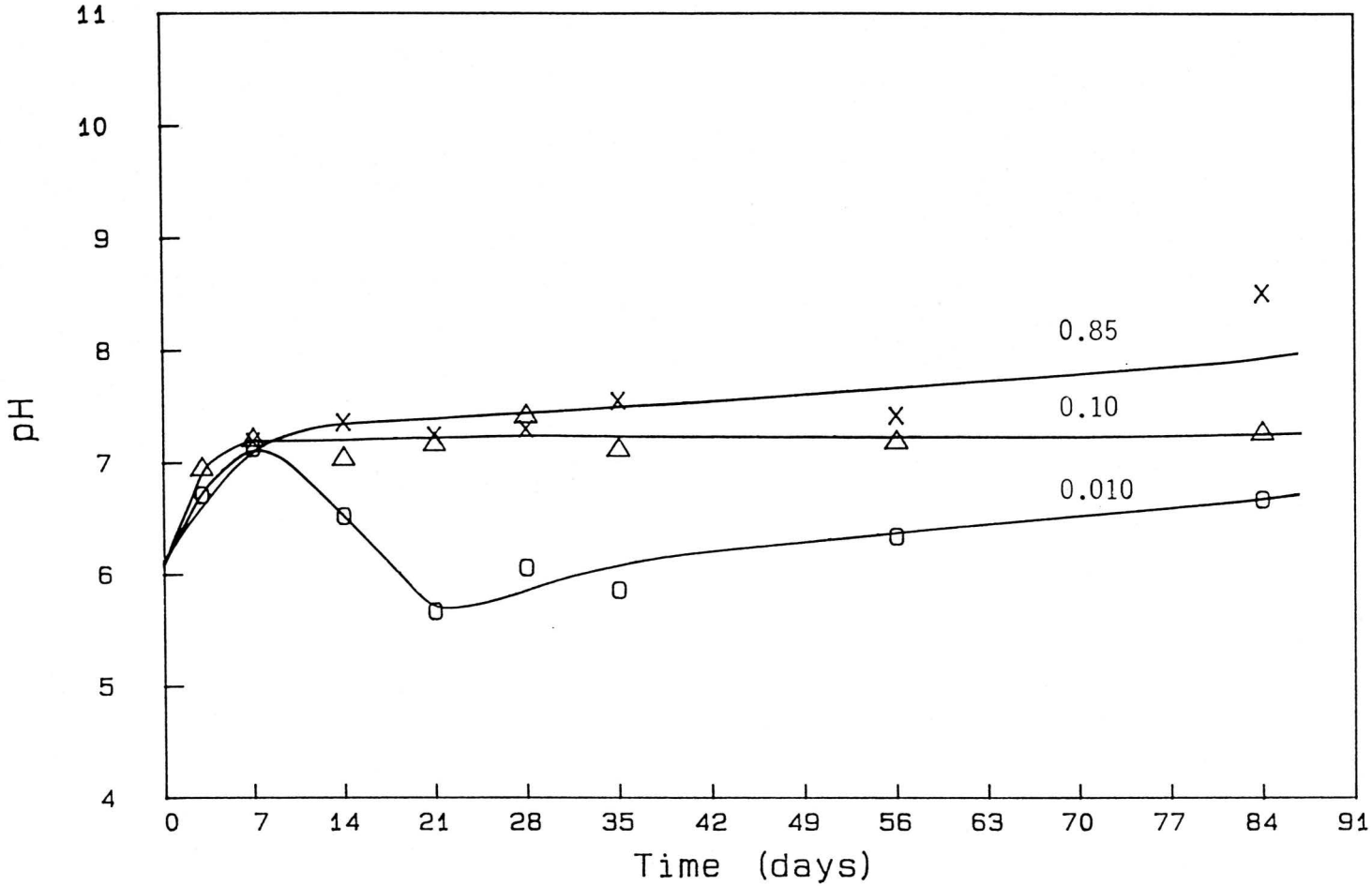

Figure 4.13. Plots of leachate pH for I-117 Glass leached in distilled deionized water at SA/V = 0.010, 0.10 and 0.85 cm^{-1} and 40°C.

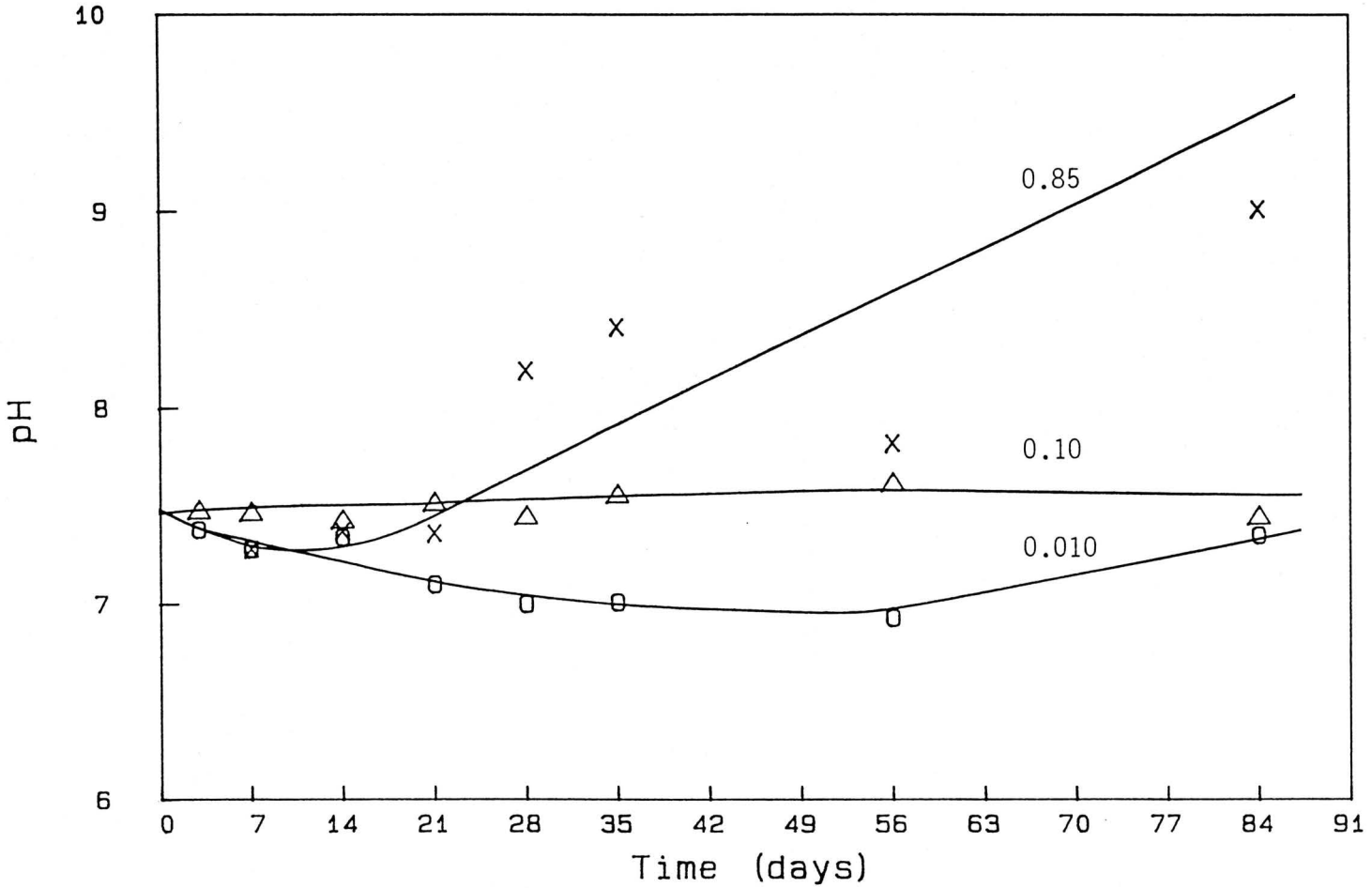

Figure 4.14. Plots of leachate pH for I-117 Glass leached in synthetic granitic groundwater at SA/V = 0.010, 0.10 and 0.85 cm^{-1} and 40°C.

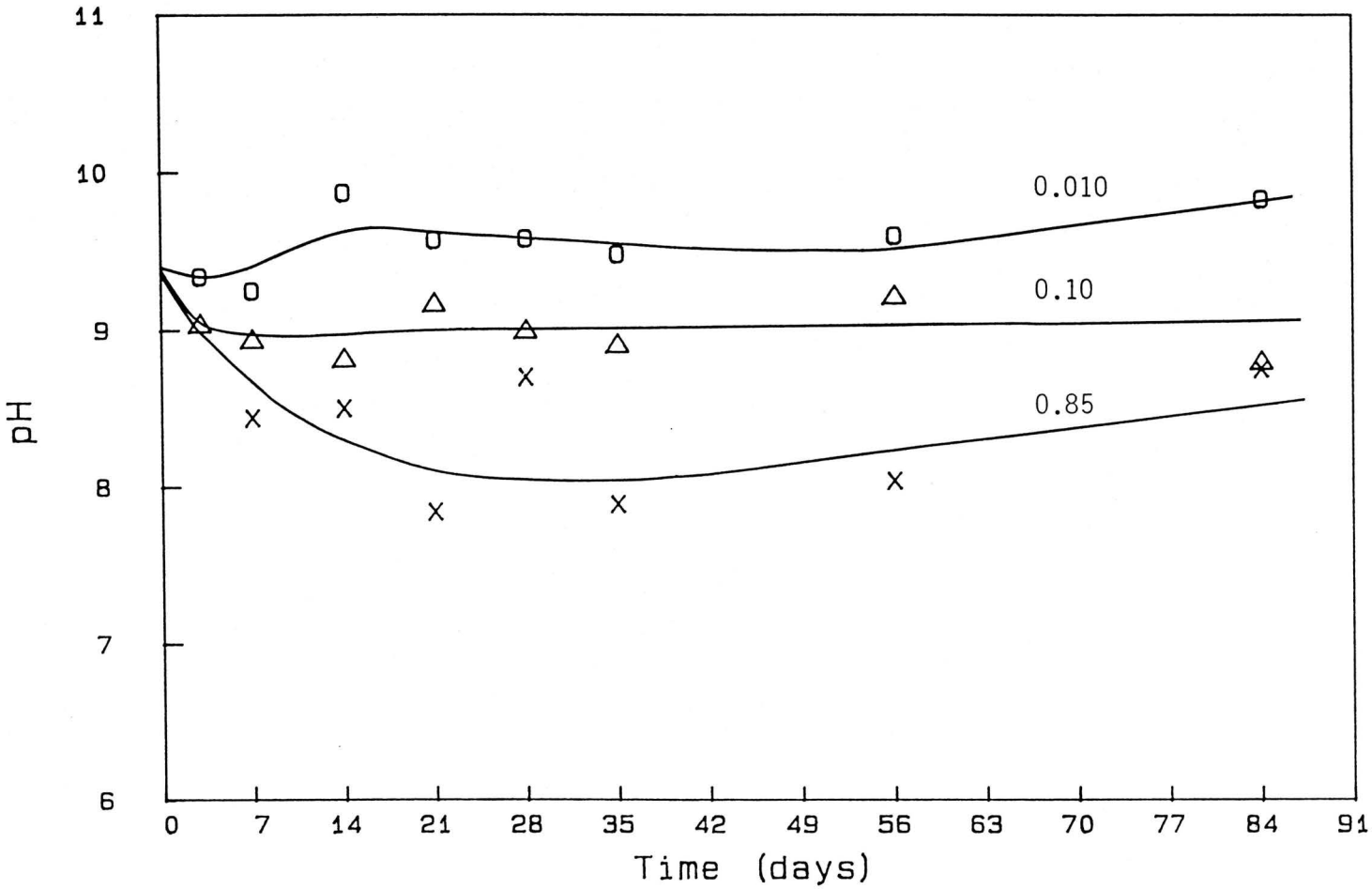

Figure 4.15. Plots of leachate pH for I-117 Glass leached in synthetic Grande Ronde basaltic groundwater at SA/V = 0.010, 0.10 and 0.85 cm^{-1} and 40°C.

ingly, the pH in the BGW leachates fell from 9.35 to 8.30. It is not clear why this decrease occurred in the BGW leachate only at 40°C and the highest SA/V ratio. Equally perplexing is the decrease in pH experienced by blank BGW solutions at both 40° and 90°C to pH 8.20 from 9.35 after 84d. It is not an experimental artifact but cannot be explained at this stage either.

Total mass loss of the glass and normalized elemental mass losses of major elements such as boron, sodium (except SA/V = 0.010 cm^{-1} at 90°C) and silicon at both 40°C and 90°C for experiments at SA/V = 0.010 and 0.10 cm^{-1} reveal that BGW is the most aggressive of the three leachants studied. Figs. 4.16 and 4.17 clearly illustrate this trend for the normalized elemental mass loss of boron and total mass loss of the glass at SA/V = 0.010 cm^{-1} and 90°C. While it may be argued that it is not surprising that BGW is the most aggressive solution considering its high initial pH and concentrations of carbonates and sulfates, it must also be remembered that this leachant is the only one which initially contained silicon.

Silicon plays an important role in the release of other elements from borosilicate glass mainly due to the fact that they are released to solution only when the SiO_2 matrix breaks down. It has been previously observed by other researchers that the rate of corrosion of glass falls when the leaching solution becomes saturated with SiO_2 (83PEDE1). The BGW leachant had an initial silicon concentration of about 35 ppm which would suggest that this solution should be approaching saturation faster than either DDW or GGW, and it should appear less aggressive. This is exactly what is observed in the experiments at SA/V = 0.85 cm^{-1} (Fig. 4.18). At SA/V = 0.010 and 0.10 cm^{-1} DDW and GGW appear less aggressive

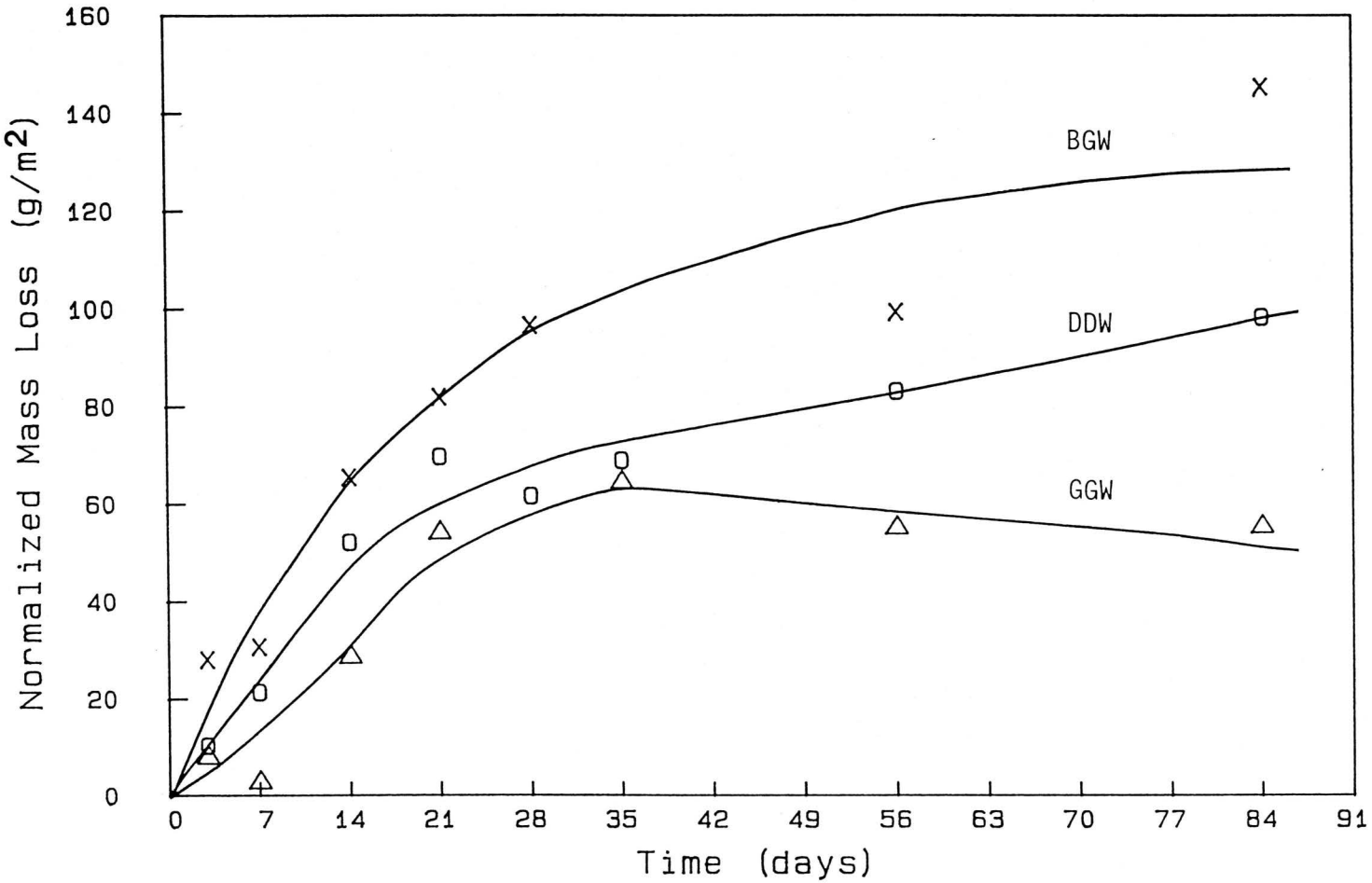

Figure 4.16. Comparison of the normalized elemental mass loss results for boron leached from I-117 Glass in synthetic Grande Ronde basaltic groundwater, distilled deionized water and synthetic granitic groundwater at SA/V = 0.010 cm^{-1} and 90°C.

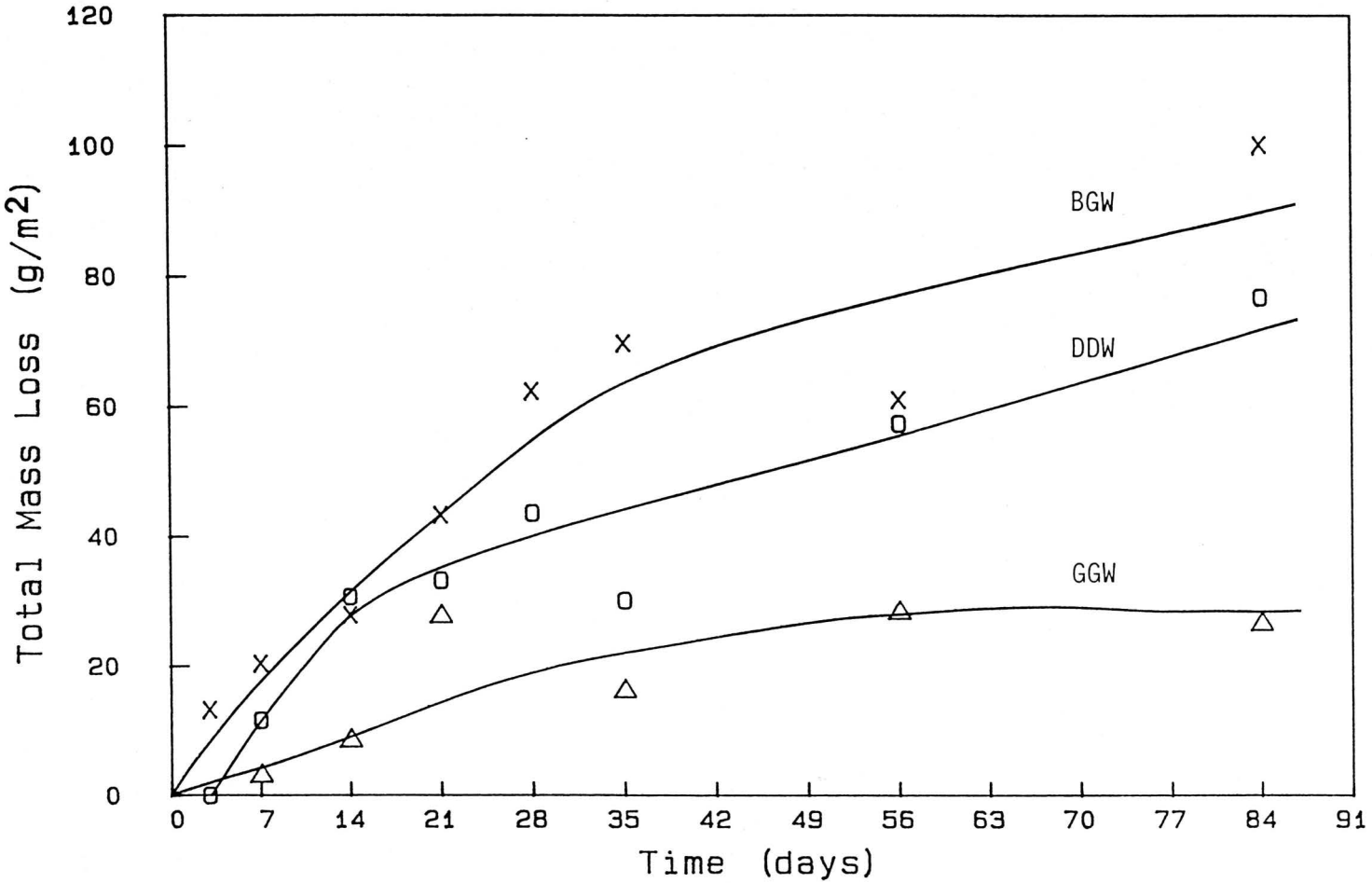

Figure 4.17. Comparison of the total mass loss of I-117 Glass leached in synthetic Grande Ronde basaltic groundwater, distilled deionized water and synthetic granitic groundwater at SA/V = 0.010 cm^{-1} and 90°C.

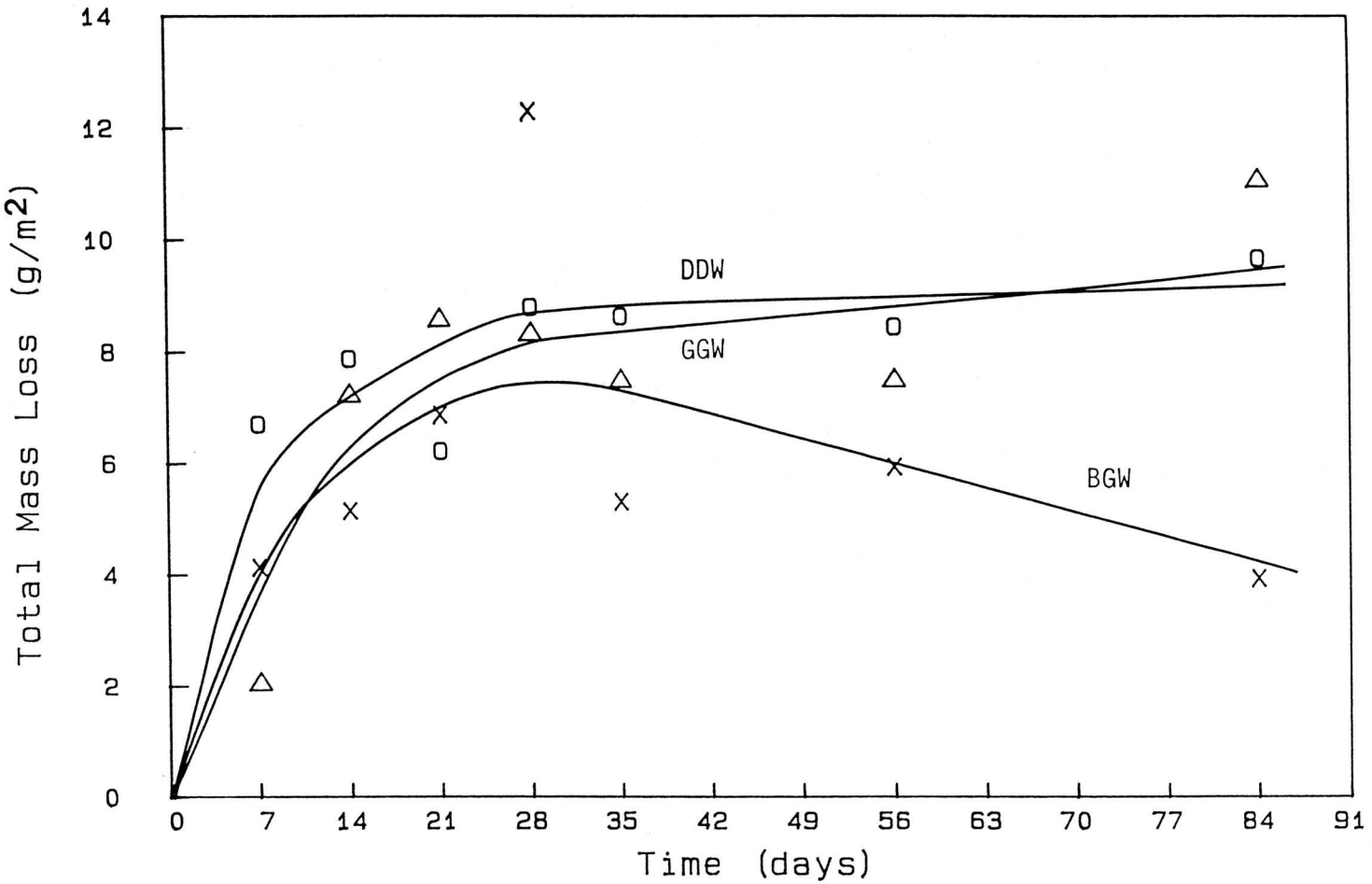

Figure 4.18. Comparison of the total mass loss of I-117 Glass leached in distilled deionized water, synthetic granitic groundwater and synthetic Grande Ronde basaltic groundwater at SA/V = 0.85 cm^{-1} and 90°C.

because of their pH. At a pH > 9, as in the case of BGW, there is an increase in reaction rate because of the behavior of dissolved silicic acid; its deprotonated form is dominant and is more soluble. DDW and GGW in these two experiments had pH values of 4.5-8.0, and H_4SiO_4 is predominant at this pH and had a constant low solubility. Since the release of so many elements are related to the release of silicon, it is understandable that the total mass loss of the glass at the two lowest SA/V ratios in DDW and GGW was lower than in BGW under the same conditions. The influence of pH on the silicic acid is not as noticeable in the experiments at SA/V = 0.85 cm^{-1}, especially at 90°C, since all three leachant solutions very quickly attained a pH > 9.

At 40°C and SA/V = 0.85 cm^{-1}, DDW still appears to be the most aggressive leachant although only a little more so than GGW and BGW whose leachates have slightly higher pH values than those of DDW. Apparently the pH of these solutions is not so much higher than DDW that the difference in the solubilities of the two forms of silicic acid exceeds the saturation effects of the silicon initially present in the solution. Further differences observed between the SA/V experiments will be dealt with in a later section.

It can be concluded from Figs. 4.16, 4.17 and 4.18 that DDW produces higher total mass losses and normalized elemental mass losses than GGW, as might be anticipated. Thus the order of leaching is BGW > DDW > GGW at SA/V = 0.010 or 0.10 cm^{-1} and DDW > GGW > BGW at SA/V = 0.85 cm^{-1}. At the SA/V ratios of 0.010 and 0.10 cm^{-1}, certain elements are leached less in BGW than in DDW or GGW even though the BGW leachant appears to be the most aggressive overall. These elements are lanthanum, manganese and

samarium. Apparently these elements are selectively removed from the glass in DDW and GGW, especially since the releases of network elements such as boron and silicon, or major components such as sodium and molybdenum are lower in these two leachants than in BGW (Fig. 4.19).

Amorphous silica is reported to have a solubility of 323 ppm in pure water at 90°C and 166 ppm at 40°C (83LANZ1). The silicon concentrations used in our experiments (2-75 ppm silicon) were obviously well below these values. Such silicon concentrations are more in line with the saturation concentration of quartz of 33.5 ppm (83LANZ1). It may be postulated that either re-precipitation of silicon has occurred, possibly through the formation of hydrated crystals, or that a very slow increase in the silica content of the solution is taking place. The silicon analysis was only carried out on leachate sampled at room temperature, as was the case for the boron analysis, because of the limited volume of leachate available. Due to the low sensitivity of NAA for silicon this element was determined by colorimetry, which meant that analysis of the precipitated material was not possible. This was unfortunate as the precipitate might have revealed a re-precipitation of this element.

When the rate of leaching and the released concentrations of other elements are compared with those of silicon, three cases can be defined:

(1) $K_i > K_{Si}$

(2) $K_i \leq K_{Si}$ $C_i > C_{Si}$

(3) $K_i \leq K_{Si}$ $C_i \leq C_{Si}$

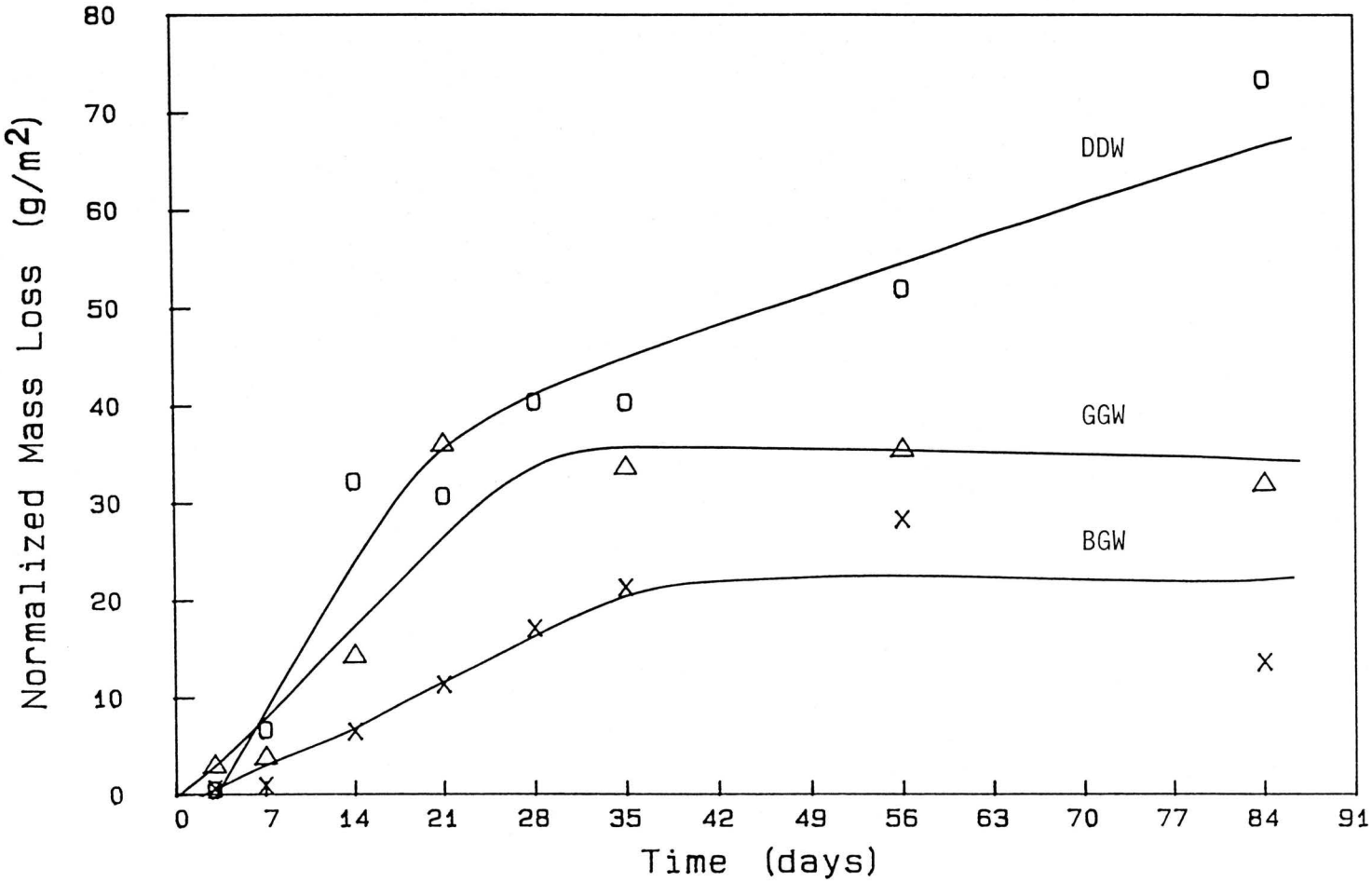

Figure 4.19. Comparison of the normalized elemental mass loss results of manganese leached from I-117 Glass in distilled deionized water, synthetic granitic groundwater and synthetic Grande Ronde basaltic groundwater at SA/V = 0.010 cm^{-1} and 90°C.

where K_i is the leach rate, and C_i is the maximum concentration of an element and is defined as the sum of saturation concentrations of all possible species in solution (82AVAG1). Elements which are not limited by the release of silicon, such as sodium, boron and molybdenum, fall in the first category. The second group of elements, such as manganese, consists of those which are not able to diffuse in glass but are released when the SiO_2 matrix breaks down. The last category is represented by elements which are enriched on the glass surface because of low solubility. The elements detected in our leaching studies have been grouped in Table 4.4 according to the above scheme.

4.D.1.A. Sodium

Sodium is a typical example of the elements in the first group. This element is not released through the dissolution of silica, but rather by diffusion through the glass as already discussed. As expected, sodium found in all experiments was in the soluble form (Table 4.5). In BGW the analysis of sodium released from glass was complicated by the initial presence of sodium at a high concentration in the leachant itself. A blank correction was required, and the error in subtracting the high sodium blank value from a marginally higher number was large. As a result, the Na normalized mass loss data is scattered at all three SA/V ratios and at both temperatures (Figs. 4.20-4.23). As suggested by data in Table 4.4, sodium is leached at a slower rate than silicon in BGW at SA/V = 0.010 cm^{-1}. This is unexpected as sodium normally leaches faster; however, when the scatter in the sodium data is considered this can perhaps be explained. This scatter made it difficult to determine which

Table 4.4. Comparison of leach rates and concentrations of individual elements with silicon for leachates at their respective temperatures and SA/V ratios

$K_i > K_{Si}$		
B	all experiments	
Mo	all experiments	
Na	all experiments, and 90°C	excluding BGW at 0.01 cm^{-1} at 40°
U	all experiments, and 90°C	excluding BGW at 0.01 cm^{-1} at 40°
Al	experiments using DDW and GGW at 0.01 cm^{-1} at 40°C	

$K_i \leq K_{Si}$ $C_i \leq C_{Si}$		
La	all experiments, and 90°C	excluding BGW at 0.85 cm^{-1} at 40°
Mn	all experiments, and 90°C	excluding BGW at 0.85 cm^{-1} at 40°
Sm	all experiments, and 90°C	excluding BGW at 0.85 cm^{-1} at 40°

K_i = Leach rate of element i

K_{Si} = Leach rate of silicon

C_i = Maximum concentration of element i

C_{Si} = Maximum concentration of silicon

Table 4.5. Predominant form of elements found in leachates after 84d

EXPERIMENT	PREDOMINANT FORM OF ELEMENT								
	Al	B	La	Mn	Mo	Na	Si	Sm	U
$0.01cm^{-1}$									
$90^{o}C$									
DDW	SOL 15X	SOL	PPT 2X	SOL 1000X	SOL	SOL	SOL	PPT 5X	PPT
GGW	SOL 1.5X	SOL	PPT	SOL 30X	SOL	SOL	SOL	PPT 10X	PPT
BGW	SOL 9X	SOL	PPT	PPT	SOL	SOL	SOL	PPT 3X	SOL 15X
$40^{o}C$									
DDW	PPT 2X	SOL	PPT	SOL 30X	SOL	SOL	SOL	PPT 10X	PPT
GGW	PPT 2X	SOL	PPT	SOL 3X	SOL	SOL	SOL	PPT 5X	PPT
BGW	SOL 3X	SOL	PPT	PPT	SOL	SOL	SOL	PPT 1.1X	SOL
$0.10cm^{-1}$									
$90^{o}C$									
DDW	SOL 3X	SOL	PPT 10X	PPT 10X	SOL 5X	SOL	SOL	PPT 10X	PPT
GGW	SOL 1.5X	SOL	PPT 20X	PPT 2X	SOL 10X	SOL	SOL	PPT 20X	PPT
BGW	SOL 10X	SOL	PPT	PPT	SOL 100X	SOL	SOL	PPT 5X	SOL 25X
$40^{o}C$									
DDW	PPT 2X	SOL	PPT 10X	SOL 5X	SOL 5X	SOL	SOL	PPT 10X	PPT
GGW	PPT 2X	SOL	PPT 5X	SOL 5X	SOL 5X	SOL	SOL	PPT 5X	PPT
BGW	SOL 5X	SOL	PPT	PPT	SOL 5X	SOL	SOL	PPT 5X	SOL 20X

SOL = Soluble, PPT = Precipitate, N.D. = Not Detected, X = Fold Excess

Table 4.5. Continued

EXPERIMENT	PREDOMINANT FORM OF ELEMENT								
	Al	B	La	Mn	Mo	Na	Si	Sm	U
$0.85cm^{-1}$									
$90^{o}C$									
DDW	SOL 3X	SOL	PPT	PPT 1.1X	SOL 60X	SOL	SOL	PPT 3X	N.D.
GGW	SOL 3X	SOL	PPT	PPT 4X	SOL 50X	SOL	SOL	PPT 3X	N.D.
BGW	SOL 10X	SOL	PPT	PPT	SOL 20X	SOL	SOL	PPT 1.5X	N.D.
$40^{o}C$									
DDW	SOL 4X	SOL	PPT 3X	PPT 2X	SOL 10X	SOL	SOL	PPT 5X	N.D.
GGW	SOL 2X	SOL	PPT 2X	SOL 2X	SOL 15X	SOL	SOL	PPT 3X	N.D.
BGW	SOL 8X	SOL	PPT	PPT	SOL	SOL	SOL	PPT 5X	N.D.

SOL = Soluble, PPT = Precipitate, N.D. = Not Detected, X = Fold Excess

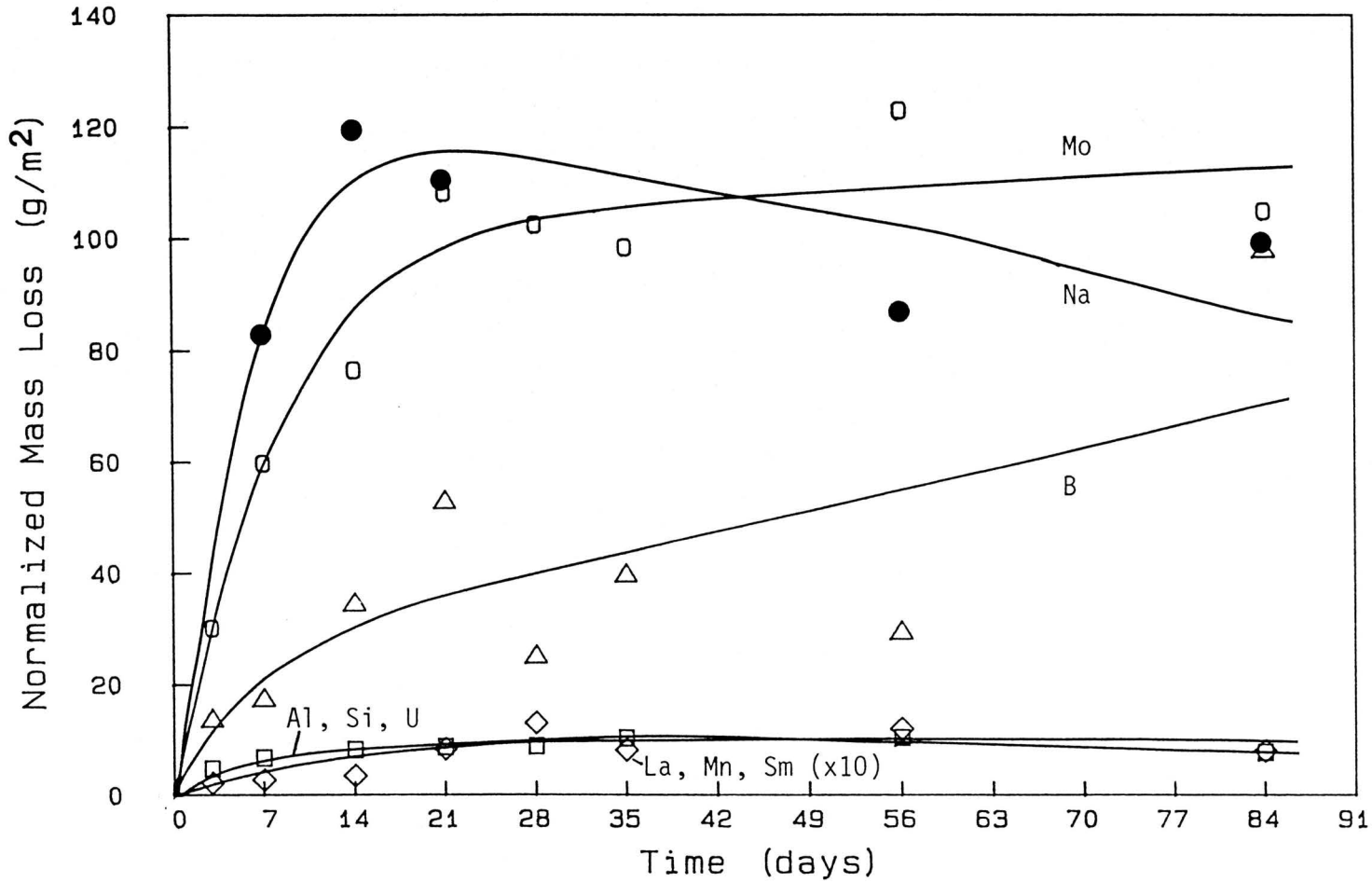

Figure 4.20. Normalized elemental mass loss results for I-117 Glass leached in synthetic Grande Ronde basaltic groundwater at SA/V = 0.10 cm^{-1} and 90°C.

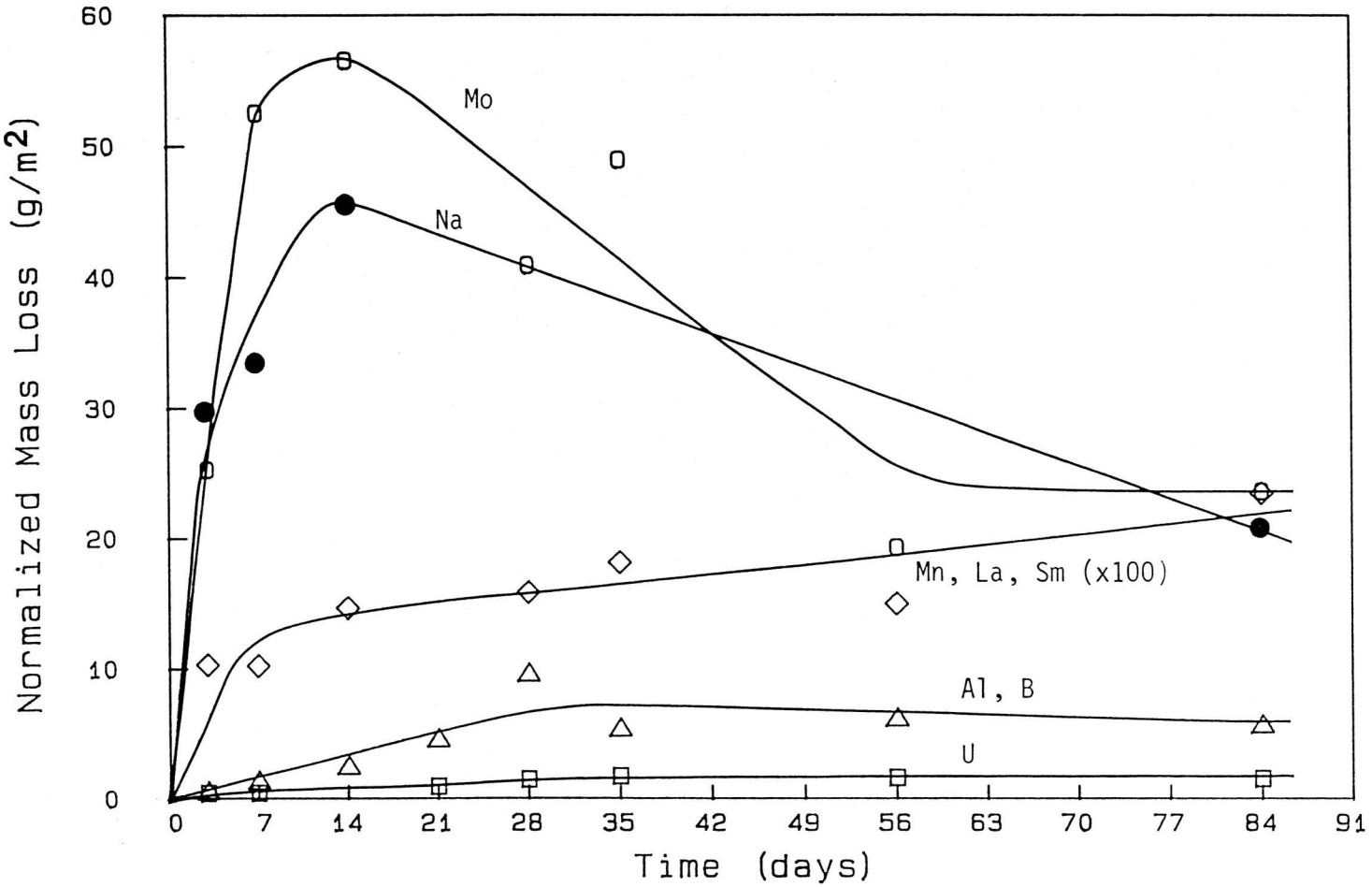

Figure 4.21. Normalized elemental mass loss results for I-117 Glass leached in synthetic Grande Ronde basaltic groundwater at SA/V = 0.10 cm^{-1} and 40°C.

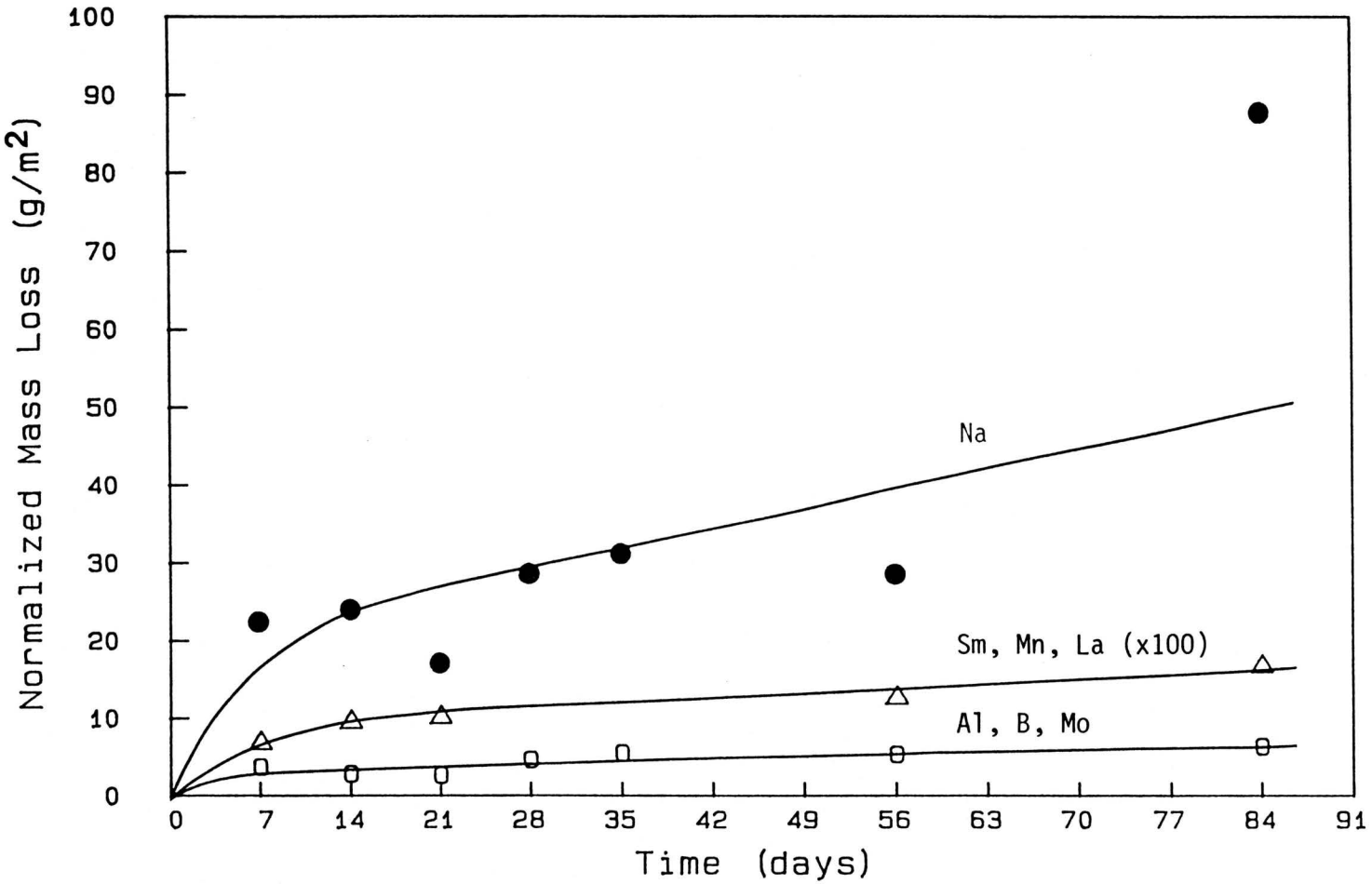

Figure 4.22. Normalized elemental mass loss results for I-117 Glass leached in synthetic Grande Ronde basaltic groundwater at SA/V = 0.85 cm^{-1} and 90°C.

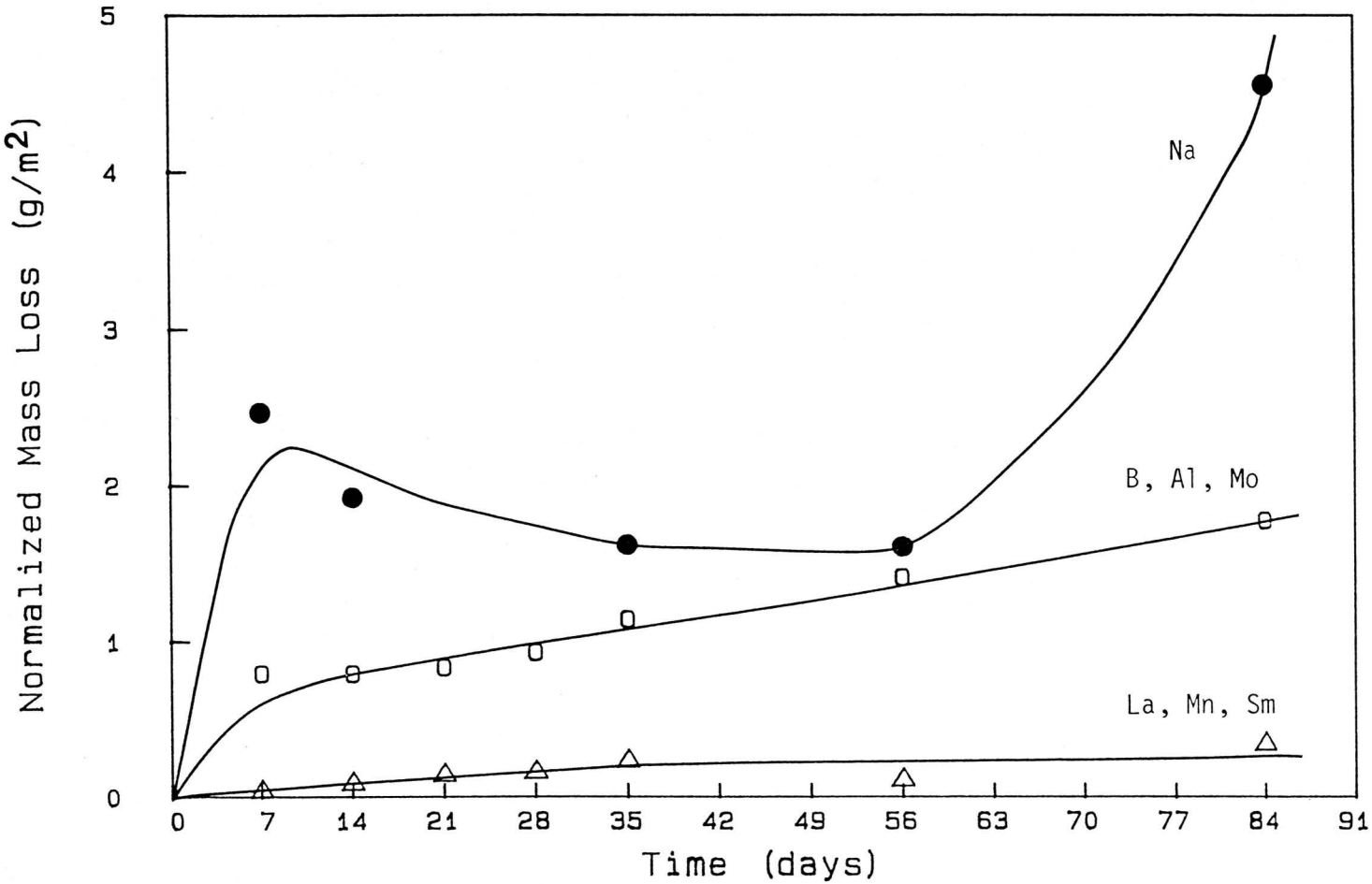

Figure 4.23. Normalized elemental mass loss results for I-117 Glass leached in synthetic Grande Ronde basaltic groundwater at SA/V = 0.85 cm^{-1} and 40°C.

element was leaching at a faster rate.

4.D.1.B. Boron

Boron and molybdenum behaved similarly to sodium in all three leachants (Table 4.4). It was discussed earlier that boron closely followed the sodium release and leached congruently in a few cases (Figs. 4.24-4.27). Often boron is a matrix element used to determine the percentage of the glass network which has been altered. Since no species is known to precipitate boron from solution, it can be used as an accurate indicator of the dissolved glass.

4.D.1.C. Molybdenum

Molybdenum forms polymeric hydroxide anions, and of these, the anionic molybdate species are usually predominant. Molybdenum content was higher in solution over the precipitate in all leaching experiments (Table 4.5). This is not unexpected when the solution pH is taken into consideration. Molybdenum will precipitate as molybdic acid at low pH values (< 4.0). Since at no time a pH < 4.0 was recorded for any of the leachates, most of the molybdenum remained in solution. Molybdenum was found completely in the soluble form only in the experiments at SA/V = 0.010 cm^{-1}, even though the DDW and GGW leachates at this SA/V ratio exhibited the lowest pH values measured (4.60-7.38), and therefore might be expected to have more molybdenum in precipitate form. Although the total amount of molybdenum leached may be highest at SA/V = 0.010 cm^{-1} due to large volume, the actual concentrations of molybdenum measured in the solutions were smaller than at the other two SA/V ratios; and apparently

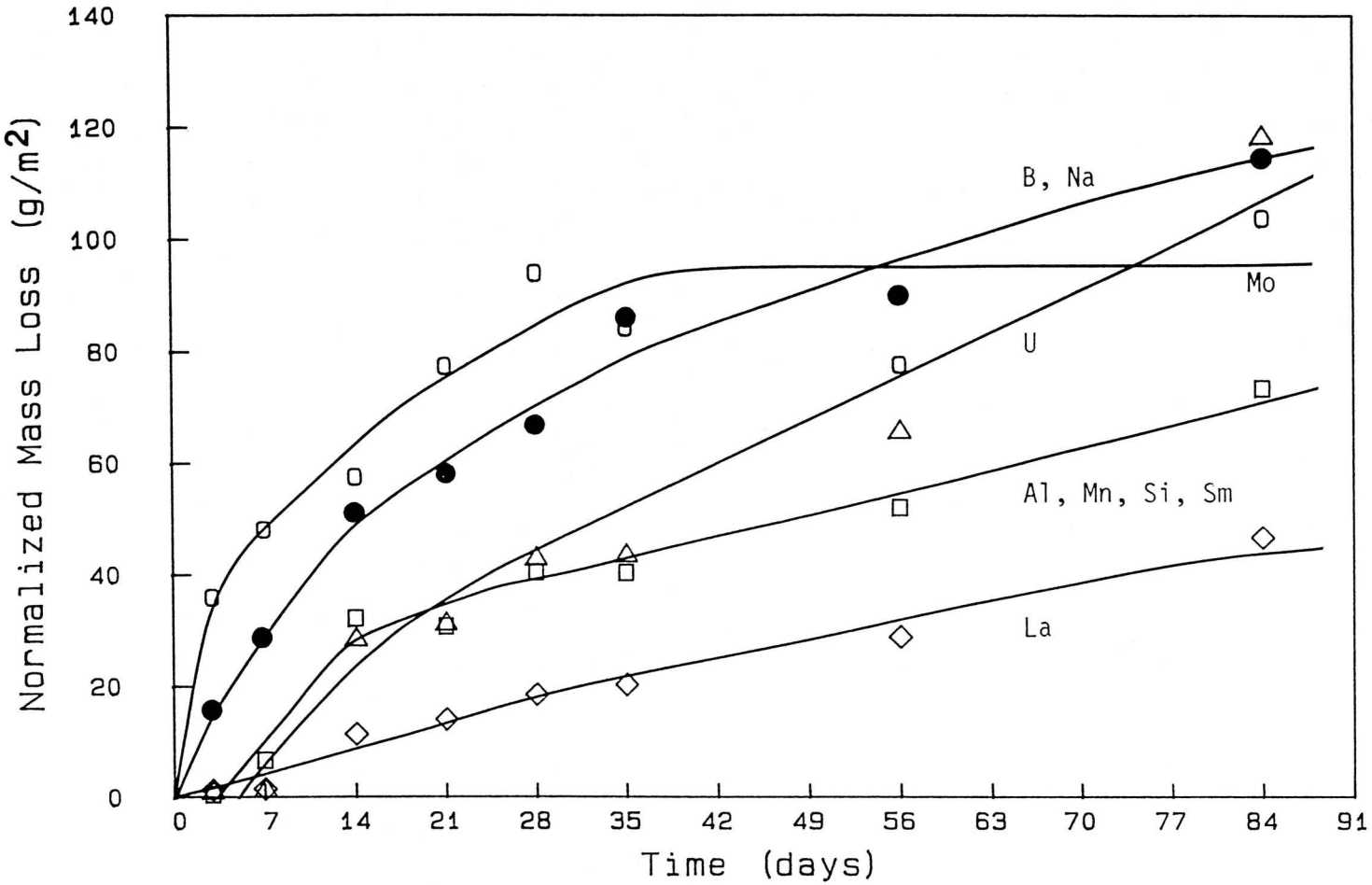

Figure 4.24. Normalized elemental mass loss results for I-117 Glass leached in distilled deionized water at SA/V = 0.010 cm^{-1} and 90°C.

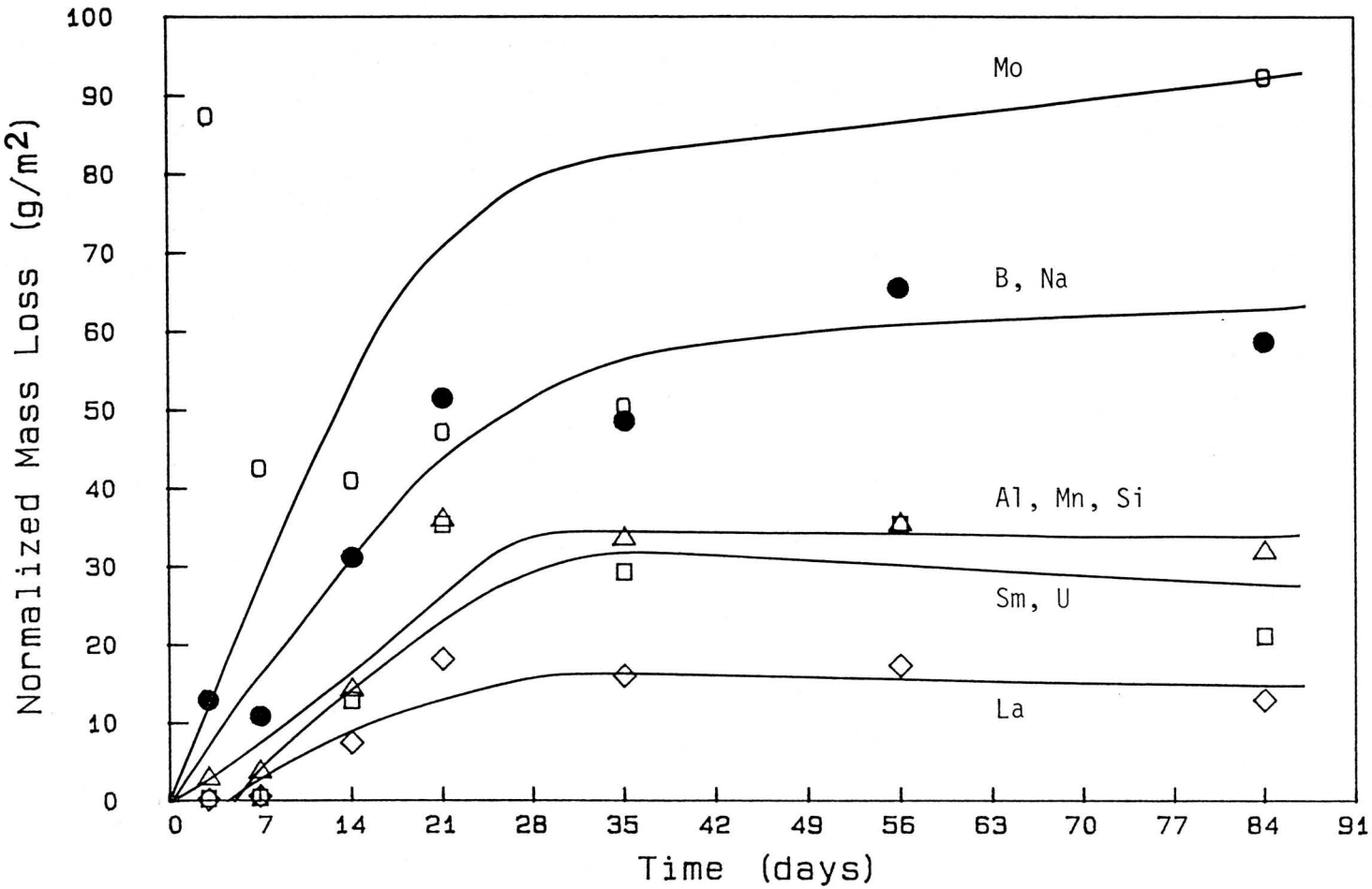

Figure 4.25. Normalized elemental mass loss results for I-117 Glass leached in synthetic granitic groundwater at SA/V = 0.010 cm^{-1} and 90°C.

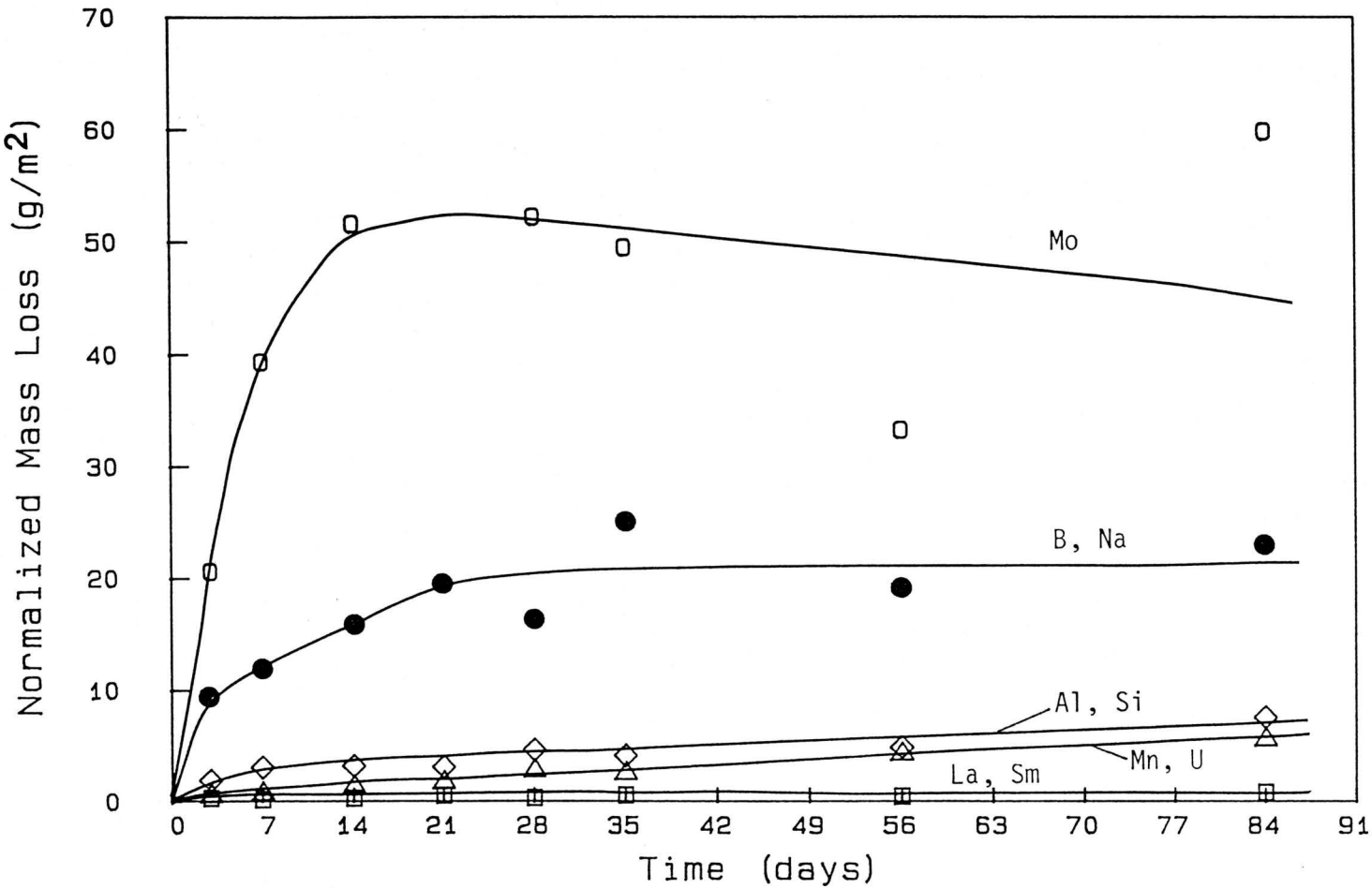

Figure 4.26. Normalized elemental mass loss results for I-117 Glass leached in distilled deionized water at SA/V = 0.10 cm^{-1} and 90°C.

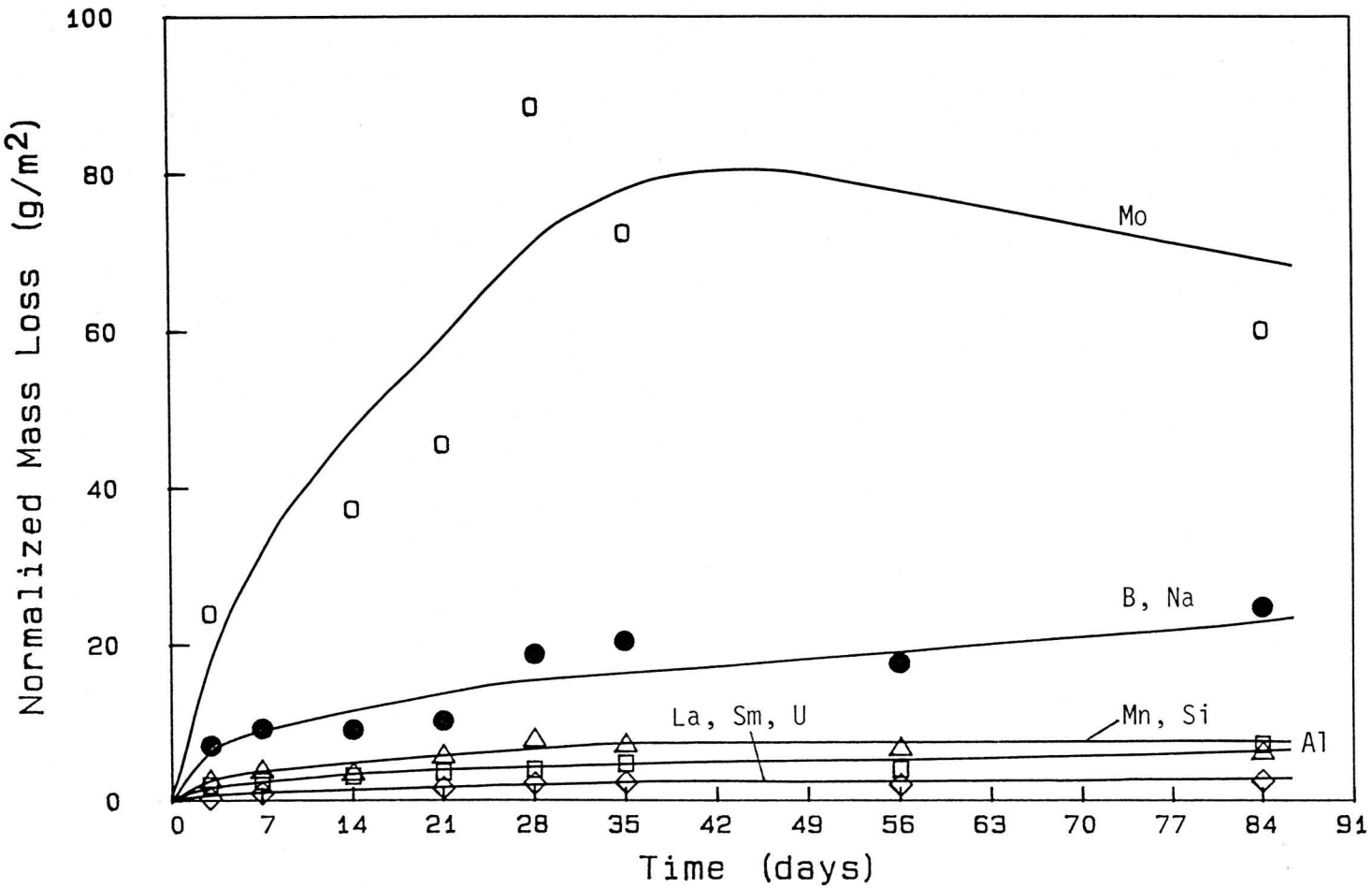

Figure 4.27. Normalized elemental mass loss results for I-117 Glass leached in synthetic granitic groundwater at SA/V = 0.10 cm^{-1} and 90°C.

were insufficient to exceed the solubility product even at lower pH. The leachates at SA/V = 0.85 cm^{-1} showed the next highest extent of solubility for molybdenum which is not surprising considering that all three leachates at 90°C had the highest pH values of any experiment, and even at 40°C the pH of the leachates were higher than in the corresponding experiments at the other SA/V ratios. The fact that any of the molybdenum remained in the precipitated form is surprising considering that the pH for most of the leachates at SA/V = 0.85 cm^{-1} were > 9. It might be that the ionic strengths of these solutions were high enough to force some of the molybdenum out of solution.

In the experiment at SA/V = 0.85 cm^{-1} and 90°C, molybdenum seems to be less soluble in the BGW leachate than in DDW or GGW leachates (Table 4.5). Since BGW has a higher SO_4^{2-} concentration, it would be expected that molybdenum would be more soluble in this groundwater. This discrepancy can only be explained by the fact that the molybdenum found in both the solution and precipitate of the BGW leachates was only slightly above the detection limits of INAA; and large errors are therefore associated with determining the amount of excess molybdenum in solution over precipitate.

Ordinarily, the normalized elemental mass loss of sodium is higher than molybdenum; however, in some of the experiments a reverse situation was observed. At SA/V = 0.010 and 0.10 cm^{-1} at both 40° and 90°C, molybdenum release was higher than Na in all three leachants (Figs. 4.28, 4.29 and 4.30). The sodium release in DDW at 90°C and SA/V = 0.010 cm^{-1} became similar to the molybdenum release by day 28 and then surpassed it. Even in the preliminary experiments involving the CEC Glass (which

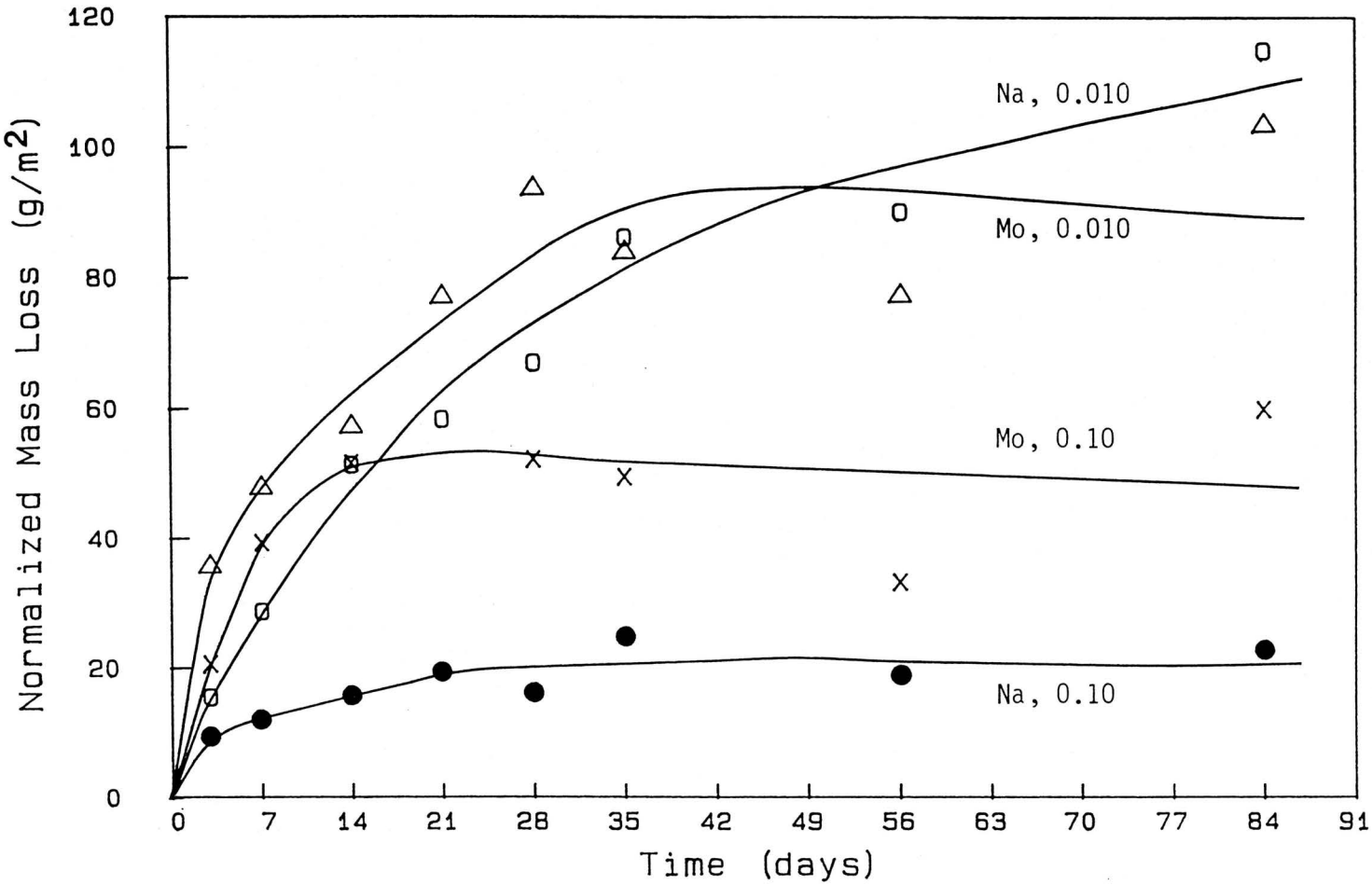

Figure 4.28. Comparison of the normalized elemental mass loss results for sodium and molybdenum leached from I-117 Glass in distilled deionized water at SA/V = 0.010 and 0.10 cm^{-1} and $90^{o}C$.

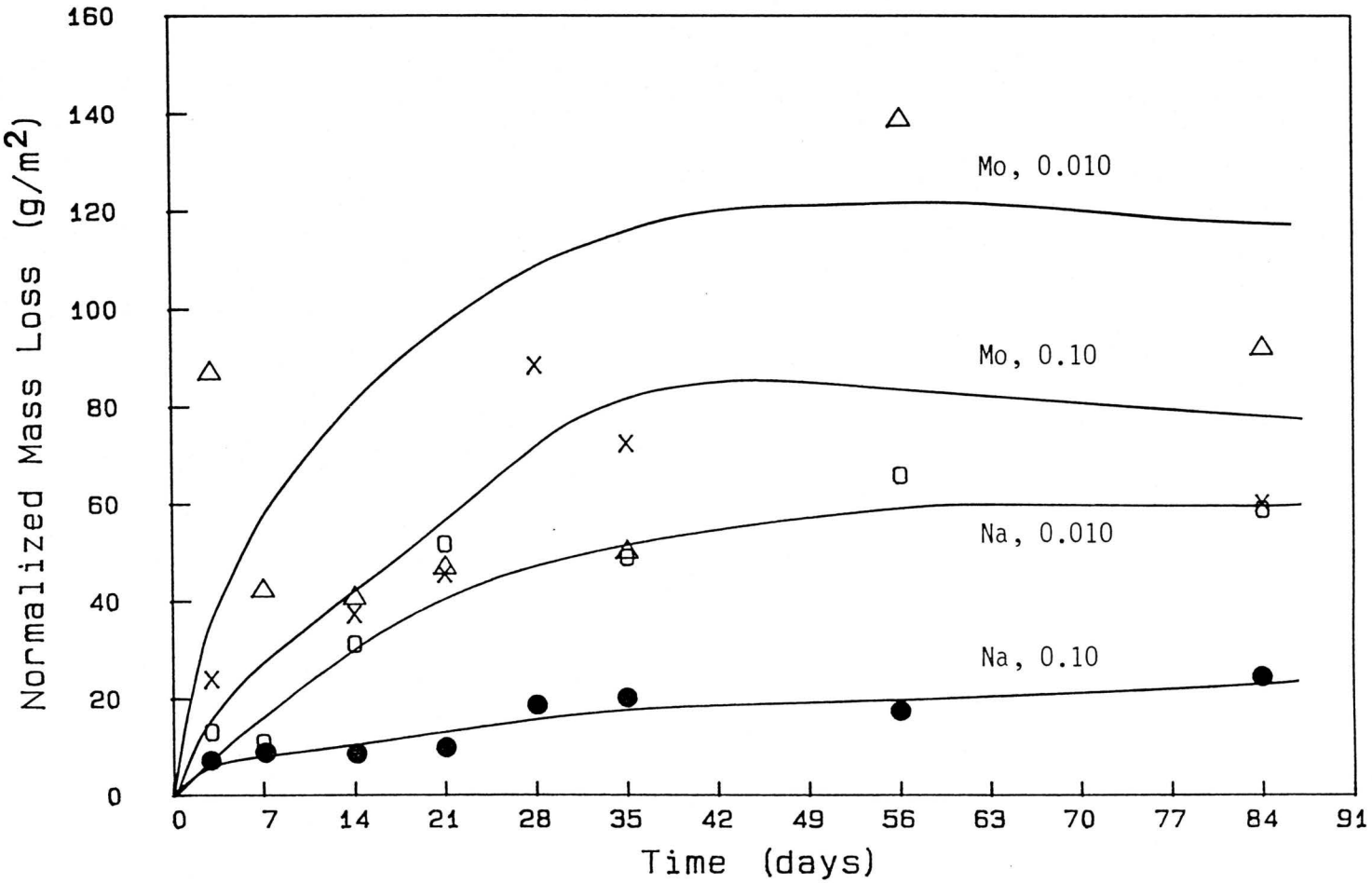

Figure 4.29. Comparison of normalized elemental mass loss results for sodium and molybdenum leached from I-117 glass in synthetic granitic groundwater at SA/V = 0.010 and 0.10 cm^{-1} at $90^{o}C$.

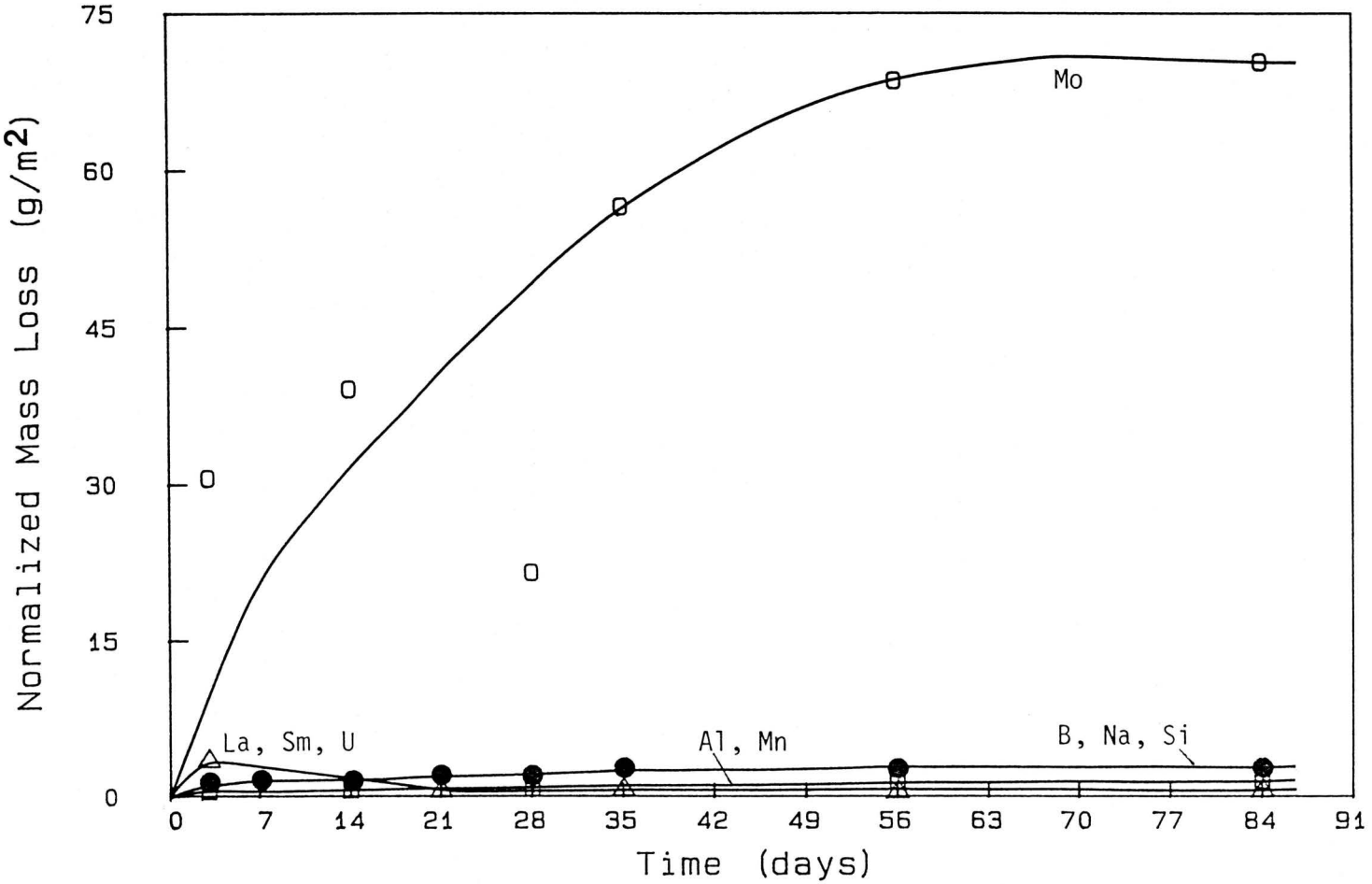

Figure 4.30. Normalized elemental mass loss results for I-117 Glass leached in synthetic granitic groundwater at SA/V = 0.10 cm^{-1} and $40^{o}C$.

closely resembles I-117 Glass), the molybdenum leach rates were higher than those of sodium (Figs. 4.3 and 4.6). The glass in these preliminary experiments was leached at room temperature and a SA/V = 0.10 cm^{-1}. Some other researchers have also observed molybdenum to leach faster than sodium. Kelm et al. leached GP98/12 glass at 100°C and 100 bar for 30d in deionized water and found the Mo leach rate to be almost double that of sodium (85IAEA1). Strachan's work also revealed a higher normalized mass loss for molybdenum leached from PNL 76-68 glass in silicate water at 90°C and SA/V = 0.10 cm^{-1} (83STRA1). The sodium normalized mass losses of all leachants at SA/V = 0.85 cm^{-1} and both temperatures in our work exceeded those of molybdenum (Fig. 4.31). The differences in the releases of sodium and molybdenum in the experiments can be explained by the difference in the glass used at SA/V = 0.010 and 0.10 cm^{-1} and that used at SA/V = 0.85 cm^{-1}. As explained previously, if the sodium incorporated in the first batch of glass was in a form which was not as easily removed from the lattice as in the second batch then this might explain why the sodium release was lower than molybdenum in the experiments at SA/V = 0.010 and 0.10 cm^{-1}.

4.D.1.D. Uranium

The behaviour of uranium leached from glass is important due to the presence of this element in spent fuel and in small quantities in the waste obtained after reprocessing. The lanthanides and in particular the actinides are of interest as these are the elements of major concern in HLW. Uranium in borosilicate glasses can exist as an equilibrium mixture of U(IV), U(V) and U(VI) where the exact concentration

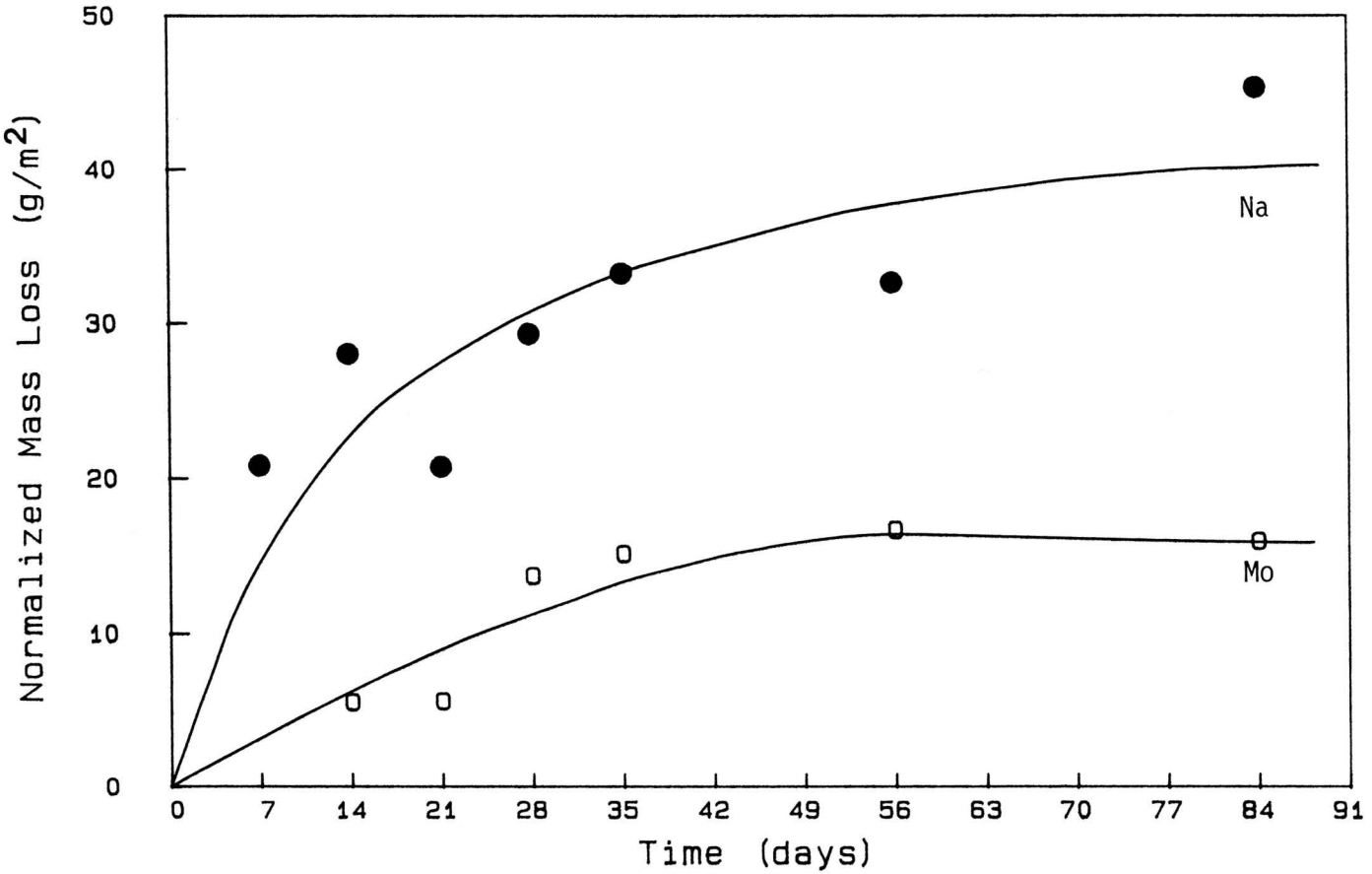

Figure 4.31. Comparison of normalized elemental mass loss results for sodium and molybdenum leached from I-117 Glass in distilled deionized water at SA/V = 0.85 cm^{-1} and 90°C.

of the individual species depends upon the melting temperature and oxygen fugacity. The characteristics of the glass will depend on the state of uranium stabilized in it, while the actual leaching can be affected in two ways: (1) through stabilization of the glass-forming network by making it more corrosion resistant and (2) through the solubility of the individual ions in the leachate as the glass dissolves. Generally U(VI) is more soluble than U(IV) in the glass melt.

A clean UO_2 surface which is exposed to an oxygen-containing solution will be rapidly oxidized, and may then dissolve to form uranyl ions or complex ions depending upon the nature of the solution (81WANG1):

$$2U_4O_9 + 16H^+ + 3O_2 \longrightarrow 8UO_2^{2+} + 8H_2O \qquad (4.8)$$

The uranyl ion, UO_2^{2+}, forms a slightly soluble hydroxide in alkaline solutions. Uranium forms complex ions with carbonates, phosphates and sulfates in natural waters, the exact nature of which depends on the solution pH. The solubility of U(VI) is greatly increased by the formation of carbonate complexes such as $UO_2(CO_3)_2^{-2}$ and $UO_2(CO_3)_3^{4-}$. Thus uranium in the +6 state is somewhat mobile in weakly acidic solutions, and again at neutral or alkaline pH in presence of carbonate ions.

Uranium in DDW and GGW at both 90°C and 40°C and at SA/V = 0.010 as well as 0.10 cm^{-1} was present in the precipitate form only (Table 4.5). This observation can be explained through pH of these solutions. Both DDW and GGW had a pH between 4.5 and 8.0 which would favour the formation of the insoluble hydroxide. In contrast, uranium detected in the BGW at these two SA/V showed a predominance of the soluble form over the

precipitate. Although BGW has a much higher pH than either DDW or GGW, suggesting hydroxide formation, it also has very high carbonate and sulfate concentrations. The fact that the uranium is mainly in the soluble form suggests that carbonate and possibly sulfate complexes were formed in the leachate. Uranium levels in the samples leached at both temperatures for SA/V = 0.85 cm^{-1} were below detection limits. This was not unexpected at the highest SA/V ratio as the uranium content of the glass used in these experiments was only 21 ppm. Typical uranium normalized mass losses are illustrated by Figs. 4.32 and 4.33 for the three leachants at SA/V = 0.010 cm^{-1} and 90°C.

4.D.1.E. Lanthanum

Lanthanum can be expected to precipitate as hydroxide at a pH around 7.8. Table 4.5 shows that the lanthanum present was in excess in the precipitate over solution in GGW and DDW at both 90°C and 40°C at SA/V = 0.10 cm^{-1}. The pH values for the leachate solutions were around 7.3, so it is not surprising that the lanthanum was distributed between solution and precipitate. In the case of BGW, all the lanthanum appeared in a solid form as expected since the pH was above 9. At SA/V = 0.010 cm^{-1}, only the DDW leachates at 90°C showed any lanthanum in a soluble form. The pH of these leachates were lower than in GGW or BGW which kept some lanthanum in the soluble form.

Since lanthanum was distributed between the solution and precipitate of the DDW and GGW leachates at SA/V = 0.10 and 0.85 cm^{-1}, it is surprising that this element was found in the precipitate alone at SA/V = 0.010 cm^{-1}, since the pH of the leachates at this SA/V ratio were lower than in the

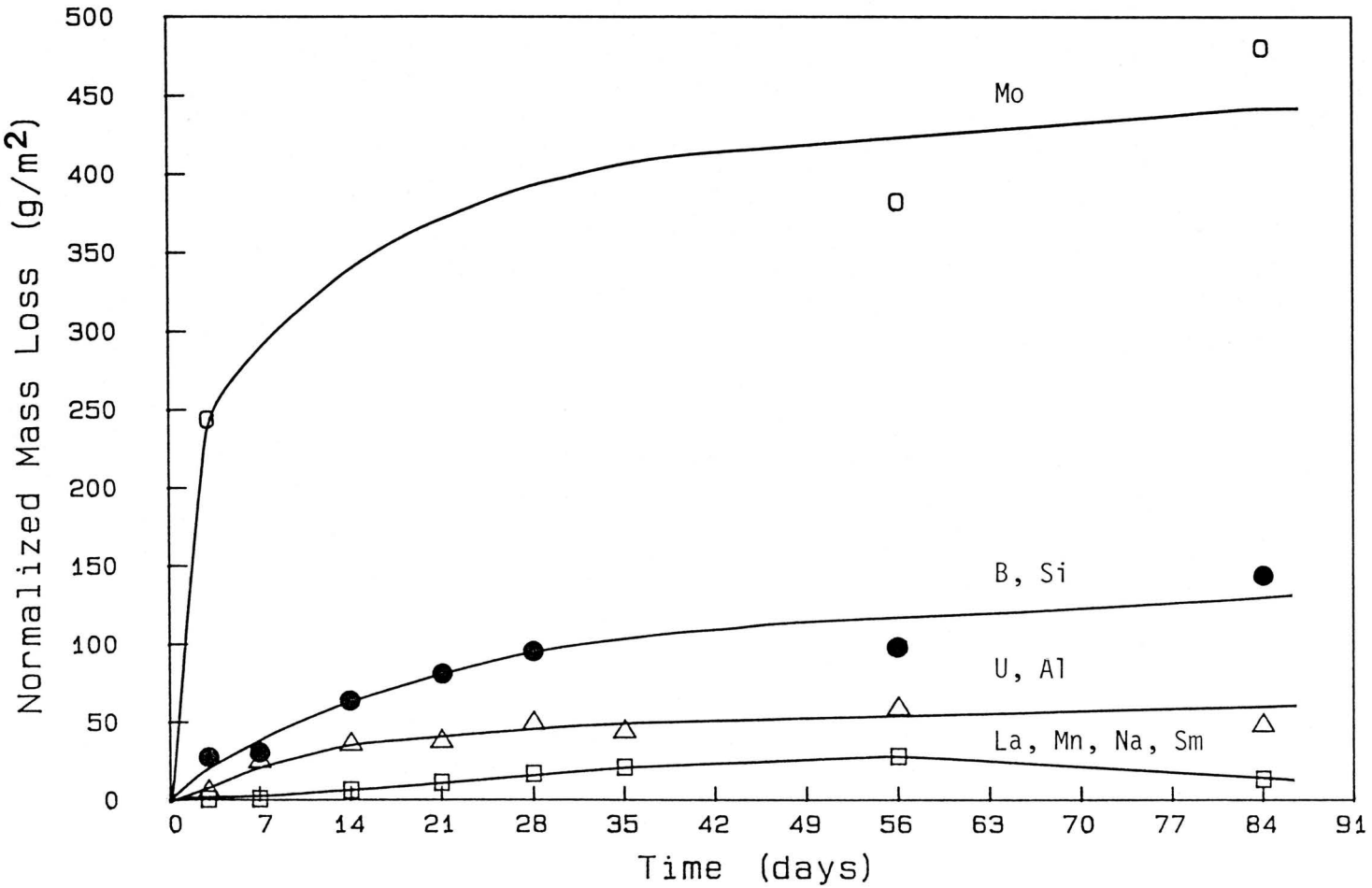

Figure 4.32. Normalized elemental mass loss results for I-117 Glass leached in synthetic Grande Ronde basaltic groundwater at SA/V = 0.010 cm^{-1} and 90°C.

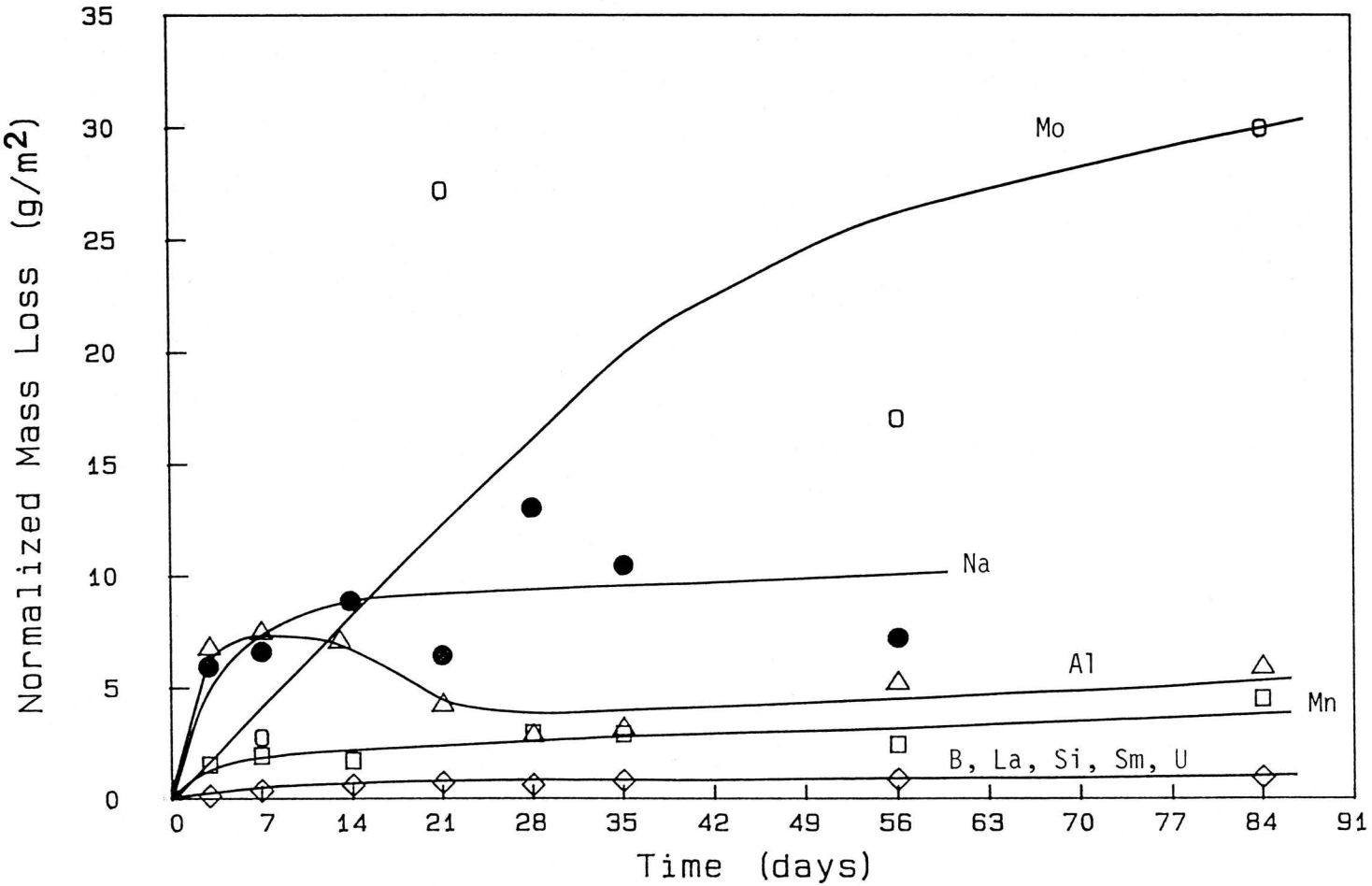

Figure 4.33. Normalized elemental mass loss results for I-117 Glass leached in synthetic granitic groundwater at SA/V = 0.010 cm^{-1} and 40°C.

other two. One explanation can be that the larger volume at SA/V = 0.010cm^{-1} experiments leads to a smaller concentration of lanthanum in solution. Although this amount of lanthanum is high enough to exceed its solubility product, the concentration of lanthanum remaining in solution is below the detection limit of the INAA method. At SA/V = 0.85 cm^{-1} all of the lanthanum detected was in the form of a precipitate except in DDW and GGW at 40°C as these were the only samples with low pH ($\sim$ 7.5 - 8). All other leachates (all BGW and DDW and GGW at 90°C) had pH values over 9. Figures 4.34 and 4.35 show the results of lanthanum normalized mass loss at SA/V = 0.85 cm^{-1} at both 40° and 90°C for DDW.

4.D.1.F. Manganese

Precipitation of manganese occurs at about pH 7, and the degree of precipitation increases in the presence of species such as carbonates or silicates in sufficient quantities. Manganese hydroxide may also form. In the BGW leachates at both temperatures and regardless of the SA/V ratio, manganese was always found exclusively in the form of a precipitate (Table 4.5). Again this may be attributed to the high pH and carbonate concentration. Manganese in DDW and GGW leachates at a SA/V ratio of 0.10 cm^{-1} and 90°C was found largely in the precipitate. A similar trend was observed at SA/V = 0.85 cm^{-1} at 90°C for DDW and GGW leachates and at 40°C for DDW as well. In all other cases involving DDW and GGW, manganese was found predominately in solution. At SA/V = 0.85 cm^{-1} and 90°C both DDW and GGW leachates had pH's above 9 suggesting manganese would be expected to precipitate almost completely as was observed. At SA/V = 0.10 cm^{-1} manganese appears to have leached to such

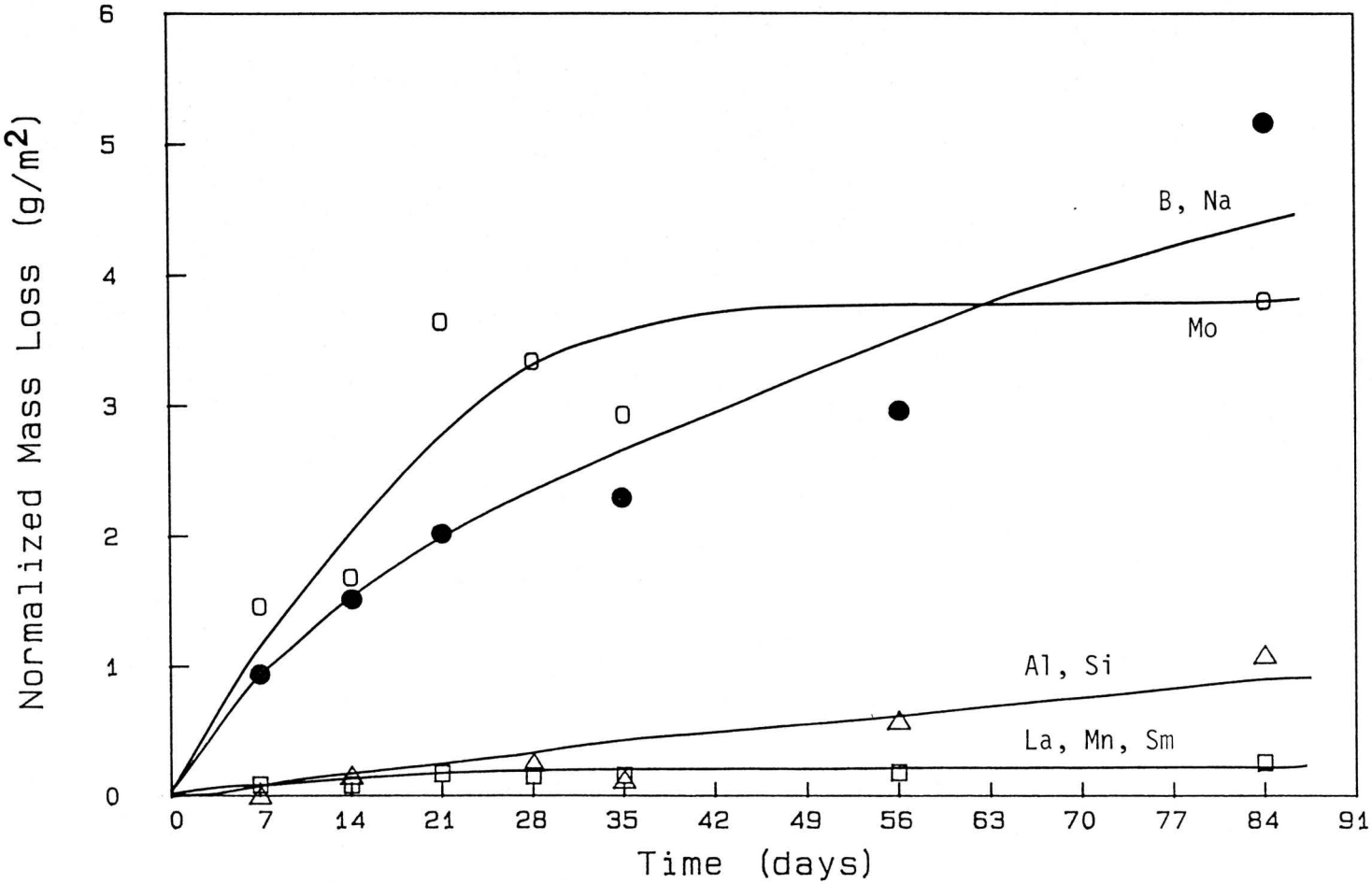

Figure 4.34. Normalized elemental mass loss results for I-117 Glass leached in distilled deionized water at SA/V = 0.85 cm^{-1} and 40°C.

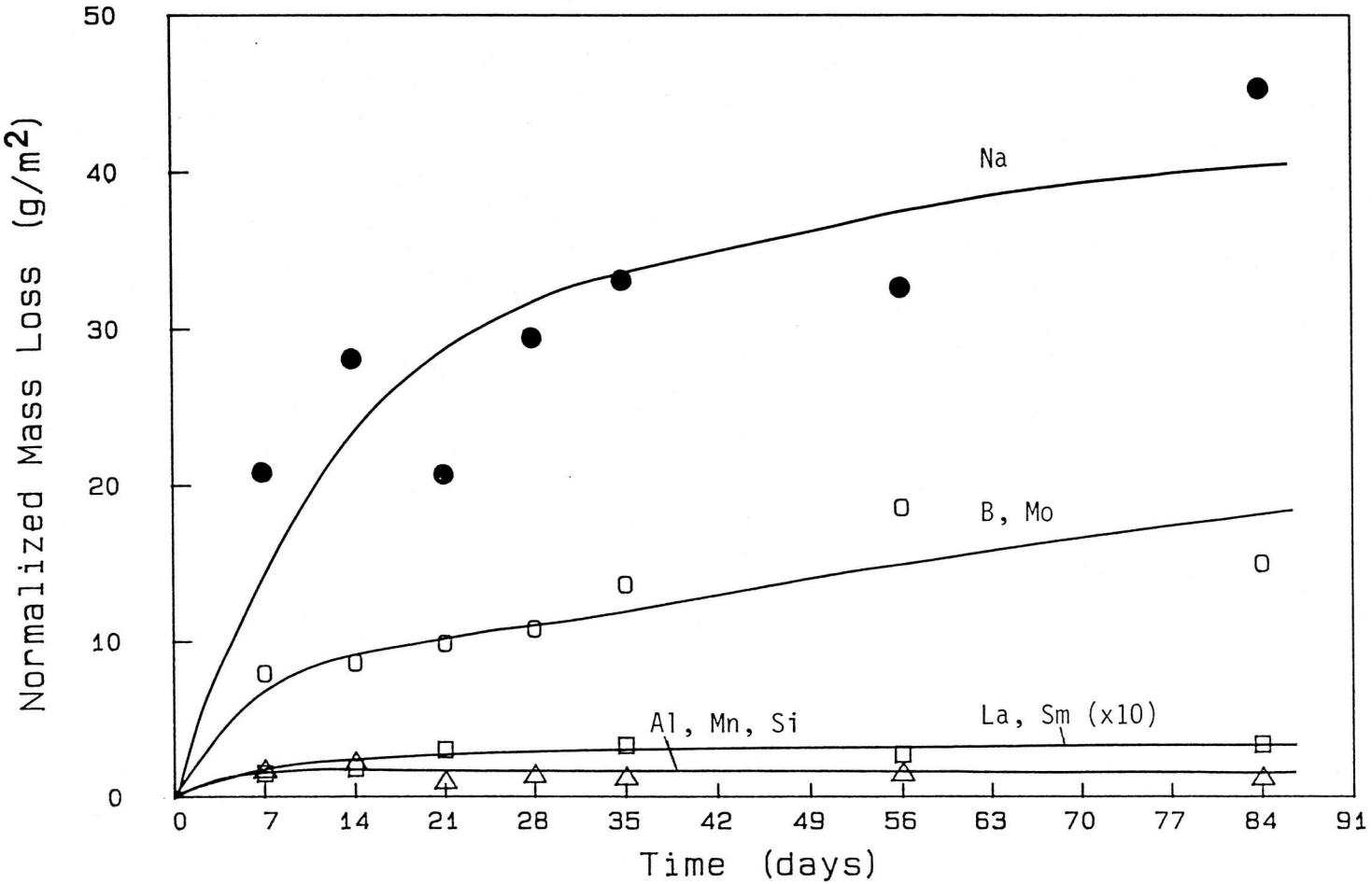

Figure 4.35. Normalized elemental mass loss results for I-117 Glass leached in distilled deionized water at SA/V = 0.85 cm^{-1} and 90°C.

an extent in DDW and GGW at 90°C that the concentration exceeded the solubility product at the solution pH, unlike the corresponding experiments at SA/V = 0.010 cm^{-1}. Again the pH of the DDW and GGW leachates at SA/V = 0.10 cm^{-1} were higher than at 0.010 cm^{-1} which explains the precipitation of manganese. Representative plots of the normalized elemental mass loss of manganese are given in Figs. 4.36 and 4.37.

Managanese is expected to leach to a smaller extent at 40°C than at 90°C; then it is not unreasonable to expect manganese to remain predominantly in solution in DDW and GGW at the two lowest SA/V ratios. The lower pH of the leachates at this temperature (5.5-7.5) also helped to keep the manganese mainly in soluble forms. At SA/V = 0.85 cm^{-1}, however, even at 40°C in DDW the concentration of manganese in solution was now high enough to have significantly exceeded the solubility product and manganese appeared more in the precipitated form.

4.D.1.G. Samarium

Figure 4.38 shows a plot of samarium normalized mass loss for GGW at SA/V = 0.85 cm^{-1} and 40°C which is typical for this element. Samarium is another element expected to precipitate as hydroxide at pH greater than 7. All samples analyzed showed the precipitate to contain an excess of samarium compared to that in solution. Although this was not unexpected, it was surprising that in the case of the BGW leachates which exhibited the highest pH from beginning to the end of the experiments, samarium content in precipitate over the solution was less than in the case of DDW and GGW. At such a high pH of BGW leachates (about 9.3) it is expected that samarium would be almost completely precipitated; however, instead

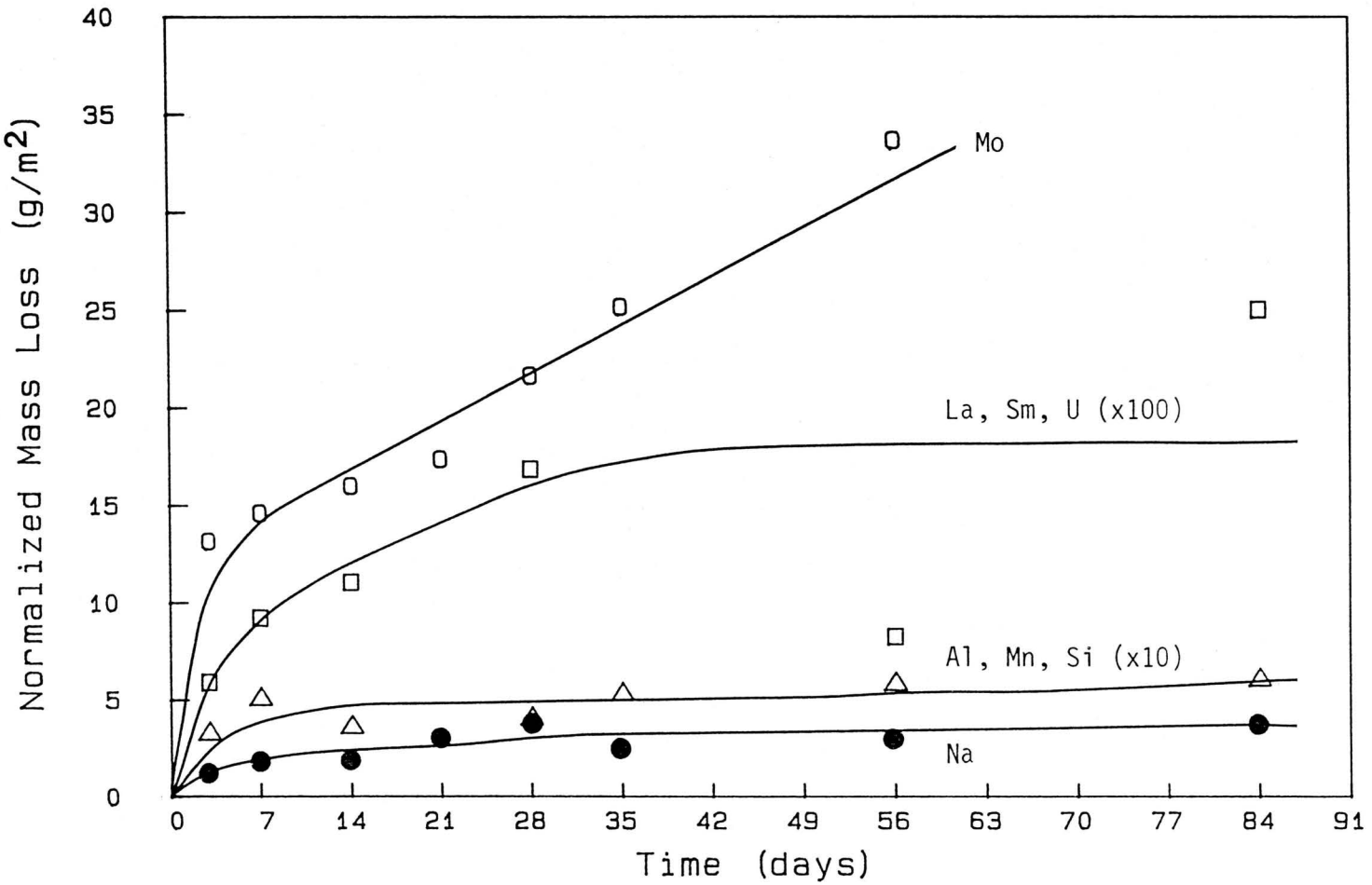

Figure 4.36. Normalized elemental mass loss results for I-117 Glass leached in distilled deionized water at SA/V = 0.10 cm^{-1} and 40°C.

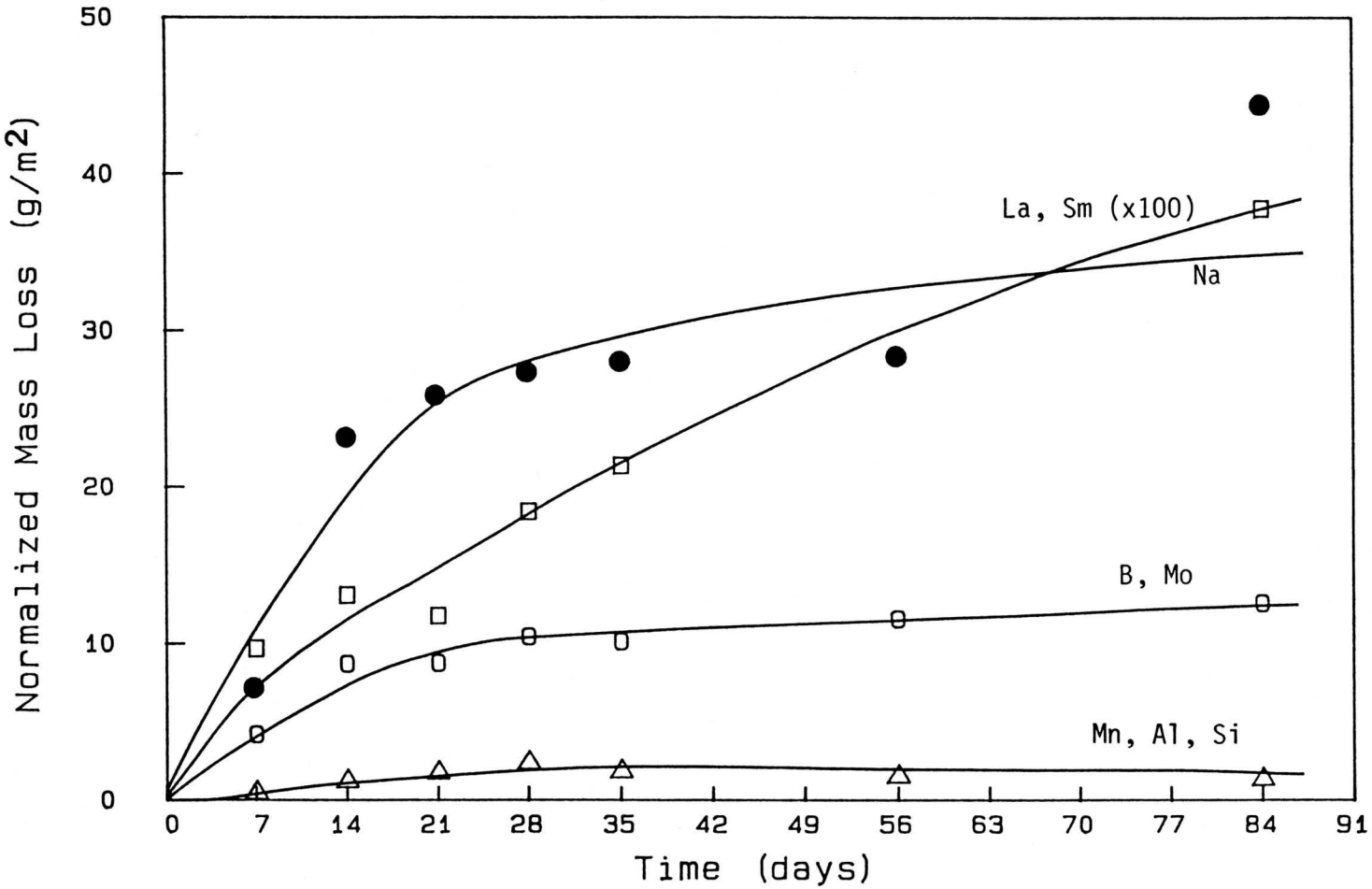

Figure 4.37. Normalized elemental mass loss results for I-117 Glass leached in synthetic granitic groundwater at SA/V = 0.85 cm^{-1} and 90°C.

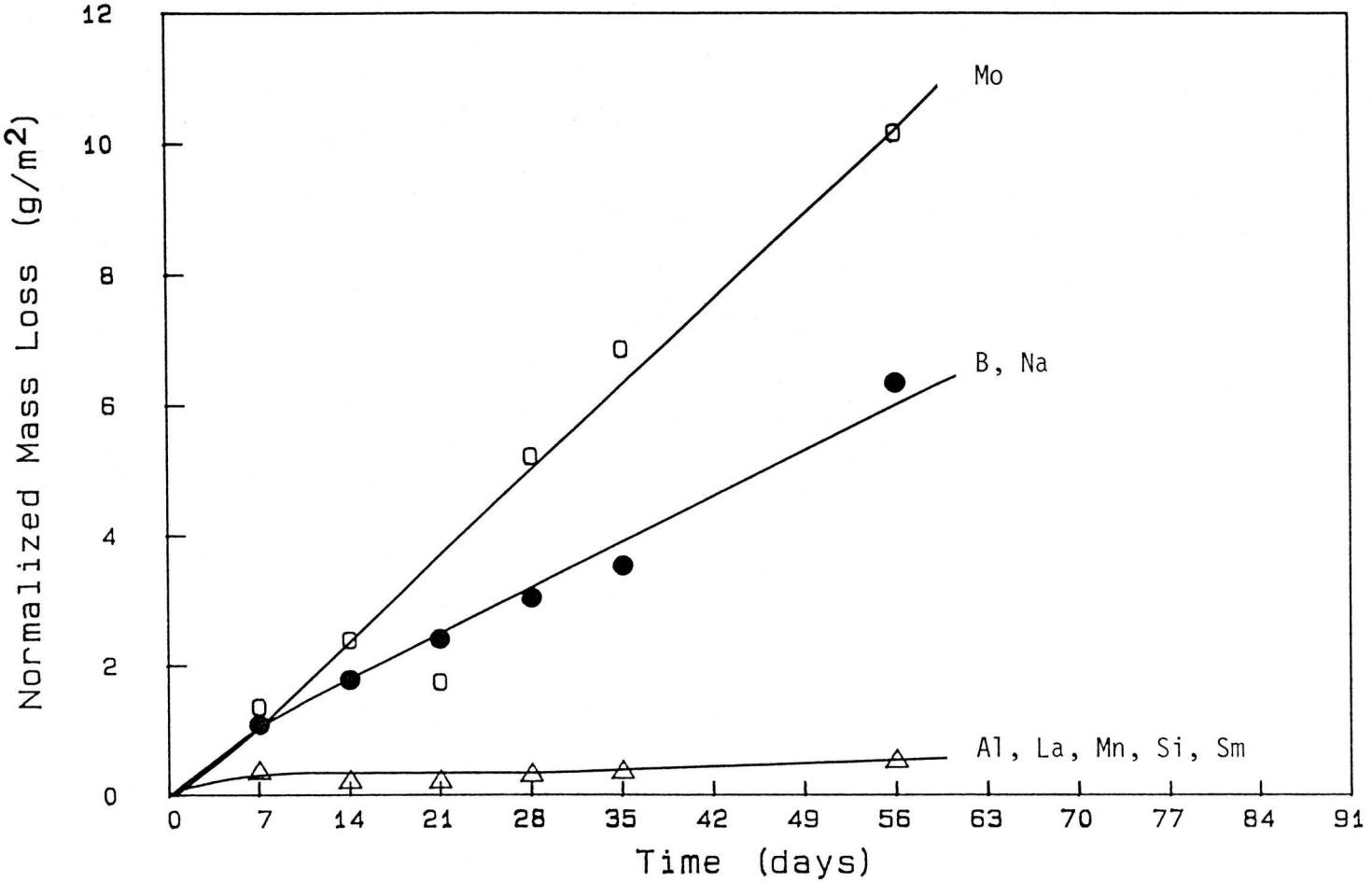

Figure 4.38. Normalized elemental mass loss results for I-117 Glass leached in synthetic granitic groundwater at SA/V = 0.85 cm^{-1} and 40°C.

samarium remained partially in solution. This situation can be explained by the formation of soluble anionic samarium complexes with the carbonate ions present in the BGW solution. These complexes are of high stability and expected to be similar to those found for europium (89RA01).

4.D.1.H. Aluminum

The precipitation of hydrated aluminum oxide and hydroxide begins at a pH slightly above 4 and increases to a maximum around 6-7, after which it again increases in solubility. This is evident from the results shown in Table 4.5. Aluminum was found predominately in the soluble form in all solutions of pH >8 (BGW leachant and all experiments at SA/V = 0.85 cm^{-1}). The only cases where aluminum was found in excess in precipitate compared to that in the soluble form was in experiments at 40°C for SA/V = 0.010 and 0.10 cm^{-1}. Since the pH of the above solutions were 5.5-7.5, this trend is understandable; however, at 90°C at these two SA/V ratios the solution pH was again about 4.5-8.2, and yet the aluminum was in excess in solution over the precipitate. This observation can be explained in terms of a temperature effect as aluminum is more soluble at the higher temperature. Examples of aluminum normalized mass loss are given in Figs. 4.39 and 4.40.

4.D.1.I. Elemental Analysis of Precipitate

The results of the elemental analyses of the precipitated material collected from the leachate solutions are presented in Tables 4.6-4.8. Each table represents the highest concentration found for the elements in terms of normalized mass loss during 84d of leaching at the respective

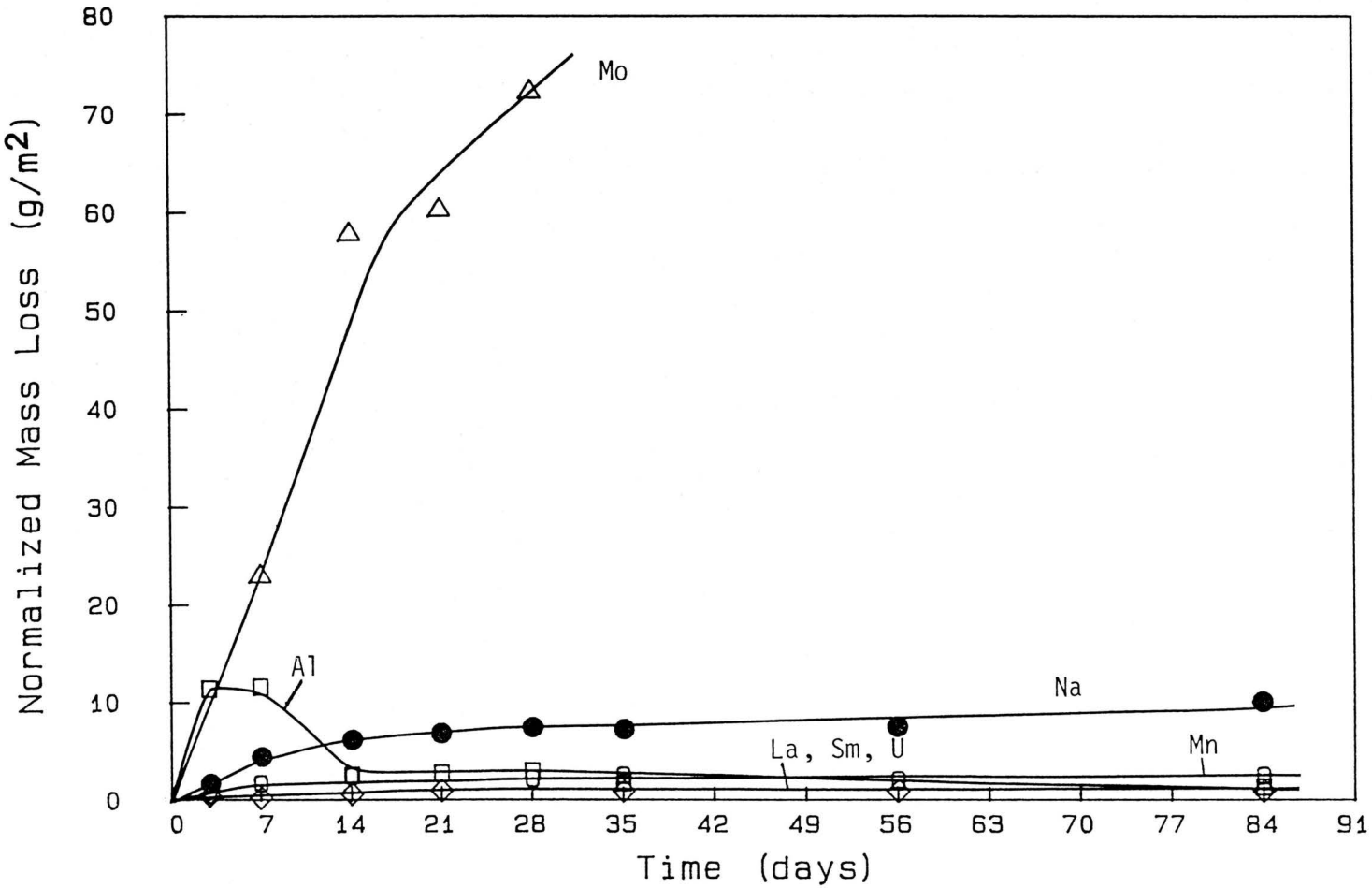

Figure 4.39. Normalized elemental mass loss results for I-117 Glass leached in distilled deionized water at SA/V = 0.010 cm^{-1} and 40°C.

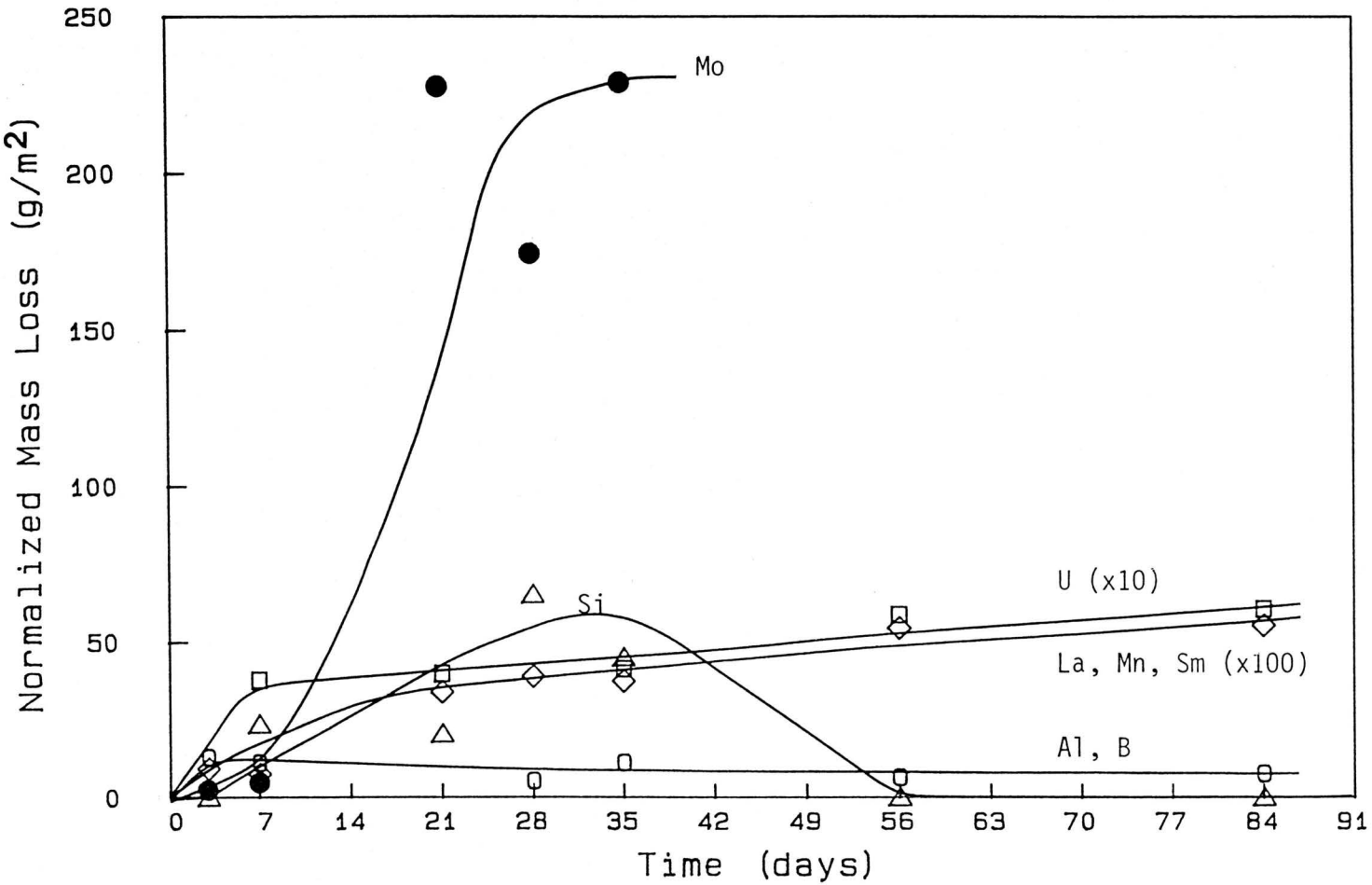

Figure 4.40. Normalized elemental mass loss results for I-117 Glass leached in synthetic Grande Ronde basaltic groundwater at SA/V = 0.010 cm^{-1} and 40°C.

Table 4.6. Maximum normalized elemental mass loss of precipitate found in leachate solutions after 84 d at SA/V = 0.010 cm^{-1}

	DDW		GGW		BGW	
ELEMENT	90°C	40°C	90°C	40°C	90°C	40°C
Al	9.31	10.8	8.79	5.85	7.12	6.47
Ce	67.6	≤ 0.193	0.531	≤ 0.941	0.367	≤ 0.973
Cs	≤ 5.83	235.8	7.62	421.8	≤ 6.97	≤ 68.1
Fe	≤ 10.9	≤ 8.85	≤ 5.61	≤ 53.6	≤ 7.83	≤ 57.4
La	41.2	0.427	16.7	1.54	3.94	0.364
Mn	1.11	1.68	11.7	0.958	14.9	1.34
Mo	≤ 0.568	≤ 0.307	≤ 0.687	≤ 0.226	≤ 1.98	≤ 0.921
Nd	569	≤ 1.39	104	≤ 7.11	14.6	≤ 7.60
Ni	≤ 21.4	≤ 16.7	≤ 11.8	≤ 101	≤ 19.4	≤ 191
Pr	59.6	≤ 0.499	17.7	≤ 1.89	3.43	≤ 1.33
Sm	77.3	0.810	34.8	0.914	8.52	0.284
U	119	1.32	46.2	1.56	5.70	≤ 0.151
W	0.939	≤ 0.643	0.934	4.10	2.88	6.46

Table 4.7. Maximum normalized elemental mass loss of precipitate found in leachate solutions after 84 d at SA/V = 0.10 cm^{-1}

	DDW		GGW		BGW	
ELEMENT	90°C	40°C	90°C	40°C	90°C	40°C
Al	3.96	1.48	4.31	1.21	1.27	1.26
Ce	6.82	12.1	32.0	10.2	3.93	2.78
Cs	3.01	11.8	5.86	4.09	1.24	27.5
Fe	5.78	5.11	10.7	12.6	$\leq$ 4.99	4.28
La	0.724	0.179	2.43	0.335	0.232	0.153
Mn	3.11	0.148	4.36	0.373	1.33	0.359
Mo	16.7	5.74	8.84	8.75	2.32	0.994
Nd	9.18	7.11	36.7	2.37	$\leq$ 0.293	1.55
Ni	13.0	$\leq$ 4.04	31.0	69.7	$\leq$ 7.21	27.1
Pr	0.918	1.12	3.33	0.321	0.0722	0.225
Sm	0.810	0.228	3.74	0.473	0.449	0.0925
U	5.72	0.162	6.32	0.661	0.497	0.146
W	2.12	1.31	2.77	1.49	1.50	0.269

Table 4.8. Maximum normalized elemental mass loss of precipitate found in leachate solutions after 84 d at SA/V = 0.85 cm^{-1}

	DDW		GGW		BGW	
ELEMENT	90°C	40°C	90°C	40°C	90°C	40°C
Al	1.13	0.648	0.947	0.723	0.780	0.540
Ce	0.180	0.162	0.0704	1.87	1.51	0.788
Cs	≤ 661	≤ 73.9	≤ 58.4	≤ 73.3	≤ 53.2	≤ 37.1
Fe	≤ 4.27	≤ 7.25	≤ 5.87	≤ 6.49	≤ 5.22	≤ 3.96
La	0.506	0.135	0.347	0.165	0.322	0.245
Mn	1.57	0.174	1.67	0.306	2.07	0.109
Mo	0.524	≤ 0.661	0.395	≤ 0.781	1.16	1.52
Nd	3.48	≤ 3.24	≤ 1.03	≤ 3.60	≤ 0.810	≤ 0.639
Ni	≤ 10.5	≤ 15.6	≤ 12.3	≤ 15.4	≤ 11.3	≤ 7.94
Pr	0.165	≤ 0.0797	≤ 0.0586	0.0672	≤ 0.0991	≤ 0.172
Sm	0.661	0.182	0.344	0.186	0.186	0.361
U	≤ 0.135	≤ 0.657	≤ 0.619	≤ 0.138	≤ 0.242	≤ 0.172
W	≤ 3.60	≤ 2.24	≤ 1.58	≤ 1.51	≤ 2.38	≤ 3.26

SA/V ratio. Some unusual occurrences were observed. Certain elements were found in the precipitate but not detected in the solution, namely Ce, Cs, Fe, Nd, Ni, Pr and W. Detection limits in terms of the decision limit (L_C) were generally higher in the leachate solutions compared to that in the precipitates due to background interferences and differences in sample geometries. It is possible that some of these elements might have been present in the solution but their concentrations were below the detection limits.

4.D.1.I.1. Cesium

Cesium was not expected to be present in the precipitates collected; however, it was found in samples at both SA/V = 0.010 and 0.10 cm^{-1} (Tables 4.6 and 4.7). Cesium, like sodium, should have remained in solution. It is possible that cesium was being sorbed by a gel layer on the corroded glass. Strachan observed that cesium was sorbed by a zinc silicate layer formed on PNL 76-68 glass leached at 90°C in deionized water and silicate water at SA/V = 0.10 cm^{-1} (83STRA1). If such a layer formed on the glass in our study and part of it flaked off during leaching, it would then be collected with the other precipitated material. Cesium can also form sparingly soluble double salts with Al, Mg, Ni, Co and some rare earth elements such as Nd and Pr (65PERE1). In addition, cesium forms compounds of low solubility with silicomolybdic acid. Cesium was found in precipitates of all three leachants at SA/V = 0.10 cm^{-1} and both temperatures (Table 4.6);however, at SA/V = 0.010 cm^{-1}, it was detected only in three types of sample (DDW at 40°C and GGW at 40° and 90°C) as shown in Table 4.7. Although the amount of cesium released

by the glass at the lower SA/V ratio (0.010 cm^{-1}) is expected to be higher than at 0.10 cm^{-1} but due to the larger volume the concentration of cesium in the solution may actually be lower. If the concentration of cesium was not high enough to exceed the solubility product, or if a sorbing layer trapped cesium and it was not flaked off, then cesium might be below the detection limits of both the solution and precipitated material. At SA/V = 0.85 cm^{-1} cesium was not found in any precipitates. The cesium concentration in the second batch of glass used at this SA/V ratio was approximately 20 times lower than in the glass used in the first two SA/V ratios, therefore it was not unexpected that cesium in the second batch of experiments would be below the detection limits.

4.D.1.I.2. Iron and Nickel

Both iron and nickel were present in detectable levels only in the precipitates collected from leachates at SA/V = 0.10 cm^{-1} (Table 4.7). These two elements can precipitate as hydrated oxides and hydroxides starting at pH 5-6. Since at this SA/V ratio the leachate solution pH values were all above pH 6, it is understandable that iron and nickel should precipitate. At SA/V = 0.010 cm^{-1} the pH of the DDW and GGW leachates ranged from 4.5- 7.5 suggesting that iron and nickel might be distributed between the solution and precipitate. The amounts of these elements found in either the solution or solid was below the detection limits of INAA. The amount of glass released to solution at SA/V = 0.85 cm^{-1} is small compared to the other two SA/V ratios; consequently, the concentrations of iron and nickel released to the solution were smaller and below the detection limits of the method.

4.D.1.I.3. Tungsten

Tungsten is expected to follow molybdenum in leaching pattern, which would suggest that any tungsten detected would be predominantly in soluble form in the leachates since tungstic acid like molybdic acid precipitates at a pH around 4. Surprisingly, all the W determined in the leachates was in the form of a precipitate. Tungstic acid, H_2WO_4 or $H_2WO_4 \cdot H_2O$ is in reality a mixture of two hydrates of tungstic oxide, and there have been some indications for the existence of the HWO_4^- ion (67RIEC1). Most tungstates are insoluble in water, and metal cations such as Ca^{2+}, Zn^{2+} or Mn^{2+} could precipitate some tungsten as tungstate. Although some of the tungsten was probably present in both solution and precipitate, its concentration was below the detection limits of the INAA method. Tungsten was not detected in any part of the leachates at SA/V = 0.85 cm^{-1} because the concentration of WO_3 in the glass used in this SA/V experiment was also below the detection limits, unlike the glass used in the first two experiments.

4.D.1.I.4. Neodymium and Praseodymium

Neodymium and praseodymium showed similar trends, as expected. At SA/V = 0.010 cm^{-1} these elements were detected only in the precipitates collected after leaching at 90°C (Table 4.6); however, at a SA/V ratio of 0.10 cm^{-1} they were found in precipitates at both the temperatures (Table 4.7). It might be that neodymium and praseodymium released at 40°C at the lower SA/V ratio remained predominantly in solution because the amount leached in a large volume was not significant enough to exceed the solubility product at the pH in question. The concentrations of

these elements in solutions were below the detection limits of the method. Neodymium or praseodymium were found only in precipitates of DDW at SA/V = 0.85 cm^{-1} and 90°C (Table 4.8). At this SA/V ratio the amount of neodymium and praseodymium leached from the glass would be small compared to either 0.010 or 0.10cm^{-1}, and since both GGW and BGW contain more anions than DDW, they could keep these elements in solution. Hence, in all but DDW at 90°C, neodymium and praseodymium appear below the detection limits in both the solution and precipitate.

Because neodymium and praseodymium do not have the same complexing abilities as samarium, there is less tendency for them to form soluble species with carbonate or other anions; however, some effect can still be seen when the leachates at the respective SA/V ratios and temperatures are compared. As expected, the precipitates collected from BGW leachate, which had a higher concentration of anions to start with than in either DDW or GGW, had lower neodymium and praseodymium contents. Even in the case of BGW there is a greater tendency for these two elements to remain in soluble form; however, their concentrations were still below the detection limits in solution.

4.D.1.I.5. Cerium

Cerium followed many of the same trends as neodymium and praseodymium except in one important instance. At a SA/V ratio of 0.10 cm^{-1} and 90°C, the normalized elemental mass losses for cerium were consistently higher than for the corresponding precipitates at SA/V = 0.010 cm^{-1}. The only exception to this statement is DDW at 90°C. As the SA/V ratio increases the mass loss values are expected to decrease which

was not observed in the case of cerium. Cerium, unlike either neodymium or praseodymium, is able to exist in both the +3 or +4 states in solution. At SA/V = 0.010 cm^{-1} more cerium should be leached than at 0.10 cm^{-1}. However, if at 90°C in GGW and BGW cerium was stabilized in the +4 state then more cerium would be present in soluble form than in the precipitate. In such a case the amount of cerium present in the precipitate at 0.10 cm^{-1} could be higher than at 0.010 cm^{-1}.

4.D.2 Effects of Temperature

Temperature is one of the most important variables influencing the leaching of glass in the repository because of the self-heating effect of the waste form resulting from radioactive decay. Obviously, the temperature of the glass in the repository depends on a number of key factors such as the age of the waste, waste loading and the thermal characteristics of the repository.

An increase in temperature significantly accelerates leaching. The extent of reaction between the glass and solution was small at 40°C after 84d of leaching in any of the leachants compared to the results at 90°C. This is shown quite clearly by comparing the total mass loss of the I-117 glass at 40°C and 90°C for each leachate at the three surface area to volume ratios (Figs. 4.41-4.49). The factor of increase in leaching with temperature after 84d for each of the three leachants at three SA/V ratios are given in Table 4.9. The greatest overall increase in leaching caused by the increase in temperature was in the BGW leachant, except at SA/V = 0.010 cm^{-1} where the largest increase occurred in DDW.

Many researchers have expressed the temperature dependence of glass

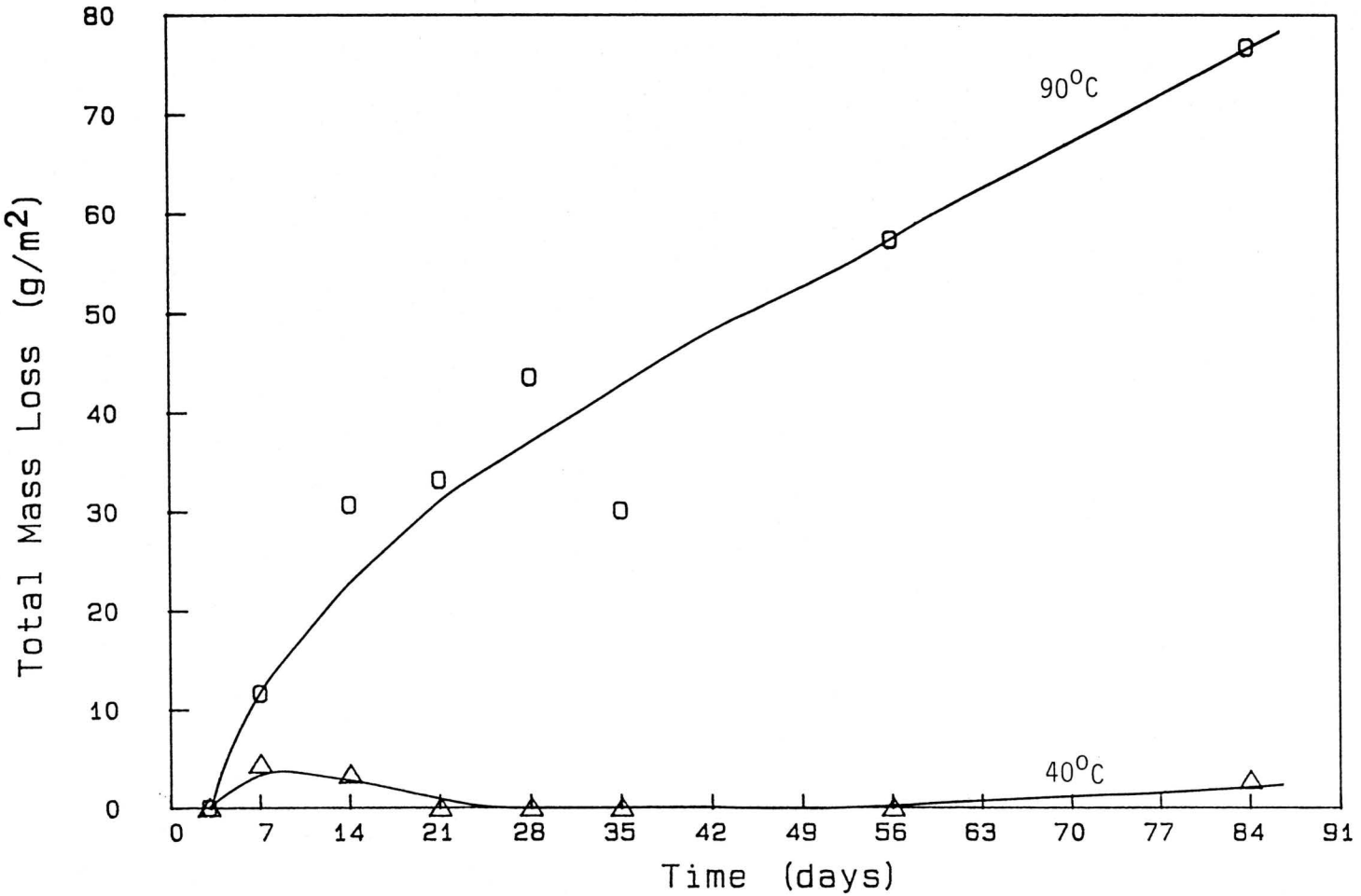

Figure 4.41. Results of total mass loss measurements of I-117 Glass leached in distilled deionized water at SA/V = 0.010 cm^{-1} and 40°C and 90°C.

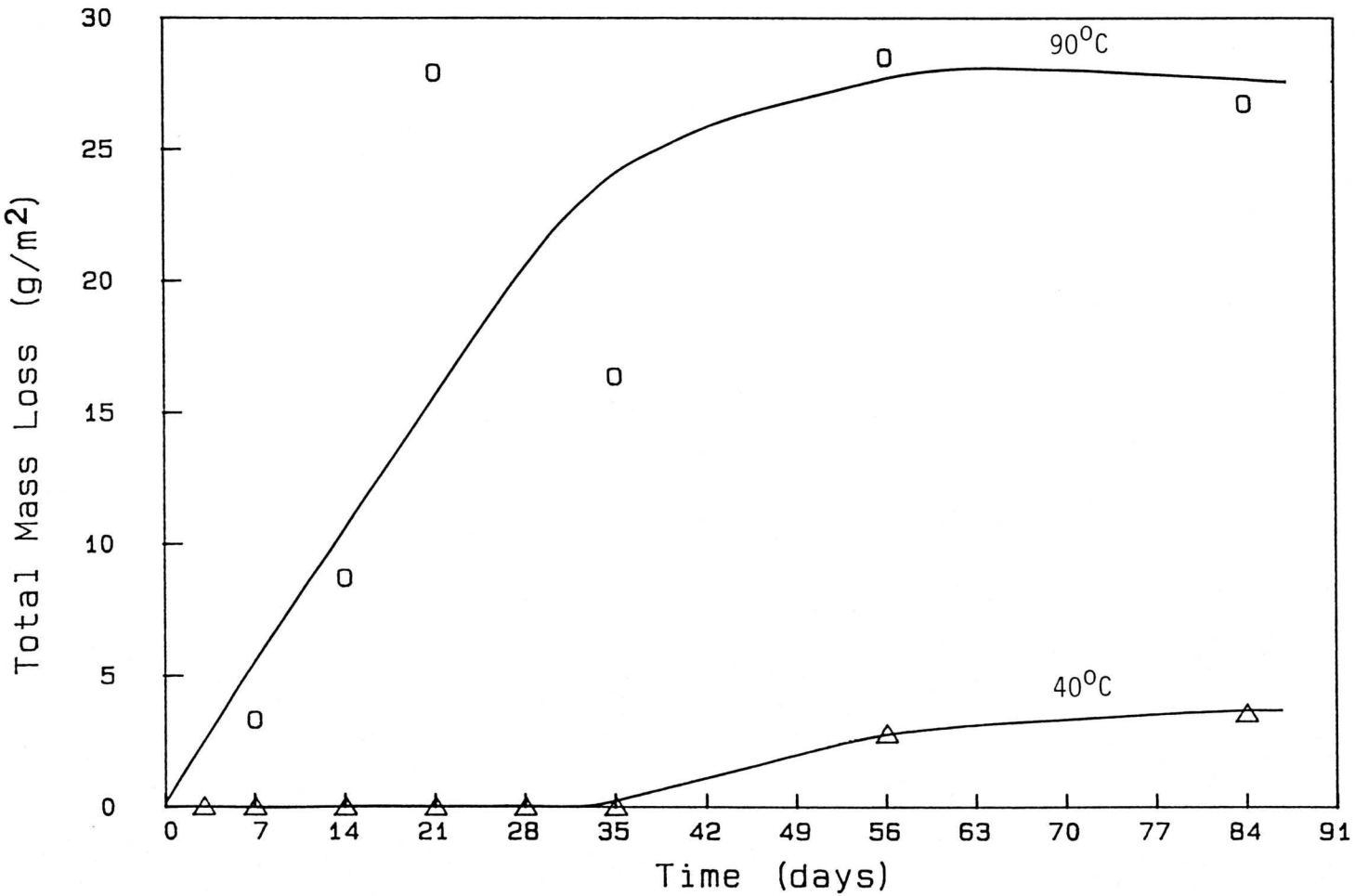

Figure 4.42. Results of total mass loss measurements of I-117 Glass leached in synthetic granitic groundwater at SA/V = 0.010 cm^{-1} and 40° and 90°C.

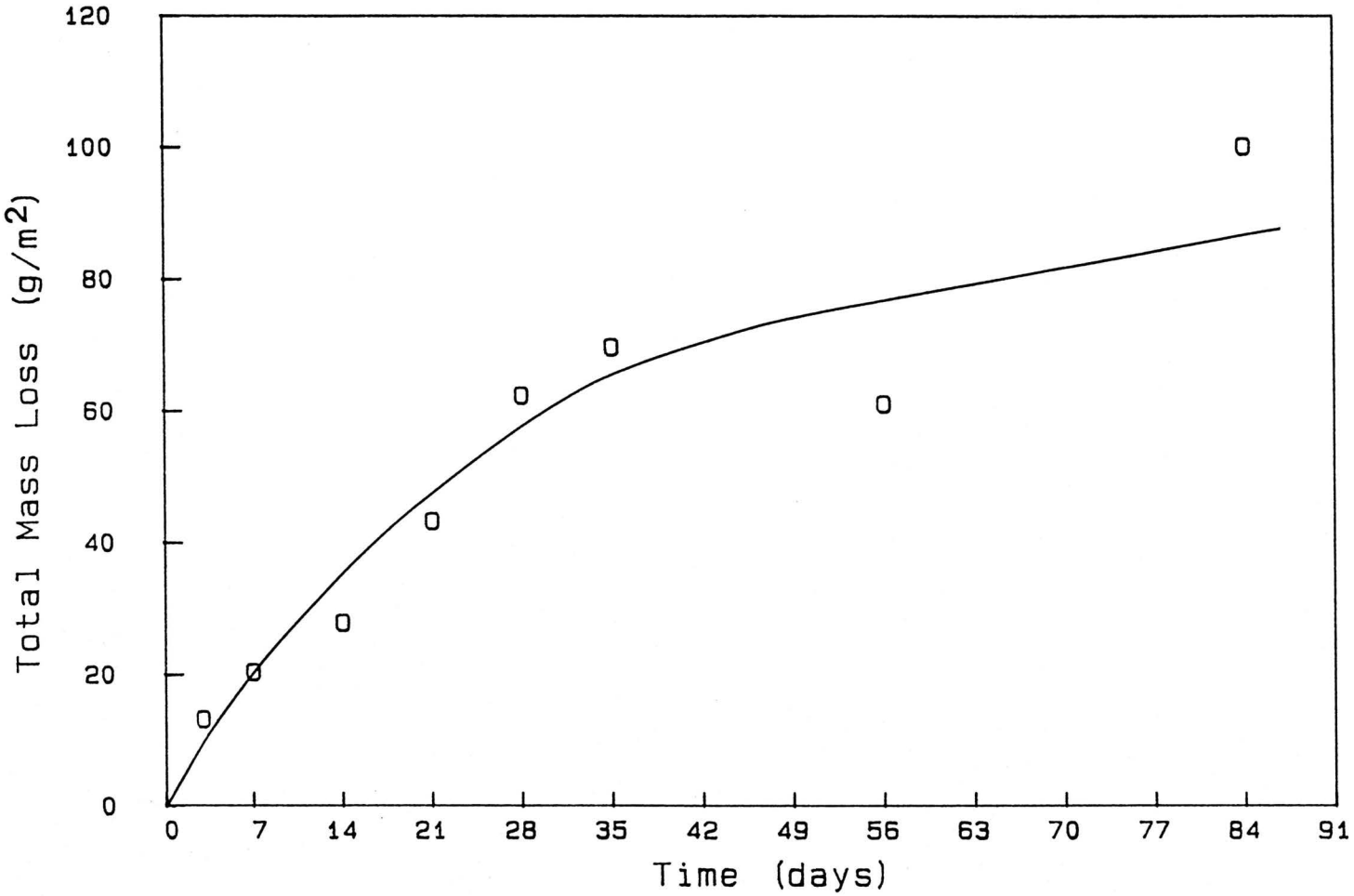

Figure 4.43. Results of total mass loss measurements of I-117 Glass leached in synthetic Grande Ronde basaltic groundwater at SA/V = 0.010 cm^{-1} and 90°C.

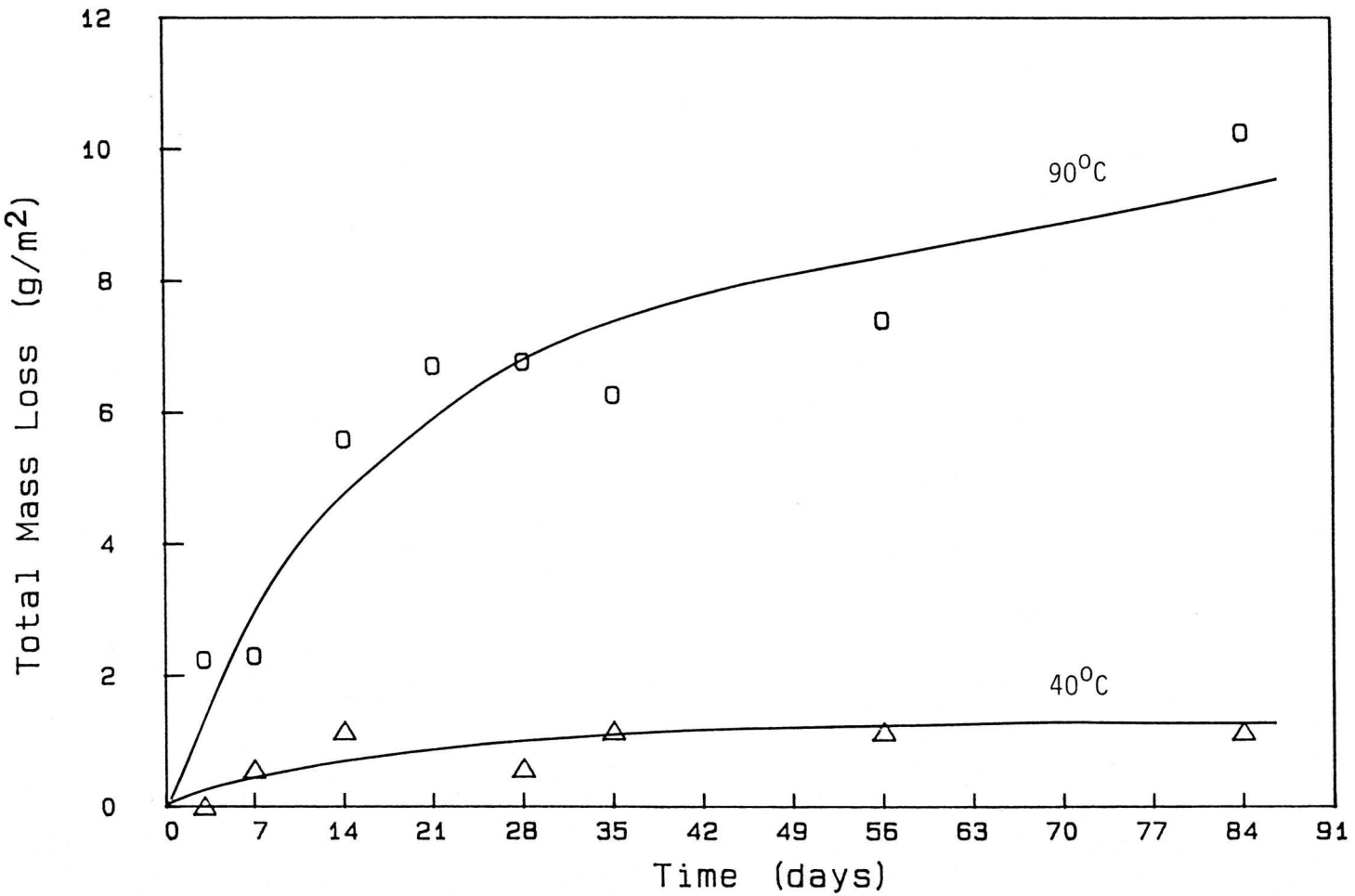

Figure 4.44. Results of total mass loss measurements of I-117 Glass leached in distilled deionized water at SA/V = 0.10 cm^{-1} and 40° and 90°C.

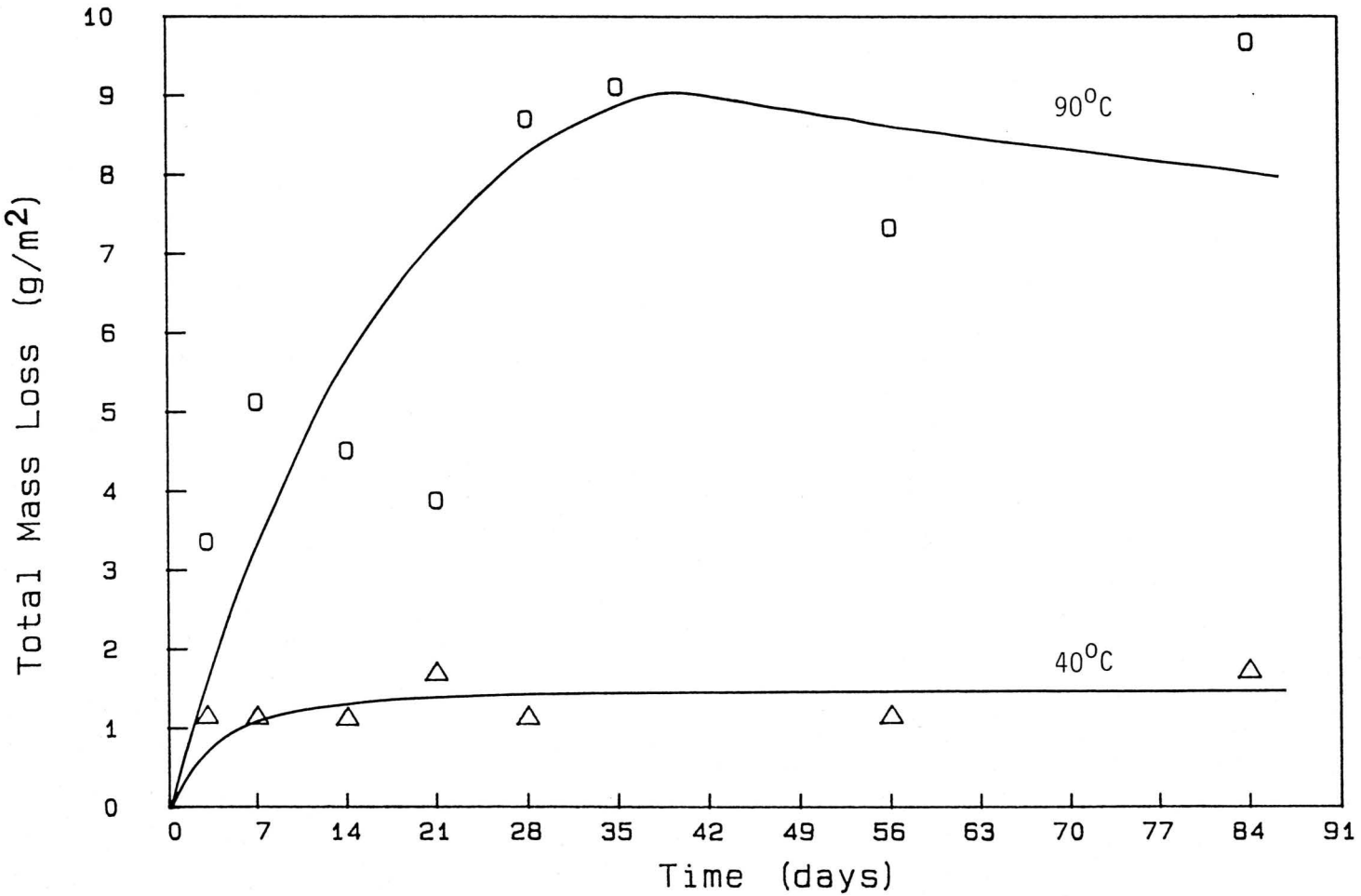

Figure 4.45. Results of total mass loss measurements of I-117 Glass leached in synthetic granitic groundwater at SA/V = 0.10 cm^{-1} and 40° and 90°C.

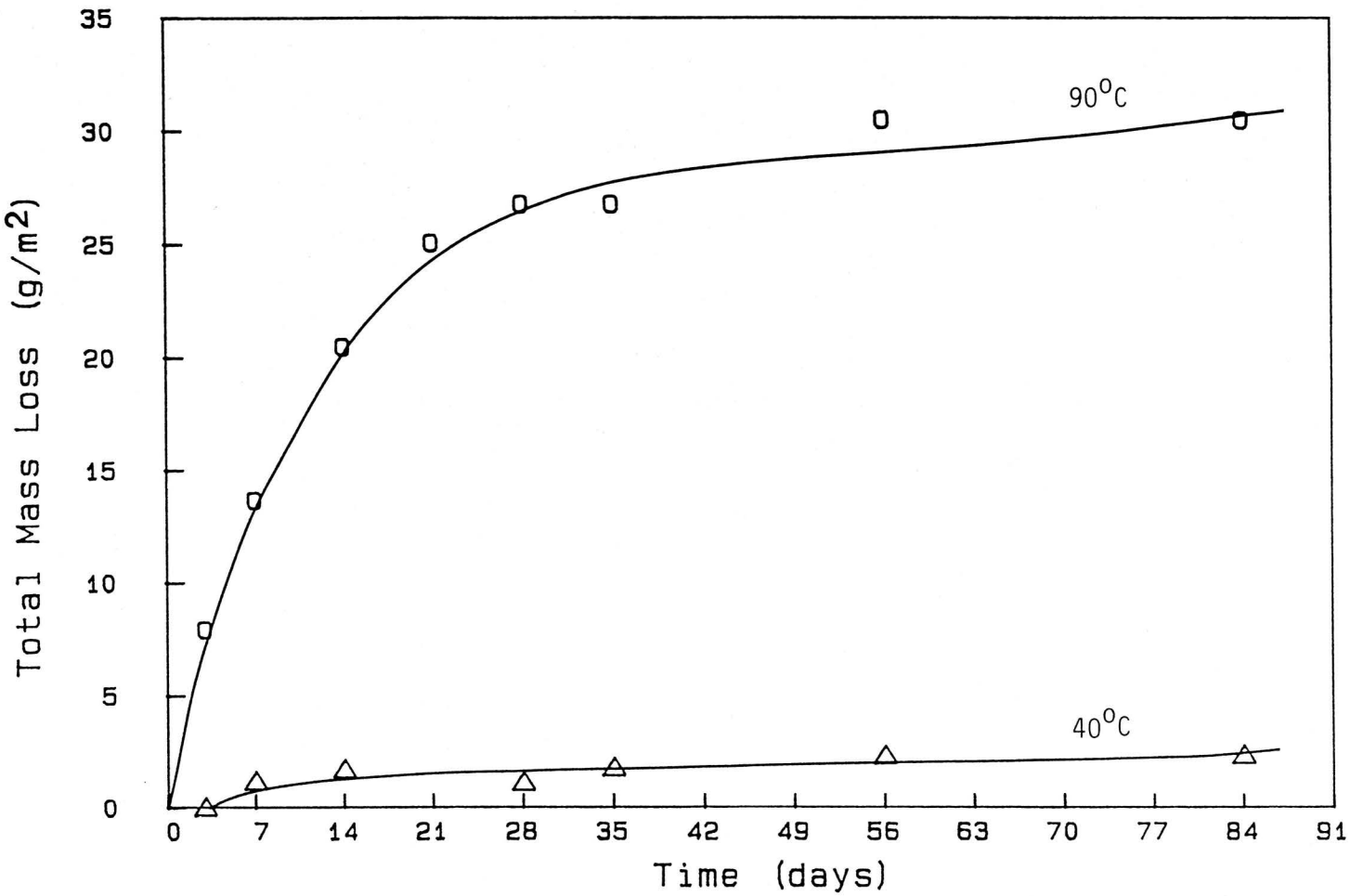

Figure 4.46. Results of total mass loss measurements of I-117 Glass leached in synthetic Grande Ronde basaltic groundwater at SA/V = 0.10 cm^{-1} and 40° and 90°C.

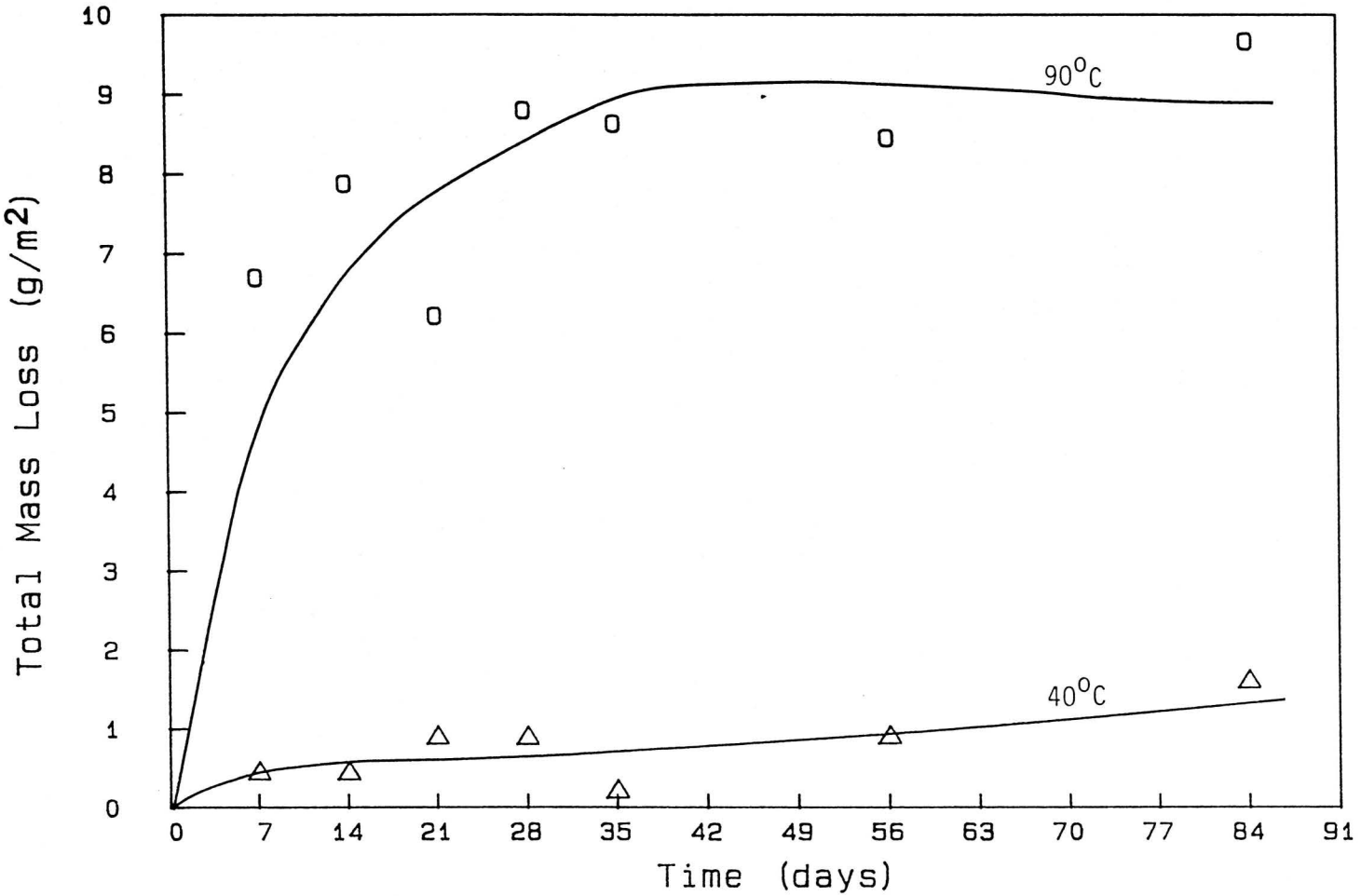

Figure 4.47. Results of total mass loss measurements of I-117 Glass leached in distilled deionized water at SA/V = 0.85 cm^{-1} and 40^{o} and $90^{o}C$.

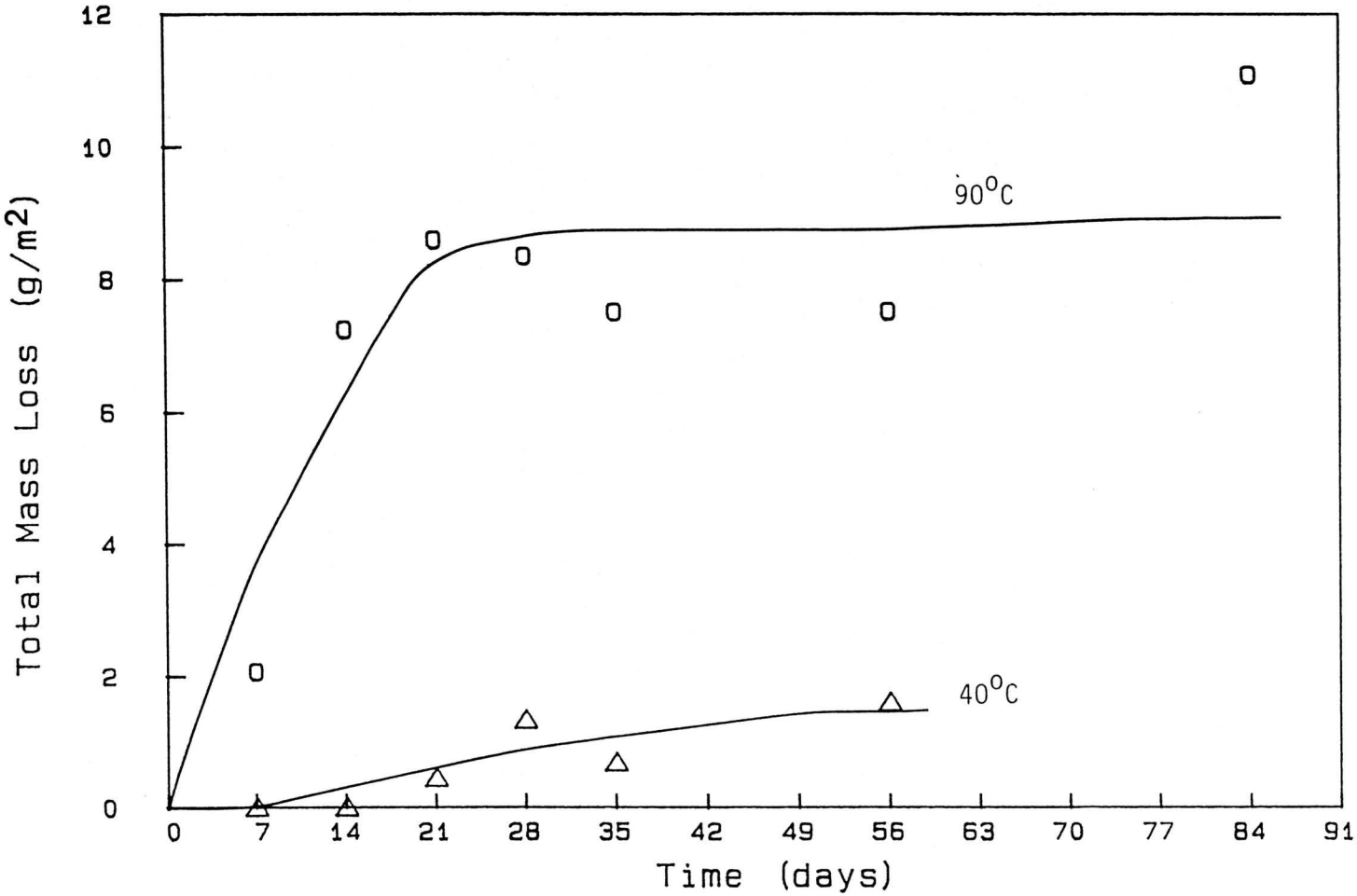

Figure 4.48. Results of total mass loss measurements of I-117 Glass leached in synthetic granitic groundwater at SA/V = 0.85 cm^{-1} and 40° and 90°C.

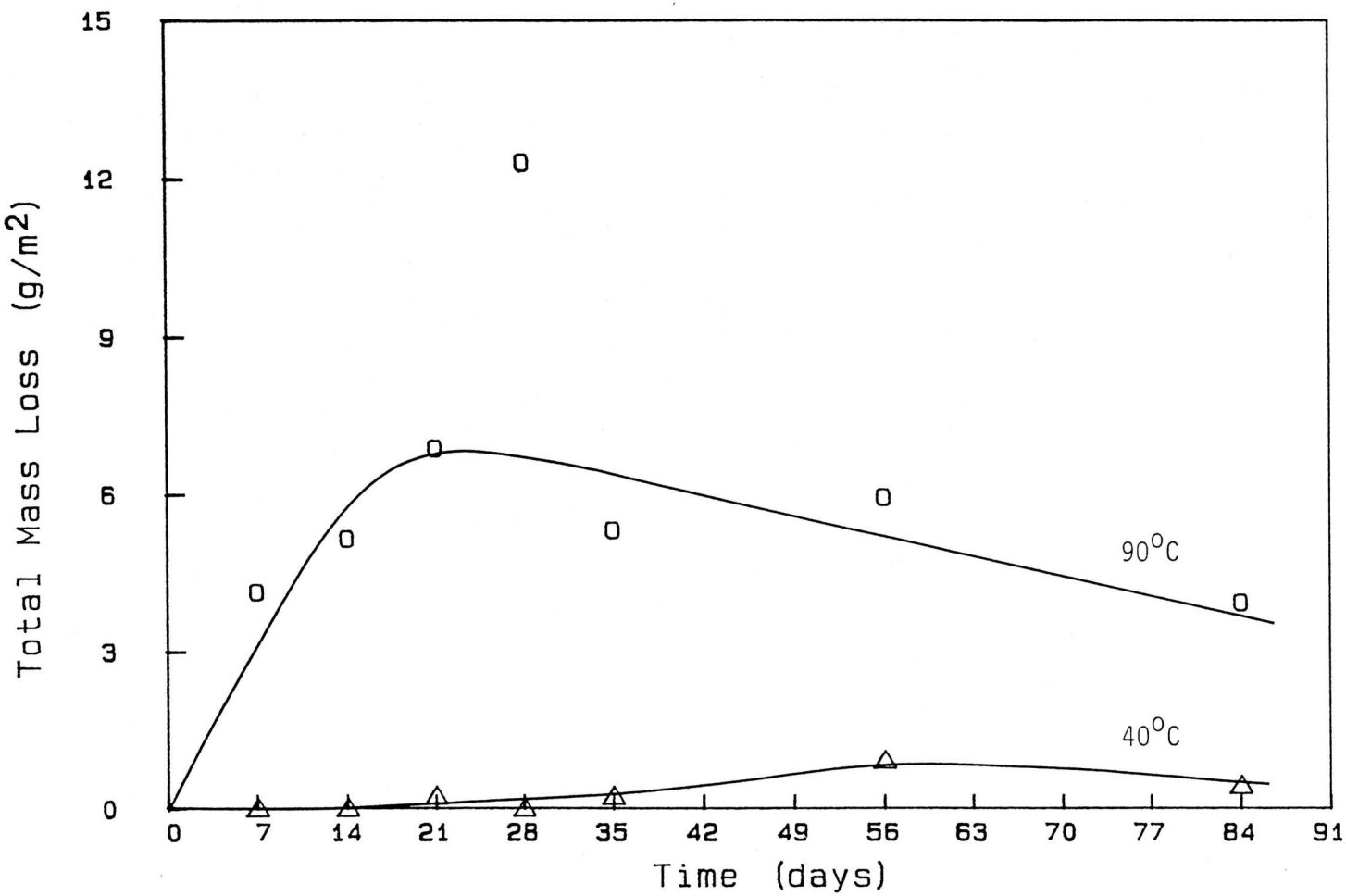

Figure 4.49. Results of total mass loss measurements of I-117 Glass leached in synthetic Grande Ronde basaltic groundwater at SA/V = 0.85 cm^{-1} and 40° and 90°C.

Table 4.9. Factor of increase in leaching of I-117 Glass at 90°C over 40°C as determined from total mass loss data after 84d

SA/V RATIO (cm^{-1})	LEACHANT	FACTOR INCREASE FOR 90° OVER 40°C
0.010	DDW	27.6
0.10	DDW	9.00
0.85	DDW	5.98
0.010	GGW	7.49
0.10	GGW	5.57
0.85	GGW	6.93
0.010	BGW	18.3
0.10	BGW	13.1
0.85	BGW	9.03

leaching as:

$$R_i = k_o \exp(-E/RT) \qquad (4.9)$$

where R_i is the leach rate in g/m^2d, k_o is a constant, R is the gas constant in J/Kmole, T is the temperature in K and E is the activation energy in J/mole (81WEST1). Activation energies for the leaching of HLW glasses have generally been found to be in the range of 50-80 kJ/mole (IAEA). The activation energies were calculated for I-117 glass leached at the three SA/V ratios in each of the three leachants from total mass losses after 84d. These results are given in Table 4.10. It is evident that the activation energy depends on pH. The highest activation energies were those calculated for the BGW leachates which also had the highest pH values. This suggests that I-117 glass in the BGW leachant would be more sensitive to temperature variation which is verified by the total mass loss curves (Figs. 4.41-4.49).

The effect of temperature is important as may be seen from the calculated normalized mass losses (Figs. 4.41-4.49). Depending upon the time from the initial disposal in the repository to the onset of leaching, the temperature encountered by the waste form will vary. It has been reported that the repository temperature could exceed 100°C within the first 100 years, and then fall to the temperature of the environment (30-60°C) after about 500 years.

4.D.3 Effect of Glass Surface Area to Leachant Volume (SA/V)

The effect of SA/V on the total mass loss and normalized release of

Table 4.10. Activation energies for I-117 Glass leached at 3 SA/V ratios in each leachant calculated from total mass loss data after 84d

SA/V RATIO (cm^{-1})	LEACHANT, pH	ACTIVATION ENERGY (kJ/mole)
0.010	DDW, 6.10	62.7
0.10	DDW, 6.10	41.5
0.85	DDW, 6.10	33.8
0.010	GGW, 7.42	38.1
0.10	GGW, 7.42	32.4
0.85	GGW, 7.42	36.6
0.010	BGW, 9.35	54.9
0.10	BGW, 9.35	48.6
0.85	BGW, 9.35	41.6

elements from I-117 glass was investigated, and as observed in the preliminary experiments, the release decreased with increased SA/V ratio (Fig. 4.50) in all three leachants at both temperatures except in the case of sodium as already discussed (Section 4.D.1). If the SA/V is high then the leachant quickly becomes saturated with leached species and the leach rate falls. However, if the volume of leachant is large (hence SA/V is small), more glass dissolves before saturation occurs. The results are summarized in Table 4.11. Taking the example of DDW at 90°C and SA/V = 0.010 cm^{-1}, 13.7% of the glass dissolved after 84d, whereas at SA/V = 0.10 cm^{-1} and all other conditions being the same, only 1.36% dissolved. Although dissolution rates of the elements decreased with increased SA/V values, they did not do so in equal proportions. This is illustrated in Fig. 4.51 which is a plot of the log of normalized elemental mass loss versus the log of SA/V ratio for samples leached in DDW at 90°C after 84d.

An accelerated attainment of the equilibrium pH was observed with increased SA/V ratio. Results for DDW at 90°C are shown in Fig. 4.52. At SA/V = 0.010 and 0.10 cm^{-1} the solution pH continued to increase slowly, while the pH rose quickly to 9.5 and did not change much upto 84d at SA/V = 0.85 cm^{-1}. This sharp increase in pH at the higher SA/V ratio has already been attributed in part to the glass used (Section 4.D.1); the SA/V is partially responsible for the results as well. Sodium present on the surface of the glass was initially released very quickly which increased the pH to basic medium through the hydrogen/alkali ion-exchange previously discussed (Section 4.D.1). In the case of DDW at SA/V = 0.85 cm^{-1} the pH at day 3 was 9.75 which dropped slightly to an equilibrium pH

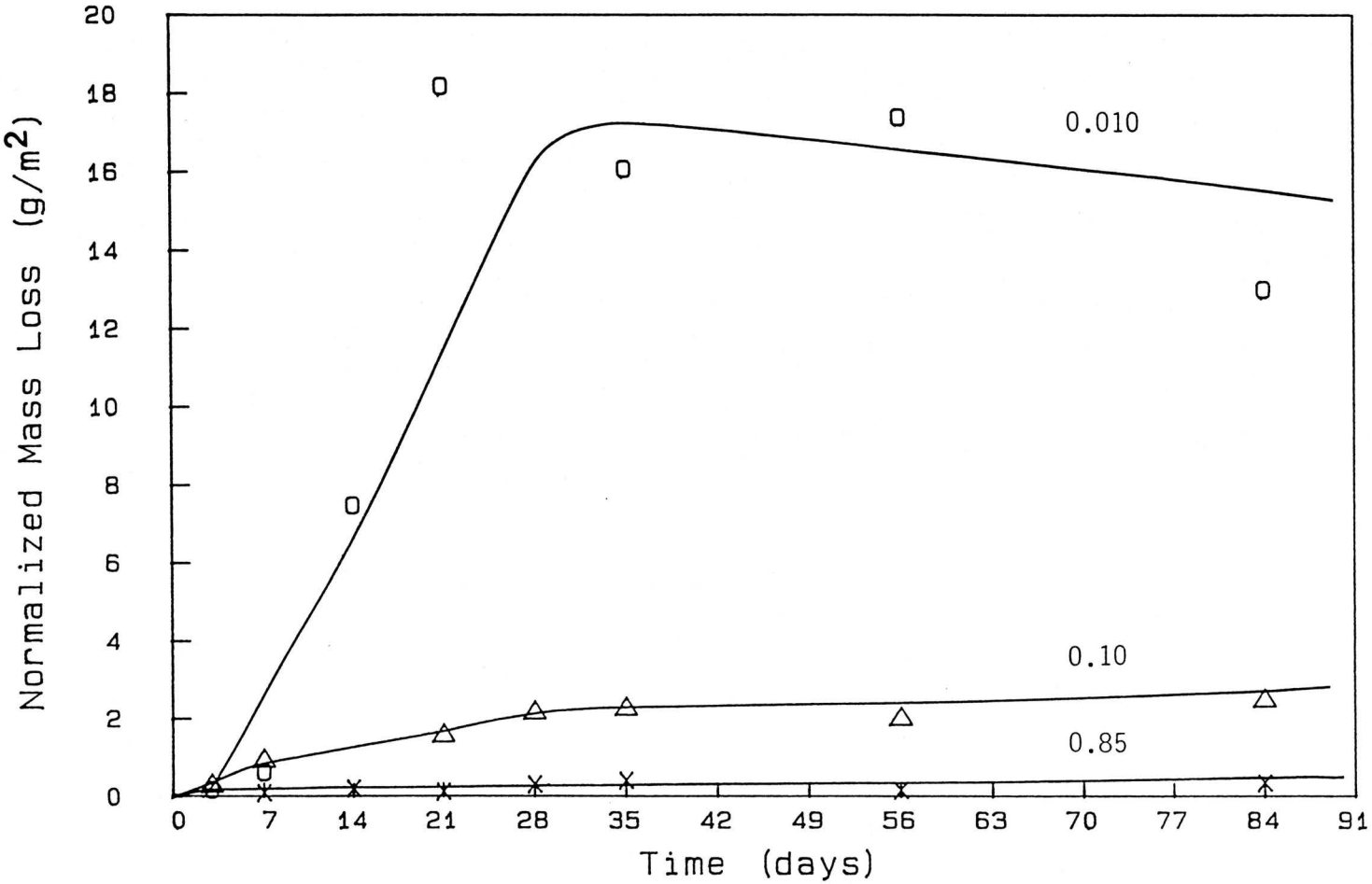

Figure 4.50. Comparison of normalized elemental mass loss results for lanthanum leached from I-117 Glass in synthetic granitic groundwater at SA/V = 0.010, 0.10 and 0.85 cm^{-1} and 90°C.

Table 4.11. Effect of surface area/volume ratio (SA/V) on the dissolution of I-117 glass at 40° and 90°C after 84d

LEACHANT	SA/V cm^{-1}	TEMPERATURE °C	% GLASS CONVERTED
DDW	0.010	90	13.7
DDW	0.10	90	1.36
DDW	0.85	90	0.502
DDW	0.010	40	0.469
DDW	0.10	40	0.144
DDW	0.85	40	0.0862
GGW	0.010	90	4.48
GGW	0.10	90	1.20
GGW	0.85	90	0.582
GGW	0.010	40	0.645
GGW	0.10	40	0.244
GGW	0.85	40	0.0954
BGW	0.010	90	18.2
BGW	0.10	90	3.51
BGW	0.85	90	0.211
BGW	0.010	40	0.870
BGW	0.10	40	0.290
BGW	0.85	40	0.0229

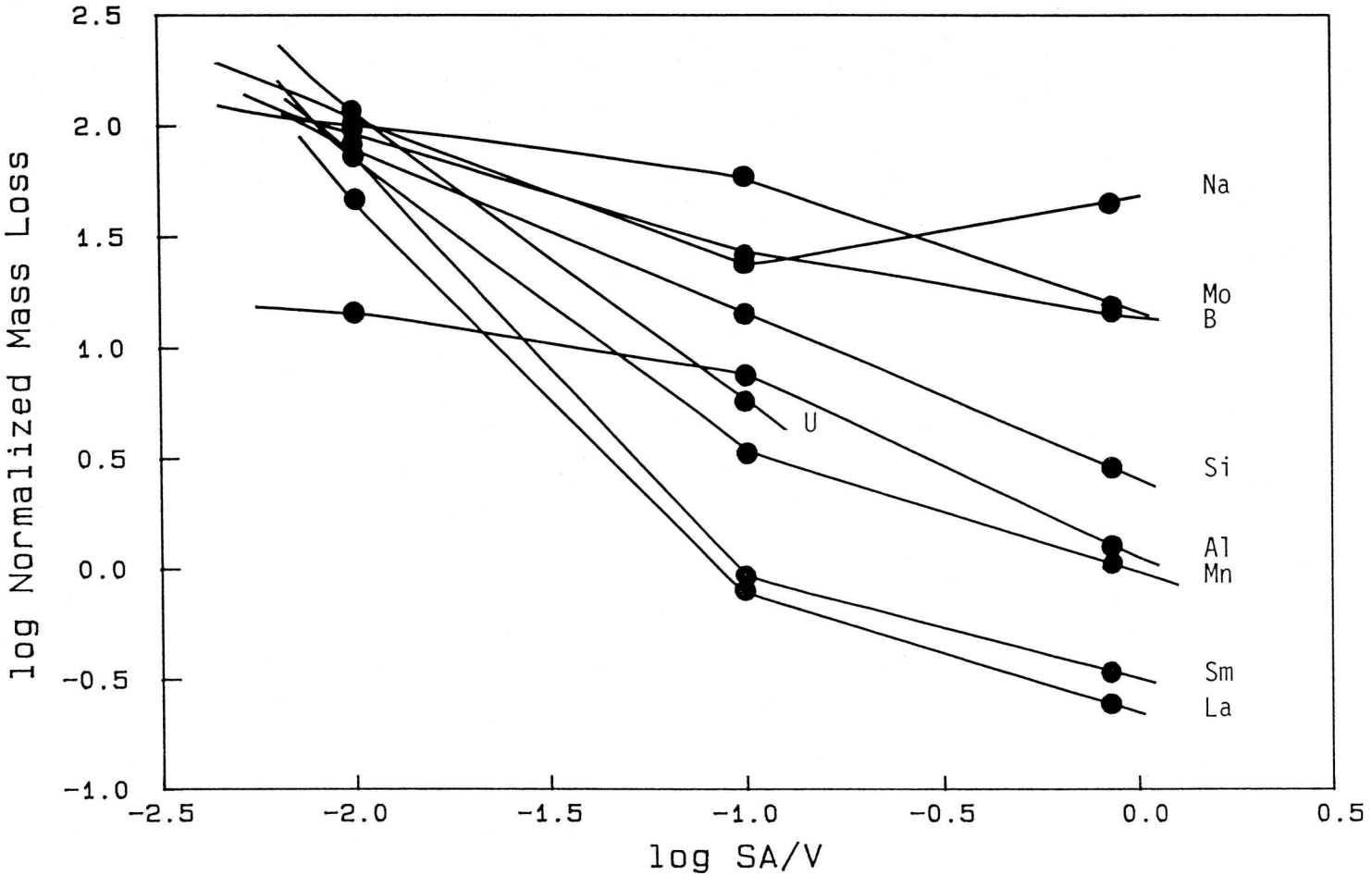

Figure 4.51. Comparison of the plots of log Normalized Elemental Mass Loss versus log SA/V for 9 elements leached from I-117 Glass in distilled deionized water at 90°C after 84 days.

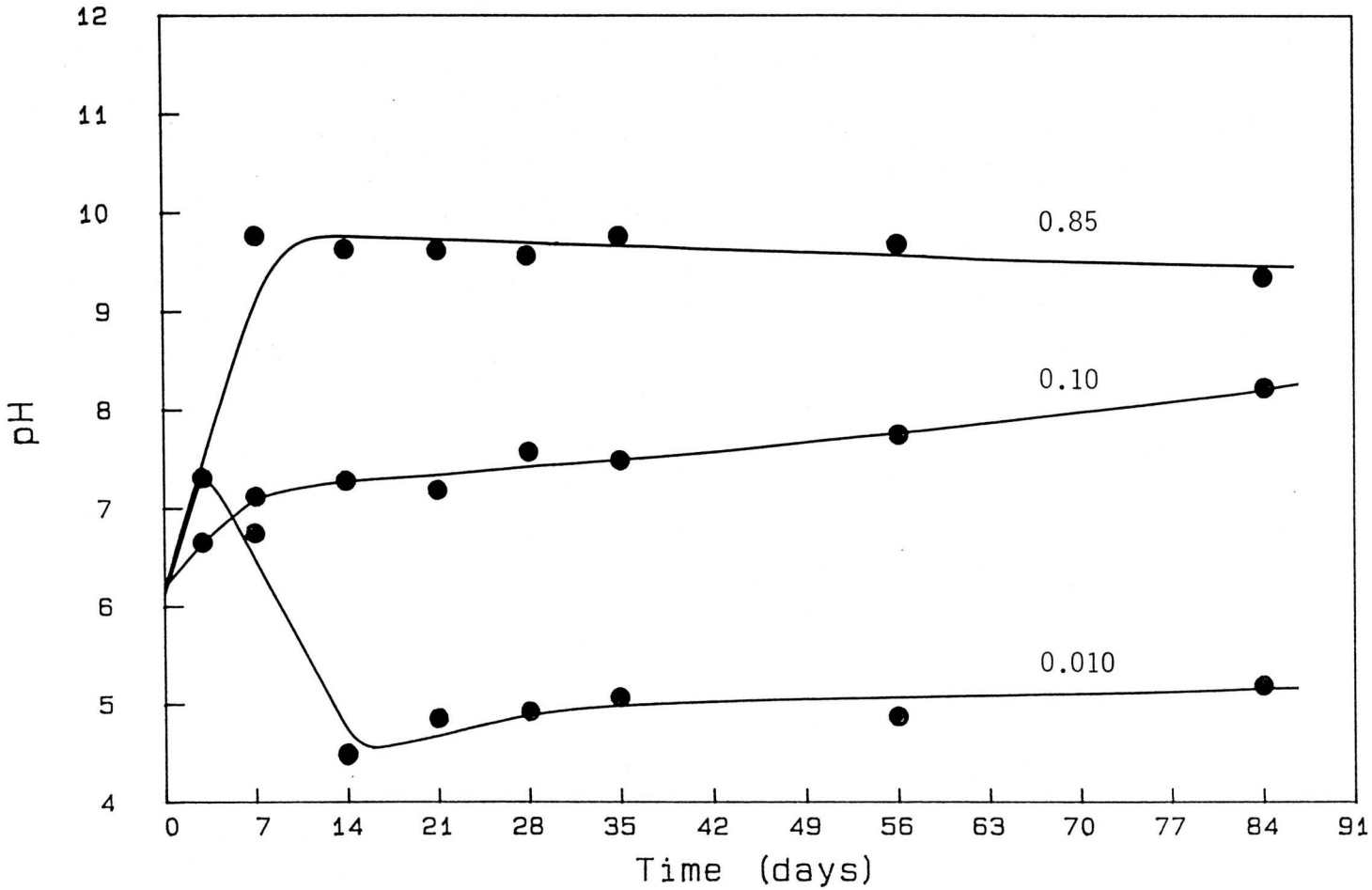

Figure 4.52. Comparison of leachate pH for I-117 Glass leached in distilled deionized water at SA/V = 0.010, 0.10 and 0.85 cm^{-1} and $90^{o}C$.

of 9.6 as the leaching continued. The higher SA/V allowed a quick burst of sodium to be released, causing an initial high pH; however, as the release of borate and other buffering components began to catch up with the sodium release, the pH fell to the equilibrium value.

4.D.4. Pseudocolloids

It has been argued that if leachate samples from experiments at elevated temperatures are allowed to cool to room temperature before an aliquot is removed, errors might be encountered (86MEAN1). Some species present in the solution are expected to precipitate as the solution cools in which case elemental concentrations would be expected to be higher in the hot leachate solution. To test this hypothesis samples of leachate in all of the main experiments conducted in this study were taken as soon as the bottles were removed from the constant temperature baths. Once the remaining leachate had cooled, a second aliquot was taken. Both aliquots were analyzed under identical conditions to see if differences in the composition did in fact exist.

The samples did show a difference; however, it was the opposite of that expected. Samples of leachate taken when the solution reached room temperature had higher concentrations of certain elements, namely lanthanum, samarium, uranium and to a lesser extent manganese. Fig. 4.53 shows these differences for samarium leachates in DDW at 0.10 cm^{-1} for 90°C and room temperature. Similar trends were observed in the other two leachants and at all three SA/V ratios. As might be expected this effect is much less pronounced at 40°C and often is unobservable.

A possible explanation for this phenomenon could be the presence of

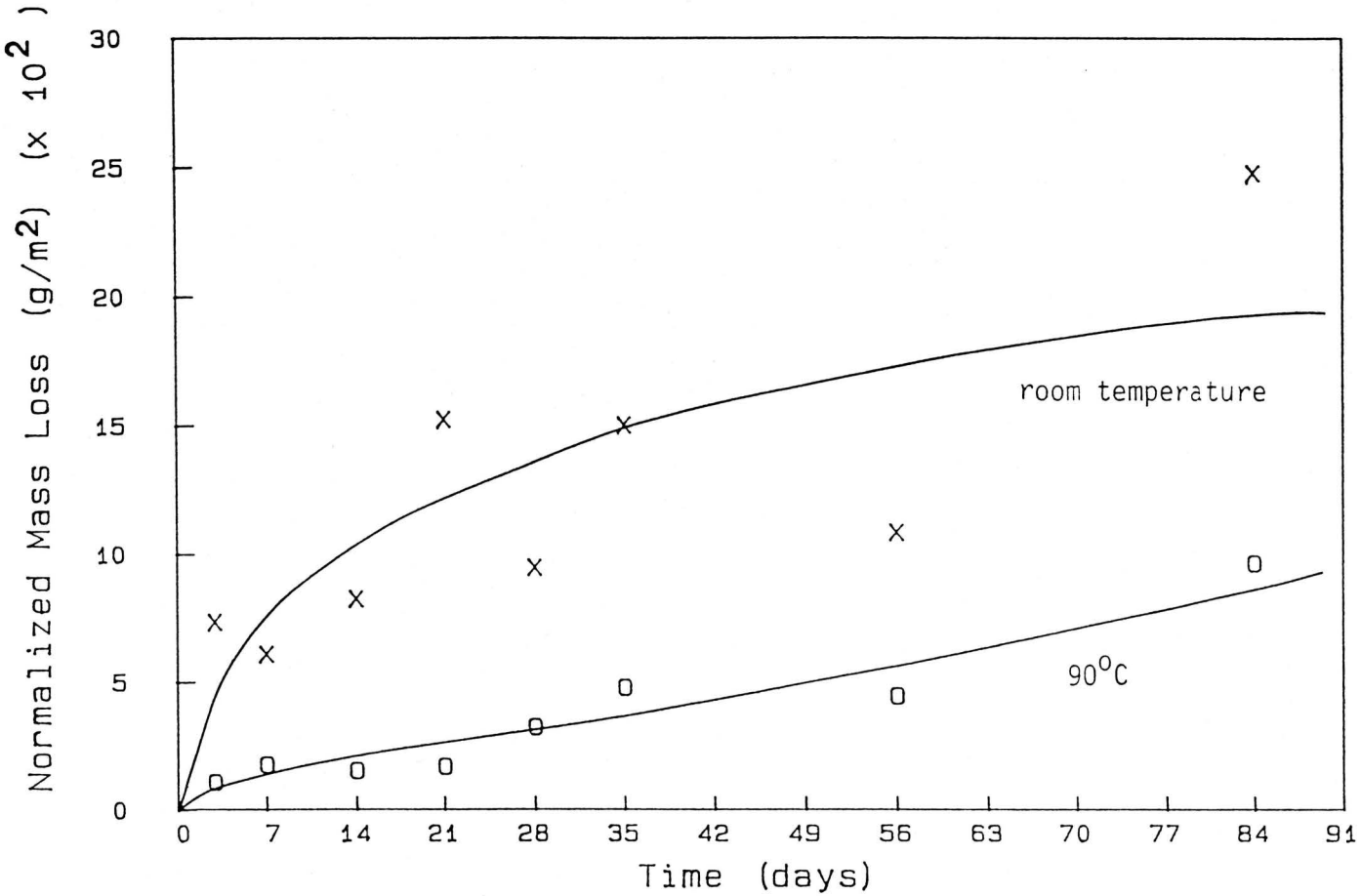

Figure 4.53. Comparison of normalized elemental mass loss results for samarium leached from I-117 Glass in synthetic granitic groundwater at SA/V = 0.10 cm^{-1} and sampled at 90°C and room temperature from the same bottle.

pseudocolloids. Normally an increase in temperature increases the rate of growth of ionic crystals; however, it does not induce larger crystal size. This is not true in the case of colloids. Heating of a solution containing cerium colloids was found to lead to an increase in the size of the particles (80BENE1). As the temperature of the leachate solution decreases the kinetic energy of particles decreases, and the chances of them meeting one another increases. Aggregation may result from partial ionic and Van der Waals' interactions between different complex species present in solution. In addition, colloids can be produced through the condensation of molecules or ions by hydrolytic or precipitation processes, assuming their concentrations are sufficiently large to exceed solubility product, and subsequent association with foreign colloidal particles present in solution as impurities. Such particles are then referred to as pseudocolloids. It is not clear as to the exact identity of such carriers for pseudocolloids; possibly a colloidally dispersed solid phase released from the walls of the vessel, or the solution may contain colloids of silicic acid which is known to be a good adsorbant. Even solutions prepared using high purity chemicals and deionized water will contain certain amounts of impurities of ionic
nature, whose state in solution can change during alteration in the solution composition. Iron is a typical example, which is a commonly encountered impurity. Colloidal particles of iron (III) hydroxide are formed on increasing solution pH. The aggregation of these particles which occurs as the sample cools would explain why the concentration appears higher in the aliquot removed after the solution reaches room temperature.

4.E. MODELS FOR LONG-TERM DISSOLUTION OF GLASS

Mathematical models reported in literature for explaining glass dissolution differ in their quality and usefulness. The most developed models are based on diffusion; however, since this process is prevalent for a limited time only, their use for long- term extrapolations results in underestimations. More sophisticated models which also take into account corrosion and processes such as phase regeneration are less well-developed.

A glass dissolution model is needed which takes into account the following effects: (1) temperature, (2) pressure, (3) leachant composition including its change in pH, buffer capacity and concentration of silicic acid, (4) formation of new phases and (5) sample geometry and glass surface area/leachant volume and its change with time. A comprehensive model which encompasses all of these factors is difficult to formulate, primarily because the chemical processes of the reactions occurring are constantly changing with time. The development of such a dissolution model is beyond the scope of this thesis. This type of model would require an enormous number of data points for each parameter investigated. However, the data which have been generated by our experiments may be used in conjunction with data from other studies by individuals working in the field of glass dissolution modelling.

Three simple equations have been suggested by Ewest for long-term extrapolation of leaching experiments (79EWES1). These equations are based on the following assumptions: (1) the glass leaches homogeneously, (2) the glass surface is considered constant until 25% of the original glass is leached and (3) the mechanical integrity of the solid glass and

the leaching conditions are maintained.

The first equation is based on a corrosion mechanism (i.e. layers of equal thickness are removed at equal times), and is given for cylinders and spheres as:

$$F = \frac{M}{M_o} = 2\left[\left(\frac{1}{p} + 1\right)\tau - \left(\frac{2}{p} + \frac{1}{2}\right)\tau^2 + \left(\frac{1}{p}\right)\tau^3\right] \qquad (4.10)$$

where M = released mass (g)

F = released mass fraction

M_o = total mass of sample (g)

$$p = \frac{L}{r} = \text{cylinder length/cylinder radius}$$

$$\tau = \frac{R(t - t_o)}{gr} = \text{dimensionless time parameter}$$

R = leach rate (g/cm^2d)

t = time (d)

t_o = start of leaching process

g = glass density (g/cm^3)

r = radius (cm)

On the other hand, if release is based on a pure diffusion mechanism (planar diffusion) then samples behave like a semi-infinite medium, (i.e. the decreasing volume does not influence the leaching) and this leads to

the second equation:

$$F = \frac{S}{M_o} 2C_o(D/\pi)^{1/2}(t - t_o)^{1/2} = \frac{S}{S_s M_o} a_1(t - t_o)^{1/2} \quad (4.11)$$

where S = surface area (cm^2)

S_s = specific surface area at the beginning of the experiment (cm^2/g)

C_o = the concentration of the diffusing component (for homogeneous leaching, C_o = density) (g/cm^3)

D = overall diffusion coefficient (all components) (cm^2/s)

a_1 = coefficient ($d^{1/2}$)

The third and final equation is the case where simultaneous corrosion and diffusion occur:

$$F = \frac{M}{M_o} = \frac{S}{M_o S_s} a_2(t - t_o)^x \quad (4.12)$$

where a_2 = coefficient (d^{-x})

x = exponent in the range $0.5 \leq X \leq 1$

Total mass loss data from this work were analyzed using these three equations. Only the data collected at 90°C for BGW at SA/V = 0.010, 0.10 and 0.85 cm^{-1} and DDW and GGW at SA/V = 0.10 cm^{-1} were used in the

calculations. Data at 40°C were not included due to the unreliability of the low total mass loss measurements. In the experiments at SA/V = 0.85 cm^{-1}, where 2 cylinders of glass were used to obtain the desired surface area, values of τ were calculated for each cylinder and then they were added together to give τ_{total}. Plots of τ vs time for these five sets of data are given in Fig. 4.54. It is evident that after approximately the 28th day, in most cases the leach rate (R) decreases and the relationship between τ and time is no longer linear. Values for R were calculated for the applicable time range in all five cases and the results are compared in Table 4.12.

As expected the highest leach rate calculated for the BGW leachant was at SA/V = 0.010 cm^{-1}. The leach rates of DDW and GGW were very similar; however, compared to that of BGW at SA/V = 0.10 cm^{-1}, these rates were approximately 3-5 times lower. The corrosion process is pH dependent; thus at very high or very low pH values, it is expected that corrosion will increase thereby increasing the leach rate. Under such conditions more free OH^- or H^+ ions are available, depending upon the pH, which can attack the glass structure, for example:

$$\text{-Si-O-Si-} + OH^- \longrightarrow \text{-Si-OH} + SiO^- \qquad (4.13)$$

The strong Si-O-Si bond is broken so that one end of the molecule becomes a silanol by proton transfer or hydroxyl ion attachment. Since the pH of BGW at SA/V = 0.10 cm^{-1} is so much higher than GGW or DDW (pH 9 compared to 7.3), the effects of corrosion are expected to be more severe, leading to a higher leach rate. A comparison of the leach rates of DDW and GGW

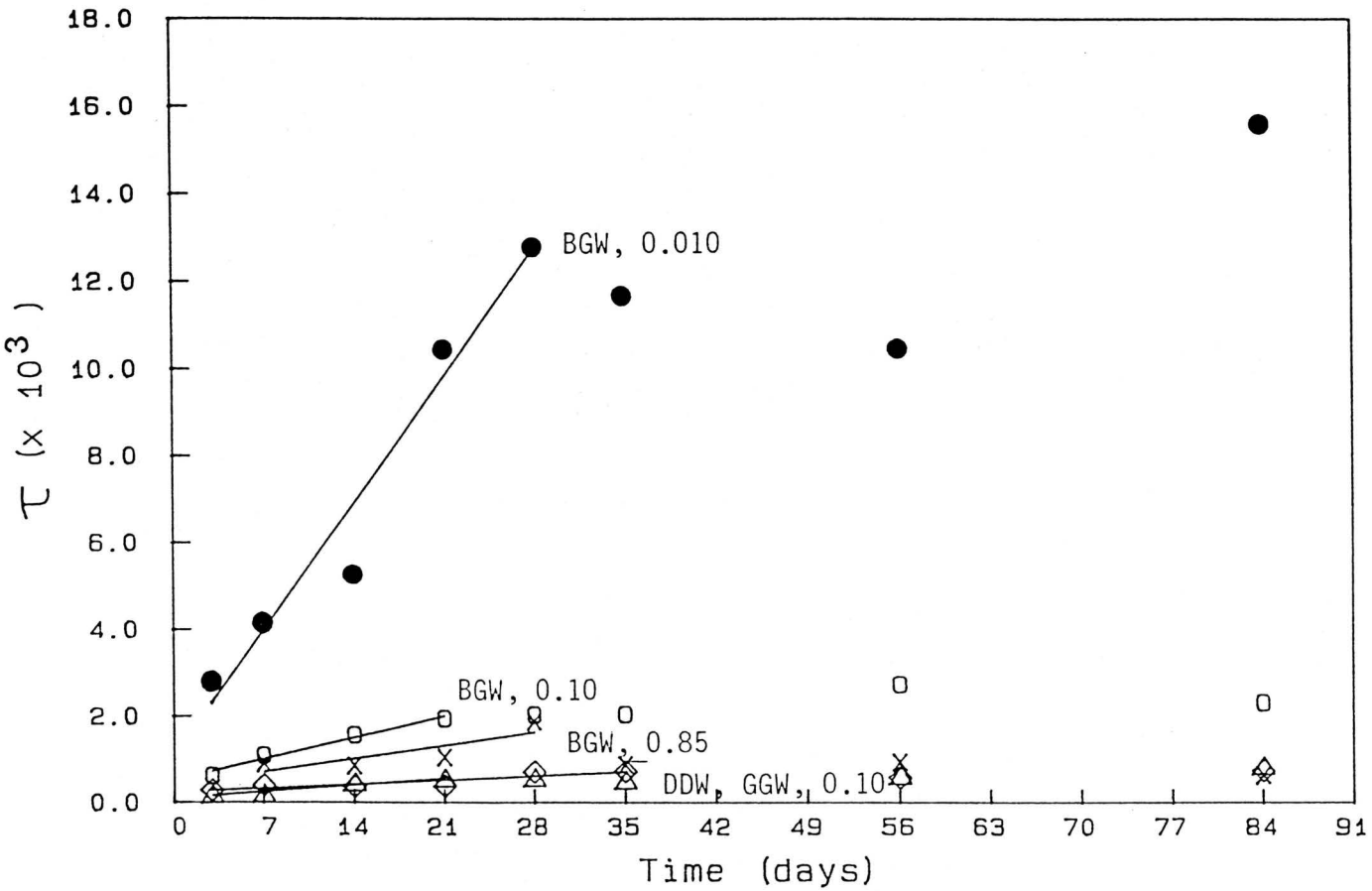

Figure 4.54. Plots of τ versus Time for I-117 Glass leached in synthetic Grande Ronde basaltic groundwater at SA/V = 0.010, 0.10 and 0.85 cm^{-1} and distilled deionized water and synthetic granitic groundwater at SA/V = 0.10 cm^{-1}, all at $90^{o}C$.

Table 4.12. Leach rates as calculated from plots of τ versus time for I-117 Glass leached at 90°C

LEACHANT	SA/V RATIO (cm^{-1})	APPLICABLE TIME RANGE (d)	LEACH RATE (g/cm^2d)
BGW	0.010	3 - 28	2.2×10^{-4}
BGW	0.10	3 - 21	9.6×10^{-5}
BGW	0.85	7 - 28	5.9×10^{-5}
DDW	0.10	3 - 21	2.4×10^{-5}
GGW	0.10	3 - 35	1.9×10^{-5}

reveals a slight difference due to pH as well. The pH of the GGW leachates were always very close to 7 while those of DDW were slightly lower. Near the neutral pH of GGW very few OH^- or H^+ ions were free to take part in the corrosion of the glass compared to the number of H^+ ions present in DDW with its slightly lower pH. As a result the leach rate of DDW is slightly higher than that of GGW. As might be expected, the effect of SA/V ratio is not that pronounced in corrosion. An increase in SA/V ratio of almost 100 times for BGW caused only a 4-fold increase in the leach rate.

Equations 4.11 and 4.12 were applied to the same data sets, and the plots are shown in Figs. 4.55 and 4.56, respectively. Values of the coefficients a_1, a_2 and x were calculated using these plots and the results are compared in Table 4.13. The value of the exponent x is expected to be between 0.5 and 1 and is indicative of the leaching process at work. A power of 1 indicates a dissolution (corrosion) process while a power of 0.5 indicates a diffusion-controlled one (82ALTE1). It can be seen from Table 4.13 that in almost all cases (excluding GGW at SA/V = 0.10 cm^{-1} where x = 0.33) x is around 0.5, and thus the dominating mechanism seems to be diffusion.

Values of x can be affected by the leaching mechanism, SA/V ratio and solution pH. If the SA/V ratio is high or the solubility is low, or a surface film forms which becomes increasingly impervious and prevents further reaction with underlying glass, then x will approach zero and the reaction will stop. If however, selective leaching carries on awhile before a steady-state is reached and the process is not limited by solubility, the rate of dissolution of the surface film finally deter-

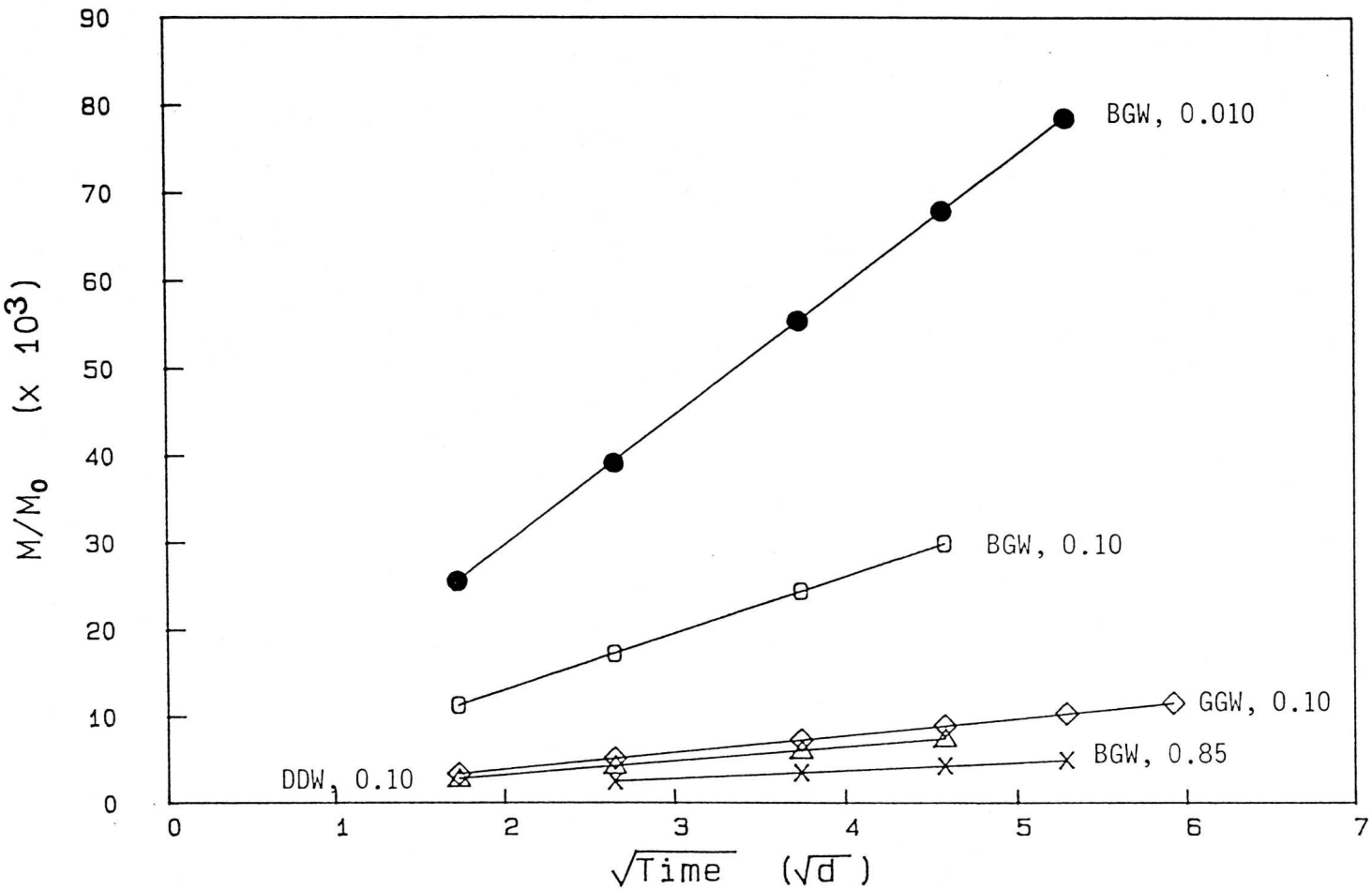

Figure 4.55. Plots of M/M_0 versus $(Time)^{1/2}$ for I-117 Glass leached in synthetic Grande Ronde basaltic groundwater at SA/V = 0.010, 0.10 and 0.85 cm^{-1} and distilled deionized water and synthetic granitic groundwater at 0.10 cm^{-1}, all at 90°C.

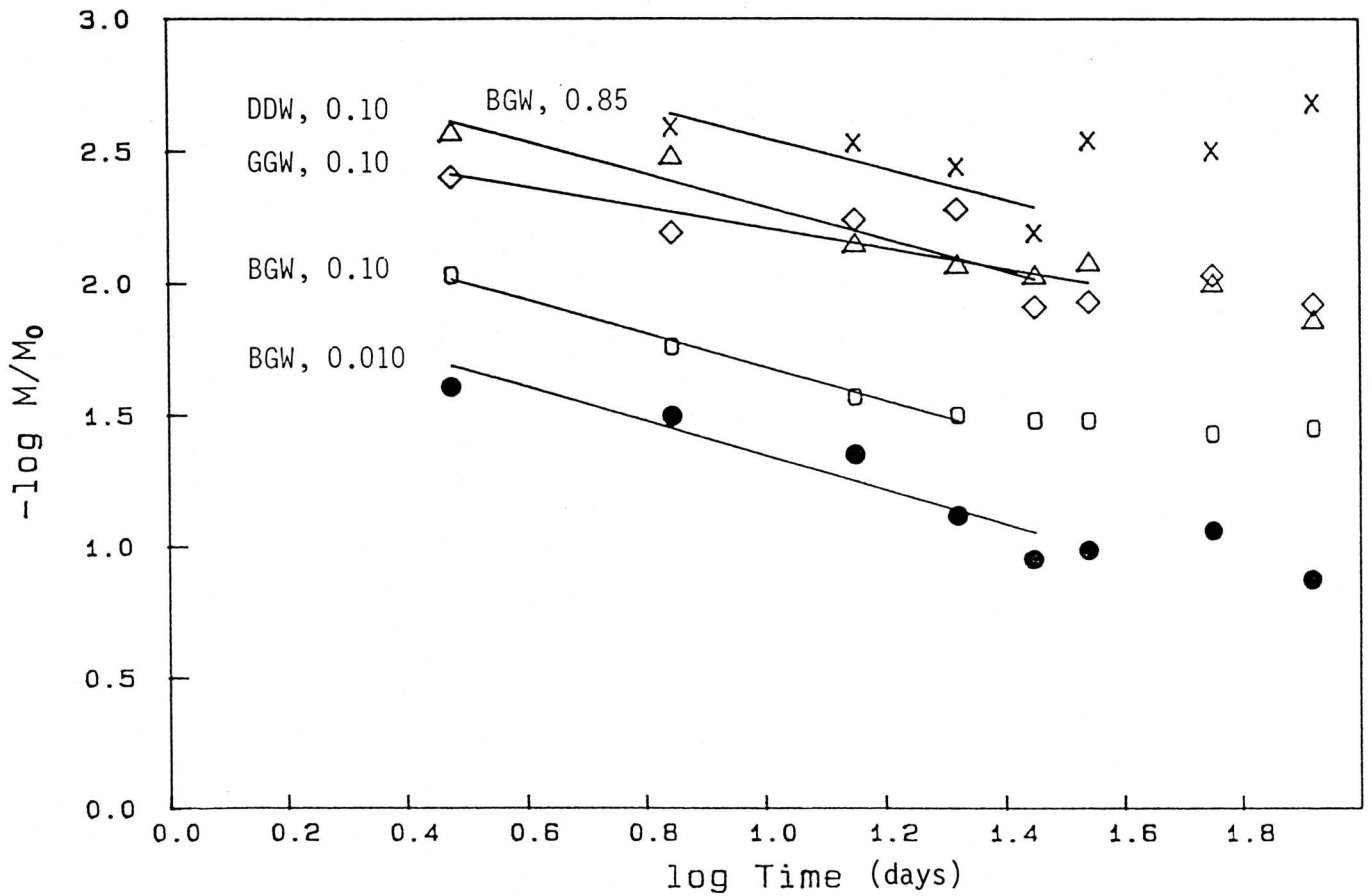

Figure 4.56. Plots of log M/M_0 versus log Time for I-117 Glass leached in synthetic Grande Ronde basaltic groundwater at SA/V = 0.010, 0.10 and 0.85 cm^{-1}, distilled deionized water and synthetic granitic groundwater at SA/V = 0.10 cm^{-1}, all at 90°C.

Table 4.13. Coefficients a_1 and a_2 and exponent x as calculated from equations 4.11 and 4.12

LEACHANT	SA/V RATIO (cm^{-1})	a_1 ($d^{-1/2}$)	a_2 (d^{-x})	x
BGW	0.010	0.015	0.010	0.647
BGW	0.10	0.0065	0.0048	0.632
BGW	0.85	0.00094	0.00073	0.594
DDW	0.10	0.0016	0.0012	0.494
GGW	0.10	0.0020	0.0025	0.326

mines the leach rate and x approaches 1. As may be observed, the SA/V ratio does have a small effect on the value of x calculated for the BGW data (Table 4.12). As the SA/V ratio increases, the value of x decreases slightly. The diffusion process depends on the leachant composition and on the surface area. As the SA/V ratio increases so should the diffusion component of the mechanism at work, and x will tend more towards 0.5. The values of x calculated for DDW and GGW at SA/V = 0.10 cm^{-1} are lower than that of the corresponding BGW leachant. The diffusion component can be decreased by the leachant composition. Since BGW initially contained the highest concentration of ions this could explain why the value of x is somewhat higher than 0.5.

The three equations (4.10-4.12) can be used for the long-term extrapolation of the data as illustrated in Table 4.14. The time periods required for complete dissolution of the glass specimen using the 5 sets of data obviously produce very different results. Application of the three equations to the BGW data reveals that with increasing SA/V ratio the time for complete dissolution increases. At SA/V = 0.010 and 0.10 cm^{-1} the times as calculated using corrosion (Equation 4.10) and diffusion (Equation 4.11) are almost equal; however, as the SA/V ratio increases the diffusion component becomes more dominant and the time for dissolution by diffusion increases significantly over that of corrosion (SA/V = 0.85 cm^{-1}). As the contribution of the diffusion component increases, the time calculated using the empirical formula (4.12) also increases. At the lowest SA/V ratios (0.010 and 0.10 cm^{-1}), where corrosion and diffusion appear equally important in the dissolution of the glass, the combined effect as calculated by Equation 4.12 produces the shortest time for

Table 4.14. Times calculated for complete dissolution of I-117 Glass specimens

LEACHANT	SA/V RATIO (cm^{-1})	TIME FOR COMPLETE DISSOLUTION		
		CORROSION (d) (Eqn. 4.10)	DIFFUSION (d) (Eqn. 4.11)	EMPIRICAL (d) (Eqn. 4.12)
BGW	0.010	2.4×10^{3}	4.5×10^{3}	1.2×10^{3}
BGW	0.10	1.4×10^{4}	2.3×10^{4}	4.6×10^{3}
BGW	0.85	2.3×10^{4}	1.1×10^{6}	2.0×10^{5}
DDW	0.10	4.6×10^{4}	3.8×10^{5}	3.9×10^{4}
GGW	0.10	7.1×10^{4}	2.6×10^{5}	1.8×10^{5}

complete dissolution. As diffusion becomes more dominant in the dissolution process compared to corrosion, the time calculated using Equation 4.12 also increases until at SA/V = 0.85 cm^{-1} where the time is similar to that calculated for corrosion only.

Since the diffusion component is more prevalent in the case of GGW and DDW, it is not surprising that the times calculated using Equation 4.11 for these leachants are higher than the corresponding BGW time (SA/V = 0.10 cm^{-1}). Since the contribution of the diffusion component is greater than that of corrosion, the combined effects as determined by the empirical formula (Equation 4.12) produces times very close or greater than those calculated by the corrosion processes alone for DDW and GGW. It has already been mentioned the diffusion process depends on the leachant composition. Since GGW contains more ions than DDW, this slows down the diffusion process; hence, the time required for complete dissolution by GGW increases compared to that of DDW as shown by calculations using the diffusion and empirical equations (Equations 4.11 and 4.12).

4.F. SUMMARY

Static leaching studies have been conducted on different types of glass in order to investigate the effects of several parameters on the leach rate. The leachant composition has been found to influence the glass dissolution process through the effects of pH and ionic concentration. High pH values such as those found in BGW leachant severely increased the rate of leaching. At high pH the matrix element silicon in the form of silicic acid could be made more soluble, thus aiding in glass

dissolution. The solubilities of other elements were affected by pH, and a number of these were found to predominate in a precipitated form. Certain anions such as carbonates and sulfates were important in making uranium, samarium and other rare earth elements more soluble. As expected, increased temperature helped to accelerate the leaching process, and as the glass surface area to leachant volume (SA/V) increased the rate of leaching decreased.

Three simple leaching models were applied to data obtained in this work to illustrate the differences in predictions of long-term results based on diffusion- and/or corrosion-controlled mechanisms. The dominant mechanism appears to be diffusion.

A difference was observed in the concentrations of elements such as lanthanum, manganese, samarium and uranium sampled while the leachate was hot compared to that after cooling to room temperature. These differences may have been due to the presence of pseudocolloids.

More information concerning the leaching of the glass might have been obtained if access to a surface analysis technique had been available. Some elements are known to be accumulated in the reactive layer which forms on the glass, or are re-precipitated on the surface. Unfortunately, surface analyses of the glass could not be performed.

CHAPTER 5

CONCLUSIONS AND RECOMMENDATIONS

5.A. CONCLUSIONS

A method for the determination of 40 major, minor and trace elements in various types of glass by INAA and EINAA was developed. The method consisted of 3 irradiations, 3 decay and 3 counting periods, namely 2-5 min, 7-10 min and 10 min, 1 h, 2d and 6h or 7 h, 5-28 d and 12h. The list of elements determined included Al, As, Ba, Br, Ca, Ce, Cl, Co, Cr, Cs, Eu, Fe, Hf, I, K, La, Mg, Mn, Mo, Na, Nd, Ni, Pr, Rb, Sb, Sc, Si, Sm, Sn, Sr, Ta, Tb, Th, Ti, Tm, U, V, W, Yb, Zn and Zr. An INAA method was also developed specifically for the determination of elements which were leached from glass, and involved 3 irradiations, 2 decays and 2 counting periods; 10 min-10 min-10 min, 7h-3d-6h and 3h-3d-3h. The elements determined using these schemes were Al, Ce, Cs, Fe, La, Mn, Mo, Na, Nd, Ni, Pr, Sm, U and W.

The precision and accuracy of this method was reasonably good ($\pm$10%) as determined through the use of the NBS SRM 92 Glass and NRCC Marine Sediment (RM MESS-1). The limits of detection were sufficiently low (0.182-125000 ppm) enough to allow the determination of the elements of interest used in evaluating glass for its suitability as a waste form immobilization matrix.

Two methods of boron determination were modified for the analysis of glass. The indirect INAA method was particularly well-suited for the

determination of high concentrations of boron (> 1% B) in glass, provided the subsequent activity of the sample was not so high as to make counting of the sample impossible within the first minute after irradiation. The spectrophotometric method was easily applied to leachates containing low boron concentrations (viz. 1-4 ppm). Low concentrations of silicon were determined in the leachates using a colorimetric method involving molybdenum blue. This method was specifically adapted for this purpose in order to remove an interference caused by fluoride in the leachates and is applicable for samples with silicon in the range of 5-100 ppm. The accuracy of the method was checked through the use of NBS SRM 1572 Citrus Leaves.

Static leaching experiments were designed to investigate the effects of time, temperature (40° and 90°C), leachant composition (distilled deionized water, synthetic granitic groundwater (GGW) and synthetic Grande Ronde basaltic groundwater (BGW)) including pH and ionic concentration, and surface area to volume ratio (SA/V) (0.010, 0.10 and 0.85 cm^{-1}) on the rate of leaching of elements from simulated waste oxide-loaded glasses. These included AECL 981 and Corning Glass JL - both sodium calcium aluminosilicate glasses, AECL 200 - a sodium borosilicate glass and CEC Glass and I-117 Glass - both simulated waste oxide-loaded sodium borosilicate glasses. Both leachate solutions as well as precipitated materials were collected for analysis.

Results of the leaching experiments indicated a strong influence of the leachant composition through both its pH and nature as well as concentrations of ions present on the leach rate. Glass leachability, as determined by total mass loss, was highest in BGW exceeding even that of

deionized water. The only exception to this observation was the leaching behaviour at the highest SA/V ratio (0.85 cm^{-1}) and was thought to be due to a different batch of glass used. The higher leachability in BGW was due primarily to its higher pH (>9) which increased the solubility of silicon in the form of silicic acid. Since silicon controls the release of other elements from the glass matrix, its solubility is extremely important. High pH also increases glass dissolution by the corrosion mechanism. Even though BGW appeared to be the most aggressive leachant overall, certain elements, namely La, Mn and Sm were preferentially leached in DDW and GGW, and their concentrations were higher than the corresponding concentrations in BGW.

Solution pH was also a factor in the precipitation of certain elements. This effect may be beneficial in some cases, such as La, Sm and U where mobility and hence migration potential to the biosphere is decreased. However, if the concentration of certain nuclides in the leachate is reduced by precipitation thereby increasing the rate of dissolution of the glass then the chance of other radionuclides reaching the biosphere is also increased. The concentration of silicon in solution is as important as that of the lanthanides. The Si concentrations found in the leachates were well below the reported solubility limits indicating the possibility that Si was re-precipitating on the glass surface. This is of concern since Si will continue to be leached, and with it other elements.

Concentrations of certain ions in BGW helped to develop its aggressiveness. Higher concentrations of anions such as carbonates and sulfates in BGW strongly affected the solubility of Sm and other lanthanides and

U possibly through the formation of soluble anionic complexes which may have considerable migration potential. The use of backfill materials incorporated in the waste disposal package are expected to trap the cationic species in the leachate, but no such screen exists to retain the anionic species.

An increase in temperature was observed to significantly accelerate glass leaching. The rate of leaching at 90°C was 5-30 times higher than that at 40°C. It is important to keep in mind that the temperature encountered will vary depending upon the time elapsed between the initial disposal in the repository and the onset of leaching. It has been estimated that the repository temperature could exceed 100°C within the first 100 years, whereas after 500 years it will have fallen to the temperature of the environment (30-60°C). Thus, the importance of the temperature effect will depend largely upon time.

Activation energies were calculated for I-117 glass at 3 SA/V ratios for each leachant. The calculated values compare well with those quoted in the literature (50-80 KJ/mole) for various glasses. Activation energies in the BGW leachant were the highest suggesting that glass leached in this solution would be more sensitive to temperature variations.

Mass losses calculated for 9 different elements from data in this study showed that the rates of leaching decreased with increasing SA/V ratio. This effect can be considered beneficial for long-term repository disposal because it is anticipated that only small quantities of water will actually come in contact with the glass. An accelerated attainment of the equilibrium pH was achieved with increased SA/V ratio.

Concentrations of La, Mn, Sm and U in leachate sampled at 90°C were found to be lower than when the same leachate was sampled after cooling to room temperature. A possible explanation for this difference was thought to be due to the presence of pseudocolloids. Species of the elements of interest can be adsorbed on colloidal particles present in solution as impurities such as Al or Fe hydroxides, forming new particles referred to as pseudocolloids. Their presence in solution can have important implications for waste management as the incorporation of actinides could increase the mobility and migration of some radionuclides.

Three long-term dissolution models based on corrosion- and diffusion-controlled mechanisms as well as a combination of both were applied to the data obtained in this work. These models revealed that the dominating mechanism of glass leaching was diffusion. As the SA/V ratio increased the diffusion component was shown to become more important. The above equations can be used for long-term extrapolation of the leaching data. Care must be exercised in using such models for evaluating the long-term safety of a disposal option as radically different results can be obtained by over- and under-estimations of various parameters.

5.B. RECOMMENDATIONS

In addition to the variables studied in this work, a few other variables which may affect the leaching process are recommended for further study. The effect of Eh on the rate of glass leaching and solubility limits needs to be given considerable attention. More research is needed

to determine the conditions under which colloids are formed, as well as under which actinides are incorporated in these colloids and the extent of their migration. Experiments in which glass is loaded with real HLW are needed to provide information on the effects of radiation on the leach rate. Finally, studies should be conducted on the impact of near-field components on the durability of the waste form. Such studies should include all components of the waste package, backfill and repository rock.

A major short-coming of our work was the unavailability of surface analysis techniques in order to determine the chemical composition of altered layers formed on the glass. Formation of surface layers is a common feature of leached borosilicate glass, and some elements are found to be more prevalent in these layers. The use of techniques such as SEM, SIMS and electron probe microanalysis could assist in this analysis.

To handle the sheer numbers of leachate samples generated in this type of work, an automated sample changer should be utilized to help in the counting of these samples after irradiations.

A comprehensive glass dissolution model which will enable long-term extrapolation is needed. This model should encompasses the variables such as temperature, pressure, leachant composition, new phase formation and changes in SA/V ratio.

CHAPTER 6

APPENDIX

6.A. NORMALIZED ELEMENTAL MASS LOSS DATA

The following pages contain tables of normalized elemental mass loss data for I-117 Glass leached in distilled deionized water (DDW), synthetic granitic groundwater (GGW), and synthetic Grande Ronde basaltic groundwater (BGW) at three SA/V ratios (0.010, 0.10 and 0.85 cm^{-1}) and two temperatures (40° and 90°C).

1st column - represents the number of days of leaching;

2nd column - represents leachate solution sampled at experimental temperature (either 40° or 90°C);

3rd column - represents precipitated material stripped from the bottle and Teflon mesh support using acid; and

4th column - represents precipitated material filtered from the leachate solution.

Values for B and Si are for leachates sampled at room temperature only. Normalized mass loss values for precipitate stripped from the bottle by acid or filtered from solution are not available for these two elements.

6.A.1. SA/V = 0.010 cm^{-1}

6.A.1.A. Sodium Normalized Mass Loss

DDW

Day	90°C	Room Temperature	Acid Strip	Precipitate
3	14.2	12.0	3.32	0.142
7	26.4	27.5	1.04	0.213
14	53.3	50.0	1.17	0.179
21	59.2	57.2	1.10	0.128
28	64.8	66.8	≤dl	0.285
35	77.7	76.7	9.28	0.250
56	87.4	88.3	0.0693	1.74
84	114	113	1.91	0.267

GGW

3	14.1	11.3	1.54	0.241
7	7.62	9.87	0.926	0.170
14	22.6	28.2	2.75	0.218
21	43.1	50.2	1.11	0.445
28	-	-	-	-
35	40.0	46.7	1.61	0.662
56	68.3	65.4	0.129	0.393
84	58.0	58.3	0.450	0.0877

BGW

3	≤dl	≤dl	2.76	0.517
7	≤dl	≤dl	3.07	0.144
14	201	46.0	3.90	1.19
21	750	417	4.35	1.09
28	≤dl	310	3.19	1.60
35	≤dl	29.3	7.61	2.56
56	508	472	5.87	2.13
84	≤dl	364	7.27	0.905

DDW

Day	40°C	Room Temperature	Acid Strip	Precipitate
3	3.39	3.53	1.84	0.257
7	2.82	3.18	0.936	0.324
14	4.20	3.61	1.98	0.713
21	5.54	5.69	0.857	0.377
28	4.21	6.15	1.12	0.209
35	5.86	6.39	0.765	0.226
56	7.01	7.49	≤dl	0.155
84	7.87	7.15	2.91	0.0822

GGW

Day	40°C	Room Temperature	Acid Strip	Precipitate
3	4.77	6.55	0.933	0.220
7	4.87	4.01	2.19	0.466
14	≤dl	3.23	5.36	0.330
21	5.36	2.44	0.969	0.210
28	5.81	4.08	0.301	8.74
35	4.66	7.98	1.94	0.586
56	5.51	6.01	0.935	0.349
84	1.70	2.94	0.150	0.175

BGW

3	≤dl	≤dl	1.16	0.224
7	≤dl	≤dl	2.67	1.59
14	≤dl	11.8	-	0.283
21	≤dl	≤dl	0.857	0.431
28	99.6	≤dl	1.66	0.441
35	67.6	13.8	1.14	1.29
56	≤dl	≤dl	3.43	1.51
84	63.5	43.3	≤dl	0.334

6.A.1.B. Manganese Normalized Mass Loss

DDW

Day	90°C	Room Temperature	Acid Strip	Precipitate
3	0.421	0.232	0.225	0.0399
7	5.55	5.59	1.07	0.0433
14	30.6	31.8	0.373	0.0362
21	31.4	30.7	≤dl	0.0303
28	36.7	40.0	0.416	0.0642
35	27.2	40.3	≤dl	0.0316
56	53.7	51.9	≤dl	0.0578
84	72.9	73.4	≤dl	0.0287

GGW

3	1.34	2.97	1.40	0.358
7	3.75	3.31	0.628	0.0319
14	16.2	14.0	0.394	0.0502
21	33.5	35.1	0.964	0.969
28	-	-	-	-
35	28.3	31.5	2.14	0.0525
56	35.1	33.5	2.12	0.0394
84	0.509	20.4	11.7	0.0485

BGW

Day	90°C	Room Temperature	Acid Strip	Precipitate
3	≤dl	≤dl	0.465	0.142
7	≤dl	≤dl	0.648	0.288
14	≤dl	≤dl	4.79	1.72
21	≤dl	≤dl	8.51	2.82
28	≤dl	≤dl	12.0	5.07
35	42.7	39.2	15.0	6.31
56	≤dl	≤dl	27.9	0.407
84	46.8	≤dl	13.1	0.512

DDW

Day	40°C	Room Temperature	Acid Strip	Precipitate
3	0.489	0.487	≤dl	0.0461
7	0.326	≤dl	1.64	0.0620
14	1.77	2.41	≤dl	0.0439
21	1.68	1.78	1.55	0.0791
28	2.16	1.23	≤dl	0.0429
35	≤dl	2.48	≤dl	0.0672
56	2.30	2.02	≤dl	0.0668
84	3.13	2.49	≤dl	0.0415

GGW

3	1.60	1.12	0.354	0.0670
7	0.974	2.41	0.904	0.0533
14	1.71	1.11	0.506	0.0976
21	≤dl	≤dl	≤dl	0.0321
28	4.03	2.83	≤dl	0.118
35	1.26	2.33	0.487	0.0935
56	2.37	1.38	≤dl	0.0709
84	3.77	≤dl	0.697	0.0309

BGW

3	≤dl	≤dl	0.443	0.0385
7	≤dl	≤dl	≤dl	0.00568
14	≤dl	≤dl	-	0.0620
21	≤dl	≤dl	0.629	0.0513
28	≤dl	≤dl	≤dl	0.134
35	≤dl	≤dl	0.867	0.118
56	≤dl	≤dl	≤dl	0.0486
84	≤dl	≤dl	1.19	0.152

6.A.1.C. Uranium Normalized Mass Loss

DDW

Day	90°C	Room Temperature	Acid Strip	Precipitate
3	≤dl	≤dl	1.17	≤dl
7	≤dl	1.42	≤dl	0.108
14	3.74	4.48	28.1	0.565
21	≤dl	≤dl	31.2	0.243
28	≤dl	1.54	40.9	0.638
35	≤dl	2.35	40.5	0.860
56	3.22	≤dl	64.3	1.64
84	1.29	≤dl	117	1.55

GGW

3	1.20	≤dl	≤dl	0.112
7	≤dl	≤dl	≤dl	0.1369
14	≤dl	≤dl	0.994	1.20
21	1.39	≤dl	11.4	0.342
28	-	-	-	-
35	1.80	≤dl	18.1	18.1
56	≤dl	≤dl	41.6	2.13
84	≤dl	≤dl	28.5	≤dl

BGW

3	6.62	≤dl	≤dl	≤dl
7	22.4	26.2	≤dl	0.0908
14	23.4	33.1	3.34	0.659
21	34.6	33.1	4.51	1.19
28	40.4	47.5	1.86	1.21
35	0.161	44.2	≤dl	1.08
56	51.5	57.1	3.02	≤dl
84	43.8	46.7	2.47	0.181

DDW

Day	40°C	Room Temperature	Acid Strip	Precipitate
3	≤dl	≤dl	≤dl	0.0987
7	≤dl	≤dl	≤dl	≤dl
14	≤dl	≤dl	≤dl	0.110
21	≤dl	≤dl	1.32	≤dl
28	≤dl	≤dl	≤dl	≤dl
35	≤dl	≤dl	0.871	≤dl
56	≤dl	≤dl	≤dl	0.0870
84	≤dl	≤dl	0.837	0.0895

GGW

Day	40°C	Room Temperature	Acid Strip	Precipitate
3	≤dl	≤dl	≤dl	≤dl
7	1.78	≤dl	≤dl	0.117
14	≤dl	≤dl	1.56	≤dl
21	4.37	≤dl	≤dl	≤dl
28	≤dl	≤dl	≤dl	0.0562
35	≤dl	≤dl	≤dl	0.0858
56	1.00	0.901	≤dl	≤dl
84	≤dl	1.00	≤dl	≤dl

BGW

3	≤dl	≤dl	6.89	≤dl
7	≤dl	3.79	≤dl	≤dl
14	≤dl	4.89	-	≤dl
21	3.99	≤dl	≤dl	≤dl
28	≤dl	≤dl	≤dl	0.0741
35	4.14	7.79	≤dl	≤dl
56	4.97	4.56	1.32	≤dl
84	≤dl	6.06	≤dl	≤dl

6.A.1.D. Samarium Normalized Mass Loss

DDW

Day	90°C	Room Temperature	Acid Strip	Precipitate
3	≤dl	0.0166	0.0592	0.0217
7	0.394	0.316	2.08	0.585
14	7.60	13.5	11.9	0.389
21	2.91	4.60	24.2	0.345
28	3.11	4.19	36.5	0.569
35	3.72	5.43	27.6	1.07
56	8.81	8.94	44.0	1.57
84	5.97	7.16	75.4	1.87

GGW

3	0.0343	0.0788	0.104	0.112
7	0.0262	0.0427	0.239	0.138
14	0.840	1.30	10.6	0.937
21	6.65	9.54	25.5	0.308
28	-	-	-	-
35	0.198	0.299	28.8	0.274
56	0.216	0.581	34.6	0.254
84	0.0235	≤dl	21.1	0.0195

BGW

Day	90°C	Room Temperature	Acid Strip	Precipitate
3	0.0959	0.106	0.0848	0.0702
7	0.187	0.223	0.0466	0.635
14	0.143	0.742	3.60	4.56
21	≤dl	1.08	4.78	3.73
28	≤dl	1.86	1.89	5.99
35	0.451	0.410	2.19	7.70
56	≤dl	≤dl	9.10	0.0293
84	≤dl	≤dl	0.499	0.0695

DDW

Day	40°C	Room Temperature	Acid Strip	Precipitate
3	0.0194	0.0193	0.378	0.0509
7	0.0649	0.0613	0.0727	0.0996
14	0.209	0.202	0.243	0.166
21	0.147	0.157	0.413	0.397
28	0.0363	0.0659	0.393	0.0738
35	0.164	0.189	0.612	0.131
56	0.510	0.522	0.275	0.145
84	0.492	0.513	0.224	0.207

GGW

3	0.0440	0.0220	0.0830	0.0273
7	0.0262	0.0807	0.213	0.0687
14	0.0566	0.0566	0.253	0.295
21	0.0827	0.119	0.344	0.253
28	0.0411	0.0770	0.439	0.102
35	0.129	0.114	0.566	0.126
56	0.179	3.15	0.550	0.146
84	0.835	0.0799	0.833	0.0805

BGW

3	≤dl	≤dl	0.0718	0.0207
7	≤dl	≤dl	0.0545	0.0207
14	0.241	0.337	-	0.165
21	≤dl	0.177	0.0387	0.125
28	≤dl	0.106	0.104	0.180
35	0.215	0.134	0.0704	0.0894
56	0.303	0.378	0.0654	0.102
84	0.348	0.320	0.0753	0.158

6.A.1.E. Lanthanum Normalized Mass Loss

DDW

Day	90°C	Room Temperature	Acid Strip	Precipitate
3	≤dl	0.449	0.705	0.0866
7	0.562	0.502	0.503	0.480
14	3.91	7.88	3.32	0.166
21	2.33	4.71	9.11	0.157
28	3.10	3.04	15.2	0.218
35	3.40	4.45	15.0	0.594
56	6.24	7.62	20.6	0.543
84	5.41	5.41	35.8	5.41

GGW

3	≤dl	≤dl	0.116	0.0543
7	≤dl	≤dl	0.484	0.136
14	1.13	1.58	5.45	0.435
21	5.92	9.05	9.00	0.110
28	-	-	-	-
35	≤dl	≤dl	15.9	0.155
56	1.06	0.627	16.6	0.130
84	≤dl	≤dl	13.0	0.0110

BGW

3	≤dl	≤dl	≤dl	≤dl
7	3.29	≤dl	≤dl	0.372
14	≤dl	≤dl	1.76	1.82
21	≤dl	≤dl	2.53	1.40
28	≤dl	≤dl	1.09	3.10
35	≤dl	≤dl	1.51	2.89
56	≤dl	≤dl	5.36	0.0112
84	≤dl	≤dl	0.279	0.0262

DDW

Day	40°C	Room Temperature	Acid Strip	Precipitate
3	≤dl	≤dl	≤dl	≤dl
7	≤dl	≤dl	0.0858	0.0835
14	≤dl	≤dl	≤dl	0.159
21	≤dl	≤dl	≤dl	0.309
28	0.372	0.521	0.349	0.0829
35	≤dl	≤dl	0.351	0.0755
56	1.03	0.474	0.212	0.0934
84	0.703	0.473	0.135	0.109

GGW

Day	40°C	Room Temperature	Acid Strip	Precipitate
3	0.192	0.191	0.0959	≤dl
7	≤dl	≤dl	0.165	≤dl
14	≤dl	≤dl	0.202	0.185
21	≤dl	≤dl	0.341	0.173
28	0.256	0.348	0.349	0.0652
35	≤dl	0.492	0.662	0.1028
56	≤dl	0.270	≤dl	0.0778
84	≤dl	≤dl	1.49	0.0482

BGW

3	≤dl	≤dl	≤dl	≤dl
7	≤dl	≤dl	≤dl	≤dl
14	≤dl	≤dl	-	0.0447
21	≤dl	≤dl	≤dl	0.0466
28	≤dl	≤dl	0.156	0.0653
35	≤dl	≤dl	0.122	0.0492
56	≤dl	≤dl	≤dl	0.265
84	≤dl	≤dl	0.293	0.0716

6.A.1.F. Molybdenum Normalized Mass Loss

DDW

Day	90°C	Room Temperature	Acid Strip	Precipitate
3	33.4	≤dl	≤dl	2.50
7	78.8	48.1	≤dl	≤dl
14	57.5	29.8	≤dl	≤dl
21	77.1	77.4	≤dl	≤dl
28	54.9	86.3	7.69	≤dl
35	84.2	55.1	≤dl	≤dl
56	57.0	76.4	≤dl	1.17
84	68.2	103	≤dl	1.20

GGW

3	62.3	74.1	11.36	1.97
7	42.6	64.9	≤dl	≤dl
14	33.4	41.0	≤dl	≤dl
21	35.2	47.2	≤dl	≤dl
28	-	-	-	-
35	50.5	38.3	≤dl	≤dl
56	111	123	≤dl	16.1
84	94.5	92.3	≤dl	≤dl

BGW

Day	90°C	Room Temperature	Acid Strip	Precipitate
3	164	228	12.1	3.37
7	243	≤dl	≤dl	≤dl
14	277	≤dl	≤dl	≤dl
21	≤dl	≤dl	≤dl	≤dl
28	≤dl	≤dl	≤dl	≤dl
35	≤dl	≤dl	≤dl	0.872
56	406	382	≤dl	≤dl
84	363	480	≤dl	0.407

DDW

Day	40°C	Room Temperature	Acid Strip	Precipitate
3	≤dl	≤dl	≤dl	≤dl
7	≤dl	23.1	≤dl	≤dl
14	≤dl	43.7	14.3	≤dl
21	≤dl	60.4	≤dl	≤dl
28	86.6	72.5	≤dl	≤dl
35	25.3	≤dl	≤dl	≤dl
56	≤dl	≤dl	≤dl	≤dl
84	21.0	13.7	≤dl	≤dl

GGW

3	51.8	34.5	16.5	≤dl
7	19.0	≤dl	≤dl	2.76
14	29.6	≤dl	≤dl	≤dl
21	58.5	27.2	≤dl	≤dl
28	≤dl	≤dl	≤dl	≤dl
35	28.7	≤dl	≤dl	≤dl
56	≤dl	17.0	≤dl	≤dl
84	43.5	30.0	≤dl	≤dl

BGW

3	≤dl	≤dl	≤dl	1.76
7	204	≤dl	≤dl	4.17
14	≤dl	≤dl	-	≤dl
21	≤dl	228	≤dl	≤dl
28	≤dl	165	8.83	0.455
35	253	229	≤dl	≤dl
56	≤dl	≤dl	≤dl	≤dl
84	265	≤dl	≤dl	≤dl

6.A.1.G. Aluminum Normalized Mass Loss

DDW

Day	90°C	Room Temperature	Acid Strip	Precipitate
3	4.74	4.92	9.31	≤dl
7	6.84	6.36	6.33	≤dl
14	34.7	36.8	4.26	≤dl
21	35.0	32.8	2.41	≤dl
28	42.5	37.9	4.46	≤dl
35	37.8	36.7	1.86	0.128
56	52.7	47.3	2.02	≤dl
84	75.9	72.6	4.60	0.0622

GGW

3	11.8	11.8	8.79	≤dl
7	6.66	7.13	6.25	≤dl
14	-	13.7	4.67	0.188
21	37.4	40.5	2.50	≤dl
28	-	-	-	-
35	5.68	6.49	4.30	≤dl
56	16.4	14.7	4.62	≤dl
84	11.6	8.45	6.36	≤dl

BGW

3	9.73	≤dl	6.88	0.241
7	60.8	31.7	3.32	≤dl
14	38.3	≤dl	3.80	0.665
21	32.7	26.4	4.83	1.00
28	23.4	75.2	5.92	1.05
35	12.2	29.9	6.01	0.830
56	27.5	28.5	3.32	0.0867
84	11.8	31.3	6.88	0.188

DDW

Day	40°C	Room Temperature	Acid Strip	Precipitate
3	4.06	3.25	7.13	0.255
7	2.18	0.798	10.8	≤dl
14	1.96	0.801	0.600	≤dl
21	1.19	1.69	1.08	≤dl
28	10.1	1.09	1.89	≤dl
35	0.713	0.436	1.31	≤dl
56	0.479	2.66	3.87	≤dl
84	0.853	1.12	0.0963	0.150

GGW

Day	40°C	Room Temperature	Acid Strip	Precipitate
3	0.600	2.42	4.42	≤dl
7	2.12	1.68	5.85	≤dl
14	2.36	2.04	5.09	≤dl
21	4.84	4.26	0.0386	≤dl
28	2.60	2.09	0.822	≤dl
35	1.38	3.18	≤dl	0.0335
56	1.93	2.22	3.04	0.0238
84	2.72	1.22	4.37	0.382

BGW

3	20.0	19.9	6.47	≤dl
7	≤dl	≤dl	24.4	≤dl
14	≤dl	≤dl	-	≤dl
21	≤dl	≤dl	0.563	≤dl
28	≤dl	2.46	0.723	0.171
35	≤dl	12.3	0.809	≤dl
56	48.7	≤dl	3.62	0.0875
84	13.2	5.75	2.76	0.301

6.A.1.H. Boron Normalized Mass Loss

90°C

Day	DDW	GGW	BGW
3	10.2	8.22	28.0
7	21.3	3.12	30.6
14	52.1	28.9	65.4
21	69.7	54.4	81.9
28	61.6	-	96.6
35	68.9	64.8	45.5
56	83.1	55.4	99.3
84	98.2	55.6	145

40°C

Day	DDW	GGW	BGW
3	≤dl	≤dl	12.9
7	≤dl	1.84	11.2
14	2.92	2.20	-
21	3.11	0.691	2.84
28	1.50	2.92	5.40
35	4.81	1.29	11.3
56	5.00	0.146	6.60
84	5.67	2.94	7.75

6.A.1.I. Silicon Normalized Mass Loss

90°C

Day	DDW	GGW	BGW
3	≤dl	8.69	34.2
7	≤dl	4.73	32.7
14	25.2	6.59	103
21	40.7	34.0	98.2
28	27.9	-	85.3
35	31.5	17.7	341
56	67.2	18.7	121
84	84.1	36.3	138

40°C

Day	DDW	GGW	BGW
3	≤dl	≤dl	≤dl
7	1.47	2.15	23.5
14	≤dl	1.46	-
21	1.98	≤dl	20.5
28	≤dl	1.29	65.2
35	7.75	≤dl	45.0
56	3.61	1.94	≤dl
84	5.60	≤dl	≤dl

6.A.2 SA/V 0.10 cm^{-1}

6.A.2.A. Sodium Normalized Mass Loss

DDW

Day	90°C	Room Temperature	Acid Strip	Precipitate
3	8.84	8.99	0.396	≤dl
7	8.65	11.6	0.381	≤dl
14	16.6	15.9	0.168	≤dl
21	18.9	19.4	0.350	≤dl
28	15.7	16.1	0.336	≤dl
35	23.7	24.7	0.504	≤dl
56	18.1	19.0	0.351	≤dl
84	21.8	21.8	1.37	≤dl

GGW

Day	90°C	Room Temperature	Acid Strip	Precipitate
3	6.70	6.85	0.256	≤dl
7	9.26	9.10	0.156	≤dl
14	8.74	8.74	0.357	≤dl
21	10.1	10.1	0.222	≤dl
28	17.8	18.6	0.333	≤dl
35	19.4	19.9	0.708	≤dl
56	16.4	16.6	0.498	≤dl
84	22.5	24.0	0.862	≤dl

BGW

3	268	213	0.879	≤dl
7	46.3	82.4	0.492	≤dl
14	113	119	0.794	≤dl
21	113	110	0.763	≤dl
28	43.1	44.4	1.06	≤dl
35	65.1	62.9	0.823	≤dl
56	33.5	86.3	0.738	≤dl
84	104	97.8	1.08	≤dl

DDW

Day	40°C	Room Temperature	Acid Strip	Precipitate
3	0.888	0.817	0.364	≤dl
7	1.42	1.69	0.456	≤dl
14	1.65	1.69	0.182	≤dl
21	1.73	1.97	0.991	≤dl
28	2.96	3.02	0.762	≤dl
35	2.54	2.36	0.117	≤dl
56	2.86	2.85	0.206	≤dl
84	3.72	3.78	0.0498	≤dl

GGW

3	0.743	0.893	0.273	≤dl
7	1.17	1.19	0.308	-
14	1.22	1.48	0.221	≤dl
21	1.91	1.79	0.360	≤dl
28	1.46	1.66	0.617	≤dl
35	2.44	2.35	0.458	≤dl
56	2.46	2.65	0.158	≤dl
84	2.60	2.86	0.0277	≤dl

BGW

Day	40°C	Room Temperature	Acid Strip	Precipitate
3	37.8	29.1	0.591	≤dl
7	18.2	33.1	0.349	≤dl
14	38.1	45.2	0.409	≤dl
21	≤dl	≤dl	0.647	≤dl
28	18.9	≤dl	0.687	≤dl
35	12.5	≤dl	0.388	≤dl
56	≤dl	≤dl	0.266	≤dl
84	18.0	20.5	0.258	≤dl

6.A.2.B. Manganese Elemental Mass Loss

DDW

Day	90°C	Room Temperature	Acid Strip	Precipitate
3	0.204	0.194	0.146	0.0247
7	≤dl	0.105	0.448	0.0541
14	0.129	0.204	1.09	0.167
21	0.173	0.277	2.27	0.305
28	≤dl	0.0603	1.86	0.182
35	0.0633	0.209	1.37	0.103
56	≤dl	≤dl	2.74	0.0684
84	0.145	0.261	2.85	0.258

GGW

3	2.66	2.09	0.839	0.200
7	3.03	3.30	0.600	0.218
14	1.64	1.82	0.563	0.407
21	2.04	3.30	2.56	1.20
28	3.44	3.95	2.76	0.503
35	2.41	2.63	3.51	0.524
56	1.92	2.02	2.80	0.414
84	1.37	1.78	3.35	1.01

BGW

3	≤dl	≤dl	0.207	0.00986
7	≤dl	≤dl	0.163	0.111
14	≤dl	≤dl	0.249	0.0979
21	≤dl	≤dl	0.548	0.281
28	≤dl	≤dl	1.08	0.224
35	≤dl	8.23	0.684	0.129
56	≤dl	≤dl	0.701	0.498
84	≤dl	10.1	0.603	0.194

DDW

Day	40°C	Room Temperature	Acid Strip	Precipitate
3	0.256	0.214	0.0769	0.0443
7	0.376	0.365	0.121	0.0282
14	0.319	0.314	≤dl	0.0541
21	0.377	0.436	0.910	0.144
28	0.263	0.279	0.0978	0. 0362
35	0.500	0.539	≤dl	≤dl
56	0.642	0.445	0.0442	0.00493
84	0.496	0.514	0.100	≤dl

GGW

Day	40°C	Room Temperature	Acid Strip	Precipitate
3	0.445	0.423	0.0465	0.0474
7	0.335	0.472	0.0419	-
14	0.469	0.549	0.0395	0.0788
21	0.604	0.802	0.105	0.338
28	0.650	0.663	0.0910	0.0544
35	1.12	1.35	0.145	0.175
56	1.17	1.30	0.0607	0.125
84	1.40	1.18	0.114	0.259

BGW

3	≤dl	≤dl	0.0746	0.0387
7	≤dl	≤dl	0.0604	0.149
14	≤dl	≤dl	0.0373	0.218
21	≤dl	≤dl	0.130	0.178
28	≤dl	≤dl	0.0652	0.279
35	≤dl	≤dl	0.0325	0.327
56	≤dl	≤dl	0.0721	0.00774
84	≤dl	≤dl	0.0983	0.0268

6.A.2.C. Uranium Normalized Mass Loss

DDW

Day	90°C	Room Temperature	Acid Strip	Precipitate
3	≤dl	≤dl	0.605	0.0429
7	≤dl	0.0902	0.532	0.244
14	≤dl	≤dl	1.36	0.0938
21	0.253	0.103	1.24	0.505
28	0.106	≤dl	2.81	0.0937
35	≤dl3	≤dl	2.65	0.0300
56	≤dl	≤dl	4.42	≤dl
84	≤dl	≤dl	5.67	0.0478

GGW

Day	90°C	Room Temperature	Acid Strip	Precipitate
3	0.487	≤dl	0.398	0.108
7	≤dl	0.102	1.04	0.243
14	≤dl	≤dl	0.801	0.108
21	≤dl	≤dl	2.40	0.136
28	≤dl	≤dl	4.42	0.183
35	≤dl	0.206	5.79	0.261
56	≤dl	≤dl	4.98	0.114
84	≤dl	0.168	6.02	0.308

BGW

3	4.42	4.46	0.324	≤dl
7	5.65	6.53	0.164	0.0452
14	7.04	7.97	0.107	0.118
21	7.57	8.27	0.294	0.153
28	8.66	8.37	0.406	0.0945
35	9.06	9.82	≤dl	0.497
56	7.36	10.1	0.229	0.101
84	6.71	7.24	0.304	0.182

DDW

Day	40°C	Room Temperature	Acid Strip	Precipitate
3	≤dl	≤dl	≤dl	0.0372
7	0.0700	≤dl	≤dl	0.0320
14	≤dl	0.140	0.0863	0.0638
21	≤dl	≤dl	0.492	0.173
28	≤dl	≤dl	≤d18	0.0524
35	≤dl	≤dl	0.0982	≤dl
56	≤dl	≤dl	0.162	≤dl
84	≤dl	≤dl	0.102	0.0196

GGW

3	≤dl	≤dl	≤dl	0.0359
7	0.116	≤dl	0.117	-
14	0.145	≤dl	≤dl	0.170
21	≤dl	0.207	0.139	0.371
28	≤dl	≤dl	0.0682	0.0748
35	≤dl	0.382	0.0430	0.465
56	0.0847	0.217	0.0921	0.229
84	≤dl	0.0901	0.264	0.397

BGW

Day	40°C	Room Temperature	Acid Strip	Precipitate
3	≤dl	0.409	≤dl	0.0189
7	0.657	0.290	0.103	0.0431
14	1.13	1.78	≤dl	0.0366
21	1.17	0.846	≤dl	0.122
28	1.68	1.47	≤dl	0.0317
35	1.81	1.73	≤dl	0.0422
56	0.799	1.65	≤dl	≤dl
84	1.29	1.58	≤dl	≤dl

6.A.2.D. Samarium Normalized Mass Loss

DDW

Day	90°C	Room Temperature	Acid Strip	Precipitate
3	0.0113	0.0310	0.464	0.0297
7	-	0.0430	0.104	0.0479
14	0.0541	0.0341	0.157	0.0954
21	0.0984	0.333	0.389	0.167
28	0.00426	0.0265	0.217	0.0666
35	0.0111	0.0596	0.558	0.0701
56	0.00727	0.0207	0.494	0.0305
84	0.0640	0.114	0.677	0.133

GGW

3	0.0108	0.0733	0.156	0.0615
7	0.0176	0.0607	0.904	0.188
14	0.0153	0.0823	0.271	0.146
21	0.0340	0.304	1.84	0.396
28	0.0324	0.0946	2.77	0.211
35	0.0478	0.150	2.79	0.273
56	0.0445	0.108	2.54	0.239
84	0.0962	0.248	3.37	0.368

BGW

3	0.0210	0.0230	0.191	0.00991
7	0.0148	0.0400	0.0136	0.0881
14	0.0368	0.0300	0.0139	0.0291
21	0.0269	0.0502	0.210	0.184
28	0.0413	0.0272	0.305	0.143
35	0.0286	0.0335	0.0228	0.0792
56	0.0438	0.0536	0.0622	0.0231
84	0.0482	0.0585	0.0399	0.0285

DDW

Day	40°C	Room Temperature	Acid Strip	Precipitate
3	0.0133	0.00561	0.0213	0.0322
7	0.00323	0.00720	0.0696	0.0154
14	0.0143	0.00769	0.0482	0.0546
21	0.0109	0.0278	1.19	0.186
28	0.00910	0.0212	0.111	0.0367
35	0.00438	0.00586	0.0398	0.0145
56	0.00578	0.00807	0.0594	0.0152
84	0.0134	0.0222	0.190	0.0382

GGW

3	0.0158	0.0122	0.0159	0.0428
7	0.0265	0.210	0.0615	-
14	0.0492	0.0279	0.0129	0.115
21	0.0826	0.123	0.140	0.305
28	0.0402	0.0155	0.0174	0.121
35	0.0555	0.146	0.323	0.289
56	0.0522	0.104	0.116	0.172
84	0.236	0.104	0.177	0.196

BGW

3	0.0341	0.0196	0.0522	0.0312
7	0.0266	0.0424	0.0230	0.0370
14	0.0390	0.0506	0.0282	0.0679
21	0.0647	0.0898	0.183	0.229
28	0.0706	0.0817	0.00711	0.0696
35	0.0729	0.0890	0.0119	0.0806
56	0.0831	0.113	0.0243	0.0153
84	0.151	0.142	0.0611	0.0317

6.A.2.E. Lanthanum Normalized Mass Loss

DDW

Day	90°C	Room Temperature	Acid Strip	Precipitate
3	≤dl	≤dl	0.276	0.0175
7	-	0.0312	0.104	0.0314
14	0.0437	0.0188	0.199	0.0675
21	0.0426	0.105	0.345	0.0926
28	≤dl	0.0294	0.247	0.0548
35	≤dl	≤dl	0.507	0.0532
56	≤dl	≤dl	0.431	0.0259
84	0.0724	0.0817	0.659	0.0654

GGW

Day	90°C	Room Temperature	Acid Strip	Precipitate
3	0.0318	0.0665	0.213	0.0407
7	≤dl	0.0270	0.798	0.134
14	0.0895	0.0448	0.298	0.334
21	≤dl	0.0626	1.05	0.493
28	≤dl	0.104	1.99	0.0988
35	0.0478	0.105	2.07	0.120
56	≤dl	0.0662	1.82	0.155
84	0.0395	0.0834	2.32	0.106

BGW

3	≤dl	≤dl	0.106	0.00370
7	≤dl	≤dl	0.0475	0.0451
14	≤dl	≤dl	0.0153	0.00716
21	≤dl	≤dl	0.116	0.0939
28	≤dl	≤dl	0.162	0.0699
35	≤dl	≤dl	0.0139	0.0282
56	≤dl	≤dl	0.0598	0.0143
84	≤dl	≤dl	0.0277	0.0107

DDW

Day	40°C	Room Temperature	Acid Strip	Precipitate
3	0.0150	0.0211	0.0288	0.0132
7	0.00337	0.00520	0.0497	0.00964
14	≤dl	0.00358	0.0430	0.0206
21	≤dl	≤dl	0.589	0.0991
28	≤dl	0.0136	0.0578	0.0216
35	≤dl	0.0210	0.0264	0.00736
56	≤dl	≤dl	0.0564	0.00971
84	≤dl	0.0213	0.165	0.0142

GGW

3	0.00985	0.00827	0.0392	0.0180
7	0.0216	0.0230	0.0344	-
14	0.0386	0.0167	0.0582	0.0812
21	0.0635	0.118	0.0819	0.142
28	≤dl	≤dl	0.101	0.0519
35	≤dl	0.0660	0.211	0.125
56	0.0462	0.0623	0.0795	0.108
84	0.0757	0.0860	0.110	0.120

BGW

Day	40°C	Room Temperature	Acid Strip	Precipitate
3	≤dl	≤dl	0.0294	0.0144
7	≤dl	≤dl	0.00825	0.0145
14	≤dl	≤dl	0.0191	0.0275
21	≤dl	≤dl	0.0438	0.0820
28	≤dl	0.0718	≤dl	0.0385
35	≤dl	≤dl	0.00615	0.147
56	≤dl	0.0729	0.0207	0.00665
84	0.0709	≤dl	0.0596	0.0162

6.A.2.F. Molybdenum Normalized Mass Loss

DDW

Day	90°C	Room Temperature	Acid Strip	Precipitate
3	4.88	20.7	12.7	3.06
7	-	-	3.62	4.31
14	2.19	36.8	6.54	8.26
21	27.3	26.6	≤dl	0.852
28	36.3	35.5	9.49	7.20
35	34.1	36.3	9.71	3.50
56	30.7	29.6	4.15	0.689
84	55.6	55.5	2.36	1.89

GGW

3	63.2	55.6	2.46	5.49
7	54.7	52.0	2.38	5.97
14	32.8	30.1	1.38	5.86
21	34.3	36.7	1.36	7.48
28	63.2	81.0	1.61	5.83
35	66.7	65.6	2.39	4.43
56	133	137	2.29	6.60
84	50.8	54.7	1.84	3.55

BGW

Day	90°C	Room Temperature	Acid Strip	Precipitate
3	66.6	28.5	1.34	0.199
7	48.6	58.2	0.693	0.792
14	89.0	76.1	≤dl	0.297
21	106	106	1.28	1.05
28	81.4	101	1.03	0.412
35	92.6	97.1	0.980	0.300
56	101	122	0.830	0.748
84	113	103	0.995	0.406

DDW

Day	40°C	Room Temperature	Acid Strip	Precipitate
3	9.44	8.99	1.13	3.03
7	6.60	7.72	1.96	4.92
14	12.0	10.3	1.82	3.92
21	9.62	13.9	2.18	1.31
28	15.1	17.3	2.03	2.27
35	25.1	25.2	≤dl	≤dl
56	33.1	33.7	≤dl	≤dl
84	14.6	14.7	0.701	0.759

GGW

3	27.4	30.4	≤dl	0.207
7	43.2	41.8	5.65	-
14	33.0	30.4	2.51	6.23
21	39.7	44.0	3.68	13.5
28	26.7	18.6	1.05	1.85
35	46.1	48.1	3.29	5.12
56	64.1	64.3	0.875	3.34
84	61.4	58.7	1.79	9.82

BGW

3	23.1	25.1	≤dl	0.223
7	45.0	51.5	0.834	0.160
14	54.3	56.2	≤dl	0.359
21	8.27	10.7	≤dl	0.350
28	47.9	40.6	≤dl	0.319
35	54.2	48.7	≤dl	0.263
56	20.1	18.3	0.994	≤dl
84	26.9	23.1	0.458	0.0744

6.A.2.G. Aluminium Normalized Mass Loss

DDW

Day	90°C	Room Temperature	Acid Strip	Precipitate
3	0.776	0.868	0.906	0.0975
7	1.11	1.14	1.74	0.176
14	2.08	1.90	0.728	0.374
21	2.06	2.27	0.517	0.306
28	3.23	3.42	0.932	0.265
35	3.18	3.25	0.766	0.110
56	4.76	4.30	0.532	0.0136
84	3.74	3.59	2.30	1.67

GGW

Day	90°C	Room Temperature	Acid Strip	Precipitate
3	1.37	0.992	0.703	0.280
7	1.51	1.66	0.425	0.404
14	2.11	1.74	0.620	0.798
21	1.51	1.77	0.868	1.03
28	2.15	2.30	0.877	0.805
35	2.61	2.73	1.30	0.750
56	1.90	2.27	1.34	0.410
84	3.09	2.91	2.82	1.49

BGW

3	13.3	13.1	1.27	≤dl
7	16.5	15.5	≤dl	0.255
14	16.6	17.2	0.139	0.0831
21	≤dl	1.44	0.552	0.246
28	8.88	4.88	0.679	0.141
35	0.215	0.504	0.718	0.240
56	5.32	6.49	0.0882	0.0533
84	13.2	13.9	≤dl	0.00292

DDW

Day	40°C	Room Temperature	Acid Strip	Precipitate
3	0.157	0.0755	0.288	0.116
7	0.375	0.168	0.172	0.196
14	0.124	0.0231	0.157	0.146
21	0.259	0.257	1.33	0.277
28	0.138	0.382	0.269	0.0699
35	0.174	0.256	0.394	≤dl
56	0.301	0.203	0.141	≤dl
84	0.166	0.177	0.734	≤dl

GGW

Day	40°C	Room Temperature	Acid Strip	Precipitate
3	0.333	0.223	0.0889	0.110
7	-	-	-	-
14	0.226	0.0647	0.283	0.246
21	0.500	0.442	0.429	0.783
28	0.143	0.145	0.308	0.151
35	0.271	0.677	0.559	0.487
56	0.305	0.442	0.230	0.199
84	0.374	0.401	0.265	0.485

BGW

Day	40°C	Room Temperature	Acid Strip	Precipitate
3	1.62	≤dl	0.342	0.179
7	2.67	1.56	1.02	0.240
14	≤dl	≤dl	0.950	0.217
21	≤dl	≤dl	0.320	0.248
28	≤dl	1.31	0.114	0.237
35	2.55	4.78	0.188	0.121
56	≤dl	≤dl	0.0433	≤dl
84	1.27	3.84	0.473	0.0301

6.A.2.H. Boron Normalized Mass Loss

90°C

Day	DDW	GGW	BGW
3	8.62	6.46	13.8
7	10.9	9.16	17.5
14	16.0	7.49	34.6
21	33.7	10.8	53.0
28	9.86	11.0	25.2
35	15.6	13.7	39.8
56	13.0	10.3	29.6
84	25.7	15.5	98.1

40°C

Day	DDW	GGW	BGW
3	≤dl	≤dl	≤dl
7	1.24	0.24	1.39
14	1.32	1.02	2.53
21	3.84	1.44	4.62
28	2.72	0.98	9.67
35	2.37	5.53	5.44
56	2.87	2.25	6.23
84	3.65	2.39	5.72

6.A.2.I. Silicon Normalized Mass Loss

$90^{o}C$

Day	DDW	GGW	BGW
3	0.995	2.75	4.16
7	2.09	4.00	7.01
14	1.17	3.67	5.91
21	10.7	5.87	31.5
28	4.97	7.97	20.6
35	8.20	7.30	32.7
56	8.01	6.87	22.6
84	14.1	6.36	12.7

$40^{o}C$

Day	DDW	GGW	BGW
3	0.232	$\leq$dl	0.448
7	1.19	0.66	0.581
14	1.12	1.16	9.43
21	$\leq$dl	1.14	3.95
28	1.12	1.49	$\leq$dl
35	0.827	1.74	$\leq$dl
56	0.761	2.05	$\leq$dl
84	0.857	2.02	0.715

6.A.3. SA/V 0.85 cm^{-1}

6.A.3.A. Sodium Normalized Mass Loss

DDW

Day	$90^{o}C$	Room Temperature	Acid Strip	Precipitate
7	19.6	20.8	0.0108	0.0357
14	26.2	27.5	0.366	0.171
21	21.0	20.6	0.0411	0.0201
28	29.3	29.3	0.119	0.0640
35	31.8	33.0	0.138	0.0691
56	33.1	32.5	0.165	0.0314
84	44.9	45.2	0.236	0.0107

GGW

7	7.26	6.96	0.0992	0.0356
14	22.1	23.1	0.182	0.0215
21	25.6	26.5	0.197	0.0261
28	27.8	27.2	0.0907	0.0486
35	27.0	27.8	0.128	0.0631
56	29.0	28.1	0.200	0.0622
84	38.6	40.4	2.10	1.94

BGW

Day	90°C	Room Temperature	Acid Strip	Precipitate
7	18.6	22.1	0.0297	0.0207
14	15.7	23.6	0.0483	0.0536
21	17.2	17.0	0.145	0.0353
28	25.9	28.1	0.343	0.0353
35	31.0	22.4	0.0527	0.0715
56	28.6	27.3	0.156	0.0327
84	81.6	87.6	0.178	0.0732

DDW

Day	40°C	Room Temperature	Acid Strip	Precipitate
7	0.803	0.825	0.0765	0.0450
14	1.55	1.35	0.151	0.0329
21	1.64	1.72	0.245	0.0574
28	0.915	1.45	0.0857	0.0353
35	2.14	2.16	0.119	0.0194
56	2.86	2.82	0.133	0.0165
84	4.75	4.79	0.342	0.0357

GGW

7	0.641	0.475	0.320	0.334
14	1.55	1.73	0.00222	0.0634
21	2.06	2.39	0.00541	0.0304
28	3.09	2.84	0.0993	0.120
35	3.55	3.33	0.129	0.0783
56	6.43	6.24	0.0902	0.0203

BGW

7	2.13	2.29	0.122	0.0637
14	4.07	1.59	0.133	0.204
21	$\leq$dl	$\leq$dl	0.154	0.0427
28	0.895	$\leq$dl	0.0677	0.0480
35	1.65	1.40	0.194	0.0319
56	0.945	1.29	0.292	0.0367
84	4.16	4.02	0.502	0.0439

6.A.3.B. Manganese Normalized Mass Loss

DDW

Day	90°C	Room Temperature	Acid Strip	Precipitate
7	0.107	0.140	0.131	0.0487
14	0.139	0.145	0.320	0.0713
21	0.149	0.317	0.239	0.0398
28	0.716	0.917	0.800	0.228
35	0.688	0.658	0.384	0.226
56	0.813	0.895	0.350	0.268
84	0.480	0.574	0.295	0.198

GGW

7	0.0809	0.0672	0.325	0.206
14	0.410	0.405	0.785	0.137
21	0.765	0.866	0.627	0.377
28	0.716	0.844	1.27	0.397
35	0.689	1.08	0.784	0.105
56	0.391	0.300	1.13	0.232
84	≤dl	0.279	1.06	0.151

BGW

7	≤dl	≤dl	0.0438	0.0550
14	≤dl	≤dl	0.0811	0.112
21	≤dl	≤dl	0.0916	0.164
28	2.27	≤dl	0.578	1.49
35	1.28	≤dl	0.0820	0.178
56	≤dl	1.62	0.121	0.112
84	≤dl	≤dl	0.124	0.0646

DDW

Day	40°C	Room Temperature	Acid Strip	Precipitate
7	0.0393	0.00237	0.0924	0.0159
14	0.0630	0.0641	0.0482	0.0106
21	0.0587	0.0257	0.147	0.02660
28	0.0325	0.0400	0.0533	0.0205
35	0.0434	0.0445	0.0497	0.0204
56	0.0390	0.0563	0.823	0.0186
84	0.0427	0.0428	0.121	0.0271

GGW

Day	40°C	Room Temperature	Acid Strip	Precipitate
7	0.142	0.595	0.0532	0.177
14	0.0663	0.153	0.0624	0.0174
21	0.176	0.133	0.0374	0.0227
28	0.177	0.200	0.0642	0.684
35	0.415	0.264	0.115	0.00118
56	0.0154	0.241	0.188	0.118

BGW

7	≤dl	≤dl	0.0394	0.0138
14	≤dl	≤dl	0.0492	0.0939
21	≤dl	≤dl	0.0813	0.0143
28	10.6	≤dl	0.0958	0.0386
35	≤dl	≤dl	0.0935	0.0160
56	≤dl	≤dl	0.0894	0.0253
84	≤dl	≤dl	0.0912	0.0176

6.A.3.C. Samarium Normalized Mass Loss

DDW

Day	90°C	Room Temperature	Acid Strip	Precipitate
7	0.0306	0.0385	0.0423	0.0706
14	0.00935	0.0192	0.116	0.0493
21	0.0681	0.114	0.164	0.0265
28	0.0618	0.152	0.215	0.194
35	0.161	0.130	0.119	0.0824
56	0.113	0.0970	0.105	0.0730
84	0.0736	0.220	0.0793	0.0402

GGW

7	0.0112	0.0141	0.0631	0.0198
14	0.0200	0.0116	0.101	0.0186
21	0.0282	0.0331	0.0544	0.0256
28	0.0266	0.0377	0.0896	0.0570
35	0.0432	0.0851	0.0955	0.0341
56	0.0266	0.0400	0.0872	0.0343
84	0.0593	0.0334	0.306	0.0380

BGW

Day	90°C	Room Temperature	Acid Strip	Precipitate
7	0.0307	0.0288	0.0168	0.0248
14	0.0441	0.0362	0.0262	0.0352
21	0.0385	0.0468	0.0213	0.0358
28	0.152	0.257	0.0694	0.217
35	0.0992	0.0876	0.0665	0.119
56	0.0408	0.0503	0.0323	0.0467
84	0.0992	0.0745	0.0562	0.0390

DDW

Day	40°C	Room Temperature	Acid Strip	Precipitate
7	0.0120	0.00991	0.0565	0.0185
14	0.106	0.0140	0.0550	0.0152
21	0.0202	0.0135	0.120	0.0392
28	0.0227	0.0259	0.0984	0.0305
35	0.0238	0.0236	0.0979	0.0372
56	0.0160	0.0196	0.142	0.0203
84	0.0651	0.0754	0.122	0.0598

GGW

7	0.00588	0.0170	0.0747	0.226
14	0.0117	0.0176	0.0663	0.136
21	0.0295	0.0401	0.0663	0.0311
28	0.0246	0.0641	0.0747	0.103
35	0.0300	0.0502	0.0779	0.0943
56	0.0537	0.0839	0.106	0.0804

BGW

7	0.0202	0.0173	0.338	0.0225
14	0.0195	0.0213	0.0595	0.112
21	0.0221	0.0408	0.141	0.0251
28	0.0578	0.0788	0.102	0.0568
35	0.0287	0.0339	0.196	0.0297
56	0.0287	0.0407	0.0747	0.0376
84	0.0383	0.0491	0.200	0.0273

6.A.3.D. Lanthanum Normalized Mass Loss

DDW

Day	90°C	Room Temperature	Acid Strip	Precipitate
7	≤dl	≤dl	0.0490	0.0214
14	0.00658	0.0340	0.102	0.0249
21	0.0673	≤dl	0.153	0.0218
28	0.0907	≤dl	0.248	0.113
35	≤dl	≤dl	0.0986	0.0658
56	0.200	≤dl	0.151	0.0490
84	0.103	0.123	0.109	0.0162

GGW

7	≤dl	≤dl	0.0765	0.0136
14	≤dl	0.0702	0.119	0.0124
21	≤dl	≤dl	0.0964	0.0239
28	≤dl	0.126	0.146	0.0370
35	0.0615	0.239	0.145	0.0249
56	≤dl	≤dl	0.125	0.0313
84	≤dl	≤dl	0.339	0.00793

BGW

7	≤dl	≤dl	0.0270	0.0166
14	≤dl	≤dl	0.0390	0.0228
21	≤dl	≤dl	0.0288	0.0228
28	≤dl	≤dl	0.105	0.217
35	0.191	≤dl	0.0812	0.0956
56	0.121	≤dl	0.0508	0.0390
84	≤dl	≤dl	0.112	0.0280

DDW

Day	40°C	Room Temperature	Acid Strip	Precipitate
7	≤dl	≤dl	0.0726	0.0103
14	≤dl	0.0158	0.0408	0.0094
21	≤dl	0.0194	0.0878	0.0243
28	≤dl	0.0362	0.0666	0.0199
35	0.0275	≤dl	0.0807	0.0213
56	≤dl	≤dl	0.121	0.0138
84	≤dl	0.0506	0.108	0.0316

GGW

Day	40°C	Room Temperature	Acid Strip	Precipitate
7	0.0187	≤dl	0.0636	0.141
14	≤dl	≤dl	0.0529	0.0103
21	0.0370	0.0801	0.0836	0.0322
28	0.0205	0.111	0.0336	0.0626
35	0.0215	≤dl	0.0867	0.0801
56	≤dl	0.0858	0.121	0.0435

BGW

7	≤dl	≤dl	0.0367	0.0129
14	≤dl	≤dl	0.0606	0.0385
21	≤dl	≤dl	0.137	0.0168
28	≤dl	≤dl	0.129	0.0432
35	≤dl	≤dl	0.215	0.0291
56	0.107	≤dl	0.0884	0.0349
84	0.140	0.109	0.215	0.0298

6.A.3.E. Molybdenum Normalized Mass Loss

DDW

Day	90°C	Room Temperature	Acid Strip	Precipitate
7	10.9	14.2	≤dl	0.524
14	9.49	5.55	≤dl	≤dl
21	5.55	5.07	≤dl	0.0788
28	15.0	13.5	≤dl	0.212
35	12.6	14.9	≤dl	0.299
56	19.3	6.68	≤dl	≤dl
84	19.0	16.0	≤dl	≤dl

GGW

7	5.57	5.21	≤dl	0.395
14	12.8	13.9	≤dl	0.252
21	8.82	8.49	≤dl	0.318
28	4.64	6.31	≤dl	0.175
35	10.8	10.8	≤dl	0.133
56	12.2	12.4	≤dl	≤dl
84	9.45	10.7	≤dl	≤dl

BGW

Day	90°C	Room Temperature	Acid Strip	Precipitate
7	≤dl	12.9	≤dl	0.310
14	12.7	9.87	≤dl	0.384
21	4.86	≤dl	≤dl	0.217
28	13.6	23.6	≤dl	0.332
35	14.9	≤dl	≤dl	0.684
56	7.90	8.99	≤dl	0.569
84	13.7	≤dl	1.16	≤dl

DDW

Day	40°C	Room Temperature	Acid Strip	Precipitate
7	2.29	1.33	≤dl	0.126
14	2.09	1.32	≤dl	0.359
21	3.41	3.44	≤dl	0.200
28	3.31	3.04	≤dl	0.301
35	2.08	2.27	≤dl	0.661
56	5.00	5.06	≤dl	≤dl
84	2.99	3.80	≤dl	≤dl

GGW

7	1.13	1.27	≤dl	0.0902
14	3.68	2.20	≤dl	0.188
21	2.51	1.35	≤dl	0.395
28	4.31	4.93	≤dl	0.278
35	7.16	5.30	≤dl	1.56
56	9.21	9.58	0.587	0.127

BGW

7	≤dl	≤dl	≤dl	0.0965
14	4.40	≤dl	≤dl	≤dl
21	≤dl	≤dl	1.38	0.145
28	≤dl	≤dl	0.572	0.372
35	≤dl	≤dl	≤dl	0.383
56	≤dl	≤dl	≤dl	≤dl
84	≤dl	≤dl	≤dl	0.158

6.A.3.F. Aluminum Normalized Mass Loss

DDW

Day	90°C	Room Temperature	Acid Strip	Precipitate
7	1.23	1.45	0.289	0.0226
14	0.606	1.13	0.822	0.304
21	0.784	0.832	0.171	0.0441
28	0.755	1.03	0.242	0.178
35	1.06	0.746	0.243	0.00858
56	0.615	0.600	0.0261	≤dl
84	0.451	1.00	0.238	0.0529

GGW

7	1.08	1.20	0.478	0.0533
14	0.783	1.53	0.443	0.0572
21	0.737	0.840	0.241	0.0858
28	0.748	0.953	0.236	0.109
35	9.55	1.18	0.175	0.102
56	0.610	0.744	0.280	0.111
84	1.24	0.652	0.530	0.417

BGW

7	0.443	5.23	3.28	0.0155
14	2.87	2.68	0.143	0.0327
21	2.49	1.39	0.142	0.0391
28	3.90	6.15	0.200	0.581
35	6.06	5.42	0.0938	0.0744
56	5.35	4.30	0.0447	0.00570
84	6.18	4.05	0.144	0.0941

DDW

Day	40°C	Room Temperature	Acid Strip	Precipitate
7	0.343	0.427	0.305	0.0301
14	0.339	0.438	0.109	≤dl
21	0.441	0.0525	0.634	0.0140
28	0.401	0.397	0.130	0.000317
35	0.263	0.324	0.0649	≤dl
56	0.227	0.249	0.0737	≤dl
84	0.253	0.181	0.237	0.0427

GGW

Day	90°C	Room Temperature	Acid Strip	Precipitate
7	0.270	0.354	0.440	0.283
14	0.159	0.440	0.142	0.00576
21	0.245	0.278	0.105	≤dl
28	0.187	0.339	0.284	0.0788
35	0.109	0.158	0.0406	0.0392
56	0.157	0.312	0.112	0.0835

BGW

7	≤dl	0.565	0.204	0.0162
14	0.774	0.183	0.393	0.147
21	0.633	0.511	0.395	0.00185
28	1.34	1.14	0.155	0.0174
35	1.35	1.71	0.202	≤dl
56	1.22	0.112	0.0871	0.00186
84	1.76	0.177	0.137	≤dl

6.A.3.G. Boron Normalized Mass Loss

90°C

Day	DDW	GGW	BGW
7	7.93	4.20	5.33
14	8.62	8.71	8.73
21	9.85	8.76	7.76
28	10.8	10.5	11.8
35	13.6	10.1	8.10
56	18.6	11.6	8.34
84	15.0	12.6	4.32

40°C

Day	DDW	GGW	BGW
7	0.637	0.319	0.792
14	1.01	1.18	0.792
21	1.46	1.65	0.833
28	1.26	2.52	0.929
35	2.23	3.37	1.14
56	2.94	2.67	1.41
84	4.10		1.77

6.A.3.H. Silicon Normalized Mass Loss

90°C

Day	DDW	GGW	BGW
7	3.28	2.95	≤dl
14	3.33	2.89	0.802
21	3.11	2.43	3.70
28	1.02	1.34	≤dl
35	3.42	1.53	≤dl
56	3.79	2.30	≤dl
84	2.92	1.90	0.313

40°C

Day	DD^W	GGW	BGW
7	≤dl	0.251	0.101
14	0.152	0.382	≤dl
21	≤dl	0.103	≤dl
28	0.250	1.04	≤dl
35	0.120	1.22	≤dl
56	0.578	0.610	≤dl
84	1.08		≤dl

CHAPTER 7
BIBLIOGRAPHY

79ALLA1 B. Allard, H. Kipatsi, B. Torstenfelt, "Nuclide transport by groundwater in Swedish bedrock", **Scientific Basis for Nuclear Waste Management**, 1, G.J. McCarthy, ed., Plenum Press, New York (1979) p.403.

84ALLA1 B. Allard, "Actinide and technetium solubility limitations in groundwaters of crystalline rocks", **Scientific Basis for Nuclear Waste Management**, 7, G.L. McVay, ed., North-Holland, New York (1984) p.219.

82ALLE1 C.C. Allen, "Stability and alteration of naturally occurring low-silica glasses: implications for the long term stability of waste form glasses", **Scientific Basis for Nuclear Waste Management**, 5, W. Lutze, ed., North-Holland, New York (1982) p.37.

81ALTE1 F.K. Altenhein, W. Lutze, G. Malow, "The mechanisms for hydrothermal leaching of glass and glass-ceramic nuclear waste forms", **Scientific Basis for Nuclear Waste Management**, 3, J.G. Moore, ed., Plenum Press, New York (1981) p.363.

82ALTE1 F.K. Altenhein, W. Lutze, "Long-term radioactivity release from solidified high-level waste-Part I: An approach to evaluating experimental data", **Scientific Basis for Nuclear Waste Management**, 5, W. Lutze, ed., North-Holland, New York (1982) p.45.

80ANTO1 M. Antonini, P. Camagni, F. Lanza, A. Manara, "Atomic displacements and radiation damage in glasses incorporating HLW", **Scientific Basis for Nuclear Waste Management**, 2, C.J.M. Northrup, Jr., ed., Plenum Press, New York (1980) p.127.

85APTE1 M.J. Apted, R. Adiga, "The effect of groundwater flow on release rate behavior of borosilicate glass", **Material Research Society Symposia Proceedings**, 44 (1985) p.163.

82AVAG1 A. Avagadro, F. Lanza, "Relationship between glass leaching mechanism and geochemical transport of radionuclides", **Scientific Basis for Nuclear Waste Management**, 5, W. Lutze, ed., North-Holland, New York (1982) p.103.

85BANB1 T. Banba, T. Murakami, "The leaching behavior of a glass waste-form - Part II: the leaching mechanisms", **Nuclear Technology**, 70 (1985) p.243.

84BARK1 A. Barkatt, W. Sousanpour, A. Barkatt, M.A. Boroomand, "Effects of metals and metal oxides on the leaching of nuclear waste glasses", **Scientific Basis for Nuclear Waste Management**, 7, G.L. McVay, ed., North-Holland, New York (1984) p.689.

80BENE1 P. Benes, V. Majer, **Trace Chemistry of Aqueous Solutions. General Chemistry and Radiochemistry**, Elsevier Scientific Publishing Company, New York (1980).

84BIBL1 N.E. Bibler, "Characterization of borosilicate glass-containing Savannah River Plant radioactive waste", **American Chemical Society Symposium Series**, 246 (1984) p.359.

86BIDO1 G. Bidoglio, A. Avagadro, A. De Plano, "Influence of redox environments on the geochemical behavior of radionuclides", **Scientific Basis for Nuclear Waste Management**, 9, L.O. Werme, ed., Materials Research Society, Pittsburgh (1986) p.709.

78BOUL1 K.A. Boult, J.T. Dalton, A.R. Hall, A. Hough, J.A.C. Marples, "The leaching of radioactive waste storage glasses", Chemistry Division AERE Harwell, (1978).

80BRAI1 J.W. Braithwaite, "Brine chemistry effects on the durability of a simulated nuclear waste glass", **Scientific Basis for Nuclear Waste Management**, 2, C.J.M. Northrup, Jr., ed., Plenum Press, New York (1980) p.199.

80CHAP1 N. Chapman, D. Savage, "Dissolution of borosilicate glasses under repository conditions of pressure and temperature", **Scientific Basis for Nuclear Waste Management**, 2, C.J.M. Northrup, Jr., ed., Plenum Press, New York (1980) p.183.

84CHIC1 L.A. Chick, L.R. Pederson, "The relationship between reaction layer thickness and leach rate for nuclear waste glasses", **Scientific Basis for Nuclear Waste Management**, 7, G.L. McVay, ed., North-Holland, New York (1984) p.635.

82CLAR1 D.E. Clark, C.A. Maurer, A.R. Jurgensen, L. Urwongse, "Effects of waste composition and loading on the chemical durability of a borosilicate glass", **Scientific Basis for Nuclear Waste Management**, 5, W. Lutze, ed., North-Holland (1982) p.1.

84CLAR1 D.E. Clark, "An evaluation of six month burial data from Stripa", **Rivista Della Staz. Sper. Vetro**, 5 (1984) p.185.

80CRAN1 J.L. Crandall, "Development of solid radionuclide waste forms in the United States", **Scientific Basis for Nuclear Waste Management**, 2, C.J.M. Northrup, Jr., ed., Plenum Press, New York (1980) p.39.

68CURR1 L.A. Currie, "Limits for qualitative detection and quantitative determination, Application to radiochemistry", **Analytical Chemistry**, 40 (1968) p.586.

81DESI1 K.N. DeSilva, "A correction method for coincidence losses in neutron activation analysis with short-lived nuclides", Ph.D. Thesis, Dalhousie University, Halifax, NS (1981).

72DESO1 D. DeSoete, R. Gijbels, J. Hoste,**Neutron Activation Analysis**, John Wiley & Sons Ltd., (1972).

70DUCE1 F.A. Duce, S.S. Yamamura, "Versatile spectrophotometric method for the determination of silicon", **Talanta**, 17 (1970) pp. 143.

79EWES1 E. Ewest, "Calculations of radioactivity release due to leaching of vitrified high level waste", **Scientific Basis for Nuclear Waste Management**, 1, G.J. McCarthy, ed., Plenum Press, New York (1979) p.161.

85FLIN1 J.F. Flintoff, A.B. Harker, "Detailed processes fo surface layer formation in borosilicate waste glass dissolution", **Scientific Basis for Nuclear Waste Management**, 8, C.M. Jantzen, J.A. Stone, R.C. Ewing, eds., Materials Research Society, Pittsburgh (1985) p.147.

87FONG1 B.B Fong, A. Chatt, "Characterization of deep sea sediments by INAA for radioactive waste management purposes", **Journal of Radioanalytical and Nuclear Chemistry, Articles**, 110 (1987) p.135.

88FONG1 B.B. Fong, "Characterization of sub-seabed sediments for storage of radioactive wastes", Ph.D. Thesis, Dalhousie University, Halifax, NS (1988).

85GARC1 I.L. Garcia, M.H. Cordoba, C. Sanchez-Pedreno, "Sensitive method for the spectrophotometric determination of boron in plants and waters using crystal violet", **Analyst**, 110 (1985) p. 1259.

85GARL1 J.A. Garland, W.B. White, "Determination of early stages of glass dissolution by pH titration", **Scientific Basis for Nuclear Waste Management**, 8, C.M. Jantzen, J.A. Stone, R.C. Ewing, eds., Materials Research Society, Pittsburgh (1985) p.81.

59GRAF1 P.R. Graff, F.J. Langmyhr, "Studies in the spectrophotometric determination of silicon in materials decomposed by hydrofluoric acid. II. Spectrophotometric determination of fluosilicic acid in hydrofluoric acid", **Analytica Chimica Acta**, 21 (1959) p. 429.

82GRAM1 B. Grambow, "The role of metal ion solubility in leaching of nuclear waste glasses", **Scientific Basis for Nuclear Waste Management**, 5, W. Lutze, ed., North-Holland, New York (1982) p.93.

84GRAM1 B. Grambow, D.M. Strachan, "Leach testing of waste glasses under near-saturation conditions", **Material Research Society Symposia Proceedings**, 26 (1984) p. 623.

83GRAU1 R. Grauer, "Glasses used in the solidification of high level radioactive waste: Their behavior in aqueous solutions", Technical Report 83-01 for the Swiss Federal institute for Reactor Research, Wurenlingen, (1983).

84GRAY1 W.J. Gray, "Gamma radiolysis effects on Grande Ronde basalt groundwater", **Scientific Basis for Nuclear Waste Management**, 7, G.L. McVay, ed., North-Holland, New York (1984) p. 147.

85HAAK1 R. Haaker, G. Malow, P. Offermann, "The effect of phase formation on glass leaching", **Scientific Basis for Nuclear Waste Managment**, 8, C.M. Jantzen, J.A. Stone, R.C. Ewing, eds., Materials Research Society, Pittsburgh (1985) p.121.

82HALL1 A.R. Hall, A. Hough, J.A.C. Marples, "Leaching of vitrified high-level radioactive waste", **Scientific Basis for Nuclear Waste Management**, 5, W. Lutze, ed., North-Holland, New York (1982) p.83.

82HARV1 K.B. Harvey, C.D. Litke, D.L. Mandolesi, J.C. Tait, "The durability of glasses", Atomic Energy of Canada Limited - Research Centre, **Proceedings of the 13th Information Meeting of the Nuclear Fuel Waste Management Program**, TR-201, 2 (1982) p. 252.

82HAYW1 P.J. Hayward et al., "SIMS depth profiling studies of sphene-based ceramics and glass ceramics leached in synthetic groundwater", Atomic Energy of Canada Limited - Research Centre, **Proceedings of the 13th Information Meeting of the Nuclear Fuel Waste Management Program**, Report TR-201, 1 (1982) p.162.

84HEIM1 R.B. Heimann, D.D. Wood, R.F. Hamon, "Multicomponent leach tests in Standard Canadian Shield Saline Solution of glasses containing simulated nuclear waste", **Material Research Society Symposia Proceedings**, 26 (1984) p.191.

86HEIM1 R.B. Heimann, "Nuclear fuel waste management and archaeology: are ancient glasses indicators of long term durability of man made materials?", **Glass Technology**, 27 (1986) p.96.

84HERM1 H-P. Hermansson, H. Christensen, D.E. Clark, I-K. Bjorner, H. Yokoyama, L. Werme, "Static leaching of radioactive glass under conditions simulating a granitic repository for high-level waste: phase 1", **Scientific Basis for Nuclear Waste Management**, 7, G.L. McVay, ed., North-Holland, New York (1984) p.671.

85HERM1 H.P. Hermansson, I.K. Bjorner, H. Christensen, T. Ohe, L, Werme, "Static leaching of fully radioactive waste glass at 90°C in the presence of bentonite, granite and stainless steel corrosion products", **Scientific Basis for Nuclear Waste Management**, 9, L.O. Werme, ed., Materials Research Society, Pittsburgh (1985) p. 179.

85HOLZ1 J. Holzbecher, A. Chatt, D.E. Ryan, "SLOWPOKE Epi-cadmium neutron flux in activation analysis of trace elements", **Canadian Journal of Spectroscopy**, 30(3) (1985) p. 67.

85IAEA1 International Atomic Energy Agency, "Chemical durability and related properties of solidified high-level waste forms", Technical Report Series no. 257, Vienna (1985).

85IAEA2 International Atomic Energy Agency, "Deep underground disposal of radioactive wastes: Near-field effects", Technical Report Series no. 251, Vienna (1985).

83ISHI1 K. Ishiguro, N. Kawanishi, N. Sasaki, H. Nagaki, M. Yamamoto, "Growth of surface layer during the leaching of the simulated waste glass and its barrier effects on leaching", **Material Research Society Symposia Proceedings**, 15 (1983) p.35.

84JANT1 C.M. Jantzen, "Methods of simulating low redox potential (Eh) for a basalt repository", **Scientific Basis for Nuclear Waste Management**, 7, G.L. McVay, ed., North-Holland, New York (1984) p.613.

80KENN1 B.T. Kenna, K.D. Murphy, "Mechanism for elevated temperature leaching", **Scientific Basis for Nuclear Waste Management**, 2, C.J.M. Northrup, Jr., ed., Plenum Press, New York (1980) p.191.

83KESS1 S.E. Kesson, A.E. Ringwood, "Safe Disposal of Spent Nuclear Fuel", **Radioactive Waste Management and the Nuclear Fuel Cycle**, 4(2) (1983) p. 159.

84KRIS1 A. Krischer, R.A. Simon, "Results of a round robin leaching test for vitrified radioactive wastes", **Rivista Della Staz. Sper. del Vetro**, 5 (1984) p.179.

81LANZ1 F. Lanza, E. Parnisari, "Influence of film formation and its composition on the leaching of borosilicate glasses", **Nuclear and Chemical Waste Management**, 2 (1981) p.131.

82LANZ1 F. Lanza, C. Ronsecco, "Influence of a backfilling material on borosilicate glass leaching", Commission of the European Communities personal communication (1982).

83LANZ1 F. Lanza, U. Demicheli, E. Parnisari, "Development of a test method for leaching glasses immersed in a porous media", Technical note, (1983).

85LEE1 C.T. Lee, D.E. Clark, "Electrokinetics, adsorption and colloid study of simulated nuclear waste glasses leached in aqueous solutions", **Scientific Basis for Nuclear Waste Management**, 8, C.M. Jantzen, J.A. Stone, R.C. Ewing, eds., Materials Research Society, Pittsburgh (1985) p.221.

80LEVI1 H.W. Levi, "Survey of high-level radioactive waste forms and their role in waste management", **Scientific Basis for Nuclear Waste Management**, 2, C.J.M. Northrup, Jr., ed., Plenum Press, New York (1980) p.21.

83LONG1 G.L. Long, J.D. Winefordner, "Limit of detection: a closer look at the IUPAC definition", **Analytical Chemistry**, 55 (1983) p. 712A.

80MACD1 D. MacDougall et al., "Guidelines for data acquisition and data quality evaluation in environmental chemistry", **Analytical Chemistry**, 52 (1980) p. 2242.

79MALO1 G. Malow, H. Andresen, "Helium formation from α-decay and its significance for radioactive waste glasses", **Scientific Basis for Nuclear Waste Management**, 1, G.J. McCarthy, ed., Plenum Press, New York (1979) p.109.

81MALO1 G. Malow, R.C. Ewing, "Nuclear waste glasses and volcanic glasses: A comparison of their stabilities", **Scientific Basis for Nuclear Waste Management**, 3, J.G. Moore, ed., Plenum Press, New York (1981) p.315.

76MARC1 Zygmunt Marczenko, **Spectrophotometric Determination of Elements**, John Wiley and Sons Inc., New York (1976) p. 163.

82MATT1 Georg Matthess, **The Properties of Groundwater**, John Wiley and Sons Inc., New York (1982).

84MCGR1 B.P. McGrail, A. Kumar, "Sodium diffusion and leaching of simulated nuclear waste glass", **American Ceramic Society**, 67 (1984) p.463.

86MEAN1 J.L. Means, E.D. Spinosa, "Simulated nuclear waste glass leaching: alteration layer artifacts produced by reprecipitation of solutes during cooling", **Ceramic Bulletin**, 65 (1986) p.780.

83MEND1 J.E. Mendel, "The scientific basis for long-term prediction of waste-form performance under repository conditions", **Scientific Basis for Nuclear Waste Management**, 6, D.G. Brookins, ed., North-Holland, New York (1983) p.1.

85MILE1 E.L. Miles, K.N. Lee, E.M. Carlin, "Nuclear waste disposal under the seabed", **Policy Papers in International Affairs**, (1985).

87MOIR1 D.L. Moir, A. Chatt, "Characterization of simulated vitrified highly active waste and its leachates by neutron activation", **Journal of Radioanalytical and Nuclear Chemistry**, Articles, 116(2) (1987) p. 389.

85MURA1 Y. Muramatsu, R.M. Parr, **Survey of Currently Available Reference Materials for Use in Connection with the Determination of Trace Elements in Biological and Environmental Materials**, International Atomic Energy Agency (1985).

82NBS1 National Bureau of Standards, Standard Reference Material 92, Washington, D.C. (1982).

82NOGU1 J.L. Nogues, L.L. Hench, J. Zarzycki, "Comparative study of seven glasses for solidification of nuclear wastes", **Scientific Basis for Nuclear Waste Management**, 5, W. Lutze, ed., North-Holland, New York (1982) p.211.

82OLOF1 U. Olofsson, B. Allard, B. Torstenfelt, K. Andersson, "Properties and mobilities of actinide colloids in geologic systems", **Scientific Basis for Nuclear Waste Management**, 5, W. Lutze, ed., North-Holland, New York (1982) p.755.

82OSHI1 M. Oshima, K. Fujimoto, S. Motomizu, K. Toei, "Extraction-spectrophotometric determination of boron with 2,6-dihydroxybenzoic acid and 4-(4-diethyl-aminophenylazo)-N-methylpyridinium iodide, with application to steels", **Analytica Chimica Acta**, 134 (1982) p. 73.

83PEDE1 L.R. Pederson, C.Q. Buckwalter, G.L. McVay, "The effects of surface area to solution volume on waste glass leaching", **Nuclear Technology**, 62 (1983) p.151.

83PEDE2 L.R. Pederson, G.L. McVay, "Influence of gamma irradiation on leaching of simulated nuclear waste glass: temperature and dose rate dependence in deaerated water", **Journal of the American Ceramic Society**, 66 (1983) p.863.

65PERE1 F.M. Perel'man, **Rubidium and Caesium**, The MacMillan Company, New York (1965).

82PETI1 J.C. Petit, Y. Langevin, J.M. Lameille, J.C. Dran, "On the leaching behavior of a simple borosilicate glass in a confined environment", **Scientific Basis for Nuclear Waste Management**, 5, W. Lutze, ed., North-Holland, New York (1982) p.203.

82PICK1 S. Pickering, C.T. Walker, "Leaching of actinides from simulated nuclear waste glass", **Scientific Basis for Nuclear Waste Management**, 5, W. Lutze, ed., North-Holland, New York (1982) p.113.

89RAO1 R.R. Rao, A. Chatt, "Complexation of Europium (III) with carbonate ions in groundwater", **Scientific Basis for Nuclear Waste Management**, 12, W. Lutze, R.C. Ewing, eds., Materials Research Society, Pittsburgh (1989) p.897.

67RAWS1 H. Rawson, **Inorganic Glass-Forming Systems**, Academic Press, New York (1967) Eds. J.P. Roberts, P. Popper.

67RIEC1 G.D. Rieck, **Tungsten and its compounds**, Pergamon Press, New York (1967).

84RIGB1 Z. Rigbi, G. Schonwald, "The influence of pH on the dissolution rate of phase separated lithium borosilicate glass", **Glass Technology**, 25 (1984) p.157.

82RING1 T. Ringwood, "Immobilization of radioactive wastes in SYNROC", **American Scientist**, 70 (1982) p.202.

79ROY1 R. Roy, "Science underlying radioactive waste management: status and needs", **Scientific Basis for Nuclear Waste Management**, 1, G.J. McCarthy, ed., Plenum Press, New York (1979) p.1.

79RUSI1 J.M. Rusin, M.F. Browning, G.J. McCarthy, Development of multibarrier nuclear waste forms", **Scientific Basis for Nuclear Waste Management**, 1, G.J. McCarthy, ed., Plenum Press, New York (1979) p.169.

78RYAN1 D.E. Ryan, D.C. Stuart, A. Chattopadhyay, "Rapid multielemental neutron activation analysis with a SLOWPOKE reactor", **Analytica Chimica Acta**, 100 (1978) p. 87.

81SALE1 H.B. Sales, C.C. Dantas, "Determination of boron in water solution by indirect neutron activation technique", **Radiochemical and Radioanalytical Letters**, 50 (1981) p. 105.

82SALE1 B.C. Sales, L.A. Boatner, H. Naramoto, C.W. White, "Rutherford backscattering investigation of the corrosion of borosilicate nuclear waste glass", **Journal of Non-Crystalline Solids**, 53 (1982) p.201.

83SALE1 B.C. Sales, C.W. White, L.A. Boatner, "A comparison of the corrosion characteristics of synthetic monazite and borosilicate glass containing simulated nuclear defense waste", **Nuclear and Chemical Waste Management**, 4 (1983) p.281.

83SALE2 B.C. Sales, C.W. White, L.A. Boatner, "Application of ion implantation and backscattering techniques to the analyses of nuclear waste glass corrosion", **Materials Letters**, 2 (1983) p.1.

84SALE1 B.C. Sales, C.W. White, G.M. Begun, L.A. Boatner, "Surface layer formation on corroded nuclear waste glasses", **Journal of Non-Crystalline Solids**, 67 (1984) p.245.

85SALE1 B.C. Sales, L.A. Boatner, "Lead-iron phosphate glass: A stable storage medium for high-level nuclear waste", **Science**, 226 (4670) (1984) p. 45-48.

82SAVA1 D. Savage, J.E. Robbins, "The interaction of borosilicate glass and granodiorite at 100°C, 50MPa: implications for models of radionuclide release", **Scientific Basis for Nuclear Waste Management**, 5, W. Lutze, ed., North-Holland, New York (1982) p.145.

85SCHI1 E. Schiewer, W. Lutze, L.A. Boatner, B.C. Sales, "Characterization of lead-iron phosphate nuclear waste glasses", **Scientific Basis for Nuclear Waste Management**, 9, L.O. Werme, ed., Materials Research Society, Pittsburgh (1985) p.231.

69SCHL1 J.A. Schleicher, D.B. Heck, "Alternate methods for the determination of boron in silicates", **Develop ments in Applied Spectroscopy**, 8 (1969) p. 138.

82SCHO1 H. Scholze, R. Conradt, H. Engelke, H. Roggendrof, "Determination of the corrosion mechanisms of high-level waste containing glass", **Scientific Basis for Nuclear Waste Management**, 5, W. Lutze, ed., North-Holland, New York (1982) p.173.

69SELE1 A. Selecki, Z. Nowakowska, "Determination of boron in solid boron-organic compounds by indirect neutron activation", **Radiochemical and Radioanalytical Letters**, 1 (1969) p. 247.

82SIMO1 R.A. Simon, S. Orlowski, "Management of radioactive wastes in Europe (EC) history, philosophy and plans for the next five years", **Scientific Basis for Nuclear Waste Management**, 6, D.G. Brookins, ed., North-Holland, New York (1982) p. 733.

82STAP1 B.A. Staples, D.A. Pavlica, H.S. Cole, "Properties of formula 127 glass prepared with radioactive zirconia calcine", Exxon Nuclear Idaho Company, Inc. prepared for the U.S. Dept. of Energy (1982).

83STRA1 D.M. Strachan, "Results from long-term use of the MCC-1 static leach test method", **Nuclear and Chemical Waste Management**, 4 (1983) p.177.

83STRA2 D.M. Strachan, "Effect of gamma irradiation on simulated waste glass leaching and on the leach vessel", **Journal of the American Ceramic Society**, 66 (1983) p.158.

84STRA1 D.M. Strachan, R.O. Lokken, "Long-term leaching of two simulated waste glasses", **Advances in Ceramics**, 8 Nuclear Waste Management, (1984) p.39.

84STRA2 D.M. Strachan, K.M. Krupka, B. Grambow, "Solubility interpretations of leach tests on nuclear waste glass", **Nuclear and Chemical Waste Management**, 5 (1984) p.87.

85STRA1 D.M. Strachan, L.R. Pederson, R.O. Lokken, "Results from the long-term interaction and modeling of SRL-131 glass with aqueous solutions", **Scientific Basis for Nuclear Waste Management**, 9, L.O. Werme, ed., Materials Reserach Society, Pittsburgh (1985) p.195.

85TROL1 G. Troll, A. Sauerer, "Determination of trace amounts of boron in geological samples with carminic acid after extraction with 2-ethylhexane-1,3-diol", **Analyst**, 110 (1985) p. 283.

82VAND1 T.T. Vandergraaf, "Interaction of dissolved radionuclides with geological materials and their implications for contaminant transport", Atomic Energy of Canada Limited - Research Centre, **Proceedings of the 13th Information Meeting of the Nuclear Fuel Waste Management Program**, TR-201, 2 (1982) p. 252.

82VANI1 P. Ph. Van Iseghem, W. Timmermans, R. De Batist, "Chemical Stability of simulated HLW forms in contact with clay media", **Scientific Basis for Nuclear Waste Management**, 5, W. Lutze, ed., North-Holland, New York (1982) p.219.

85VANI1 P.Ph. Van Iseghem, W. Timmermans, R. De Batist, "Parametric study of the corrosion behavior in static distilled water of simulated European reference high level waste glasses", **Scientific Basis for Nuclear Waste Management**, 8, C.M. Jantzen, J.A. Stone, R.C. Ewing, eds., Materials Research Society, Pittsburgh (1985) p.55.

86VILK1 P. Vilks, D.J. Drew, "The effect of colloids on actinide migration", (1986).

81WANG1 R. Wang, Y.B. Katayama, "Probable leaching mechanisms for UO_2 and spent fuel", **Scientific Basis for Nuclear Waste Management**, 3, J.G. Moore, ed., Plenum Press, New York (1981) p.379.

83WEBE1 W.J. Weber, "A review of the current status of radiation effects in solid nuclear waste forms", **Scientific Basis for Nuclear Waste Management**, 6, D.G. Brookins, ed., North-Holland, New York (1983) p.407.

81WEST1 J.H. Westsik, Jr., R.D. Peters, "Time and temperature dependence of the leaching of a simulated high-level waste glass", **Scientific Basis for Nuclear Waste Management**, 3, J.G. Moore, ed., Plenum Press, New York (1981) p.355.

82WICK1 G.G. Wicks, W.C. Mosley, P.G. Whitkop, K.A. Saturday, "Durability of simulated waste glasseffects of pressure and formation of surface layers", **Journal of Non-Crystalline Solids**, 49 (1982) p.413.

82WICK2 G.G. Wicks, B.M. Robnett, W.D. Rankin, "Chemical durability of glass containing SRP waste - leachability characteristics, protective layer formation, and repository system interactions", **Scientific Basis for Nuclear Waste Management**, 5, W. Lutze, ed., North-Holland, New York (1982) p.15.

86WICK1 G.G. Wicks, "Nuclear waste vitrification - the geology connection", **Journal of Non-Crystalline Solids**, 84 (1986) p.241.

86WICK2 G.G. Wicks, "Interactions of SRP waste glass with potential canister and overpack metals", **Journal of Non-Crystalline Solids**, 84 (1986) p. 258.

85YAMA1 S. Yamanaka, J. Akagi, M. Hattori, "Reaction of Pyrex type borosilicate glass with water in autoclave", **Journal of Non-Crystalline Solids**, 70 (1985) p.279.